UNIVERSITY OF CANBERRA

Virulence factors in rabbit calicivirus infections

A thesis submitted in fulfilment
of the requirements for the degree of
Doctor of Philosophy

Submitted by

Elena Smertina

Faculty of Science and Technology

University of Canberra

December 2022

Contents

Funding

Publications

- <u>Smertina E</u>, Urakova N, Strive T, Frese M. Calicivirus RNA-dependent RNA polymerases: evolution, structure, protein dynamics, and function. *Frontiers in Microbiology*, 2019; 10:1280. doi: 10.3389/fmicb.2019.01280

- <u>Smertina E</u>, Hall RN, Urakova N, Strive T, Frese M. Calicivirus Non-structural proteins: potential functions in replication and host cell manipulation. *Frontiers in Microbiology*, 2021; 12:712710. doi: 10.3389/fmicb.2021.712710

- Kardia E, Frese M, <u>Smertina E</u>, Strive T, Zeng Z-L, Estes MK, Hall RN. Culture and differentiation of rabbit intestinal organoids and organoid-derived cell monolayers. *Scientific reports*, 2021; 11(1):5401. doi: 10.1038/s41598-021-84774-w

- Mahar JE, Jenckel M, Huang N, <u>Smertina E</u>, Holmes EC, Strive T, Hall RN. Frequent intergenotypic recombination between the non-structural and structural genes is a major driver of epidemiological fitness in caliciviruses. *Virus Evolution*, 2021; https://doi.org/10.1093/ve/veab080

- <u>Smertina E</u>, Carroll AJ, Boileau J, Emmott E, Jenckel M, Vohra H, Rolland V, Hands P, Hayashi J, Neave MJ, Liu J-W, Hall RN, Strive T, Frese M. Lagovirus non-structural protein p23: a putative viroporin that interacts with heat shock proteins and uses a disulfide bond for dimerization. *Frontiers in Microbiology*, 2022; https://doi.org/10.3389/fmicb.2022.923256

- Kardia E, Fakhri O, Pavy M, Mason H, Huang N, <u>Smertina E</u>, Estes MK, Strive T, Frese M, Hall RN. Hepatobiliary organoids derived from leporids support the replication of hepatotropic lagoviruses. *Preprint*, 2022; https://doi.org/10.1101/2022.04.07.487566.

Conference abstracts

- <u>Smertina E</u>, Frese M, Strive T, Hall R. Virulence factors in Rabbit calicivirus infections (Science and Technology HDR Student Conference 2019, oral presentation)
- <u>Smertina E</u>, Jenckel M, Hall R, Frese M, Strive T. Quantitative proteomics to investigate the Rabbit haemorrhagic disease virus infection (the 26th Annual Lorne Proteomics Symposium 2021, oral presentation and poster)
- <u>Smertina E</u>, Hall R, Frese M, Strive T. Studying uncharacterised non-structural proteins of Rabbit haemorrhagic disease virus (the 25th Annual Lorne Proteomics Symposium 2020, oral presentation and poster)
- <u>Smertina E</u>, Hall R, Frese M, Strive T. Studying uncharacterised non-structural proteins of RHDV (7th International Calicivirus Conference 2019, poster)
- <u>Smertina E</u>, Carroll AJ, Boileau J, Emmott E, Jenckel M, Vohra H, Rolland V, Hands P, Hayashi J, Neave MJ, Liu J-W, Hall RN, Strive T, Frese M. Lagovirus non-structural protein p23 is a viroporin that interacts with heat shock proteins and affects Ca^{2+} transmembrane transport (The Australian & New Zealand Society for Mass Spectrometry Conference 2021).

Awards

- 7th International Calicivirus Conference 2019 in Sydney, Australia, travel grant.
- University of Canberra Higher Degree by Research additional funding competition winner in 2020.

Acknowledgments

List of abbreviations

°C	Degree Celsius
β-me	β-mercaptoethanol
bp	Base pairs
CAPS	N-cyclohexyl-3-aminopropanesulfonic acid
CRFK	Crandell-Rees feline kidney cells
DMEM	Dulbecco's modified eagle medium
DNA	Deoxyribonucleic acid
EBHSV	*European brown hare syndrome virus*
E. coli	*Escherichia coli*
EDTA	Ethylenediaminetetraacetic acid
e.g.	exempli gratia (for example)
eIF	Eukaryotic initiation factor
ER	Endoplasmic reticulum
FCV	*Feline calicivirus*
FMDV	*Foot and mouth disease virus*
G (RCF)	Relative centrifugal force
GFP	Green fluorescent protein
gRNA	Genomic RNA
h	Hour
HAE	Hereditary acute angioedema
HBGA	Histo-blood group antigen
Hsp	Heat shock protein
i.e.	id est (that is)
IFN	Interferon
IP	immunoprecipitation
IPTG	Isopropyl-β-d-1-thiogalactopyranoside
kB	Kilobase
kDa	Kilodalton
LB	Luria Bertani
LC	Leader of capsid
LLC-MK2	Rhesus monkey kidney epithelial cells
MEM	Minimum essential medium
MNV	*Murine norovirus*
min	minute
MW	Molecular weight
NLS	Nuclear localisation signal
NS	Non-structural
NTPase	Nucleoside-triphosphatase
nt	Nucleotide
OD	Optical density
o/n	Overnight
ORF	Open reading frame
PBS	Phosphate buffered saline
PCR	Polymerase chain reaction
PDB	Protein data bank
pI	Isoelectric point

PSIPRED	PSI-blast based secondary structure PREDiction
RaV	*Rabbit vesivirus*
RCV	*Rabbit calicivirus*
RdRp	RNA-dependent RNA polymerase
RHD	Rabbit haemorrhagic disease
RHDV	*Rabbit haemorrhagic disease virus*
RK	Rabbit kidney
RNA	Ribonucleic acid
rpm	Rounds per minute
SDS-PAGE	Sodium dodecyl sulfate-polyacrylamide gel electrophoresis
sgRNA	Subgenomic RNA
SILAC	Stable isotope labelling of amino acids in cell culture
SOC	Super optimal broth with catabolites repression
TB	Terrific broth
TBST	Tris buffered saline, 0.1% Tween-20
TCA	Trichloroacetic acid
TURBS	Termination upstream ribosomal binding site
UT	Untransfected
UTR	Untranslated region
VESV	*Vesicular exanthema of swine virus*
VLP	Virus-like particle
VP	Viral protein
VPg	Virion protein, genome-linked

List of figures

List of tables

Abstract

Rabbit caliciviruses belong to the family *Caliciviridae,* genus *Lagovirus* and are used in Australia to manage the numbers of European rabbits (*Oryctolagus cuniculus*), introduced vertebrate pest species. Feral rabbit populations damage the environment leading to extinction of native plant and animal species and causing agricultural losses. The *Rabbit haemorrhagic disease virus* (RHDV) is a pathogenic lagovirus that causes liver failure and haemorrhages in adult, but not young rabbits. Another lagovirus, RHDV2, frequently kills both adult and young rabbits. These viruses are thought to have evolved from non-pathogenic rabbit caliciviruses that infect intestinal, and not liver tissues. In the Iberian Peninsula, lagomorphs are important elements of the environment and farmed rabbits represent a food source. RHDV outbreaks in farmed rabbits are not desirable and rabbit vaccination is implemented. Despite the use of lagoviruses as a biocontrol agent in Australia and efforts to prevent outbreaks in Europe, many aspects of their virology remain poorly understood. This is mostly due to the inability of researchers to grow rabbit caliciviruses in the laboratory, as they cannot be propagated in a conventional cell culture system. Recent advances towards organoid culture systems may soon improve our knowledge in this area.

Caliciviridae have a small positive-sense single-stranded RNA genome that encodes structural (capsid) and non-structural proteins. The non-structural proteins are responsible for virus replication and modification of the host cell to accommodate virus replication. Thus, these proteins are likely important virulence determinants of lagoviruses. For example, one of the previously discovered virulence factors is the RNA-dependent RNA polymerase (RdRp). This enzyme replicates the genome and was shown to rearrange Golgi membranes in transfected cells. The crystal structure of RdRp for most caliciviruses had been resolved and all the functional RNA polymerase motifs have been identified. In this work, however, we described a novel motif that is characteristic for caliciviruses and picornaviruses. This motif (termed motif I) was found to be conserved across the order *Picornavirales*. The exact function of this motif is yet to be identified.

Another knowledge gap in lagovirus virology is the unknown function(s) of several non-structural proteins of lagoviruses, namely p16, p23 and p29. I used various *in vitro* and *in silico* approaches to study these proteins, e.g., their localisation in transfected cells and presence of functional motifs in their sequences. Currently, the most studied protein of the three is p23. This protein was shown to localise to the cytoplasm and oligomerise. Adding to this information, I showed that this protein has two amphipathic helices at the C-terminus, that may form a channel

upon the oligomerisation of p23. Moreover, this protein interacts with heat shock proteins (Hsp70 and 110), which may assist its correct folding and oligomerisation process. The exact localisation of this protein was also demonstrated in this study, suggesting that p23 forms channels in the endoplasmic reticulum (ER). Remarkably, cytoplasmic Ca^{2+} concentration was increased in p23 transfected cells, further supporting my hypothesis that p23 is a viroporin, as the ER is known to be the most important cellular Ca^{2+} depot.

Thesis structure

This thesis represents a combination of published and unpublished works, organised according to the *HDR Thesis Submission & Examination Guidelines*. Individual chapters consist of published or accepted for publication manuscripts, or unpublished results that are accompanied by a general introduction (chapter 1) and discussion (chapter 6). Some of the figures from my published works were used in the general introduction with a due reference. In line with the guidelines, I am the lead author for most, but not all the included publications. The publications for which I was not the lead author can be found in the appendix. My contribution to individual papers/manuscripts is stated at the beginning of each chapter in authorship declaration forms.

Chapter 1

A general introduction for all following chapters is given in this chapter.

Chapter 2

Smertina E, Urakova N, Strive T, Frese M. Calicivirus RNA-dependent RNA polymerases: evolution, structure, protein dynamics, and function. *Frontiers in Microbiology*, 2019; 10:1280. doi: 10.3389/fmicb.2019.01280

[Frontiers | Calicivirus RNA-Dependent RNA Polymerases: Evolution, Structure, Protein Dynamics, and Function | Microbiology (frontiersin.org)](#)

In this publication, a new conserved motif for calicivirus RNA-dependent RNA polymerases (RdRps) was described. This motif is of high significance as it was found to be also conserved at the level of the order Picornavirales which includes 8 viral families with broad host range.

Chapter 3

Smertina E, Hall RN, Urakova N, Strive T, Frese M. Calicivirus Non-structural proteins: potential functions in replication and host cell manipulation. *Frontiers in Microbiology*, 2021; 12:712710. doi: 10.3389/fmicb.2021.712710

[Frontiers | Calicivirus Non-structural Proteins: Potential Functions in Replication and Host Cell Manipulation | Microbiology (frontiersin.org)](#)

In this publication, a function is proposed for protein p23 (NS2) of Caliciviridae. This protein has characteristic features of a viroporin, and this function is likely to be conserved across the Caliciviridae family.

Chapter 4

Smertina E, Carroll AJ, Boileau J, Emmott E, Jenckel M, Vohra H, Rolland V, Hands P, Hayashi J, Neave MJ, Liu J-W, Hall RN, Strive T, Frese M. Lagovirus non-structural protein p23: a putative viroporin that interacts with heat shock proteins and uses a disulfide bond for dimerization. *Frontiers in Microbiology*, 2022; doi: 10.3389/fmicb.2022.923256

https://www.frontiersin.org/articles/10.3389/fmicb.2022.923256/full

In this publication, a viroporin activity is described for lagovirus non-structural protein p23. The mechanism behind p23 oligomerisation is revealed and elevated calcium levels detected in p23-transfected cells.

Chapter 5

This chapter describes my results on RHDV non-structural proteins expression in bacterial and mammalian cells.

Chapter 6

General discussion on the results presented in chapters 2–5.

Appendix

All publications, including those for which I was not the lead author can be found here. These publications provide evidence for extensive collaborations during my PhD studies:

1. Kardia E, Frese M, Smertina E, Strive T, Zeng XL, Estes MK & Hall RN. Culture and differentiation of rabbit intestinal organoids and organoid-derived cell monolayers. *Scientific Reports*, 2021; 1–12. https://doi.org/10.1038/s41598-021-84774-w.
2. Mahar JE, Jenckel M, Huang N, Smertina E, Holmes EC, Strive T & Hall RN. Frequent intergenotypic recombination between the non-structural and structural genes is a major driver of epidemiological fitness in caliciviruses. *Virus Evolution*, 2021; 7(2), 1–14. https://doi.org/10.1093/ve/veab080.
3. Kardia E, Fakhri O, Pavy M, Mason H, Huang N, Smertina E, Estes MK, Strive T, Frese M, Hall RN. Hepatobiliary organoids derived from leporids support the replication of hepatotropic lagoviruses. *Preprint*, 2022; https://doi.org/10.1101/2022.04.07.487566.

Data availability

- The scripts used to analyse the data presented in chapter 4 can be found here: https://github.com/sme229

- The proteomics data sets (label-free quantification) were deposited to the ProteomeXchange Consortium via the PRIDE repository with PXD031027 identifier. The SILAC data set was deposited to the ProteomeXchange Consortium via the PRIDE repository with PXD031619 identifier.

- The RNA sequencing data that I re-analysed for this study, were deposited in the NCBI Sequence Read Archive under the BioProject accession No. PRJNA434149 (https://www.ncbi.nlm.nih.gov/sra/?term=PRJNA434149).

Animal ethics statement

Rabbit liver samples that were used in this study for global proteome and transcriptome characterisation were initially prepared for a previous study (Neave et al., 2018) and subsequently stored at -20°C. Animal ethics approval was received for that study earlier: "Animal experiments were conducted at the Commonwealth Scientific and Industrial Research Organisation (CSIRO) Black Mountain Laboratories following the Australian Code for the Care and Use of Animals for Scientific Purposes (2013) and approved by the CSIRO Ecosystem Sciences Animal Ethics Committee (permit identifiers: CESAEC DOMRAB, SEAEC 10-12, ESAEC 13-10)."

Therefore, there was no need for animal ethics approval to conduct this study.

Chapter 1. General introduction

Overview

The *Caliciviridae* family consists of 11 genera (*Norovirus, Nebovirus, Sapovirus, Lagovirus, Vesivirus, Nacovirus, Bavovirus, Recovirus, Salovirus, Minovirus* and *Valovirus*) (**Figure 1**). The genus *Lagovirus* comprises viruses that infect lagomorphs, but members of this genus differ greatly in their pathogenicity. For example, the *Rabbit haemorrhagic disease virus* (RHDV) causes acute hepatitis, liver failure and haemorrhages in European rabbits (*Oryctolagus cuniculus*), leading to death within 72 hours after infection. While RHDV has >90% case fatality rate, the closely related *Rabbit calicivirus Australia-1* (RCV-A1) causes almost no disease manifestations (Abrantes et al., 2012a). Since the mid-1990s, RHDV has been used to control feral rabbit populations in Australia and New Zealand (reviewed in Kerr et al., 2021).
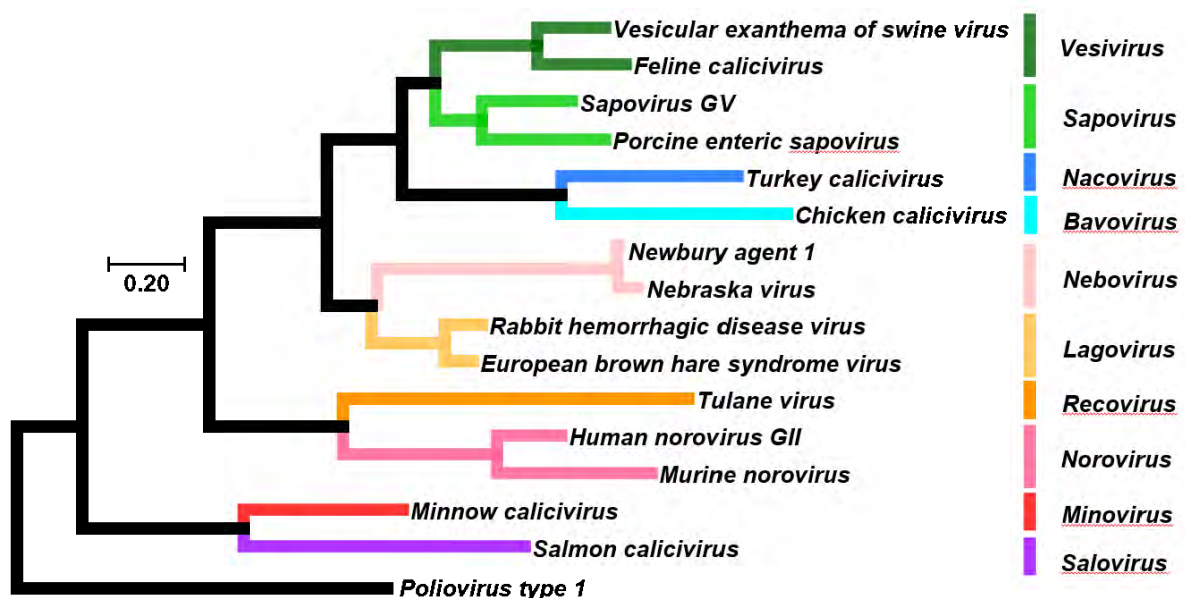
Figure 1. Phylogenetic analysis of calicivirus RNA-dependent RNA polymerase (RdRp) protein sequences using Maximum Likelihood algorithm (D. T. Jones et al., 1992). The tree is drawn to scale, with branch lengths representing the number of substitutions per site. The Phylogenies were rooted using *Poliovirus type 1* (GenBank accession NC_002058). The following sequences were used: *Vesicular exanthema of swine virus* (VESV; NC_002551), *Feline calicivirus* (FCV; NC_001481), *Sapovirus genogroup V* (MG012434), *Porcine enteric sapovirus* (NC_000940), *Turkey calicivirus* (NC_043516), *Chicken calicivirus* (NC_033081), *Newbury agent 1* (NC_007916), *Nebraska virus* (NC_004064), *Rabbit haemorrhagic disease virus* (NC_001543), *European brown hare syndrome virus* (EBHSV; NC_002615), *Tulane*

virus (NC_043512), *Human norovirus GII* (NC_039477), *Murine norovirus* (MNV; NC_008311), *Minnow calicivirus* (NC_035675) and *Salmon calicivirus* (NC_024031). Evolutionary analyses were conducted in MEGA7 (Kumar et al., 2016).

In 1995, RHDV testing on wild rabbits started in Wardang island (South Australia). This field trial aimed to evaluate the rates of virus transmission and mortality in wild rabbits. For this trial, a 50-ha enclosure was built with electrified cat- and rabbit-proof fence and strict quarantine protocols were implemented. The trials were initiated by infecting two rabbits on the site, which died after 42 hours. Overall, RHDV spread poorly in the wild when the only mechanism of spreading was by direct contact with infected rabbits (Cooke & Fenner, 2002).

Later that year, RHDV escaped to the mainland, presumably transferred by flies – an additional mechanism of virus spread (Cooke & Fenner, 2002). This RHDV strain was subsequently named RHDV1 (GI.1). A different lagovirus, newly emerged RHDV2 (GI.2), was detected in France in 2010. In 2015, this virus was detected in Australia after it has spread around the world (Hall et al., 2015; Hall et al., 2017; Le Gall-Reculé et al., 2011). Both viruses cause acute haemorrhagic disease in infected adult rabbits. However, RHDV2 (in contrast to RHDV1) was shown to cause disease not only in adult rabbits but also in young rabbits (kittens) and in hares (Dalton et al., 2012; Lopes et al., 2015). The possible mechanisms underlying the resistance of young rabbits to RHDV1-caused disease have been studied using RNA-sequencing of RHDV1- and RHDV2-infected liver samples (Neave et al., 2018). The findings suggest that constitutive activation of innate immune system components in kittens, such as overexpression of MHC class II genes, may play a role in the innate resistance of young animals to the disease. Furthermore, MHC class I gene expression was downregulated in RHDV2-infected kittens, suggesting that this virus is able to suppress part of the immune response, which may aid disease progression (Neave et al., 2018).

Rabbits are native to Europe and are an important part of the food chain (Delibes-Mateos et al., 2008). In the Iberian Peninsula, where European rabbits originated, RHDV outbreaks are causing dramatic population decreases in the wild and kill domestic as well as commercially-bred rabbits (Abrantes et al., 2012a). The latter leads to economic losses in the fur and meat industry. Moreover, the decrease in wild rabbit population also threatens natural rabbit predators (Angulo et al., 2002). Therefore, in these areas, RHDV immunisation is in use to protect the valuable rabbits.

These two aspects of lagoviruses, being extremely 'useful' in one part of the world and 'harmful' in the other, render the necessity and importance to study these viruses.

Lagovirus nomenclature

The current taxonomy for lagoviruses is based on the major capsid protein VP60 sequence alignments (**Figure 2**) (Le Pendu et al., 2017). This nomenclature is based on genogroups, e.g., RHDV and RCV are closely related and belong to the genogroup GI, whereas *European brown hare syndrome virus* (EBHSV) and other hare lagoviruses belong to genogroup GII. Further, if ≥15% of nucleotides differ across the VP60 coding sequences between clades within a genogroup, genogroups are divided into genotypes, GI.1, GI.2 and so on. Finally, subgroups within genotypes can be defined as variants, e.g., GI.1a. Genetic distance of ≥6% between subgroups accounts for variants. However, the short denominations can still be used for convenience, e.g., RHDV, RHDV2, RCV (Le Pendu et al., 2017).
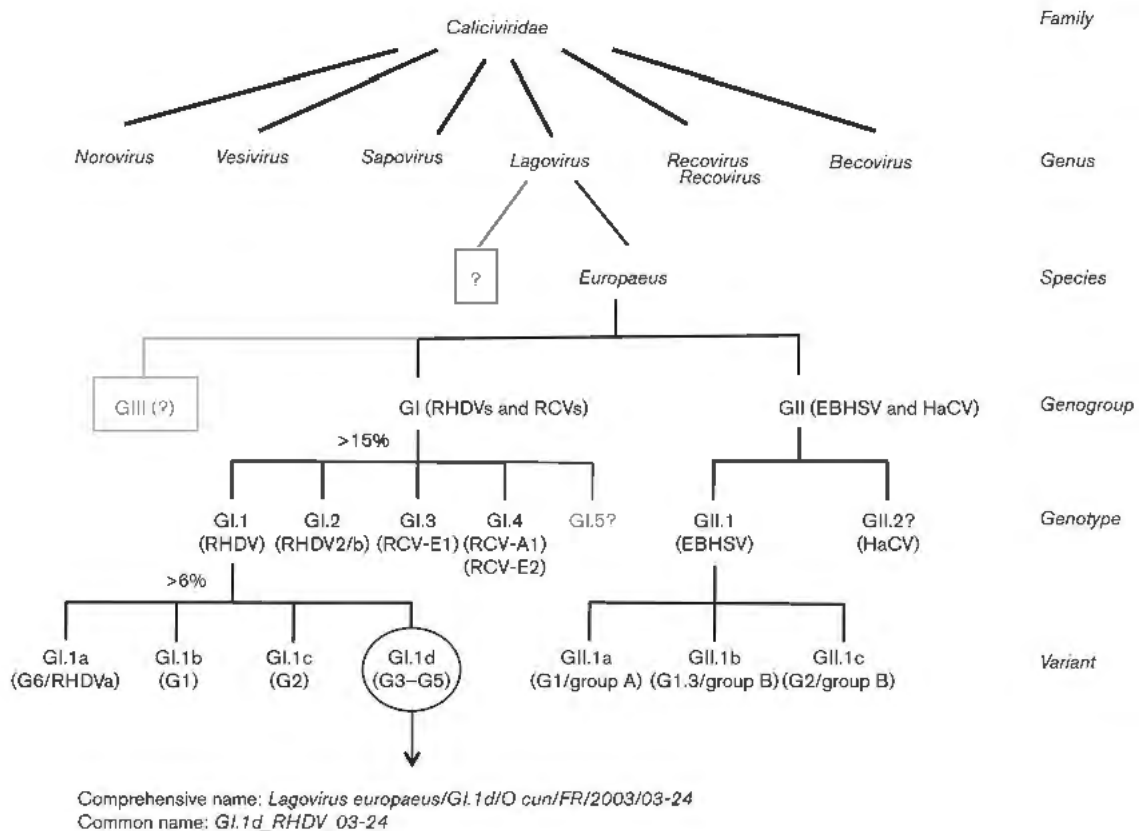
Figure 2. Taxonomy of the genus *Lagovirus*. Virus species are classified into genogroups, GI (rabbit caliciviruses) and GII (hare caliciviruses). Genogroups are further divided into genotypes, e.g., GI.1 (RHDV). Variants can be further distinguished within genotypes and are indicated by a letter, GI.1a. Undiscovered part of the genus are coloured light grey. Figure from Le Pendu et al., 2017.

Calicivirus genome organisation

The genome of caliciviruses consists of positive-sense, single-stranded RNA that contains coding sequences in two or more partially overlapping open reading frames (ORFs) (**Figure 3**). The coding sequences are flanked by untranslated regions (UTRs) at both the 5' and 3' ends. Genomic RNA is covalently linked at the 5' end to a viral protein (VPg, for "virion protein, genome-linked") and is polyadenylated at the 3' end. Calicivirus particles contain a genomic (full-length) RNA of about 7.5 kb or one or more copies of a subgenomic RNA of about 2 kb (Ehresmann & Schaffer, 1977; Meyers et al., 1991b, 1991a). The number of ORFs varies from two to four in full-length genomic RNAs and from two to three in subgenomic RNAs (McFadden et al., 2011; Wirblich et al., 1996). ORF1 is the largest of the reading frames and encodes a polyprotein that is subsequently cleaved into five non-structural proteins and VPg (genus *Norovirus* and *Vesivirus*) or five non-structural proteins, VPg and the major capsid protein VP1 (genus *Lagovirus*, *Nebovirus* and *Sapovirus*) (Martín Alonso et al., 1996; Meyers et al., 2000). The second and third ORFs in the genomic RNA of noroviruses encode the structural proteins VP1 and VP2, respectively. The subgenomic RNAs of all genera are very similar to each other; they contain the 5' UTR and the VP1 and VP2 coding sequences (Boga et al., 1992; Meyers et al., 1991b, 1991a, 2000).
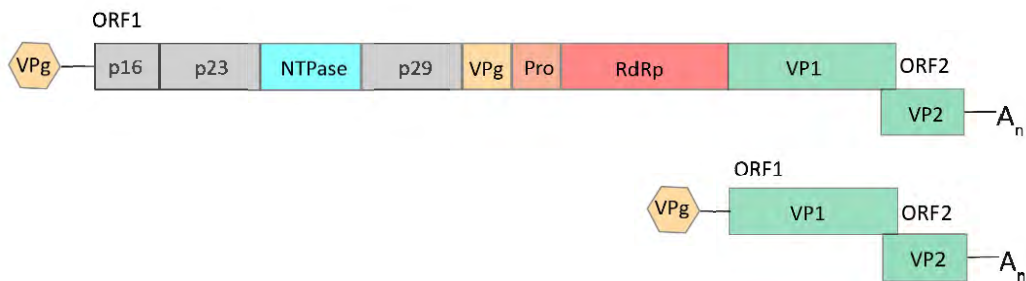
Figure 3. Lagovirus genome organisation. Genomic full-length RNA of about 7.5 kb (top) in size contains two ORFs. Subgenomic RNA of about 2.1 kb (bottom) in size with two ORFs encodes the main structural proteins, VP1 (VP60) and VP2 (VP10). Coloured boxes represent coding sequences that are flanked by untranslated regions (shown as lines). Yellow hexagons represent VPg proteins that are covalently bound to the 5' end of all genomic and subgenomic RNAs; A_n represents the poly(A) tail at the 3'-end of all genomic and subgenomic RNAs. Figure from Smertina et al., 2019 with modifications.

In lagoviruses, the 5' terminal sequences of the genomic and subgenomic RNAs demonstrate a high level of homology (Meyers et al., 1991). The RdRp-VP1 junction is also

highly conserved, and this enables recombination events within and between lagovirus variants and genotypes. The recombination occurs through template switching mechanism, where an RdRp starts replicating one genome and at the sequence of the RdRp-VP1 junction switches to a different genome template. This results in new virus variants that have non-structural and structural genes from different genotypes or variants (Abrantes et al., 2020; Mahar et al., 2021). The recombination events are considered as a major source of diversity for caliciviruses (Ludwig-Begall et al., 2018; Mahar et al., 2021; Parra, 2019).

Life cycle

The calicivirus life cycle begins with the entry of viral particles into the host cells. The primary target of RHDV infection is liver, however, the virus can also be detected in lung and spleen macrophages (Abrantes et al., 2012). The receptor that RHDV uses to enter liver cells has not yet been discovered. Histo-blood group antigens (HBGAs) H type 2, A type 2 and B type 2 expressed on the surface of intestines and trachea were identified as the receptors for RHDV attachment (Ruvoën-Clouet et al., 2000) (Rademacher et al., 2007). Because HBGAs are not expressed on the surface of hepatocytes, it is likely that HBGAs are used by RHDV as attachment factors and other molecules serve as entrance receptors in the liver. After the attachment and virus internalisation, the genome is released into the cytoplasm. It was further proposed that the internalisation occurs not through a single receptor, but through the interaction of viral capsid proteins with cell surface nucleolin, resulting in clathrin-dependent endocytosis (Zhu et al., 2018). However, these data have not yet found confirmation in other studies; moreover, a successful infection of cultured cells with an RHDV replicon constructed earlier (Zhu et al., 2017) and used in this study has not been reproduced by other researchers.

Once in the cytoplasm, the genome of this positive-sense RNA virus is directly translated by the host cell translation machinery. In caliciviruses, VPg plays a key role in the initiation of translation, substituting the cap structure of host cell mRNAs (Goodfellow, 2011). For example, the VPg of FCV binds eIF4E, a cap-binding translation initiation factor (Goodfellow et al., 2005). For MNV, it was shown that VPg also interacts with eIF4G, another translation initiation factor, and this interaction is essential for viral translation (Leen et al., 2016). Caliciviruses encode a polyprotein that is subsequently cleaved into several non-structural and structural (capsid) proteins by a virus encoded protease (3C-like) (Meyers et al., 2000), in some cases, cellular proteases are also involved in the cleavage process. For example, norovirus protein NS1/2 is cleaved by caspase-3 (Lee et al., 2019). After all viral proteins are produced and enough capsid protein is accumulated, viral genome replication starts. The RdRp

replicates the genome in association with the helicase (2C-like) that unwinds RNA helices (reviewed in Smertina et al., 2019). Nucleotidylated VPg (covalently bound to either GTP or UTP) serves as a primer for RNA replication (reviewed in Eruera et al., 2021). The first replication step results in the synthesis of a complementary, negative-sense RNA that serves as a template to produce multiple copies of positive-sense RNA (full length and subgenomic RNAs). The newly synthesised genomic RNA is translated into more polyprotein or packaged into viral particles. The subgenomic RNA translation boosts capsid protein expression and promotes the assembly of new virions.

Calicivirus proteins

Structural (capsid) proteins

The structural protein VP1 (termed VP60 in lagoviruses) forms an icosahedral, non-enveloped capsid of about 25–40 nm in diameter (Parra & Prieto, 1990; Prasad et al., 1994, 1999). A typical calicivirus capsid contains 90 VP1 dimers. Protruding VP1 domains create a surface topography that resembles cup-shaped depressions when viewed using an electron microscope, which inspired the name 'calicivirus' (from Latin 'calyx' = cup) (**Figure 4A**). The atomic structure of the RHDV capsid was resolved using cryo-electron microscopy and crystallography and deposited to Protein Data Bank (PDB) under the 3J1P identifier (Wang et al., 2013) (**Figure 4B;** https://www.rcsb.org/3d-view/3J1P/1).

The second structural protein VP2 (termed VP10 in lagoviruses) is present in the capsid in much smaller numbers, binding VP1 at the virion interior (Vongpunsawad et al., 2013). In the absence of VP2, assembly of virus-like particles (VLPs) still occurs in noroviruses, however, VP2 was shown to regulate the stability of virus capsid (Bertolotti-Ciarlet et al., 2003). This protein also plays a role in virus replication and maturation of infectious virus particles (Sosnovtsev et al., 2005). Recent studies on FCV demonstrate that VP2 forms a portal-like structure that facilitates the delivery of viral RNA into the cytoplasm in the early stages of infection (Conley et al., 2019). The translation of VP2 in caliciviruses occurs through a termination/re-initiation mechanism as this protein is encoded downstream of VP1 in ORF2 (*Lagovirus, Nebovirus* and *Sapovirus* genera) or ORF3 (*Norovirus* and *Vesivirus* genera) (Napthine et al., 2009; Wennesz et al., 2019; Zinoviev et al., 2015). According to this mechanism, an RNA motif at the end of the VP1 coding sequence retains the ribosome until it is reloaded with translation initiation factors. This motif was named 'termination upstream ribosomal binding site' (TURBS) and allows the re-initiation of translation without a start AUG codon.

A

B
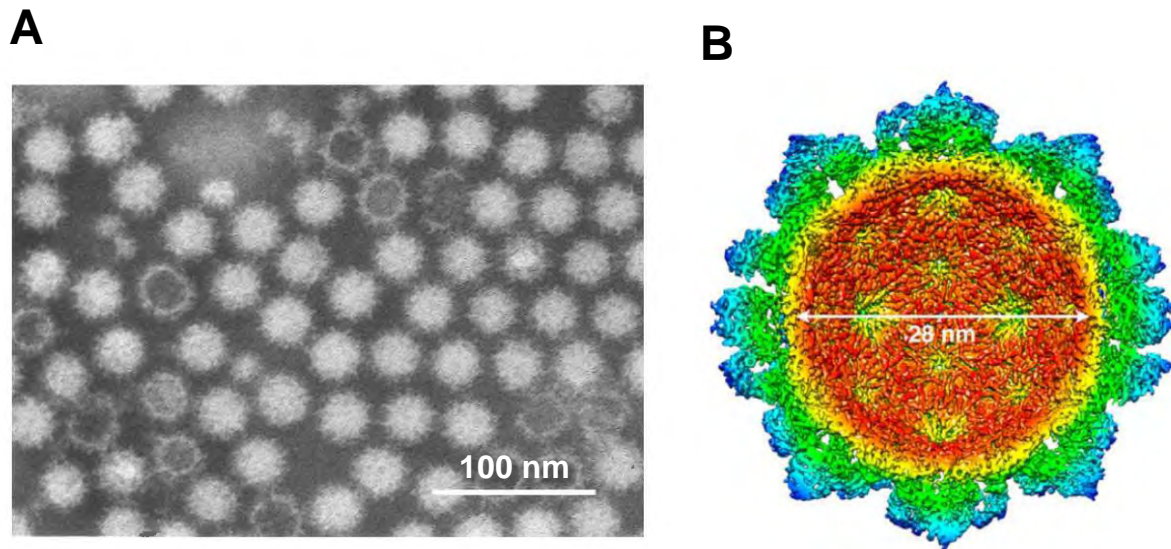
Figure 4. Electron micrograph of RHDV particles (A) and cryo-electron microscopy-resolved virion structure (B). The typical calicivirus particle size is 25–40 nm. Figures from Cooke & Fenner, 2002 and Wang et al., 2013 with modifications.

In lagoviruses, the structural proteins VP60 and VP10 are responsible for host and tissue tropism (Mahar et al., 2021). This was demonstrated by analysing recombinant virus variants. The viral genome sequence at the RdRp-VP60 junction area is highly conserved, which enables template switching during replication when a host cell is infected by different lagoviruses. As a result of such an event, two viruses 'swap' their structural and non-structural genes producing recombinant virus variants (Mahar et al., 2021). Recombinant viruses that contained the non-structural genes from a benign GI.4 genotype (RCV) and structural genes from a pathogenic GI.2 genotype (RHDV2) were pathogenic and hepatotropic (Mahar et al., 2021). This observation means that RHDV2 structural proteins define the tropism and are correlated with virulence (Mahar et al., 2021).

Non-structural proteins

RNA-dependent RNA polymerase (RdRp)

The ORF1 of caliciviruses encodes the non-structural proteins that are involved in replication and in the modification of the host cell environment (**Figure 3**). The non-structural proteins can be categorised into those with known functions, i.e., 2C-like helicase, 3C-like protease and RdRp and those for which a clear role has not yet been defined (NS1, NS2 and NS4). The functions of some non-structural proteins were deduced by comparing calicivirus and picornavirus sequences and by searching for conserved motifs. For example, a 2C-like

helicase (NTPase) was identified after a typical nucleotide-binding site was detected (Neill, 1990). The p58 cleavage product of the RHDV polyprotein was found to resemble the 3D polymerase of poliovirus, and its role in RNA replication was subsequently confirmed using functional assays (Lopez Vazquez et al., 1998; Wirblich et al., 1996). Similarly, the sequence preceding the RdRp gene was found to encode a 3C-like protease (Jiang et al., 1993; Neill, 1990). Similar to the picornavirus proteins, calicivirus proteases are responsible for the processing of the polyprotein and the formation and accumulation of a 3CD-like polymerase precursor. Interestingly, this precursor protein demonstrates only a protease activity in picornaviruses, whereas in caliciviruses it also acts as a polymerase (Sosnovtseva et al., 1999; Thumfart & Meyers, 2002; Marcotte et al., 2007).

All viral RdRps have a similar structure with three domains: fingers, palm and thumb (**Figure 5A**). The domains can be further subdivided into homomorphs (**Figure 5B**). The homomorphs are named alphabetically from A to H. Each of these homomorphs (apart from the homomorph H) accommodates a conserved functional motif, which retain the homomorphs' nomenclature (**Figure 5C**). All these motifs are conserved and involved in the functional activity of the enzyme, being essential for RNA replication.
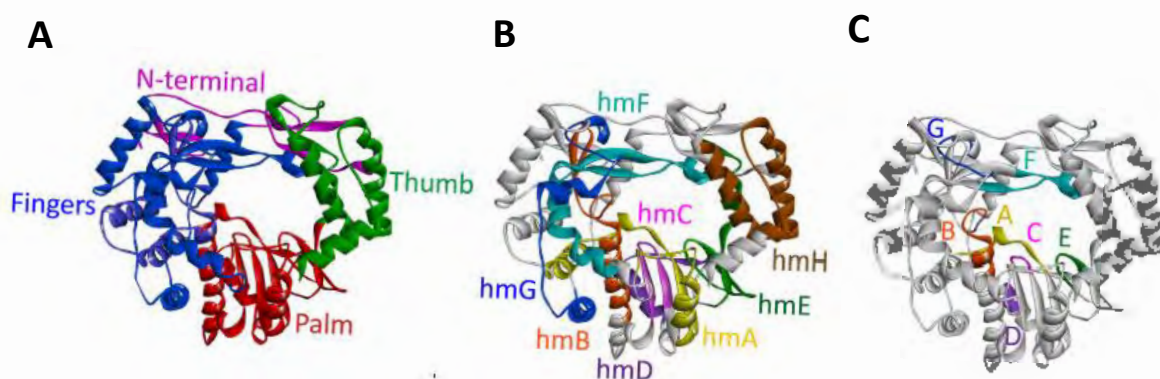
Figure 5. Domains and motifs of calicivirus RdRps. (**A**) Ribbon diagram of the RHDV RdRp (PDB ID: 1KHW) with three structural domains (fingers, thumb and palm), fingers and thumb domains are connected by the N-terminal structure; (**B**) homomorphs and (**C**) functional motifs (A–G). Figure modified from Smertina et al., 2019.

In this work, I, together with my colleagues, identified a putative new conserved motif in calicivirus and picornavirus RdRps (**Figure 6A**). This motif was termed 'I motif' (as the letter 'H' already refers to a known homomorph) and it resides in the N-terminal connection between the thumb and fingers domains (**Figure 6B**, **C**) (Smertina et al., 2019). This motif is conserved in the order *Picornavirales*, which comprises the families *Caliciviridae* and

Picornaviridae as well as other families, e.g., viruses that infect plants (family *Secoviridae*) and insects (family *Dicistroviridae*). Our data suggest an important role of the I motif in virus replication; however, its exact function is yet to be identified. Presumably, this motif of the RdRps is involved in the regulation of fidelity of RNA replication, as substitutions in this region of foot-and-mouth disease virus (FMDV, family *Picornaviridae*) led to higher frequency of mutations in newly synthesised RNA (Xie et al., 2014). The results of this work are published and presented in chapter 1.
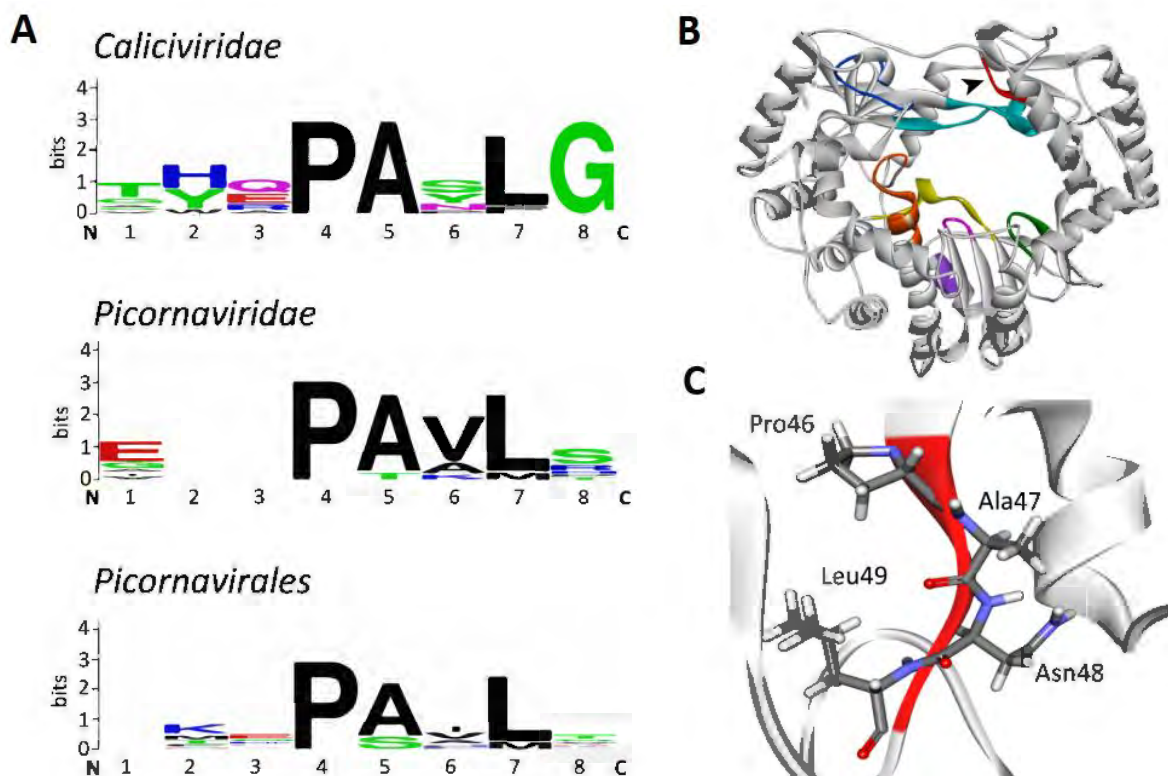
Figure 6. Putative new motif I in calicivirus and picornavirus RdRps. (**A**) Sequence logo alignment of the putative new motif in families *Caliciviridae*, *Picornaviridae* and order *Picornavirales*. The amino acids P (proline), A (alanine) and L (leucine) are highly conserved as measured by bits and indicated by the height of each letter. Amino acids are coloured based on their physicochemical properties: polar amino acids (Gly, Ser, Thr, Tyr, Cys, Gln, Asn), green; basic (Lys, Arg, His), blue; acidic (Asp, Glu), red; and hydrophobic (Ala, Val, Leu, Ile, Pro, Trp, Phe, Met), black (Crooks et al., 2004). (**B**) Ribbon diagram of RHDV RdRp (PDB ID: 1KHW) that shows the location of the new motif I (highlighted red and pointed by the black arrowhead). (**C**) Structure of the motif I in RHDV. Figure modified from Smertina et al., 2019.

Proteins p16, p23 and p29

To identify potential virulence factors, I studied the non-structural lagovirus proteins for which any functions have not yet been described. These proteins are p16 (NS1), p23 (NS2) and p29 (NS4). In other caliciviruses, these proteins can recruit cellular membranes for the formation of viral replication sites by disassembling cellular organelles such as the ER and Golgi. Some of them also counteract host immune responses (**Table 1**, from Smertina et al., 2021 with modifications). For example, the human norovirus proteins NS1/2 (p48) and NS4 (p22) induce Golgi membrane rearrangements in transfected cells (Fernandez-Vega et al., 2004). Moreover, NS4 also blocks trafficking of vesicles from ER to Golgi (Sharp et al., 2010). In *Murine norovirus* and human noroviruses, the cleavage product of NS1/2, NS1 is secreted, and the secreted protein mediates resistance to IFN-λ (Lee et al., 2019). A murine norovirus variant with a defective NS1/2 cleavage site lost its ability to secrete NS1 and to replicate in wild-type mice but successfully replicated in IFN-λ-signaling deficient mice (Lee et al., 2019).

A remarkable advance in the understanding of calicivirus non-structural proteins was made by studying the Tulane virus (genus *Recovirus*) protein NS1/2. Strtak et al. (2019) showed that the NS1/2 protein of this virus is a viroporin, i.e., it forms ion channels in cellular membranes upon oligomerisation. The authors also showed that NS1/2 localises to the ER and that the channel formation leads to a release of Ca^{2+} into the cytoplasm.

Table 1. Functions of the non-structural proteins in *Caliciviridae*.

Protein name	Intracellular localisation	Major functions/features	Reference
Human norovirus (genus *Norovirus*)			
NS1	Extracellular	NS1 is secreted and counteracts innate immune responses mediated by IFN-λ	Lee et al., 2019
NS1/2	Golgi	Golgi disassembly; inhibition of cellular protein secretion	Fernandez-Vega et al., 2004 Ettayebi and Hardy, 2003
NS4	ER/Golgi	Golgi disassembly; inhibition of cellular protein secretion; formation of membranous web (replication factories)	Sharp et al., 2010 Doerflinger et al., 2017

Murine norovirus (genus Norovirus)			
NS1	Extracellular	NS1 is secreted and counteracts innate immune responses mediated by IFN-λ	Lee et al., 2019
NS1/2	ER	NS1/2 dimerisation; NS1/2 cleavage is associated with persistence and apoptosis	Hyde and Mackenzie, 2010 Baker et al., 2012 Lee et al., 2019 Robinson et al., 2019
NS4	Golgi, endosomes	Golgi disassembly; moderate inhibition of cellular protein secretion	Sharp et al., 2012 Hyde and Mackenzie, 2010
Feline calicivirus (genus Vesivirus)			
NS2	ER	Dimerisation; formation of membranous web (replication factories)	Bailey et al., 2010 Kaiser, 2006
NS4	ER	Formation of membranous web (replication factories); counteracts IFN response	Bailey et al., 2010 Tian et al., 2020
Leader of capsid	Mitochondria	Oligomerisation and viroporin activity; apoptosis induction	Peñaflor-Téllez et al., 2022
Rabbit haemorrhagic disease virus (genus Lagovirus)			
NS1 (p16)	Nucleus and cytoplasm	Unknown	Urakova et al., 2015 Smertina et al., 2022
NS2 (p23)	ER	Oligomerisation; viroporin activity	
NS4 (p29)	Cytoplasm	Unknown	
Tulane virus (genus Recovirus)			
NS1/2	ER	Oligomerisation; viroporin activity	Strtak et al., 2019

Interestingly, the NS1/2 homologs of other caliciviruses also localise to the ER. For example, in RHDV, p23 shows an ER-like localisation pattern, the murine norovirus NS1/2 and its feline calicivirus (FCV) homolog p32 localise to the ER (Bailey et al., 2010; Hyde and

Mackenzie, 2010; Urakova et al., 2015). In contrast, the human norovirus NS1/2 (p48) appears to interact with Golgi rather than ER membranes (Fernandez-Vega et al., 2004). In addition, similar to the Tulane virus NS1/2, the NS1/2 and NS2 of other caliciviruses oligomerise. In RHDV, oligomerisation of p23 was first shown using a 'translocation assay', for which cells were co-transfected with plasmids that encode two p23 protein variants. One plasmid encoded a FLAG-tagged p23 and the other encoded a myc-tagged p23. One of them also encoded a nuclear localisation signal (NLS). Subsequently, both myc and FLAG-tagged p23 were detected in the nucleus, demonstrating a strong interaction or dimerisation of these proteins (Urakova et al., 2015).

Another recent work showed that *Feline calicivirus* (genus *Vesivirus*) also encodes a viroporin; however, in this case, it was not the positional homolog of NS1/2, but the leader of capsid protein (LC, a protein unique for vesiviruses) that is encoded upstream from the major capsid protein VP1 (Peñaflor-Téllez et al., 2022). Viroporins are classified by the number of transmembrane helices that mediate membrane integration: class I viroporins contain a single helix and class II viroporins contain two helices (Nieva et al., 2012). Interestingly, the LC protein does not contain transmembrane helices and is therefore an unconventional viroporin. Similarly, the Ebola virus viroporin 'delta peptide' permeates the membranes without the use of amphipathic helices, but by forming a disulfide cross-linked hairpin (He et al., 2017). Oligomerisation and membrane integration of protein LC is also mediated by inter- and intramolecular disulfide bonds (Peñaflor-Téllez et al., 2022).

In my work, I further investigated the function of the lagovirus protein p23, hypothesising that this protein is a viroporin. This protein has not yet been crystallised and its 3D structure is still unknown. I attempted to express and purify this protein in *E. coli* cells but did not succeed, likely because this protein is cytotoxic (see chapter 5). Thus, I used secondary structure prediction tools to identify candidate motifs that may suggest an intracellular localisation and/or a function for this protein. Similar to Tulane virus NS1/2, I found two amphipathic transmembrane helices at the C-terminus of p23 (**Figure 7**) (Smertina et al., 2021), but these helices do not allow the protein to form a membrane channel in its monomeric state. Oligomerisation is usually required for pore-forming proteins such as viroporins to insert and span the membrane (Fischer et al., 2002). Further investigations revealed that p23 forms dimers and perhaps higher order oligomers (i.e., trimers and tetramers). Of note, p23 only formed oligomers under non-reducing conditions and, therefore, I proposed that it might be a disulfide bond that stabilises the oligomerisation. Protein sequence of p23 contains three cysteine residues and using site-directed mutagenesis, I identified a residue essential for the dimerisation

(cysteine at position 41). This covalent bond stabilises p23 dimers, revealing the mechanistic details behind p23 dimerisation (Smertina et al., 2022). An altered protein mobility was observed in p23 variants where other cysteine residues were substituted with serine, suggesting a formation of intramolecular disulfide bonds. The exact mechanism underlying formation of the higher order oligomers is yet to be revealed.

Furthermore, I identified several cellular interaction partners of protein p23. Stable isotope labelling of amino acids in cell culture (SILAC) coupled with immunoprecipitation revealed that p23 interacts with the cytoplasmic heat shock proteins Hsp70 and Hsp110. This interaction is likely essential for the membrane association of p23, as heat shock proteins are known to 'guide' partially hydrophobic proteins that lack a signal sequence towards membranes (Martinez-Gil and Mingarro, 2015). Confocal microscopy and quantitative co-localisation assays confirmed the previous observation of the ER-like localisation of p23.
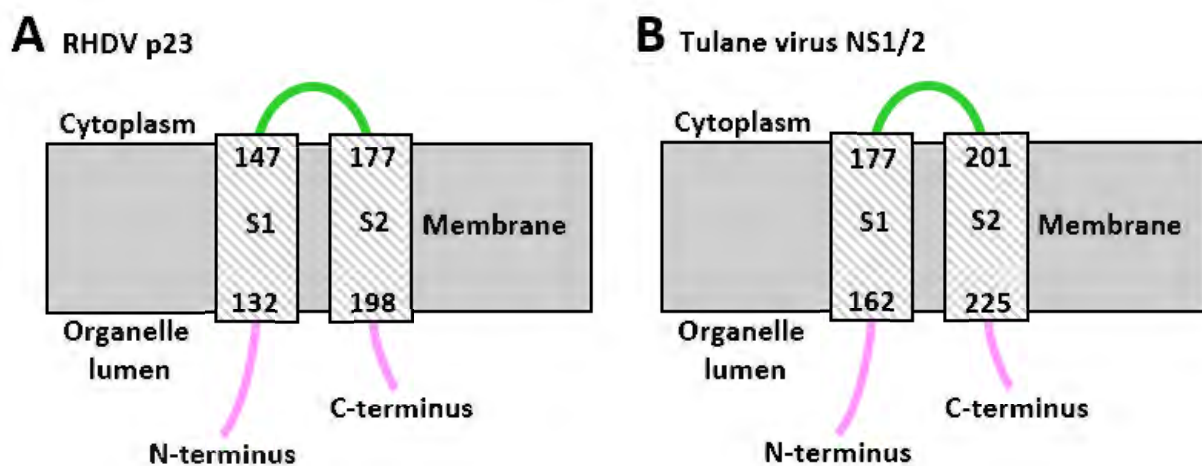
Figure 7. Protein secondary structure prediction using PSIPRED. Secondary structure prediction for the protein sequence of (**A**) RHDV p23 and (**B**) Tulane virus NS1/2. The sequences were submitted to PSIPRED server (http://bioinf.cs.ucl.ac.uk/psipred/; Buchan & Jones, 2019). Two amphipathic membrane-spanning helices are located at the C-terminus of both proteins.

Of note, my experiments were performed using rabbit kidney (RK-13) cells that were transiently transfected with FLAG-tagged p23. Transient protein expression served as the main tool in this work because there is no cell culture available yet that supports lagovirus replication. To investigate events that occur during a genuine viral replication, I used liver samples from virus-infected rabbits. These samples were stored in a freezer and were originally prepared for a different study (Neave et al., 2018) and re-used in this work. To identify global transcriptome

and proteome changes in RHDV2-infected animals, infected liver samples were compared to healthy rabbit liver samples. One of the altered pathways in infected cells was the regulation of the calcium transmembrane transport (**Figure 8**) (Smertina et al., 2022). These data further support the hypothesis that lagovirus p23 is a viroporin similar to the Tulane virus NS1/2. The results of this work are presented in chapters 3 and 4.
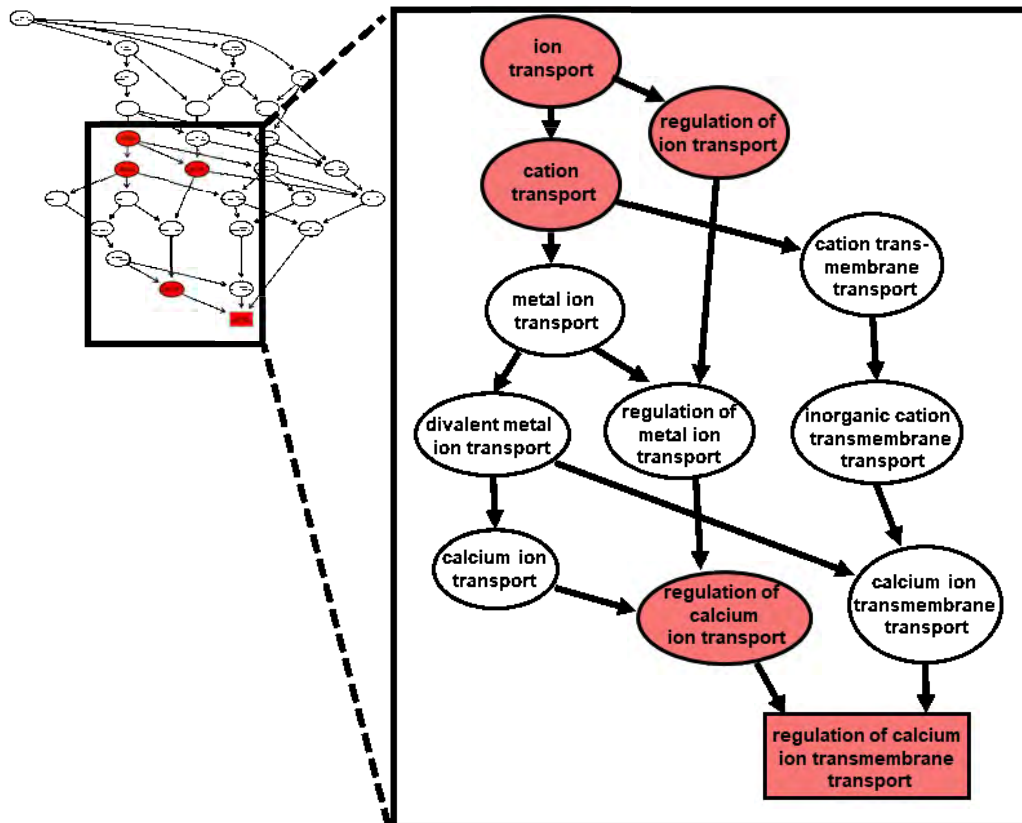
Figure 8. Pathway network analysis of differentially expressed genes in RHDV-infected liver samples. Regulation of calcium transmembrane transport is altered in infected liver cells. The colour indicates statistical significance with red indicating higher significance. The analysis was performed using R package TopGO (Alexa & Rahnenfuhrer, 2020).

Advances in cell culture system development for lagoviruses

Some caliciviruses can be grown in a cell culture, e.g., viruses of the genus *Recovirus* (*Tulane virus*), genus *Vesivirus* including FCV and *Rabbit vesivirus* (RaV). Some noroviruses can also be cultured and are therefore well-studied, e.g., MNV. MNV is an important model virus for studying human noroviruses, pathogens of the gastrointestinal tract and the leading cause of gastroenteritis worldwide (Parra et al., 2017).

In 2006, Liu et al reported the construction of an infectious RHDV clone (G. Liu et al., 2006). In this work, a cDNA clone was transcribed *in vitro* and transfected into RK-13 cells. The authors reported that this resulted in virus recovery and replication (G. Liu et al., 2006). However, the described construct had not been shared with other researchers and no other laboratory was able to reproduce this result. Therefore, unfortunately, for the majority of lagovirus researchers, these viruses remain uncultivable.

Recent breakthroughs towards culturing of human noroviruses in the laboratory made it possible to study this virus in more detail. Human norovirus replication has been achieved in a continuous human B cell line, in zebrafish larvae and in human enteroids (Ettayebi et al., 2016; M. K. Jones et al., 2014; van Dycke et al., 2019). However, these systems are not yet fully robust and require further optimisation. In our laboratory, a successful culture system for rabbit intestinal organoids derived from rabbit intestines was established (Kardia et al., 2021). Rabbit intestinal organoids were generated with the aim of cultivating of enterotropic RCV/GI.4 viruses. However, virus replication has not been detected in this system and, therefore, the next aim was set to create rabbit liver-derived organoids suitable for RHDV/GI.1/GI.2 infection. The results of this ongoing work are presented in the appendix.

Aims and objectives

Aims

- Characterisation of the RHDV RdRp

  The motif was described and named 'motif I'. This aim is addressed in chapter 2.

- Determine the functions of RHDV non-structural proteins

  Initially, I aimed to identify functions for all three proteins with unknown functions: p16, p23 and p29. Evidence has been accumulating that protein p23 is a viroporin and hence this protein received more focus in this work. This aim is addressed in chapters 3-5.

- Develop and optimise a culture system (organoids) for lagoviruses

  This work was done as a collaboration and the relevant publications can be found in the appendix.

Objectives

- Establish an immunoprecipitation assay to identify interaction partners of RHDV non-structural proteins

  For this objective, I used stable isotope labelling of amino acids in cell culture (SILAC) proteomics approach coupled with immunoprecipitations to quantitatively identify cellular interactors of viral proteins.

- Develop protocols for the expression and purification of non-structural proteins in bacteria

  For this objective, I used various E. coli strains and different expression conditions.

- Identify the precise subcellular localisation of p23

  Confocal microscopy and quantitative colocalisation analysis were used to precisely identify the subcellular localisation of p23.

- Characterise the gene expression in infected rabbit liver samples

  Label-free protein quantification was used to characterise the changes at the proteome level and RNA sequencing data was used to characterise the changes at the transcriptome level.

- Understand the *modus operandi* of p23 oligomerisation

  For this objective, I used site-directed mutagenesis to reveal which amino acid residue is responsible for p23 oligomerisation.

List of constructs and critical reagents

Reagent/consumable	Code	Manufacturer
Proteomics		
MEM SILAC	88368	Thermo Fisher Scientific
FBS, dialysed	30067334	Thermo Fisher Scientific
Heavy lysine, K8, $^{13}C_6$ $^{15}N_2$	608041	Sigma Aldrich
Heavy arginine, R10, $^{13}C_6$ $^{15}N_4$	608033	Sigma Aldrich
Light L-lysine	L5501	Sigma Aldrich
Light L-arginine	A5006	Sigma Aldrich
ANTI-FLAG® M2 Affinity Gel	A2220	Sigma Aldrich
Iodoacetamide	A3221	Sigma Aldrich
S-trap sample prep columns	C02-micro-40	Protifi
TEAB	T7408	Sigma Aldrich
Sequencing grade modified trypsin	V5113	Promega
NP-40 Surfact-Amps™ Detergent Solution	85124	Thermo Fisher Scientific
Rabbit kidney (RK-13) cells	00021715	Sigma Aldrich, European Collection of Cell Cultures
Benzonase nuclease, ultrapure grade	E8263-5KU	Sigma Aldrich
COMPLETE(TM), MINI protease inhibitor cocktail	4693124001	Sigma Aldrich
Lipofectamine 3000	L3000015	Thermo Fisher Scientific
Western blotting		
Nitrocellulose membrane 0.45 um, Nitrobind		MSI
SIGMAFAST™ 3,3′-Diaminobenzidine tablets	D4293	Sigma Aldrich
TRUPAGE(TM) precast gels, 4-20%, 10 x 8 cm	PCG2012-10EA	Sigma Aldrich
CAPS	C2632	Sigma Aldrich
Rat a-FLAG antibodies Novus DYKDDDDK Epitope Tag Antibody	NOVNBP106712SS	In vitro technologies

Mouse monoclonal a-β-actin	ab8226	Abcam
Rabbit monoclonal anti-Hsp70	ab45133	Abcam
Goat anti-mouse IgG HRP	170-6516	Bio-Rad
Goat anti-rat IgG HRP	3050-05	Cambridge Bioscience
Cloning and _E. coli_ strains		
Q5® Site-Directed Mutagenesis Kit	E0554	New England BioLabs
pCMV-Tag2C cloning vector		Agilent Technologies
pet28a cloning vector		Provided by Michelle Williams
E. coli TOP10 chemically competent	Prepared in house	
BL21DE3 _E. coli_ chemically competent		Provided by Michelle Williams
One Shot™ BL21(DE3) pLysE Chemically Competent _E. coli_	C656503	Thermo Fisher Scientific
Single-use BL21(DE3) pLysS	L1195	Promega
Flow cytometry		
Fluo-4 AM, cell permeant	F14201	Thermo Fisher Scientific
DMSO anhydrous	276855	Thermo Fisher Scientific
DPBS	14190136	Thermo Fisher Scientific
Ionomycin	I0634	Sigma Aldrich
Immunofluorescence		
Rabbit polyclonal anti-calnexin	ab75801	Abcam
Rabbit polyclonal anti-α-tubulin	PA5-19489	Thermo Fisher Scientific
Secondary goat anti-rabbit Alexa Fluor 488	ab150077	Abcam
Secondary goat anti-rat Alexa Fluor 555	3050-05	Cambridge Bioscience
Nunc Lab-Tek II Chamber Slide system	154453	Thermo Fisher Scientific
Fluoroshield	F4680	Sigma Aldrich
4',6-diamidino-2-phenylindole (DAPI)	D9542	Sigma Aldrich

Construct	Insertion	Vector	Selection in bacteria	Primers for cloning (5'->3')	Restriction sites
FLAG:p29 RHDV1	p29	pCMVTag2C	Kanamycin	F: ATATAGAATTCTTATGGGTGCCAACAAATTTAACTTTG R: ATATACTCGAGCTACTGAAAAGCTTTCGTTGCAACTG	*Eco*RI (5')-*Xho*I (3')
FLAG:GFP	GFP	pCMVTag2C	Kanamycin	F: ATATAGGATCCTTATGGTGAGCAAGG R: ATATAAAGCTTCTACTACTTGTACAGCTCGTC	*Bam*HI (5')-*Hind*III (3')
FLAG:RdRp RHDV1	RdRp	pCMVTag2C	Kanamycin	F: ATATAGAATTCTTATGACGTCAAACTTCTTCTGTGG R: ATATAGTCGACCTACTCCATAACATTCACAAATTC	*Eco*RI (5')-*Sal*I (3')
FLAG:VPg RHDV1	VPg	pCMVTag2C	Kanamycin	F: ATATAGGATCCAAGGCGTGAAAGGCAAGACAAAAC R: ATATAAAGCTTTTACTCATAGTCATTGTCATAAAAGCCACC	*Bam*HI (5')-*Hind*III (3')
Helicase RHDV2 in pCMVTag2C	Helicase	pCMVTag2C	Kanamycin	F: ATATAAAGCTTTTGACACTGTCCCCACGGG R: ATATAGTCGACTTACTCAAAAGAGGCTACATCAGG	*Hind*III (5')-*Sal*I (3')
RHDV1 3CD in pCMVTag2C	3CD	pCMVTag2C	Kanamycin	F: ATATAGGATCCAAGGTTTACCTGGGTTCATG R: ATATACTCGAGCTACTCCATAACATTCACAAATTC	*Bam*HI (5')-*Xho*I (3')
p16 into pET28a (codon optimised)	p16	pET28a	Kanamycin	F: ATATACCATGGGCTTAACAGG R: TATATCTCGAGTTCGAAGATCG	*Nco*I (5')-*Xho*I (3')
p23 into pET28a (codon optimised)	p23	pET28a	Kanamycin	F: ATATACCATGGGCGGAGAAG R: TATATCTCGAGCTCGAAGGTGTC	*Nco*I (5')-*Xho*I (3')
p29 into pET28a (codon optimised)	p29	pET28a	Kanamycin	F: ATATACCATGGGCGGAGC R: TATATCTCGAGCTGGAAGGC	*Nco*I (5')-*Xho*I (3')
VPD domain deletion in FLAG:p23	VPD deletion	pCMVTag2C	Kanamycin	F: ATCGATACCGTCGACCTCGAG R: TCAGTCCACGGCAATGACGTTGTG	Q5 PCR mutagenesis

FLAG:p23 insertion of a missing stop codon	Stop codon	pCMVTag2C	Kanamycin	F: ACATTTGAGTAAGCTTATCGATAC R: GTCAAACAGCCTCTTG	Q5 PCR mutagenesis
FLAG:p23 Cys451Ser	Substitution	pCMVTag2C	Kanamycin	F: AAGGTGGTCAGTGCAACGGAC R: GTCCCAGAAACTCTTCACACC	Q5 PCR mutagenesis
FLAG:p23 Cys456Ser	Substitution	pCMVTag2C	Kanamycin	F: ACGGACCGCAGTTTTGACTTGC R: TGCACAGACCACCTTGTCC	Q5 PCR mutagenesis
FLAG:p23 Cys41Ser	Substitution	pCMVTag2C	Kanamycin	F: GACGAACCCAGTTTGACATCA R: AACATCAACAAACTTGTCCATC	Q5 PCR mutagenesis
FLAG:TV_NS1/2	Tulane virus NS1/2	pCMVTag2C	Kanamycin	F (M13): GTAAAACGACGGCCAGT R (M13): GTCATAGCTGTTTCCTG Amplified from Twist plasmid, digested and ligated into pCMVTag2C	*Bam*HI (5')-*Hind*III (3') From Twist synthetised plasmid
mCherry into FLAG:p23	Gibson assembly insert mCherry	pCMVTag2C	Kanamycin	Vector: F: TGTACAAGATGGGGGAGGTTGACG R: TCACCATGGGCTTCTTATCGTCGTCATC Fragment: F: AAGAAGCCCATGGTGAGCAAGGGC R: TCCCCCATCTTGTACAGCTCGTCCATG	

Chapter 2. Calicivirus RNA-dependent RNA polymerases: evolution, structure, protein dynamics, and function

For use in theses which include co-authored publications. This declaration must be completed for each co-authored publication and to be placed at the start of the thesis chapter in which the publication appears, or as a preface to the thesis.

Declaration for Thesis Chapter 2

DECLARATION BY CANDIDATE

Declaration for the following publication: Calicivirus RNA-Dependent RNA Polymerases: Evolution, Structure, Protein Dynamics, and Function. Front. Microbiol., 6 June 2019 | https://doi.org/10.3389/fmicb.2019.01280

Nature of Contribution	Extent of Contributions (%)
Conducted the literature search, wrote the first draft, revised as per reviewers' suggestions	70%

The following co-authors contributed to the work:

Name	Nature of Contribution	Contributor is also a UC student (Yes/No)
Nadya Urakova	Contributed to literature search and provided suggestions; some of the findings from Nadya's PhD thesis were used in this review	No
Tanja Strive	Supervisor: developed the idea and plan of the review; revised the review	No
Michael Frese	Supervisor; provided help with the structure of the review; revised the review	No

_____
Candidate's Signature   Date   21/04/2022

DECLARATION BY CO-AUTHORS

The undersigned hereby certify that:

(1) the above declaration correctly reflects the nature and extent of the candidate's contribution to this work, and the nature of the contribution of each of the co-authors;

(2) they meet the criteria for authorship in that they have participated in the conception, execution, or interpretation, of at least that part of the publication in their field of expertise;

(3) they take public responsibility for their part of the publication, except for the responsible author who accepts overall responsibility for the publication;

(4) there are no other authors of the publication according to these criteria;

(5) potential conflicts of interest have been disclosed to (a) granting bodies, (b) the editor or publisher of journals or other publications, and (c) the head of the responsible academic unit; and

(6) the original data are stored at the following location(s) and will be held for at least five years from the date indicated below:

[Please note that the location(s) must be institutional in nature, and should be indicated here as a department, centre or institute, with specific campus identification where relevant.]

Location(s):	CSIRO Black Mountain, University of Canberra

Signatures	Date
	20/04/2022
Nadya Urakova	20/04/2022
(Michael Frese)	20-04-2022

1 of 1

Calicivirus RNA-Dependent RNA Polymerases: Evolution, Structure, Protein Dynamics, and Function

Elena Smertina[1,2], Nadya Urakova[3], Tanja Strive,[1,4] and Michael Frese[2]*

[1] Commonwealth Scientific and Industrial Research Organisation, Health and Biosecurity, Canberra, ACT, Australia

[2] Faculty of Science and Technology, University of Canberra, Canberra, ACT, Australia

[3] Department of Entomology, The Pennsylvania State University, PA, USA

[4] Invasive Animals Cooperative Research Centre, University of Canberra, Canberra, ACT, Australia

* Correspondence:
Michael Frese
michael.frese@canberra.edu.au

Abstract

The *Caliciviridae* are viruses with a positive-sense, single-stranded RNA genome that is packaged into an icosahedral, environmentally stable protein capsid. The family contains five genera (*Norovirus*, *Nebovirus, Sapovirus*, *Lagovirus*, and *Vesivirus*) that infect vertebrates including amphibians, reptiles, birds, and mammals. The RNA-dependent RNA polymerase (RdRp) replicates the genome of RNA viruses and can speed up evolution due to its error-prone nature. Studying calicivirus RdRps in the context of genuine virus replication is often hampered by a lack of suitable model systems. Enteric caliciviruses and RHDV in particular are notoriously difficult to propagate in cell culture; therefore, molecular studies of replication mechanisms are challenging. Nevertheless, research on recombinant proteins has revealed several unexpected characteristics of calicivirus RdRps. For example, the RdRp of RHDV and related lagoviruses possesses the ability to expose a hydrophobic motif, to rearrange Golgi membranes, and to copy RNA at unusually high temperatures. This review is focused on the structural dynamics, biochemical properties, kinetics, and putative interaction partners of these RdRps. In addition, we discuss the possible existence of a conserved but as yet undescribed structural element that is shared amongst the RdRps of all caliciviruses.

Introduction

The *Caliciviridae* family currently consists of five genera (*Norovirus*, *Nebovirus, Sapovirus*, *Lagovirus*, and *Vesivirus*) (**Figure 1**). The establishment of three additional genera (i.e., *Recovirus*, *Valovirus*, and *Balovirus*) has been proposed (Farkas et al., 2008; L'Homme et al., 2009; Wang et al., 2017). The exponential increase in metagenomic sequence data is likely to reveal an even higher degree of diversity for this virus family. Not surprisingly, many of the currently known caliciviruses are highly pathogenic (a characteristic that usually leads to discovery), but research using metagenomics is likely to discover more non-pathogenic family members (Mahar et al., 2018). Viruses from the genera *Norovirus* and *Sapovirus* are a common cause of gastroenteritis in humans and animals. For example, *Norwalk virus* and other human noroviruses are responsible for almost half of all gastroenteritis cases globally (Atmar and Estes, 2006). These viruses are easily transmitted either directly from person to person or through contaminated food and water. Infections are especially dangerous for elderly, young, and immunocompromised individuals such as transplant recipients (Schwartz et al., 2011). Despite the high socioeconomic costs associated with human norovirus outbreaks, no approved vaccines or small molecule inhibitors are currently available to prevent or cure infections. Viruses from the genus *Vesivirus*, such as *Feline calicivirus* (FCV) and *Vesicular exanthema of swine virus* (VESV), are highly contagious in animals and can cause persistent infection. FCV causes fever and acute upper respiratory tract and oral cavity disease in all feline species and can lead to a virulent systemic disorder (Hurley and Sykes, 2003). VESV affects pigs and marine mammals, causing fever and epithelial lesions around the mouth, nostrils, and on the feet (Neill et al., 1995). The genus *Lagovirus* comprises only viruses that infect lagomorphs, especially rabbits and hares. Pathogenicity among lagoviruses can differ dramatically. The *Rabbit haemorrhagic disease virus* (RHDV) causes acute necrotizing hepatitis and disseminated intravascular coagulation in European rabbits (*Oryctolagus cuniculus*), which leads to death 48−72 hours post-infection, while the *Rabbit calicivirus* (RCV) causes only mild disease manifestations (Abrantes et al., 2012). Since the mid-1990s, RHDV has been used to control rabbit populations in Australia and New Zealand following the introduction of the European rabbit in the late 1800s (Cooke, 2002; Cooke and Fenner, 2002). Even though RHDV is an important biocontrol agent, it has not yet been studied in great detail; many aspects of viral replication and the function of several proteins remain unknown.
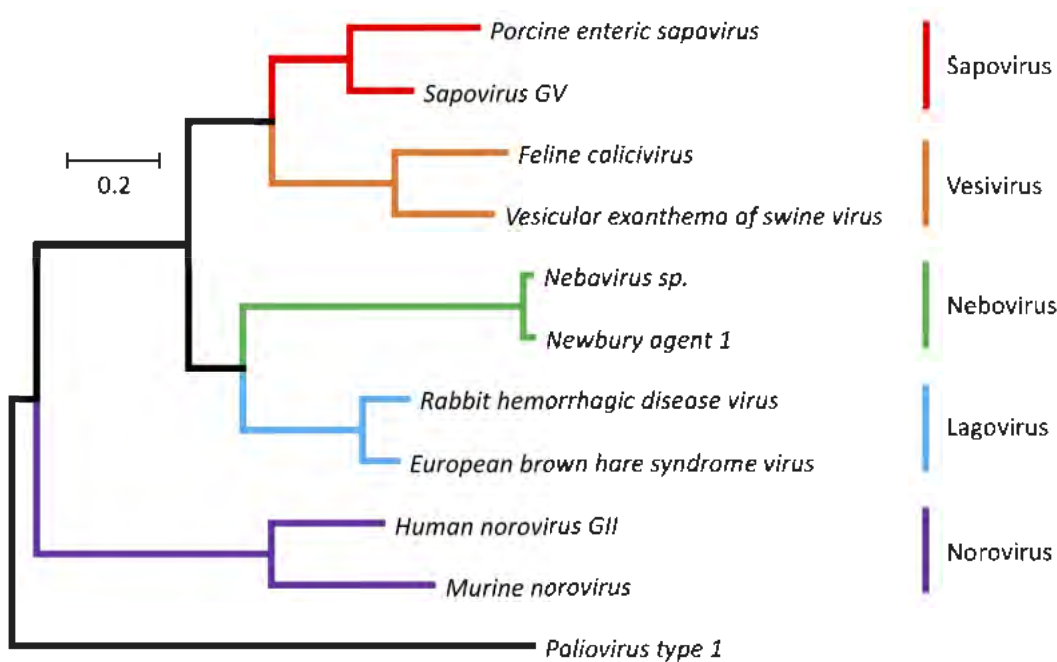
Figure 1. Phylogenetic tree for RdRp protein sequences of the family *Caliciviridae* and *Poliovirus type 1* (Mahoney strain). The evolutionary history was inferred using the Maximum Likelihood method (Jones et al., 1992). The tree is drawn to scale, with branch lengths representing the number of substitutions per site. The analysis involved amino acid sequences from 11 caliciviruses (*Porcine enteric sapovirus*, A0A348BR93 (UniProt); *Sapovirus GV*, NP783310 (NCBI Protein); *Feline calicivirus*, NP786896 (NCBI Protein); *Vesicular exanthema of swine virus*, AYN44917 (NCBI Protein); *Nebovirus sp.*, YP529897 (NCBI Protein); *Newbury agent 1*, NP740332 (NCBI Protein); *Rabbit haemorrhagic disease virus*, NP786902 (NCBI Protein); *European brown hare syndrome virus*, D0UGI3 (UniProt); *Human norovirus GII*, AWB14625 (NCBI Protein); *Murine norovirus*, P03300 (UniProt)) and a poliovirus (*Poliovirus type 1*, Q6IX02 (UniProt)). Evolutionary analyses were conducted using the MEGA7 program package (Kumar et al., 2016). Different colors are used for different calicivirus genera.

Viruses of the *Caliciviridae* family share a number of features. The genome consists of positive-sense, single-stranded RNAs that contain coding sequences in two or more partially overlapping open reading frames (ORFs). The coding sequences are flanked by untranslated regions (UTRs) at both the 5' and 3' ends. Genomic RNAs are covalently linked at the 5' end to a viral protein (VPg, for "virion protein, genome-linked") and are polyadenylated at the 3' end. Calicivirus particles contain two types of RNA, a genomic (full-length) RNA of about 7.5 kb and one or more copies of a subgenomic RNA of about 2 kb (Ehresmann and Schaffer, 1977; Meyers et al., 1991a, 1991b). The number of ORFs varies from two to four in full-length

genomic RNAs and from two to three in subgenomic RNAs (McFadden et al., 2011; Wirblich et al., 1996) (**Figure 2**). ORF1 is always the largest of the reading frames and encodes a polyprotein that is subsequently cleaved into five non-structural proteins and VPg (genus *Norovirus* and *Vesivirus*) or five non-structural proteins, VPg and the major capsid protein VP1 (genus *Lagovirus*, *Nebovirus*, and *Sapovirus*) (Martín Alonso et al., 1996; Meyers et al., 2000). The second and third ORFs in the genomic RNA of noroviruses encode the structural proteins VP1 and VP2, respectively. In vesiviruses, ORF2 encodes the VP1 precursor protein that is subsequently cleaved into a mature VP1 and a small leader peptide (leader of the capsid protein, LC). The LC protein of FCV is cytopathic and promotes virus spread (Abente et al., 2013). The subgenomic RNAs of all genera are very similar to each other; they contain the 5' UTR and the VP1 and VP2 coding sequences (Boga et al., 1992; Meyers et al., 1991a, 1991b, 2000). In *Murine norovirus* (MNV), there is an additional ORF in the VP1 coding region of both genomic and subgenomic RNAs that encodes the viral factor 1 (VF1), an antagonist of the innate antiviral immune response (McFadden et al., 2011).
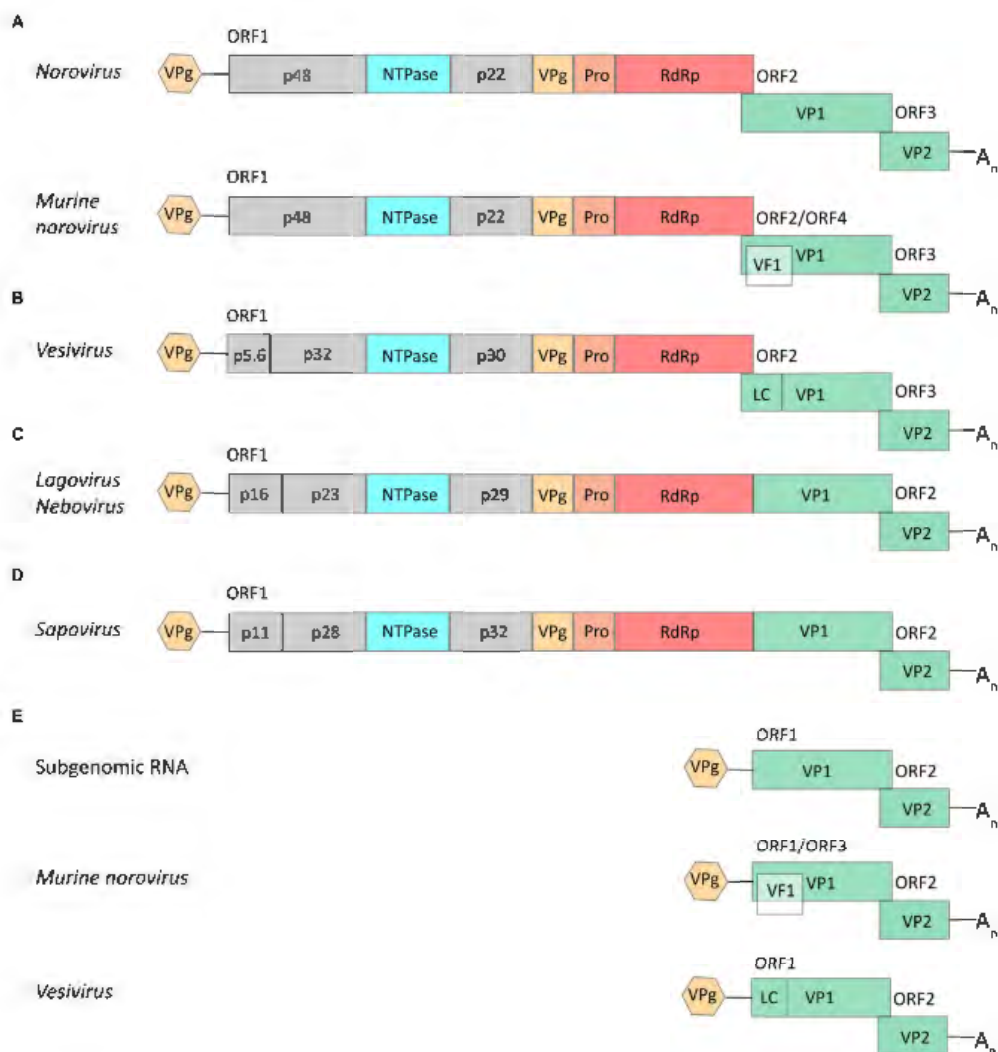
Figure 2. Schematic representations of typical calicivirus genome organizations. (**A**–**D**) Genomic full-length RNAs of about 7.5 kb in size contain either two ORFs (in viruses of the genera *Lagovirus*, *Nebovirus*, and *Sapovirus*) or three ORFs (*Norovirus* and *Vesivirus*), except for the genomic RNA of *Murine norovirus* (MNV; genus *Norovirus*) that may contain an additional ORF (encoding the VF1 protein). (**E**) All caliciviruses except MNV and vesiviruses have subgenomic RNAs of about 2.1 kb in size with two ORFs that encode the main structural proteins, VP1 and VP2; the subgenomic RNA of MNV includes three ORFs (similar to the corresponding genomic RNA) and the subgenomic RNA of vesiviruses encodes—apart from proteins VP1 and VP2—a small leader of the capsid protein (LC). Colored boxes represent coding sequences that are flanked by untranslated leader and trailer sequences (shown as lines). Hexagons represent VPg proteins that are covalently bound to the 5' end of all genomic and subgenomic RNAs; A_n represents the poly(A) tail at the 3' end of all genomic and subgenomic RNAs.

The structural protein VP1 forms an icosahedral, non-enveloped capsid of about 25–40 nm in diameter (Parra and Prieto, 1990; Prasad et al., 1994, 1999). A typical calicivirus capsid contains 90 VP1 dimers. Protruding VP1 (VP60 in RHDV) domains create a surface topography that resembles cup-shaped depressions when viewed using electron microscopy, which inspired the name "calicivirus" (Latin "*calyx*" = cup). The basic VP2 protein has also been found associated with virus particles (although in much smaller numbers) and plays a role in RNA replication and the maturation of infectious virus particles (Sosnovtsev et al., 2005). In addition, recent studies of FCV suggest a role for VP2 in the formation of a portal-like structure facilitating the delivery of viral RNA into the cytoplasm in the early stages of infection (Conley et al., 2019).

The VPg protein is also found in virus particles and should therefore be categorized as a structural protein, since the components of a mature virus particle are defined as structural proteins. The VPg is covalently linked to the 5' end of both the full-length genomic and subgenomic RNAs (Black et al., 1978; Burroughs J. N., 1978; Meyers et al., 1991a). Mass-spectrometry-based assays showed that both FCV and MNV VPg proteins are linked to a guanosine diphosphate moiety via tyrosine residues, which is consistent with the presence of a highly conserved 5' guanosine nucleotide in the genome of all caliciviruses (Olspert et al., 2016). The association between VPg and RNA was recognized for the first time when, following phenol extraction, a significant amount of caliciviral RNA was found in the interphase, along with other viral and cellular proteins. However, when the samples were treated

with protease K prior to the extraction, the viral RNA was found in the aqueous phase. Furthermore, when purified RHDV RNA was labelled with ^{125}I, autoradiography revealed two protein bands corresponding to genomic and subgenomic RNAs. The subsequent treatment of the labelled RNAs with RNase produced a single band of about 15 kDa on SDS-PAGE (sodium dodecyl sulfate-polyacrylamide gel electrophoresis) (Meyers et al., 1991a). The VPg protein also plays a critical role in RNA replication. Following nucleotidylation by the RNA-dependent RNA polymerase (RdRp) or an RdRp precursor, VPg can act as a primer for genome replication (Belliot et al., 2008; Goodfellow, 2011).

The non-structural proteins can be categorized into those with known functions (NTPase, 3C-like protease, and RdRp) and unknown functions (all remaining proteins). The first one or two N-terminal proteins of the full-length genomic RNA (e.g. p16, p23, and p29 in lagoviruses, or p48 and p22 in noroviruses) may have functions similar to the so-called "security proteins" of the *Picornaviridae* family that counteract host defense mechanisms (Agol and Gmyl, 2010). This hypothesis is based on the fact that the coding sequence for the calicivirus proteins and the picornavirus security proteins have a similar position in the genome of the respective viruses. Although the calicivirus proteins do not share detectable sequence homologies with their picornavirus counterparts, accumulating data from functional studies suggest that these proteins do indeed impede immune responses, e.g. those that depend on cellular secretory pathways. The Norwalk virus protein p48 (when expressed as a recombinant protein in transfected cells) induces Golgi membrane rearrangements (Fernandez-Vega et al., 2004). The p48 protein of both MNV and human noroviruses interacts with the vesicle-associated membrane protein-associated protein A (VAP-A). VAP-A is a soluble N-ethylmaleimide-sensitive factor attachment protein receptor (SNARE)-regulator and is involved in vesicle transport (Ettayebi and Hardy, 2003; Weir et al., 1998). This interaction is likely to disrupt intracellular protein trafficking, as cells that express p48 were unable to expose the vesicular stomatitis G glycoprotein on the cell surface (Ettayebi and Hardy, 2003). Moreover, strand-specific quantitative PCR revealed a delayed accumulation of positive and negative strand MNV RNAs in VAP-A deficient cells (McCune et al., 2017). The p22 protein of Norwalk virus also contributes to Golgi disaggregation and blocks trafficking of vesicles from the ER to the Golgi (Sharp et al., 2010). However, the corresponding proteins in other calicivirus genera have not yet been functionally characterized and, to date, no conserved motifs have been identified that would suggest particular functions. Therefore, their exact role in virus replication and/or pathogenesis remains unknown.

The functions of the remaining non-structural proteins were deduced by comparing calicivirus and picornavirus sequences and by searching for conserved motifs. A 2C-like helicase (named NTPase in **Figure 2**) was identified after the detection of a nucleotide-binding site that is typical for viral proteins (Neill, 1990). Later, this enzyme was shown to be associated with the replication complex and to destabilize double-stranded RNA in an NTP-independent manner, representing an unexpected RNA chaperone-like activity (Han et al., 2018; Li et al., 2017). Thereafter, the p58 cleavage product of the RHDV polyprotein was found to resemble the 3D polymerase of poliovirus, and its role in RNA replication was subsequently confirmed using functional assays (Vazquez et al., 1998; Wirblich et al., 1996). Similarly, the sequence preceding the RdRp gene was suggested to code for a 3C-like protease (Jiang et al., 1993; Neill, 1990). Similar to the picornavirus proteases, the calicivirus homologs are responsible for the processing of the polyprotein (on a par with cellular proteases) and for the formation and accumulation of a 3CD-like polymerase precursor (Sosnovtseva et al., 1999; Thumfart and Meyers, 2002; Oka et al., 2005).

Table 1. Polymerase crystal structures and amino acid sequence information for representative members of the *Caliciviridae* family

Genus	Species	PDB code	UniProt entry	Reference
Norovirus	*Norwalk virus*	1SH0	Q83883	Ng et al., 2004
	Murine norovirus (MNV)	3NAH	Q80J95	Lee et al., 2011
Vesivirus	*Feline calicivirus* (FCV)	No data	Q66914	
	Vesicular exanthema of swine virus (VESV)	No data	Q9DUN3	
Sapovirus	*Sapporo virus*	2CKW	Q69014	Fullerton et al., 2007
Lagovirus	*Rabbit haemorrhagic disease virus* (RHDV)	1KHW	P27411	Ng et al., 2002
	Rabbit calicivirus (RCV)	No data	A0A1B2RX11	

RdRps are the key proteins responsible for viral replication. In all caliciviruses, the RdRp coding sequence follows that of the viral protease at the 3'end of ORF1. Mature RdRps

are proteins of about 60 kDa (75 kDa in the precursor form). Remarkably, the calicivirus RdRp precursor protein is also an active polymerase enzyme (Wei et al., 2001). RdRps are usually among the best-characterized proteins of any given virus species; RdRps from several caliciviruses have been crystallized and studied (**Table 1**).

Features common to all calicivirus RdRps

The shape of all RdRps resembles a right hand with fingers, palm, thumb, and an N-terminal domain that links the finger and thumb domains (**Figure 3A, B**). The active site of the enzyme is located in the palm domain and its architecture is highly conserved. So far, seven highly conserved amino acid sequence motifs have been identified: four motifs in the palm domain (motifs A, B, C, and D), one motif in the thumb domain (motif E), and two motifs in the fingers domains (motifs F and G) (**Figure 3A, D**) (Koonin, 1991; Poch et al., 1989). Whereas these short functional motifs have highly conserved amino acid sequences, the so-called homomorphs encompassing these motifs (except for the newly discovered homomorph H (Černý et al., 2014)) represent protein regions with a conserved structure but no recognizable consensus sequence (Lang et al., 2013) (**Figure 3C**).
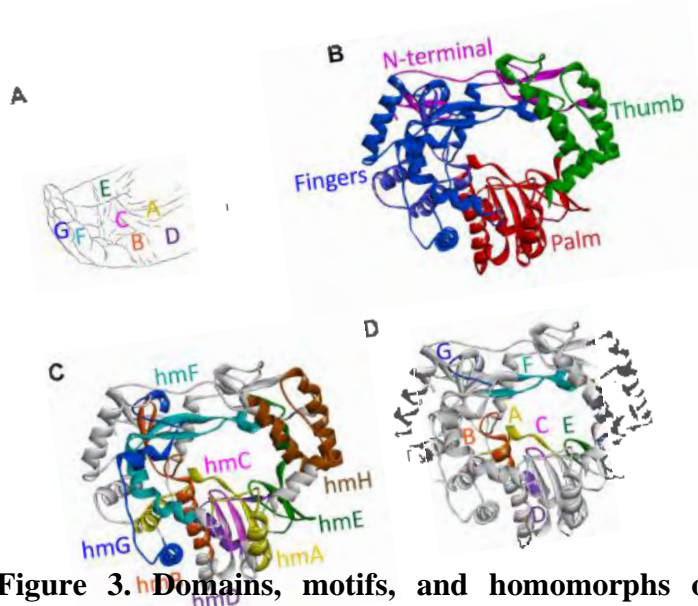
Figure 3. Domains, motifs, and homomorphs of a typical calicivirus RdRp. (**A**) Representation of a slightly cupped right hand resembling an RdRp with the position of motifs A to G on fingers, palm, and thumb. (**B**–**D**) Ribbon diagrams of the RHDV RdRp (PDB ID: 1KHW); (**B**) fingers, palm, and thumb domains colored blue, red, and green, respectively, and the N-terminal domain colored magenta; (**C**) structurally conserved homomorphs (hmA to hmH); and (**D**) functional motifs A to G (the positions of homomorphs and corresponding motifs are indicated by the same color). Ribbon diagrams were generated using Discovery

Studio (Dassault Systèmes BIOVIA, Discovery Studio Visualizer v17.2.0, San Diego: Dassault Systèmes, 2016).

Individual motifs cooperate to perform highly specialized functions. Motifs B, D, E, and F are involved in nucleotide recognition and coordination, motifs B and G coordinate template and primer binding, and motifs A and C execute the catalysis of nucleotide binding (Choi, 2012; Ng et al., 2008) (**Table 2**). Motif A comprises two Asp residues separated by up to five amino acids, whereas motif C includes an Asp-Asp dipeptide, forming the highly conserved Gly-Asp-Asp motif (Poch et al., 1989). The Asp residues in motifs A and C coordinate two divalent metal ions that are essential for catalysis, typically Mg^{2+} or Mn^{2+}. Motif F contains the positively charged residues Arg and Lys that mediate interactions with the triphosphate moieties of incoming nucleoside triphosphates (NTPs) (Butcher et al., 2001; Gong and Peersen, 2010; Lang et al., 2013; Ng et al., 2008). Motif G is located in the template cleft and is involved in protein primer orientation during the initiation of RNA replication (Gorbalenya et al., 2002; Ng et al., 2002).

Table 2. Conserved motifs and their functions

Motif*	Residue numbers**	Function	References
G	123–134	Correct orientation of a template and a primer	Gorbalenya et al., 2002; Ng et al., 2002
F	173–191	Coordination of the triphosphate moiety of NTPs	Butcher et al., 2001; Gong and Peersen, 2010; Lang et al., 2013; Ng et al., 2008
A	250–259	M^{2+***} coordination, NTP binding, catalysis	Choi, 2012; Ng et al., 2008
B	308–318	Template and NTPs positioning, selection of NTPs over dNTPs	Ferrer-Orta et al., 2007; Gohara et al., 2000; Gong and Peersen, 2010
C	353–355	M^{2+} coordination, NTP binding, catalysis	Kamer and Argos, 1984
D	373–376	NTPs binding, active site closure, export of PP_i from the active site, fidelity determination	Castro et al., 2007, 2009; Yang et al., 2012
E	400–404	Formation of NTPs entry tunnel, template and nascent strand binding	Han et al., 2017; Jacobo-Molina et al., 1993; Poch et al., 1989

* Motifs are listed according to their position in the protein, starting with the motif closest to the amino-terminus (N-terminus).
** Amino acid positions refer to the RHDV RdRp (UniProt ID: P27411).
*** M = Metal.

The thumb domain of calicivirus and picornavirus RdRps is small compared with that of other RdRps and DNA-dependent DNA polymerases. The domain consists of only four helices and forms a relatively large, 15 Å-wide central cleft (also named a channel) that leads to the active site (Ferrer-Orta et al., 2004, 2006). This cleft accommodates both the template and a VPg-linked primer (Choi, 2012).

The main function of RdRps is to copy RNA. This process is based on transferring the α-phosphate moiety of a complementary nucleotide to the 3'-OH end of the nascent strand. This reaction depends on two divalent metal ions (usually Mn^{2+} or Mg^{2+}) in the active site. The metal ions are coordinated by the Asp residues of motifs A and C. One of the ions interacts with the 3'-OH group of the primer, which reduces the affinity of this group for the hydrogen and enables a nucleophilic attack of the negatively charged 3'-O⁻ on the α-phosphate residue of the incoming complementary nucleotide (Steitz, 1998). The second metal ion is involved in positioning the incoming NTP and the release of a pyrophosphate (PP_i). As a result of the nucleophilic attack, a new phosphoester bond between the 3'-OH terminal group of the protein-linked primer and the α-phosphate of nucleoside monophosphate (NMP) is created and PP_i is released (Joyce and Steitz, 1995; Steitz, 1998).

Structural and functional characteristics of norovirus and lagovirus RdRps

Noroviruses

The overall structure of norovirus RdRps is similar to that of other caliciviruses, but some differences exist. For example, the carboxyl terminus (C-terminus) of the protein is located within the active site cleft close to the two catalytic Asp residues (Ng et al., 2004) (**Figure 4A**). Therefore, the C-terminus is suitably positioned to take part in the initiation of RNA replication. This configuration is similar to that in the RdRps of the *Hepatitis C virus* (HCV) and the φ6 bacteriophage, in which C-terminal amino acids help to stabilize primers in the active site (Butcher et al., 2001; Laurila et al., 2002; Ranjith-Kumar et al., 2002). This C-terminal addition to the active site would not allow the entry of RNA in the form of a duplex with a long primer, but it does not prevent an interaction of the template with a short dinucleotide primer (Ng et al., 2004). RNA binding to the active site of the norovirus RdRp also causes the rotation of the main helix of the thumb domain (residues 435–449) by 22°, thus forming a suitable groove for a protein-linked primer (Zamyatkin et al., 2008). Sapovirus RdRps share many features with those of noroviruses, e.g. the C-terminus of the sapovirus RdRp is located within the active site cleft (Fullerton et al., 2007) (**Figure 4D**).
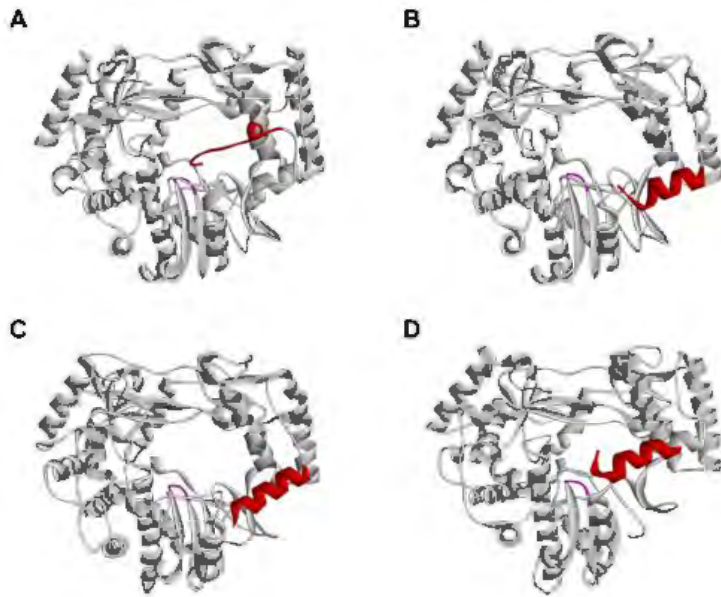
Figure 4. Position of the C-terminus in different calicivirus RdRps. (**A**) *Norwalk virus* (PDB ID: 1SH0); (**B**) MNV (PDB ID: 3NAH); (**C**) RHDV (PDB ID: 1KHW); (**D**) *Sapporo virus* (PDB ID: 1CKW) RdRps, presented as ribbon diagrams. C-terminal amino acids are colored red; the highly conserved motif C is colored magenta. Ribbon diagrams were generated using Discovery Studio (Dassault Systèmes BIOVIA, Discovery Studio Visualizer v17.2.0).

Lagoviruses

Several lines of evidence suggest that lagovirus RdRps exist as a 3CD-like precursor protein and a mature protein. Both the *in vitro* translation of viral RNA with a subsequent precipitation of the products using region-specific antisera, as well as the *in vivo* analysis of proteins present in RHDV-infected primary hepatocytes revealed a 72 kDa protein corresponding to an uncleaved 15 kDa 3C-protease and 58 kDa polymerase (König et al., 1998; Martín Alonso et al., 1996). Subsequent *in vitro* studies with recombinant proteins suggest that this 3CD-like precursor possesses both protease and polymerase activities and is able to uridylate VPg (Machín et al., 2009).

Many RNA viruses, including caliciviruses, recruit cellular membranes to protect and act as a scaffold for their RNA replication machinery (Green et al., 2002). A number of viral proteins recruit intracellular membranes (e.g., p48 of Norwalk virus) but polymerases are usually not involved. One of the most remarkable findings with lagovirus RdRps is their apparent ability to interact with intracellular membranes and to change the architecture of the Golgi apparatus. The expression of recombinant RHDV and RCV RdRps induced a striking

rearrangement of cis/medial and medial/trans Golgi membranes (Urakova et al., 2015, 2017a). However, all immunofluorescence studies on the intracellular localization of the recombinant lagovirus RdRps that have been conducted so far have failed to detect a colocalization of RdRps with Golgi (or other) intracellular membranes (Urakova et al., 2015, 2017a). Furthermore, the overexpression of recombinant proteins without viral replication may result in more RdRp proteins being available to change the localization of Golgi membranes (as compared to the situation in virus-infected cells). This may explain why barely detectable amounts of RdRps were observed to be sufficient to induce dramatic changes to the Golgi apparatus (Urakova et al., 2015, 2017b). The enzymatic activity of the RdRp is not required for the RdRp to disaggregate the Golgi apparatus, as active site (motif C) variants with Gly-Asp-Asp to Gly-Asn-Asp and Gly-Asp-Asp to Gly-Ala-Ala substitutions had the same effect on Golgi membranes as proteins with the wild type sequence (Urakova et al., 2017a). The observed Golgi membrane disruption is most likely a consequence of cellular membrane recruitment for the formation of a membranous vesicle network on which virus replication occurs, similar to the membrane recruitment in other caliciviruses and picornaviruses (Green et al., 2002; Schlegel et al., 1996). A hydrophobic motif (positions 189–210) that might be responsible for the interaction with Golgi membranes has been identified (Urakova et al., 2017b) (**Figure 5A**). This motif is located next to the F motif within the F homomorph (this newly identified hydrophobic motif should not be confused with the 'classic' conserved motifs A to G). Truncated RHDV RdRp variants without the hydrophobic motif showed a diffuse cytoplasmic localization when expressed in transiently transfected cells. None of these variants accumulated in the distinct cytoplasmic foci that are typical for the intracellular localization of the wild type RdRp (Urakova et al., 2017b). Furthermore, the hydrophobic motif is able to change the localization pattern of other proteins, as it has been demonstrated using the green fluorescent protein (Urakova et al., 2017b). A similar hydrophobic motif was observed in the RdRp of RCV, also in the F homomorph and in the same position as in the RHDV RdRp, but the motif does not exist, or is less obvious in more distantly related caliciviruses (Urakova et al., 2017b). The importance of the hydrophobic amino acids within the motif was demonstrated using variants in which individual Val residues were changed to Ser residues. A variant with two Val to Ser substitutions in the C-terminal part of the motif exhibited a diminished ability to rearrange Golgi membranes, and a variant with four such mutations completely lost this feature (Urakova et al., 2017b).

Research into the newly identified hydrophobic motif revealed an unexpected structural flexibility of calicivirus RdRps, as exposure of the partially buried hydrophobic motif requires

a series of conformational changes. Molecular dynamics simulations suggest that four regions surrounding the motif possess a high degree of mobility (loops 1–3 in **Figure 5B**). Two of these loops (loops 1 and 2) flank the 'point of access' to the motif, and the third loop covers the motif, much like a 'trap door'. The following sequence of movements is thought to bring the RdRp close to an intracellular membrane and allow exposure of the hydrophobic motif (Urakova et al., 2017b): firstly, three collinear, positively charged Lys residues at the edge of a solvent-exposed helix next to the loop 1 interact with the negatively charged surface of the membrane. Next, hydrophobic interactions, including those between the partially hydrophobic loop 2 and the membrane, draw the protein further towards the membrane to a point, at which hydrophobic loop 3 makes contact with the membrane, moves out of the way, and allows the hydrophobic motif to become exposed and to insert itself into the membrane.
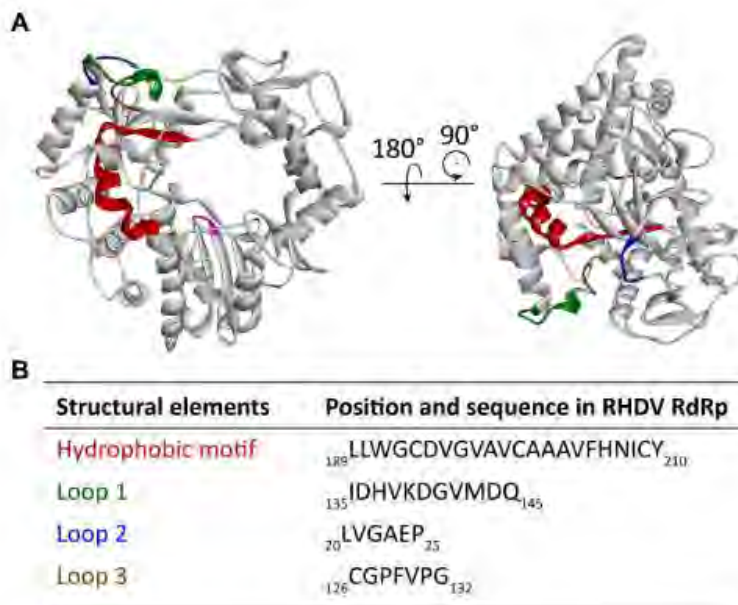
Figure 5. Localization of a partially buried hydrophobic membrane interaction motif in the RHDV RdRp. (**A**) Ribbon diagrams of RHDV RdRp (PDB ID: 1KHW). The hydrophobic motif is colored red, loop 1 green, hydrophobic loop 2 blue, and hydrophobic loop 3 brown. The active site (motif C) is highlighted magenta to provide a reference point for the position of the hydrophobic motif in the RdRp. (**B**) Amino acid positions and sequences of the structural elements highlighted in the diagrams above. Ribbon diagrams were generated using Discovery Studio (Dassault Systèmes BIOVIA, Discovery Studio Visualizer v17.2.0).

Genomic and subgenomic RNA replication

Detailed studies on calicivirus replication and pathogenicity often lag behind those in other RNA virus families. For decades, studies on human norovirus and other enteric caliciviruses have been hampered by the lack of a robust cell culture system. Of note, it has been reported that replication competent RHDV RNAs can be generated from plasmids using a T7 promotor and a hepatitis D virus ribozyme (Zhu et al., 2017), but these findings have not yet been independently reproduced. Very recently, however, ground-breaking progress was made in enteroid cultivation methods that show great potential for providing new cell culture systems for noroviruses and lagoviruses (Ettayebi et al., 2016; Jones et al., 2015). The new methods complement and supplant previously developed cell culture models for MNV that relied on bone marrow-derived murine macrophages and dendritic cells. These MNV cell cultures were used as surrogate models to study human norovirus (Wobus et al., 2004, 2006). However, there is still no general agreement on certain steps of the calicivirus replication process, such as the mechanism of the replication initiation.

Terminal transferase activity of RdRps

RdRps vary in their ability to add nucleotides to a nascent RNA strand. Terminal transferase activity is the ability to add nucleotides to the 3' end in a template independent manner. Similar to poliovirus (Arnold et al., 1999) and HCV RdRps (Ranjith-Kumar et al., 2001), human norovirus RdRps possess terminal transferase activity (Rohayem et al., 2006a). The activity is thought to serve as a repair system for 3' ends that were damaged by cellular exonucleases and, in some cases, it facilitates the initiation of RNA synthesis through the addition of non-templated nucleotides (Wu and Kaper, 1994). For example, the terminal adenylyl transferase activity of the poliovirus 3D polymerase restores the infectivity of poliovirus RNA genomes that lack a poly(A) tail (Neufeld et al., 1994). The terminal transferase activity of calicivirus RdRps generates not only a protective poly(A) tail but may also generate the poly(C) tail that has been suspected to play a critical role in the initiation of genomic and subgenomic RNA synthesis.

Initiation of RNA synthesis

In calicivirus replication, the initiation of RNA synthesis occurs differently for genomic and antigenomic RNAs (**Figure 6A, B**). The former may occur in a primer independent manner (Rohayem et al., 2006b), and the latter is generally thought to depend on a nucleotidylated VPg primer. However, according to Subba-Reddy and coworkers, the synthesis of negative sense

RNAs can be initiated *de novo* (Subba-Reddy et al., 2012). This article was later retracted (Subba-Reddy et al., 2017), although the authors maintain that the overall conclusion in the original article is still valid ("[…] that the norovirus major capsid protein could modulate norovirus RdRp activity has been confirmed in both the Kao and the Goodfellow labs"). Clearly, more research is warranted to better understand the initiation of norovirus RNA synthesis. Interestingly, the VPg of human noroviruses consists of 133 amino acids, which is substantially larger than the 22 amino acids of the homologous protein in picornaviruses. Nevertheless, the larger size does not prevent the norovirus VPg from serving as a protein primer. As shown by Rohayem and coworkers in a series of *in vitro* experiments, the norovirus RdRp is able to initiate synthesis on subgenomic RNA that is polyadenylated and carries a VPg protein in the absence of a short poly(U) RNA primer but in the presence of VPg, confirming the notion of a protein-primed initiation (Rohayem et al., 2006b). For anti-subgenomic RNA replication to occur, a protein primer is probably not required, as an RNA product is yielded in the absence of exogenous primers (Rohayem et al., 2006b). Interestingly, a poly(C) stretch was detected at the 3' terminus of newly produced anti-subgenomic norovirus RNA, which may have been the result of a terminal transferase activity of the norovirus RdRp (**Figure 6C**). Based on these observations, it was proposed that the initiation of subgenomic RNA synthesis occurs *de novo* on a short 3'-terminal poly(C) stretch of anti-subgenomic RNA, a scenario that is in line with the general observation that the *de novo* initiation on RNA genomes usually starts on pyrimidines (Kao et al., 2001; Rohayem et al., 2006b). However, other evidence suggests that the synthesis of positive sense genomic and subgenomic RNAs also depends on a VPg primer, since infectious (positive-sense) RNAs isolated from MNV-infected cells are linked to VPg (Chaudhry et al., 2006). Similar *in vitro* studies were performed using the 3'-terminal region of genomic norovirus RNA. In these studies, the norovirus RdRp was shown to initiate the synthesis of antigenomic RNA primer-independently (Fukushi et al., 2004). Moreover, a 3'-terminal region without the poly(A) sequence was replicated as effectively as RNA with the original sequence, indicating that a poly(A) sequence is not necessary for the initiation of negative strand RNA synthesis (Fukushi et al., 2004). With sapoviruses, initiation of RNA synthesis was also observed to be different for subgenomic polyadenylated RNA and anti-subgenomic RNA. In the case of subgenomic RNA synthesis, replication initiation is primer independent, whereas the synthesis of anti-subgenomic RNA is strictly primer dependent and occurs only when an oligo(U) primer is added to the reaction (Fullerton et al., 2007). Terminal transferase activity was also shown to be a feature of sapovirus RdRps (Fullerton et al., 2007).
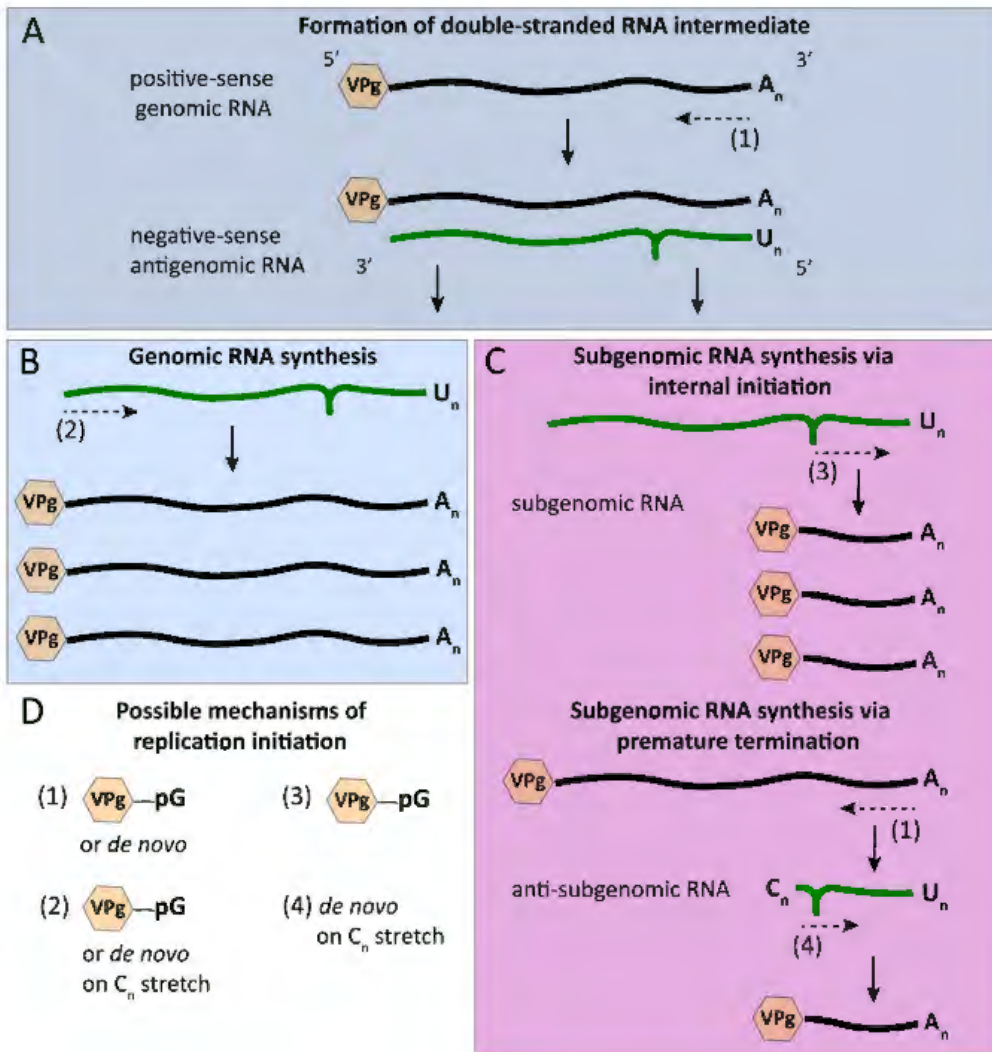
Figure 6. Initiation modes for RNA synthesis during calicivirus replication. (**A**) The synthesis of antigenomic RNA results in the formation of a double-stranded RNA intermediate; antigenomic RNA synthesis is initiated in a VPg-dependent manner or *de novo*. (**B**) The synthesis of new genomic RNA was described to start either *de novo* or from a poly(C) stretch of nucleotides that were added by the RdRp's terminal transferase activity. (**C**) The synthesis of subgenomic RNA may be initialized internally using a stem loop in the negative sense antigenomic RNA and VPg priming; according to an alternative mechanism, a premature termination of antigenomic RNA synthesis results in anti-subgenomic RNA that is then used as a template for subgenomic RNA synthesis, a process that is suggested to involve a poly(C) stretch similar to the proposed initiation of genomic RNA synthesis. (**D**) Overview of the various mechanisms that were postulated for the initiation of calicivirus RNA synthesis. Green and black lines symbolize negative and positive sense RNAs, respectively; the loop in negative sense RNAs indicates the position of a stem loop that may act as a subgenomic promoter region; dashed arrows indicate the initiation point and direction of RNA synthesis; hexagons represent

VPg proteins that are covalently bound to the 5' end of all positive-sense RNAs; pG indicates guanylation; A_n, U_n, and C_n represent poly(A), poly(U), and poly(C) sequences, respectively.

Binding of promoter regions and other RdRp-RNA interactions

The initiation of RHDV subgenomic RNA replication was studied in great detail and these observations may guide a better understanding of calicivirus promoters. There are two possible mechanisms for the synthesis of subgenomic RNA (**Figure 6C**). It can either be through an internal initiation on a negative strand of genomic RNA, or through a premature termination of genomic negative strand RNA synthesis. The latter would result in negative-sense subgenomic RNA that can be used as a template for positive sense subgenomic RNA production (Miller and Koev, 2000; Sit et al., 1998). Subgenomic RNA replication in RHDV was shown to be initialized internally on negative strand genomic RNA, and a suitable promoter region was discovered upstream of the subgenomic RNA synthesis start site (Morales et al., 2004). The localization and extent of this subgenomic RNA promoter region was analyzed by constructing deletion mutants with truncated 3'-terminal sequences on the negative strand genomic RNA. At least 50 nucleotide residues preceding the start of the subgenomic RNA were required for subgenomic RNA production (Morales et al., 2004).

Subsequent studies revealed a stable and evolutionarily conserved stem-loop in the negative strand of genomic RNA of all caliciviruses that is located six nucleotides upstream of the start of the subgenomic RNA in the RdRp coding region (Simmonds et al., 2008). The role of this stem loop in subgenomic RNA synthesis was studied by the introduction of nucleotide substitutions in the stem-loop sequence of an MNV replicon that contained the *Renilla* luciferase gene fused to the foot-and-mouth disease virus (FMDV) 2A protease coding sequence ahead of the VP2-coding region. These reporter replicon variants were used to quantify subgenomic RNA synthesis. Replicons with mutations in the stem-loop produced less luciferase compared with wild type MNV replicons, but similar amounts to a replication-defective replicon. The amount of subgenomic RNA was determined using a primer extension assay, in which a radiolabeled primer complementary to the 5' region of subgenomic RNA was used to generate a product corresponding to the start of the subgenomic RNA. Subgenomic RNA was detected in cells transfected with the wild type MNV genome but was absent in those transfected with the replicon bearing mutations in the stem-loop region. These results confirmed the hypothesis that the stem-loop in the RdRp coding region is essential for the initiation of subgenomic RNA synthesis (Yunus et al., 2015).

In the search for the protein region that is involved in RNA recognition and binding, several amino acid residues of the MNV RdRp that potentially interact with genomic RNA were identified: Lys169, Lys183 and 184, Arg185, Lys210, Arg395 and 396, and Lys422. These positively charged amino acid residues are located adjacent to the active site and well conserved across the *Caliciviridae* family. Using site-directed mutagenesis, seven MNV variants were created, in which positively charged amino acids were substituted with a nonpolar Ala (Han et al., 2017). The effect of these substitutions on protein-RNA interactions was examined using electrophoretic mobility shift assays, and the impact of these substitutions on RNA replication was studied in cell culture. The results demonstrate that RdRp variants with Ala substitutions interacted with the RNA less efficiently and were either non-viable or replicated with reduced efficiency (Han et al., 2017).

Finally, the FCV polymerase-protease precursor protein was found to interact with the ORF2 region of the viral genome. ORF2 encodes the major structural protein VP1 and the LC protein. This interaction is suspected to be required for the encapsidation of the viral RNA, although this is yet to be proven (Kaiser, 2006).

RdRp-mediated VPg nucleotidylation

VPg nucleotidylation is catalyzed much more efficiently by the human norovirus protease-polymerase precursor protein than by the mature enzyme (Medvedev et al., 2017). While nucleotidylation by the precursor protein occurs without a poly(A) template, the mature RdRp requires such a template (Belliot et al., 2008; Rohayem et al., 2006b). Unlike the poliovirus protease-polymerase precursor 3CD that shows only protease activity, the homolog of human noroviruses possesses both protease and polymerase activities, is able to initiate RNA synthesis, and can elongate the nascent RNA (Belliot et al., 2005). The FCV RdRp precursor protein was also suspected to be an active polymerase, because infected cells contain more of the uncleaved precursor than the mature enzyme (Sosnovtseva et al., 1999). Subsequent experiments confirmed that the precursor indeed possesses polymerase activity. The deletion of 164 amino acids from the amino terminus of the precursor only caused a threefold decrease in polymerase activity, but the deletion of the next amino acid resulted in a 90-fold reduction (Wei et al., 2001). This study defines the boundary of the active form of the FCV RdRp that is located either at Val135 or further towards the amino terminus (Wei et al., 2001).

During FCV replication, a direct interaction of the VPg with the polymerase-protease precursor protein was detected in an ELISA-based assay, in which purified VPg was adsorbed to the wells and the recombinant precursor protein was passed over (Kaiser, 2006; Leonard et

al., 2000). The results support the idea of a protein-primed initiation of replication, a concept that was further validated by research into RHDV replication. The RdRp of RHDV also transfers nucleotides to VPg (Machín et al., 2001). Moreover, the RHDV RdRp precursor (p72) catalyzed VPg uridylation more actively than the mature enzyme, although the mature form showed a higher *in vitro* polymerization activity when a heteropolymeric RNA was used as a template (Machín et al., 2009). Mutational analysis of the FCV VPg further confirmed the hypothesis of a protein-primed initiation of replication: the substitution of Tyr24 to Ala (as well as to Thr, Phe, and Ser) was lethal for the virus (Mitra et al., 2004). A Tyr in this position is believed to be essential for the VPg uridylation in FCV, similar to Tyr21 in the RHDV VPg. The critical amino acid in the RHDV VPg was detected by the deletion of the first 21 N-terminal residues, which completely stopped uridylation. When Tyr21 was substituted either by Phe, Ser, or Thr, the resulting variants were no longer uridylated, due to steric hindrances (in the case of Ser and Thr substitutions), or the lack of a hydroxyl group (in the case of Phe) that would have been able to act as a nucleophile in the uridylation reaction (Machín et al., 2001).

The substrate specificity of RdRps varies. For example, human norovirus RdRps nucleotidylate only human norovirus VPgs, whereas the RdRp of MNV efficiently nucleotidylates the VPgs of both human and murine noroviruses (Min et al., 2012). For the MNV RdRp, this reaction can be enhanced by *in vitro*-transcribed positive and negative strand subgenomic RNAs. Of all RNAs tested, it was the ORF3 region of the subgenomic negative strand RNA that stimulated nucleotidylation most effectively, indicating that the ORF3 region contains a cis-acting element that stimulates the reaction (Han et al., 2010).

Interactions of RdRps and other proteins

Viral interaction partners

Many calicivirus protein-protein interactions have been investigated using MNV, because this virus can be propagated in cell culture (Wobus et al., 2004). VPg clearly needs to interact with the calicivirus RdRp. However, this interaction also occurs independent of VPg-priming, because VPg variants that lack the Tyr residue needed for the nucleotidylation process still enhanced the replication process *in vitro* (Lee et al., 2018).

Further protein-protein interactions were detected using a cell-based assay in which the human norovirus GII.4 RdRp was assessed for its ability to synthesize RNA (Subba-Reddy et al., 2011). The assay uses the ability of various cellular pattern recognition receptors, such as retinoic acid-inducible gene I (RIG-I) to detect viral RNA, which leads to the activation of innate immune responses and the expression of interferon (IFN)-regulated genes (Honda et al.,

2005; Patel et al., 2003). Measuring the luciferase production that is driven by an IFN-β promoter can thus be used to quantify viral RdRp activity, as increasing virus RNA concentrations correlate with increasing expression of IFN-regulated genes (Subba-Reddy et al., 2011). Using this rather indirect reporter assay, Subba-Reddy and coworkers investigated which viral proteins had stimulatory or inhibitory effects on RNA replication. The researchers reported a stimulatory effect for the human norovirus non-structural protein p48 and the structural protein VP1, and an inhibitory effect for VP2. But when these GII.4 proteins were co-expressed with the RdRps of other viruses, they did not significantly increase virus RNA replication (again quantified via the expression of the IFN-β-dependent reporter), suggesting that these calicivirus protein-protein interactions occur in a species-specific manner (Subba-Reddy et al., 2012, 2017). Further experiments identified the part of the VP1 protein that is responsible for the interaction with RdRp. VP1 consists of two domains, a shell domain and a protruding domain. The co-expression of the RdRp with a series of truncated VP1 proteins revealed that the shell domain was sufficient to modulate the enzyme activity. The findings were confirmed using MNV replicons: the transfection of cells with a replicon defective for VP1 expression showed impaired replication, but when VP1 expression was restored by *in trans*-complementation, virus replication was rescued. Presumably, this positive feedback (the more positive-sense RNA is synthesized, the more VP1 is translated) slows at the point when VP1 starts to multimerize and assemble into new capsids, which prevents its interaction with RdRp and stops the stimulation of RNA synthesis (Subba-Reddy et al., 2012, 2017).

Cellular interaction partners

Only caliciviruses that grow in cell culture, such as FCV and MNV (Vashist et al., 2009; Wobus et al., 2006), allow investigations of RdRp interactions with cellular proteins during genuine virus replication. A redistribution of nucleolin from the nucleoli to the nucleoplasm as well as the perinuclear area was observed in FCV-infected cells. Subsequent studies showed that the FCV RdRp directly interacts and colocalizes with nucleolin, and that this interaction is necessary for efficient virus replication. Given that nucleolin interacts with both RdRp and the 3' UTR of viral RNAs, it has been suggested that the interaction promotes the formation of replication and/or translation complexes (Cancio-Lonches et al., 2011).

The FCV protease-polymerase precursor inhibits host gene transcription mediated by the cellular RNA polymerase II. The effect was observed using reporter genes under the control of either an endogenous promoter (in this case, the feline IFN-β promoter) or exogenous promoters (simian virus 40, cytomegalovirus, or bacteriophage T7 promoters). Moreover, a domain was

identified in the N-terminal region of the protease-polymerase precursor that is responsible for the observed inhibition of the RNA polymerase II (Wu et al., 2016). Similarly, the poliovirus 3C protease shuts off cellular transcription through the cleavage of the TATA-binding protein, which prioritizes the synthesis of viral proteins (Kundu et al., 2005).

Another cellular protein that affects FCV, MNV, and porcine enteric calicivirus (PEC) replication is the lysosomal endopeptidase cathepsin L, a protease that is involved in apoptosis and is primarily located in endosomes. Cathepsin L cleaves the structural protein VP1 of FCV and MNV, and VP2 of PEC. Its inhibition was shown to negatively affect the replication of FCV, MNV, and PEC in cell culture. The effect of cathepsin L inhibition is similar to the inhibition of endosomal acidification (a necessary step during viral entry), which prevents MNV and PEC from endosomal escape. These and possibly other caliciviruses enter host cells via clathrin-mediated endocytosis, thus, it should not come as a surprise that any interference with the endosomal escape of incoming virus particles blocks the initiation of virus replication (Shivanna et al., 2014a, 2014b).

Co- and post-translational modifications of calicivirus RdRps

Co- and post-translational modifications refer to a process in which a protein undergoes enzymatically driven covalent modifications during or following translation. The norovirus RdRps show signs of such modifications, e.g., the signaling kinase Akt phosphorylates the enzyme at residue Thr33 (located at the interface between finger and thumb domains) (Eden et al., 2011). Akt is a serine/threonine protein kinase involved in multiple cellular pathways; it promotes survival through the inhibition of apoptosis and the regulation of the cell cycle (Datta et al., 1999). The consequences of RdRp phosphorylation were studied by comparing the kinetic properties of the wild type enzyme to those of a Thr33 to Glu variant that mimics phosphorylation (Eden et al., 2011). In a *de novo* GTP incorporation assay that can be used to analyze enzyme kinetics (Bull et al., 2010b), the Thr33 to Glu variant showed a lower maximum enzyme velocity (100 versus 125 fmol $\times$ min^{-1}) and had a lower affinity for the GTP substrate than the wild type, suggesting that phosphorylating Thr33 modulates the activity of the enzyme (Eden et al., 2011).

Oligomerization of RdRps

Norovirus RdRps were shown to form homodimers (Högbom et al., 2009), a phenomenon that had already been described for picornavirus RdRps (Lyle et al., 2002). When different amounts of purified recombinant norovirus RdRp protein were subjected to PAGE in

native (non-denaturing) conditions, dimer formation was observed at high protein concentration and subsequently confirmed by a denaturation of the isolated proteins, SDS-PAGE, and Western blotting. The formation of dimers seems to be of biological importance, as norovirus RdRps demonstrate cooperative enzymatic activity. Increasing amounts of RNA can be synthesized in vitro with increasing concentrations of RdRp, until a plateau phase is reached. Högbom and coworkers interpret the data as a shift from active monomeric RdRps to more active dimers. They analyzed the cooperativity between RdRp monomers by calculating the Hill coefficient that, in this case, was determined to have a value greater than one, which is indicative of a positive cooperativity (Högbom et al., 2009).

In MNV, the interaction of RdRp with VPg stimulates RdRp multimerization and formation of large fibril-like structures, a reaction that can be observed by transmission electron microscopy (Lee et al., 2018). Analysis of the crystal structure of the MNV RdRp together with a truncated VPg (consisting of the first 73 amino acids) suggested that two amino acid residues of the RdRp, Asp331 and Leu354, might be involved in the interaction between RdRp and VPg. When Asp331 was changed to Ala and Leu354 to Asp, the resulting RdRp variants were still able to form hexamers in the absence of VPg, but did no longer form higher order protein structures in the presence of VPg. Moreover, the binding affinity of these variants to full length VPg decreased significantly, confirming that Asp331 and Leu354 are critical for the interaction of RdRp with VPg. It has been speculated that the formation of RdRp multimers and tubular fibrils may lead to a better coordination of replication components within larger clusters and thus enhance replication efficiency (Lee et al., 2018).

Enzymatic properties of calicivirus RdRps

Polymerase fidelity, replication speed, and evolutionary rates

Calicivirus RdRps, as well as the RdRps of other RNA viruses are known to be error-prone enzymes, because they lack the proofreading activities of many DNA polymerases. Approximately one error occurs per replication cycle for RNA viruses compared with one error per 300 cycles for DNA viruses (Drake, 1991, 1993). Comparing studies with different error reporting units is somewhat challenging, but certain trends emerge. The average error rate for HCV (family *Flaviviridae*) is 3.8×10^{-5}, measured as substitutions per nucleotide per cycle of infection (s/n/c) (Sanjuán and Domingo-Calap, 2016; Selisko et al., 2018), and the error frequency of the poliovirus RdRp ranges from 7×10^{-4} to 5.4×10^{-3}, as determined by the ratio of non-complementary nucleotides incorporation to the total number of nucleotides (Ward et

al., 1988). Similar RdRp error rates were determined for several viruses of the family *Caliciviridae*, e.g., 6.8×10^{-4} for MNV, 1.6×10^{-4} for sapovirus GI, and 9.0×10^{-4} nucleotide substitutions/site for norovirus GII.4 (Bull et al., 2010b).

RdRp properties, such as fidelity and replication rate, are important factors that shape virus evolution. For example, RdRps from norovirus GII.4 strains had higher mutation rates (determined using *in vitro* fidelity assays) compared with those of the closely related but less frequently detected GII.b and GII.7 strains (5.5–9.1×10^{-4} substitutions per site for GII.4 RdRps versus 1.5×10^{-4} and 2.2×10^{-5} substitutions per site for GII.b and GII.7, respectively). Interestingly, the GII.4 lineage showed an approximately 1.7-fold higher rate of evolution of capsid sequences and a higher frequency of non-synonymous changes compared with non-pandemic norovirus strains (Bull et al., 2010a). Furthermore, Mahar et al. reported that the acquisition of new GII.3 RdRp variants with higher mutation rates may increase genetic diversity and improve the overall fitness of viral populations under selective pressures (Mahar et al., 2013). Taken together, a low fidelity rate seems to correlate with a higher evolutionary rate.

The replication rate of a virus is another determinant of viral fitness, since viruses with an increased replication rate can produce more copies of their genome, which would result in more variants even if the RdRp error rate remains the same. For example, the RdRps from the 2006 GII.4 pandemic strains had a higher nucleotide incorporation rate (i.e. they replicated faster) than the recombinant GII.4 RdRps from earlier outbreaks and the US95/96-like pandemic GII.4 strain (the error rates were very similar). The observed increase in the incorporation rate has been associated with the appearance of a mutation outside of the active site, i.e. a Lys291 to Thr substitution in the RdRp finger domain (Bull et al., 2010a). Thus, high mutation and/or replication rate within the GII.4 lineage seem to correlate with the evolution of pandemic strains. However, high replication rates do not always correlate with a high overall fitness of a virus, this suggests that speed needs to be balanced with suitable mutation rates. For example, the GII.7 norovirus lineage, despite having a high replication rate, has a low mutation rate and limited geographic spread (Bull et al., 2010a). It is possible that the speed at which this particular virus replicated was not fast enough to balance its limited ability to produce new variants through the incorporation of mutations.

The contribution of the RdRp to the evolutionary rate of caliciviruses became even more clear with the recent success of recombinant GII.2 and GII.4 viruses that acquired a new polymerase variant. For example, the reemerged recombinant norovirus GII.P16-GII.2 that differs from previous GII.P16-GII.2 strains by 5 amino acids in the RdRp (Ruis et al., 2017),

results in high virus loads in feces, possesses a relatively high evolutionary rate (5.5×10^{-3} substitutions/site/year) and has rapidly spread across the world (Ao et al., 2018; Cheung et al., 2019). It has been suggested that the amino acid changes in the new RdRp affect the kinetic properties and the fidelity of the enzyme, but the exact mechanistic details remain unknown. Genetic recombination events have also been observed between different lagoviruses. RHDV2, originally a virus with moderate virulence and limited geographical range, evolved into a highly virulent virus, a change that is believed to be a consequence of recombination with other lagoviruses (Forrester et al., 2008; Lopes et al., 2015). Some of these recombinant viruses were found to possess the nonstructural proteins of benign rabbit calicivirus Australia-1 (RCV-A1)-like viruses (Hall et al., 2018; Lopes et al., 2015). RHDV and RCV-A1 have evolutionary rates of 2.8×10^{-3} and 5.0×10^{-3} substitutions/site/year, respectively (Eden et al., 2015; Mahar et al., 2016). The higher evolutionary rate of RCV-A1 correlates with a higher speed of its RdRp, as determined by *in vitro* assays (Urakova et al., 2016). This suggests that RHDV2 could have acquired a relatively fast polymerase, which may explain its increased virulence and evolutionary success. Within 18 months of its arrival, RHDV2 largely replaced endemic RHDV strains in Australia (Mahar et al., 2017).

The generation of a genetically highly diverse pool of genomes provides an evolutionary advantage, because a diverse virus population can more readily adapt to selective pressures (Domingo, 2002; Lauring and Andino, 2010). If the diversity is the result of a higher error rate, this can also increase the likelihood of acquiring detrimental mutations and it has therefore been suggested that most RNA viruses replicate at the edge of an error threshold that is determined by a complex interplay of several parameters such as genome size, error rates, and replication speed (Duffy et al., 2008). As such, it should not come as a surprise that both increases and decreases in RdRp fidelity can affect viral fitness (Agol and Gmyl, 2018; Arias et al., 2016; Pfeiffer and Kirkegaard, 2005; Xie et al., 2014).

Effects of temperature, pH, and salt conditions on RdRp performance

The conditions for an optimal performance of calicivirus RdRps were determined for viruses from the genera *Norovirus*, *Sapovirus*, and *Lagovirus* (**Table 3**). The activity of viral RdRps is temperature dependent, although the optimal temperature is not necessarily that of host's body. In early studies, the highest sapovirus RdRp activity was detected at 37°C (Fullerton et al., 2007). However, more recent studies indicate that many calicivirus RdRps work in an environment that does not allow for maximal performance. For example, a human norovirus RdRp demonstrated a higher activity at 30 than at 37°C according to *in vitro* assays

(Rohayem et al., 2006a). Moreover, when a broader temperature range was studied (i.e. 5, 25, 37, 55, 65, and 75°C) with human norovirus and sapovirus RdRps, the activity was highest at 25°C, and only about 50% of the optimal enzymatic activity was exhibited at 37°C (Bull et al., 2010b). Furthermore, the norovirus and sapovirus RdRps displayed only approximately 20% of their optimal activity at 5°C and only about 1% at 55°C. No activity was detected at 65 or 75°C for any of the RdRps except sapovirus RdRp, which still exhibited 13% of the optimal activity at 65°C (Bull et al., 2010b). Interestingly, the optimal temperature for some if not all lagoviruses is higher than that of human noroviruses and sapoviruses. Using recombinant proteins, it was found that the RdRps of the non-pathogenic RCV and the highly pathogenic RHDV performed best between 40–45°C (Urakova et al., 2016), a feature that can be explained as an adaptation of rabbit caliciviruses to their hosts, as the body temperature of healthy rabbits ranges from 38.3 to 39.4°C. Moreover, the fever associated with rabbit haemorrhagic disease often raises the body temperature to 42°C (Strive et al., 2010), but this temperature is not high enough to slow down the activity of the RHDV RdRp (Urakova et al., 2016). The reason why caliciviruses other than lagoviruses seem to possess a temperature optimum that is different from the core body temperature of the host is presently unknown and further research is required to answer this question.

Table 3. Enzymatic properties of calicivirus RdRps

Genera	pH optimum	Me^{2+} preference (test conditions)	Temperature optimum (°C)	References
Norovirus	7.0–8.0	Mn^{2+} (2.5 mM MnCl$_2$) Mg^{2+} (0.5–1.5 mM MgCl$_2$)	25 30 35–39	Bull et al., 2010b Rohayem et al., 2006a Urakova et al., 2016
Lagovirus	8.5	Mn^{2+} (2.5 mM MnCl$_2$) Mg^{2+} (3 mM Mg(CH$_3$COO)$_2$)	40–45	Urakova et al., 2016 Vazquez et al., 1998
Sapovirus	8.0	Mn^{2+} (0.5–5 mM MnCl$_2$)	25 37	Bull et al., 2010b Fullerton et al., 2007

The optimal pH for rabbit caliciviruses RdRps was found to be 8.5, which is higher than that of norovirus RdRps (7.0–8.0) (Bull et al., 2010b; Urakova et al., 2016). For optimal catalytic function, the norovirus and lagovirus RdRps can utilize either Mn^{2+} or Mg^{2+}, but not Fe^{2+} (Rohayem et al., 2006a; Urakova et al., 2016; Vazquez et al., 1998). Sapovirus RdRp demonstrated a higher activity with Mn^{2+}, but it was also active when Mg^{2+} was added as a cofactor to the reaction, indicating some flexibility in the use of cofactors (Fullerton et al., 2007).

A putative undescribed conserved motif in calicivirus RdRps

Our own sequence comparison of calicivirus RdRps revealed a conserved motif that had not previously been described. This short motif in the RHDV RdRp is located in the thumb domain and consists of four amino acids: $_{46}$Pro-Ala-Asn-Leu$_{49}$ (**Figure 7D, E**). The flanking amino acids Pro and Leu are significantly conserved, whereas the internal Ala and Asn are not (**Figure 7A–C**). This motif is present in all calicivirus and picornavirus RdRps, but does not extend beyond the order *Picornavirales*. We propose to name the new motif "I motif" in accordance with the established nomenclature for previously described motifs and homomorphs. A literature search revealed that several FMDV variants with amino acid substitutions in the region of the I motif have been investigated. Pro36 to Lys, Ala37 to Val, and Leu39 to Phe were all non-viable, supporting the hypothesis that this RdRp region is critical for the enzymatic function of the protein (Xie et al., 2014). Interestingly, an Ala38 to Val substitution changed the fidelity of the FMDV RdRp (Zeng et al., 2014). This variant was selected as ribavirin-resistant during exposure to ribavirin and demonstrated a 1.65-fold increase in fidelity compared with the wild type FMDV virus (Zeng et al., 2014), a finding that is in line with similar reports on other polymerases (Mansky and Cunningham, 2000; Pfeiffer and Kirkegaard, 2003). While no specific function has as yet been assigned to the I motif, its high level of conservation warrants further investigation. Future studies should be directed at its possible involvement in regulating polymerase fidelity.
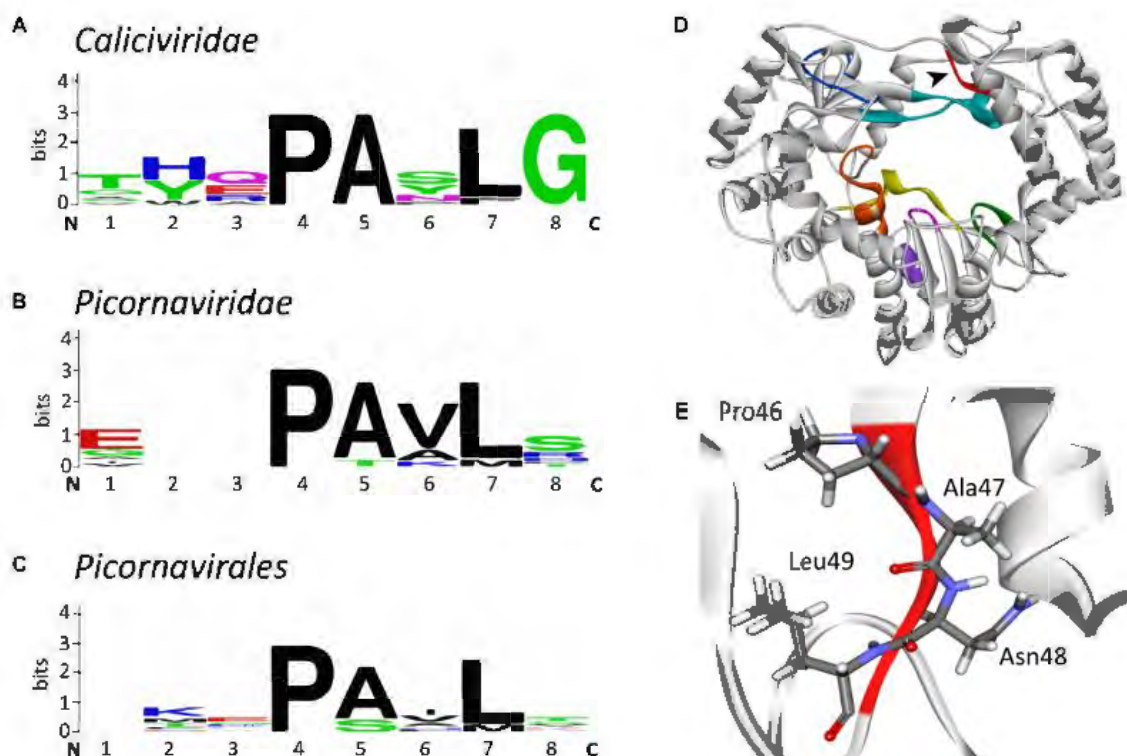
Figure 7. Sequence alignment logos of a putative new conserved motif ("motif I") and the localization of the motif in the RHDV RdRp. (**A**) Sequence logo alignment for the putative motif of the following viruses in the family *Caliciviridae*: *European brown hare syndrome virus* and RHDV (both genus *Lagovirus*)*; Norwalk virus, Lordsdale virus*, MNV (genus *Norovirus*); *Sapporo virus* (genus *Sapovirus*)*;* FCV, VESV, and *San Miguel sea lion virus* (genus *Vesivirus*); *Newbury 1 virus* (genus *Nebovirus*). (**B**) Sequence logo alignment for the putative motif of the following viruses in the family *Picornaviridae*: *Poliovirus*, *Bovine enterovirus, Coxsackievirus B3, Human rhinovirus A*, and *Echovirus* (genus *Enterovirus*); *Foot and mouth disease virus* (genus *Aphtovirus*); *Hepatitis A virus* (genus *Hepatovirus*); *Human parechovirus* (genus *Parechovirus*); *Theiler's murine encephalomyelitis virus* and *Encephalomyocarditis virus* (genus *Cardiovirus*); *Avian encephalomyelitis virus* (genus *Tremovirus*). (**C**) Sequence logo alignment for the putative motif of the following viruses in the order *Picornavirales: Poliovirus,* FMDV*, Hepatitis A virus* and *Human parechovirus (*family *Picornaviridae*); *Cricket paralysis virus* and *Drosophila C virus* (family *Dicistroviridae*); *Parsnip yellow fleck virus, Broad bean wilt virus, Cowpea mosaic virus, and Beet ringspot virus* (family *Secoviridae*). N and C indicate N- and C-terminal directions, respectively. Sequence conservation is measured in bits and is indicated by the height of each letter's stack. Amino acids are colored according to their chemical properties: polar amino acids (Gly, Ser, Thr, Tyr, Cys, Gln, Asn) green, basic (Lys, Arg, His) blue, acidic (Asp, Glu) red, and hydrophobic (Ala, Val, Leu, Ile, Pro, Trp, Phe, Met) amino acids are colored black (Crooks et al., 2004). (**D**) Ribbon diagram of RHDV RdRp (PDB ID: 1KHW). The black arrowhead points at the new motif I that is colored red, other conserved motifs are colored as in **Figure 3D**. (**E**) Structure of the motif I. Sequence alignments were performed with the multiple sequence alignment tool MUSCLE (Edgar, 2004); sequence logo pictures were created with Weblogo (Crooks et al., 2004). The ribbon diagram was generated using Discovery Studio (Dassault Systèmes BIOVIA, Discovery Studio Visualizer v17.2.0).

Calicivirus RdRp inhibitors

RdRps are attractive targets for antiviral intervention, because these enzymes are indispensable for virus replication and are very different from any of the host polymerases, which greatly reduces off target effects. RdRp inhibitors can be classified into two major groups: nucleoside analogs (NAs) and non-nucleoside inhibitors (NNIs) (**Table 4**). NAs are treated by an RdRp as 'normal' nucleotides (once an NA is phosphorylated and is in its active

form). When they are incorporated into a nascent RNA strand, they can cause a termination of the RNA synthesis or lethal mutagenesis (Costantini et al., 2012; Galmarini et al., 2001). NNIs are aimed to bind an RdRp allosterically, which means outside of the active center (Caillet-Saguy et al., 2011; Netzler et al., 2017).

Nucleoside analogs

2CMC

The active 5'-triphosphate form of 2'-C-methylcytidine (2CMC) is an HCV polymerase inhibitor that competes with the nucleotide cytidine triphosphate (CTP) for binding to the active site of RdRps. Incorporation of 2CMC into a nascent RNA strand leads to the termination of RNA synthesis. In cell culture, this compound is also active against *Dengue virus*, *Yellow fever virus*, and *West Nile virus* (Pierra et al., 2006). 2CMC also inhibits calicivirus replication in cell culture: as demonstrated by time-of-drug-addition assays, 2CMC inhibited MNV replication and plaque formation (Rocha-Pereira et al., 2012a). Furthermore, 2CMC was able to 'cure' cultured cells from Norwalk virus replicons (Rocha-Pereira et al., 2013).

Ribavirin

Ribavirin (1-β-D-ribofuranosyl-1,2,4-triazole-3-carboxamide) mimics the guanosine nucleotide and inhibits the replication of a broad range of DNA and RNA viruses (Graci and Cameron, 2006; Kanda et al., 2004; Leyssen et al., 2005). In cell culture experiments, ribavirin significantly reduced norovirus replicon production (Chang and George, 2007).
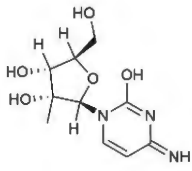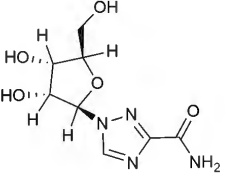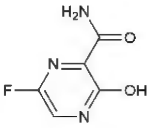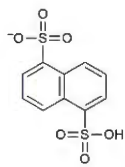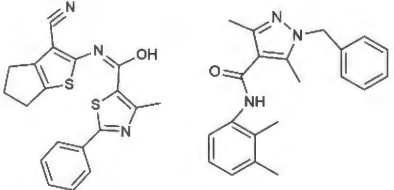
Various mechanisms of the ribavirin-mediated inhibitory effect on virus replication have been proposed, including indirect mechanisms such as guanosine triphosphate (GTP) depletion via the downregulation of inosine monophosphate dehydrogenase, an enzyme that catalyzes GTP synthesis. More direct mechanisms include the ribavirin incorporation into the nascent RNA strand, which may increase mutation frequencies and lead to an 'error catastrophe' (Graci and Cameron, 2006).
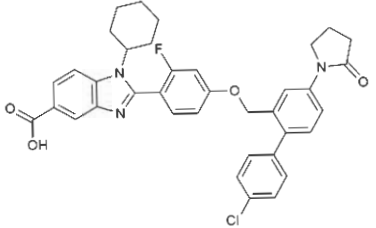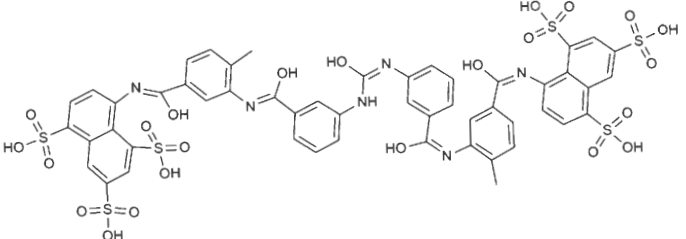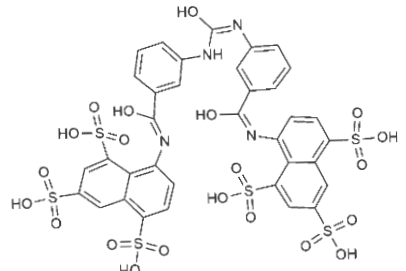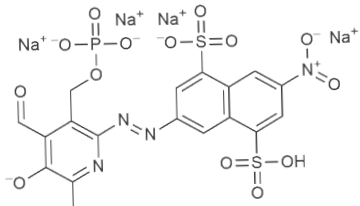
Favipiravir (T-705)

Originally, T-705 (6-fluoro-3-hydroxy-2-pyrazinecarboxamide), a purine nucleoside analogue, was developed as an influenza virus inhibitor. T-705 is a prodrug which is turned into its active form (favipiravir-ribofuranosyl-5′-triphosphate) by cellular enzymes (Furuta et al., 2002, 2013). This compound proved also to be a potent inhibitor of bunyaviruses, arenaviruses, and flaviviruses (Gowen et al., 2007; Morrey et al., 2008). Furthermore, it inhibits MNV

replication in cell culture, although at a relatively high EC_{50} (half maximal effective concentration) (Rocha-Pereira et al., 2012b). The mechanism through which favipiravir inhibits virus multiplication is most probably lethal mutagenesis, because this NA in its active form is incorporated opposite C and U by 'susceptible' RdRps (Jin et al., 2013). This hypothesis was confirmed when increased mutation frequencies were observed in MNV-infected mice after the treatment with favipiravir (Arias et al., 2014). Moreover, after the treatment of a human norovirus-infected patient with favipiravir, a distinct viral variant was observed that differed greatly from all variants that were detected before the treatment commenced and contained 118 nonsynonymous substitutions (Ruis et al., 2018).

TABLE 4 | Calicivirus RdRp inhibitors

Inhibitor	Chemical structure	Type of inhibitor	Calicivirus RdRp binding site	$EC_{50}/IC_{50}/ED_{50}$*, μM	Reference
2CMC		NA	Active site	1.6 (EC_{50}, MNV)	Carroll et al., 2003; Rocha-Pereira et al., 2012a
Ribavirin		NA	Active site	40 (ED_{50}, hNV)	Chang and George, 2007; Graci and Cameron, 2006; Witkowski et al., 1972
Favipiravir		NA	Active site	124±42 (EC_{50}, MNV)	Furuta et al., 2002; Rocha-Pereira et al., 2012b
NAF2		NNI	A-site and B-site	14±1.0 (IC_{50}, hNV)	Tarantino et al., 2014
NIC02/ NIC04		NNI	Unknown	4.8 (EC_{50}, MNV)/ 32.8 (EC_{50}, MNV)	Eltahla et al., 2014

JTK-109		NNI	B-site	6.1 (EC$_{50}$, MNV)	Hirashima et al., 2006; Netzler et al., 2017
Suramin		NNI	Across the fingers and thumb domains, at the dNTPs access (A-site)	0.07±0.003 (IC$_{50}$, MNV)	Mastrangelo et al., 2012
NF023		NNI	A-site	0.2±0.002 (IC$_{50}$, MNV)	Mastrangelo et al., 2012
PPNDS		NNI	In the thumb domain along the exit path for the synthesized RNA strand (B-site)	0.45±0.09 (IC$_{50}$, hNV**)	Mastrangelo et al., 2012; Tarantino et al., 2014

* ED$_{50}$ represents the dose required for 50% of the population to obtain the therapeutic effect; ** Human norovirus.

Non-nucleoside RdRp inhibitors

Suramin, NF023, and PPNDS

Suramin, NF023, and PPNDS are naphthylurea derivatives. Originally, Suramin was developed as a medication for African sleeping sickness and river blindness (Voogd et al., 1993). However, Suramin and NF023 also inhibit a broad range of viruses, including human norovirus and MNV. The calicivirus RdRps were inhibited in a dose-dependent manner indicating a binding of the drug to the free enzyme or enzyme-substrate complex (Mastrangelo et al., 2012). In norovirus RdRps, there are two defined binding sites for naphthylurea derivatives: one site (retrospectively named 'A-site') is located across the fingers and thumb domains where NTPs access the active site (Mastrangelo et al., 2012), the other one is named the 'B-site' and is situated in the thumb domain (Tarantino et al., 2014). The A-site was identified by studying the crystal structures of the MNV RdRp in a complex with Suramin and NF023. (Mastrangelo et al., 2012). The B-site is located along the exit path for the synthesized RNA strand and was identified by analyzing a crystal structure of the RdRp in complex with NAF2 (naphthalene-1,5-disulphonic acid). NAF2 is a fragment derived from the aforementioned compounds (Suramin and NF023) and is likely to represent the most active inhibitory part of larger naphthylurea derivatives. The naphthalene sulfonate-based compound pyridoxal-50-phosphate-6-(20-naphthylazo-60-nitro-40,80-disulfonate) tetrasodium salt (PPNDS) was selected in a docking assay (a method widely used to identify drug binding sites) for further characterization of the B-site. Subsequent studies proved that PPNDS inhibits the RdRp at a much lower IC_{50} (half maximal inhibitory concentration) value compared with NAF2 (Tarantino et al., 2014).

NIC02 and NIC04

Phenylthiazole carboxamide (NIC02) and pyrazole acetamide (NIC04) are novel compounds that inhibit GII.4 norovirus RdRps at relatively low IC_{50} values. The mode of inhibition was determined by examining the kinetics of GTP incorporation in the presence of increasing concentrations of these inhibitors. With higher inhibitor concentrations, the reaction velocity and the substrate affinity decreased, suggesting that these compounds can bind both free enzyme and the enzyme-substrate complex (Eltahla et al., 2014). The inhibitory potential of both compounds was also tested using other calicivirus RdRps from sapovirus GII, MNV, and different human norovirus strains. NIC02 has a broad inhibitory range (as far as calicivirus RdRps are concerned), which suggests that it binds within a conserved but as yet unidentified motif (Eltahla et al., 2014).

JTK-109

JTK-109 is a benzimidazole derivative that is known as an allosteric inhibitor of the HCV RdRp (Hirashima et al., 2006). JTK-109 also possesses inhibitory activity against a variety of caliciviruses (including *Norovirus*, *Sapovirus*, and *Lagovirus*), as measured in a quantitative fluorescent *de novo* RdRp activity assay (Eltahla et al., 2013; Netzler et al., 2017). In cell culture experiments, this compound inhibited MNV plaque formation and virus growth (Netzler et al., 2017). Using molecular docking, Netzler and coworkers showed that JTK-109 targets calicivirus RdRps by binding to the B-site of the thumb domain (Netzler et al., 2017).

Outlook

Caliciviruses, like almost all other RNA viruses, depend on their RdRps for genome replication. All virus RdRps possess a conserved core structure that is different from cellular polymerases. This dependency on a unique enzyme class provides a soft target for antiviral intervention. However, little information is currently available on how exactly calicivirus RdRps initiate, elongate, and terminate RNA synthesis, how they contribute to the establishment of viral replication factories, and how they escape host cell innate immune responses. Research into the replication of human caliciviruses is especially lacking compared with other small RNA viruses, such as picornaviruses. Norovirus research has long relied on surrogate models or cell-free *in vitro* studies, but recent progress with organoid culture techniques has provided new models that will soon allow the study of RdRp functions in the context of genuine virus replication and host cell countermeasures. As RdRps are often the principal targets in drug-based antiviral therapies, a better understanding of their enzymatic activities and interactions with viral and cellular partners will likely aid in the development of a new generation of highly effective and more specific antivirals.

Acknowledgements

Funding

Author Contributions Statement

TS and MF developed the conceptual outline; ES, NU, and MF wrote the manuscript (ES wrote the first draft). All authors contributed to editing and revising the manuscript. All authors read and approved the final manuscript.

Conflict of Interest Statement

The authors declare no conflict of interest.

References

Abente, E. J., Sosnovtsev, S. V., Sandoval-Jaime, C., Parra, G. I., Bok, K., and Green, K. Y. (2013). The feline calicivirus leader of the capsid protein is associated with cytopathic effect. *J. Virol.* 87, 3003–3017. doi:10.1128/JVI.02480-12.

Abrantes, J., Van Der Loo, W., Le Pendu, J., and Esteves, P. J. (2012). Rabbit haemorrhagic disease (RHD) and rabbit haemorrhagic disease virus (RHDV): A review. *Vet. Res.* 43. doi:10.1186/1297-9716-43-12.

Agol, V. I., and Gmyl, A. P. (2010). Viral security proteins: counteracting host defences. *Nat. Rev. Microbiol.* 8, 867–878. doi:10.1038/nrmicro2452.

Agol, V. I., and Gmyl, A. P. (2018). Emergency services of viral RNAs: repair and remodeling. *Microbiol. Mol. Biol. Rev.* 82, e00067-17. doi:10.1128/MMBR.00067-17.

Ao, Y., Cong, X., Jin, M., Sun, X., Wei, X., Wang, J., et al. (2018). Genetic analysis of reemerging GII.P16-GII.2 noroviruses in 2016-2017 in China. *J. Infect. Dis.* 218, 133–143. doi:10.1093/infdis/jiy182.

Arias, A., Thorne, L., Ghurburrun, E., Bailey, D., and Goodfellow, I. (2016). Norovirus polymerase fidelity contributes to viral transmission in vivo. *mSphere* 1, e00279-16. doi:10.1128/mSphere.00279-16.

Arias, A., Thorne, L., and Goodfellow, I. (2014). Favipiravir elicits antiviral mutagenesis

during virus replication in vivo. *Elife* 3, 3679. doi:10.7554/elife.03679.

Arnold, J. J., Ghosh, S. K. B., and Cameron, C. E. (1999). Poliovirus RNA-dependent RNA polymerase (3D(pol)). Divalent cation modulation of primer, template, and nucleotide selection. *J. Biol. Chem.* 274, 37060–37069. doi:10.1074/jbc.274.52.37060.

Atmar, R. L., and Estes, M. K. (2006). The epidemiologic and clinical importance of norovirus infection. *Gastroenterol. Clin. North Am.* 35, 275–290. doi:10.1016/j.gtc.2006.03.001.

Belliot, G., Sosnovtsev, S. V., Chang, K.-O., Babu, V., Uche, U., Arnold, J. J., et al. (2005). Norovirus proteinase-polymerase and polymerase are both active forms of RNA-dependent RNA polymerase. *J. Virol.* 79, 2393–2403. doi:10.1128/JVI.79.4.2393-2403.2005.

Belliot, G., Sosnovtsev, S. V., Chang, K. O., McPhie, P., and Green, K. Y. (2008). Nucleotidylylation of the VPg protein of a human norovirus by its proteinase-polymerase precursor protein. *Virology* 374, 33–49. doi:10.1016/j.virol.2007.12.028.

Black, D. N., Burroughs, J. N., Harris, T. J. R., and Brown, F. (1978). The structure and replication of calicivirus RNA. *Nature* 274, 614–615. doi:10.1038/274614a0.

Boga, J., Marín, M. S., Casais, R., Prieto, M., and Parra, F. (1992). In vitro translation of a subgenomic mRNA from purified virions of the Spanish field isolate AST/89 of Rabbit Hemorrhagic Disease Virus (RHDV). *Virus Res.* 26, 33–40. doi:10.1016/0168-1702(92)90144-X.

Bull, R. A., Eden, J. S., Rawlinson, W. D., and White, P. A. (2010a). Rapid evolution of pandemic noroviruses of the GII.4 lineage. *PLoS Pathog.* 6, 1000831. doi:10.1371/journal.ppat.1000831.

Bull, R. A., Hyde, J., MacKenzie, J. M., Hansman, G. S., Oka, T., Takeda, N., et al. (2010b). Comparison of the replication properties of murine and human calicivirus RNA-dependent RNA polymerases. *Virus Genes* 42, 16–27. doi:10.1007/s11262-010-0535-y.

Burroughs J. N., B. N. (1978). Presence of a covalently linked protein on Calicivirus RNA. *J. gen. Virol* 41, 443–446. doi:10.1099/0022-1317-41-2-443.

Butcher, S. J., Grimes, J. M., Makeyev, E. V., Bamford, D. H., and Stuart, D. I. (2001). A mechanism for initiating RNA-dependent RNA polymerization. *Nature* 410, 235–240. doi:10.1038/35065653.

Caillet-Saguy, C., Simister, P. C., and Bressanelli, S. (2011). An objective assessment of conformational variability in complexes of hepatitis C virus polymerase with non-nucleoside inhibitors. *J. Mol. Biol.* 414, 370–384. doi:10.1016/j.jmb.2011.10.001.

Cancio-Lonches, C., Yocupicio-Monroy, M., Sandoval-Jaime, C., Galvan-Mendoza, I, Ureña,

L., Vashist, S., et al. (2011). Nucleolin interacts with the Feline calicivirus 3' untranslated region and the protease-polymerase NS6 and NS7 proteins, playing a role in virus veplication. *J. Virol.* 85, 8056–8068. doi:10.1128/JVI.01878-10.

Carroll, S. S., Tomassini, J. E., Bosserman, M., Getty, K., Stahlhut, M. W., Eldrup, A. B., et al. (2003). Inhibition of hepatitis C virus RNA replication by 2′-modified nucleoside analogs. *J. Biol. Chem.* 278, 11979–11984. doi:10.1074/jbc.M210914200.

Castro, C., Smidansky, E. D., Arnold, J. J., Maksimchuk, K. R., Moustafa, I., Uchida, A., et al. (2009). Nucleic acid polymerases use a general acid for nucleotidyl transfer. *Nat. Struct. Mol. Biol.* 16, 212–218. doi:10.1038/nsmb.1540.

Castro, C., Smidansky, E., Maksimchuk, K. R., Arnold, J. J., Korneeva, V. S., Gotte, M., et al. (2007). Two proton transfers in the transition state for nucleotidyl transfer catalyzed by RNA- and DNA-dependent RNA and DNA polymerases. *Proc. Natl. Acad. Sci.* 104, 4267–4272. doi:10.1073/pnas.0608952104.

Černý, J., Bolfíková, B. Č., Valdés, J. J., Grubhoffer, L., and Růžek, D. (2014). Evolution of tertiary structure of viral RNA dependent polymerases. *PLoS One* 9, 96070. doi:10.1371/journal.pone.0096070.

Chang, K.-O., and George, D. W. (2007). Interferons and ribavirin effectively inhibit Norwalk virus replication in replicon-bearing cells. *J. Virol.* 81, 12111–12118. doi:10.1128/jvi.00560-07.

Chaudhry, Y., Nayak, A., Bordeleau, M. E., Tanaka, J., Pelletier, J., Belsham, G. J., et al. (2006). Caliciviruses differ in their functional requirements for eIF4F components. *J. Biol. Chem.* 281, 25315–25325. doi:10.1074/jbc.M602230200.

Cheung, S. K. C., Kwok, K., Zhang, L. Y., Mohammad, K. N., Lui, G. C. Y., Lee, N., et al. (2019). Higher viral load of emerging norovirus GII.P16-GII.2 than pandemic GII.4 and epidemic GII.17, Hong Kong, China. *Emerg. Infect. Dis.* 25, 119–122. doi:10.3201/eid2501.180395.

Choi, K. H. (2012). Viral polymerases. *Adv. Exp. Med. Biol.* 726, 267–304. doi:10.1007/978-1-4614-0980-9_12.

Conley, M. J., McElwee, M., Azmi, L., Gabrielsen, M., Byron, O., Goodfellow, I. G., et al. (2019). Calicivirus VP2 forms a portal-like assembly following receptor engagement. *Nature*, 1. doi:10.1038/s41586-018-0852-1.

Cooke, B. D. (2002). Rabbit haemorrhagic disease: field epidemiology and the management of wild rabbit populations. *Rev. Sci. Tech. l'OIE* 21, 347–358. doi:10.20506/rst.21.2.1337.

Cooke, B. D., and Fenner, F. (2002). Rabbit haemorrhagic disease and the biological control of

wild rabbits, *Oryctolagus cuniculus*, in Australia and New Zealand. *Wildl. Res.* 29, 689–706. doi:10.1071/WR02010.

Costantini, V. P., Whitaker, T., Barclay, L., Lee, D., McBrayer, T. R., Schinazi, R. F., et al. (2012). Antiviral activity of nucleoside analogues against norovirus. *Antivir. Ther.* 17, 981–991. doi:10.3851/IMP2229.

Crooks, G. E., Hon, G., Chandonia, J. M., and Brenner, S. E. (2004). WebLogo: A sequence logo generator. *Genome Res.* 14, 1188–1190. doi:10.1101/gr.849004.

Datta, S. R., Brunet, A., and Greenberg, M. E. (1999). Cellular survival: A play in three akts. *Genes Dev.* 13, 2905–2927. doi:10.1101/gad.13.22.2905.

Domingo, E. (2002). Quasispecies theory in virology. *J. Virol.* 76, 463–465. doi:10.1128/JVI.76.1.463-465.2002.

Drake, J. W. (1991). A constant rate of spontaneous mutation in DNA-based microbes. *Proc. Natl. Acad. Sci. USA* 88, 7160–7164.

Drake, J. W. (1993). Rates of spontaneous mutation among RNA viruses. *Proc. Natl. Acad. Sci. USA* 90, 4171–4175.

Duffy, S., Shackelton, L. A., and Holmes, E. C. (2008). Rates of evolutionary change in viruses: Patterns and determinants. *Nat. Rev. Genet.* 9, 267–276. doi:10.1038/nrg2323.

Eden, J.-S., Read, A. J., Duckworth, J. A., Strive, T., and Holmes, E. C. (2015). Resolving the origin of rabbit hemorrhagic disease virus: insights from an investigation of the viral stocks released in Australia. *J. Virol.* 89, 12217–12220. doi:10.1128/JVI.01937-15.

Eden, J.-S., Sharpe, L. J., White, P. A., and Brown, A. J. (2011). Norovirus RNA-dependent RNA polymerase is phosphorylated by an important survival kinase, Akt. *J. Virol.* 85, 10894–10898. doi:10.1128/JVI.05562-11.

Edgar, R. C. (2004). MUSCLE: Multiple sequence alignment with high accuracy and high throughput. *Nucleic Acids Res.* 32, 1792–1797. doi:10.1093/nar/gkh340.

Ehresmann, D. W., and Schaffer, F. L. (1977). RNA synthesized in calicivirus infected cells is atypical of picornaviruses. *J. Virol.* 22, 572–576.

Eltahla, A. A., Lackovic, K., Marquis, C., Eden, J. S., and White, P. A. (2013). A fluorescence-based high-throughput screen to identify small compound inhibitors of the genotype 3a hepatitis c virus RNA polymerase. *J. Biomol. Screen.* 18, 1027–1034. doi:10.1177/1087057113489883.

Eltahla, A. A., Lim, K. L., Eden, J.-S., Kelly, A. G., Mackenzie, J. M., and White, P. A. (2014). Nonnucleoside inhibitors of norovirus RNA polymerase: scaffolds for rational drug design. *Antimicrob. Agents Chemother.* 58, 3115–3123. doi:10.1128/aac.02799-13.

Ettayebi, K., Crawford, S. E., Murakami, K., Broughman, J. R., Karandikar, U., Tenge, V. R., et al. (2016). Replication of human noroviruses in stem cell-derived human enteroids. *Science (80-.).* 353, 1387–1393. doi:10.1126/science.aaf5211.

Ettayebi, K., and Hardy, M. E. (2003). Norwalk virus nonstructural protein p48 forms a complex with the SNARE regulator VAP-A and prevents cell surface expression of vesicular stomatitis virus G protein. *J. Virol.* 77, 11790–7. doi:10.1128/JVI.77.21.11790.

Farkas, T., Sestak, K., Wei, C., and Jiang, X. (2008). Characterization of a rhesus monkey calicivirus representing a new genus of Caliciviridae. *J. Virol.* 82, 5408–5416. doi:10.1128/JVI.00070-08.

Fernandez-Vega, V., Sosnovtsev, S. V, Belliot, G., King, A. D., Mitra, T., Gorbalenya, A., et al. (2004). Norwalk virus N-terminal nonstructural protein is associated with disassembly of the Golgi complex in transfected cells. *J.Virol.* 78, 4827–4837. doi:10.1128/JVI.78.9.4827.

Ferrer-Orta, C., Arias, A., Escarmís, C., Verdaguer, N., Van Duyne, G. D., and Yang, W. (2006). A comparison of viral RNA-dependent RNA polymerases. *Curr. Opin. Struct. Biol.* 16, 27–34. doi:10.1016/j.sbi.2005.12.002.

Ferrer-Orta, C., Arias, A., Perez-Luque, R., Escarmis, C., Domingo, E., and Verdaguer, N. (2007). Sequential structures provide insights into the fidelity of RNA replication. *Proc. Natl. Acad. Sci.* 104, 9463–9468. doi:10.1073/pnas.0700518104.

Ferrer-Orta, C., Arias, A., Perez-Luque, R., Escarmís, C., Domingo, E., and Verdaguer, N. (2004). Structure of foot-and-mouth disease virus RNA-dependent RNA polymerase and its complex with a template-primer RNA. *J. Biol. Chem.* 279, 47212–47221. doi:10.1074/jbc.M405465200.

Forrester, N. L., Moss, S. R., Turner, S. L., Schirrmeier, H., and Gould, E. A. (2008). Recombination in rabbit haemorrhagic disease virus: possible impact on evolution and epidemiology. doi:10.1016/j.virol.2008.03.023.

Fukushi, S., Kojima, S., Takai, R., Hoshino, F. B., Oka, T., Takeda, N., et al. (2004). Poly(A)- and primer-independent RNA polymerase of Norovirus. *J.Virol.* 78, 3889–3896. doi:10.1128/JVI.78.8.3889.

Fullerton, S. W. B., Blaschke, M., Coutard, B., Gebhardt, J., Gorbalenya, A., Canard, B., et al. (2007). Structural and functional characterization of sapovirus RNA-dependent RNA polymerase. *J. Virol.* 81, 1858–1871. doi:10.1109/BIOCAS.2017.8325071.

Furuta, Y., Gowen, B. B., Takahashi, K., Shiraki, K., Smee, D. F., and Barnard, D. L. (2013). Favipiravir (T-705), a novel viral RNA polymerase inhibitor. *Antiviral Res.* 100, 446–454.

doi:10.1016/j.antiviral.2013.09.015.

Furuta, Y., Takahashi, K., Fukuda, Y., Kuno, M., Kamiyama, T., Kozaki, K., et al. (2002). In vitro and in vivo activities of anti-influenza virus compound T-705. *Antimicrob. Agents Chemother.* 46, 977–981. doi:10.1128/AAC.46.4.977-981.2002.

Galmarini, C. M., Mackey, J. R., and Dumontet, C. (2001). Nucleoside analogues: mechanisms of drug resistance and reversal strategies.

Gohara, D. W., Crotty, S., Arnold, J. J., Yoder, J. D., Andino, R., and Cameron, C. E. (2000). Poliovirus RNA-dependent RNA polymerase (3D(pol)): Structural, biochemical, and biological analysis of conserved structural motifs A and B. *J. Biol. Chem.* 275, 25523–25532. doi:10.1074/jbc.M002671200.

Gong, P., and Peersen, O. B. (2010). Structural basis for active site closure by the poliovirus RNA-dependent RNA polymerase. *Proc. Natl. Acad. Sci.* 107, 22505–22510. doi:10.1073/pnas.1007626107.

Goodfellow, I. (2011). The genome-linked protein VPg of vertebrate viruses - A multifaceted protein. *Curr. Opin. Virol.* 1, 355–362. doi:10.1016/j.coviro.2011.09.003.

Gorbalenya, A. E., Pringle, F. M., Zeddam, J.-L., Luke, B. T., Cameron, C. E., Kalmakoff, J., et al. (2002). The palm subdomain-based active site is internally permuted in viral RNA-dependent RNA polymerases of an ancient lineage. *J. Mol. Biol* 324, 47–62. doi:10.1016/S0022-2836(02)01033-1.

Gowen, B. B., Wong, M.-H., Jung, K.-H., Sanders, A. B., Mendenhall, M., Bailey, K. W., et al. (2007). In vitro and in vivo activities of T-705 against arenavirus and bunyavirus infections. *Antimicrob. Agents Chemother.* 51, 3168–3176. doi:10.1128/AAC.00356-07.

Graci, J. D., and Cameron, C. E. (2006). Mechanisms of action of ribavirin against distinct viruses. *Rev. Med. Virol.* 16, 37–48. doi:10.1002/rmv.483.

Green, K. Y., Mory, A., Fogg, M. H., Weisberg, A., Belliot, G., Wagner, M., et al. (2002). Isolation of enzymatically active replication complexes from Feline calicivirus-infected cells. *J. Virol.* 76, 8582–8595. doi:10.1128/JVI.76.17.8582-8595.2002.

Hall, R. N., Mahar, J. E., Read, A. J., Mourant, R., Piper, M., Huang, N., et al. (2018). A strain-specific multiplex RT-PCR for Australian rabbit haemorrhagic disease viruses uncovers a new recombinant virus variant in rabbits and hares. *Transbound. Emerg. Dis.* 65, e444–e456. doi:10.1111/tbed.12779.

Han, K. R., Alhatlani, B. Y., Cho, S., Lee, J. H., Hosmillo, M., Goodfellow, I. G., et al. (2017). Identification of amino acids within norovirus polymerase involved in RNA binding and viral replication. *J. Gen. Virol.* 98, 1311–1315. doi:10.1099/jgv.0.000826.

Han, K. R., Choi, Y., Min, B. S., Jeong, H., Cheon, D., Kim, J., et al. (2010). Murine norovirus-1 3Dpol exhibits RNA-dependent RNA polymerase activity and nucleotidylylates on Tyr of the VPg. *J. Gen. Virol.* 91, 1713–1722. doi:10.1099/vir.0.020461-0.

Han, K. R., Lee, J.-H., Kotiguda, G. G., Jung, K. H., Chung, M. S., Kang, S., et al. (2018). Nucleotide triphosphatase and RNA chaperone activities of murine norovirus NS3. *J. Gen. Virol.* 99, 1482–1493. doi:10.1099/jgv.0.001151.

Hirashima, S., Suzuki, T., Ishida, T., Noji, S., Yata, S., Ando, I., et al. (2006). Benzimidazole derivatives bearing substituted biphenyls as hepatitis C virus NS5B RNA-dependent RNA polymerase inhibitors: Structure-activity relationship studies and identification of a potent and highly selective inhibitor JTK-109. *J. Med. Chem.* 49, 4721–4736. doi:10.1021/jm060269e.

Högbom, M., Jäger, K., Robel, I., Unge, T., and Rohayem, J. (2009). The active form of the norovirus RNA-dependent RNA polymerase is a homodimer with cooperative activity. *J. Gen. Virol.* 90, 281–291. doi:10.1099/vir.0.005629-0.

Honda, K., Yanai, H., Negishi, H., Asagiri, M., Sato, M., Mizutani, T., et al. (2005). IRF-7 is the master regulator of type-I interferon-dependent immune responses. *Nature* 434. doi:10.1038/nature03464.

Hurley, K. F., and Sykes, J. E. (2003). Update on feline calicivirus: new trends. *Vet. Clin. North Am. - Small Anim. Pract.* 33, 759–772. doi:10.1016/S0195-5616(03)00025-1.

Jacobo-Molina, A., Ding, J., Nanni, R. G., Clark, A. D., Lu, X., Tantillo, C., et al. (1993). Crystal structure of human immunodeficiency virus type 1 reverse transcriptase complexed with double-stranded DNA at 3.0 A resolution shows bent DNA. *Proc. Natl. Acad. Sci.* 90, 6320–6324. doi:10.1073/pnas.90.13.6320.

Jiang, X., Wang, M., Wang, K., and Estes, M. K. (1993). Sequence and genomic organization of Norwalk virus. *Virology* 195, 51–61. doi:10.1006/viro.1993.1345.

Jin, Z., Smith, L. K., Rajwanshi, V. K., Kim, B., and Deval, J. (2013). The ambiguous base-pairing and high substrate efficiency of T-705 (favipiravir) ribofuranosyl 5′-triphosphate towards influenza A virus polymerase. *PLoS One* 8, 68347. doi:10.1371/journal.pone.0068347.

Jones, D. T., Taylor, W. R., and Thornton, J. M. (1992). The rapid generation of mutation data matrices. doi:doi.org/10.1093/bioinformatics/8.3.275.

Jones, M. K., Grau, K. R., Costantini, V., Kolawole, A. O., De Graaf, M., Freiden, P., et al. (2015). Human norovirus culture in B cells HHS Public Access Author manuscript. *Nat Protoc* 10, 1939–1947. doi:10.1038/nprot.2015.121.

Joyce, C. M., and Steitz, T. A. (1995). Polymerase structures and function: Variations on a theme? *J. Bacteriol.* 177, 6321–6329. doi:10.1128/jb.177.22.6321-6329.1995.

Kaiser, W. J. (2006). Analysis of protein-protein interactions in the feline calicivirus replication complex. *J. Gen. Virol.* 87, 363–368. doi:10.1099/vir.0.81456-0.

Kamer, G., and Argos, P. (1984). Primary structural comparison of RNA-dependent polymerases from plant, animal and bacterial viruses. *Nucleic Acids Res.* 12, 7269–7282. doi:10.1093/nar/12.18.7269.

Kanda, T., Yokosuka, O., Imazeki, F., Tanaka, M., Shino, Y., Shimada, H., et al. (2004). Inhibition of subgenomic hepatitis C virus RNA in Huh-7 cells: Ribavirin induces mutagenesis in HCV RNA. *J. Viral Hepat.* 11, 479–487. doi:10.1111/j.1365-2893.2004.00531.x.

Kao, C. C., Singh, P., and Ecker, D. J. (2001). De novo initiation of viral RNA-dependent RNA synthesis. *Virology* 287, 251–260. doi:10.1006/viro.2001.1039.

König, M., Thiel, H.-J. J., and Meyers, G. (1998). Detection of viral proteins after infection of cultured hepatocytes with rabbit hemorrhagic disease virus. *J. Virol.* 72, 4492–7. doi:<p>10.3732/ajb.90.5.796</p>.

Koonin, E. V. (1991). The phylogeny of RNA-dependent RNA polymerases of positive-strand RNA viruses. *J. Gen. Virol.* 72, 2197–2206. doi:10.1099/0022-1317-72-9-2197.

Kumar, S., Stecher, G., and Tamura, K. (2016). MEGA7: molecular evolutionary genetics analysis version 7.0 for bigger datasets. *Mol. Biol. Evol.* 33, 1870–1874. doi:10.1093/molbev/msw054.

Kundu, P., Raychaudhuri, S., Tsai, W., and Dasgupta, A. (2005). Shutoff of RNA polymerase II transcription by poliovirus involves 3C protease-mediated cleavage of the TATA-binding protein at an alternative site: incomplete shutoff of transcription interferes with efficient viral replication. *J. Virol.* 79, 9702–13. doi:10.1128/JVI.79.15.9702-9713.2005.

L'Homme, Y., Sansregret, R., Plante-Fortier, É., Lamontagne, A. M., Ouardani, M., Lacroix, G., et al. (2009). Genomic characterization of swine caliciviruses representing a new genus of Caliciviridae. *Virus Genes* 39, 66–75. doi:10.1007/s11262-009-0360-3.

Lang, D. M., Zemla, A. T., and Ecale Zhou, C. L. (2013). Highly similar structural frames link the template tunnel and NTP entry tunnel to the exterior surface in RNA-dependent RNA polymerases. *Nucleic Acids Res.* 41, 1464–1482. doi:10.1093/nar/gks1251.

Laurila, M. R. L., Makeyev, E. V., and Bamford, D. H. (2002). Bacteriophage φ6 RNA-dependent RNA polymerase. Molecular details of initiating nucleic acid synthesis without primer. *J. Biol. Chem.* 277, 17117–17124. doi:10.1074/jbc.M111220200.

Lauring, A. S., and Andino, R. (2010). Quasispecies theory and the behavior of RNA viruses. *PLoS Pathog.* 6, 1–8. doi:10.1371/journal.ppat.1001005.

Lee, J. H., Alam, I., Han, K. R., Cho, S., Shin, S., Kang, S., et al. (2011). Crystal structures of murine norovirus-1 RNA-dependent RNA polymerase. *J. Gen. Virol.* 92, 1607–1616. doi:10.1099/vir.0.031104-0.

Lee, J. H., Park, B. S., Han, K. R., Biering, S. B., Kim, S. J., Choi, J., et al. (2018). Insight into the interaction between RNA polymerase and VPg for murine norovirus replication. *Front. Microbiol.* 9. doi:10.3389/fmicb.2018.01466.

Leonard, S., Plante, D., Wittmann, S., Daigneault, N., Fortin, M. G., and Laliberte, J.-F. (2000). Complex formation between potyvirus VPg and translation eukaryotic initiation factor 4E correlates with virus infectivity. doi:10.1128/JVI.74.17.7730-7737.2000.

Leyssen, P., Balzarini, J., De Clercq, E., and Neyts, J. (2005). The predominant mechanism by which ribavirin exerts its antiviral activity in vitro against flaviviruses and paramyxoviruses is mediated by inhibition of IMP dehydrogenase. *J. Virol.* 79, 1943–1947. doi:10.1128/jvi.79.3.1943-1947.2005.

Li, T.-F., Hosmillo, M., Schwanke, H., Shu, T., Wang, Z., Yin, L., et al. (2017). Human norovirus NS3 has RNA helicase and chaperoning activities. *J. Virol.* 92. doi:10.1128/jvi.01606-17.

Lopes, A. M., Dalton, K. P., Magalhães, M. J., Parra, F., Esteves, P. J., Holmes, E. C., et al. (2015). Full genomic analysis of new variant rabbit hemorrhagic disease virus revealed multiple recombination events. *J. Gen. Virol.* 96, 1309–1319. doi:10.1099/vir.0.000070.

Lyle, J. M., Bullitt, E., Bienz, K., and Kirkegaard, K. (2002). Visualization and functional analysis of RNA-dependent RNA polymerase lattices. *Science (80-.).* 296, 2218–2222. doi:10.1126/science.1070585.

Machín, Á., Martín Alonso, J. M., Dalton, K. P., and Parra, F. (2009). Functional differences between precursor and mature forms of the RNA-dependent RNA polymerase from rabbit hemorrhagic disease virus. *J. Gen. Virol.* 90, 2114–2118. doi:10.1099/vir.0.011296-0.

Machín, Á., Martín Alonso, J. M., and Parra, F. (2001). Identification of the amino acid residue involved in rabbit hemorrhagic disease virus VPg uridylylation. *J. Biol. Chem.* 276, 27787–27792. doi:10.1074/jbc.M100707200.

Mahar, J. E., Bok, K., Green, K. Y., and Kirkwood, C. D. (2013). The importance of intergenic recombination in norovirus GII.3 evolution. *J. Virol.* 87, 3687–3698. doi:10.1128/JVI.03056-12.

Mahar, J. E., Hall, R. N., and Holmes, C. (2018). The discovery of three new hare lagoviruses

reveals unexplored viral diversity in this genus. *bioRxiv*. doi:10.1101/466557.

Mahar, J. E., Hall, R. N., Peacock, D., Kovaliski, J., Piper, M., Mourant, R., et al. (2017). Rabbit hemorrhagic disease virus 2 (RHDV2; GI.2) is replacing endemic strains of RHDV in the Australian landscape within 18 months of its arrival. *J. Virol.* 92, 1374–1391. doi:10.1128/jvi.01374-17.

Mahar, J. E., Nicholson, L., Eden, J.-S., Duchêne, S., Kerr, P. J., Duckworth, J., et al. (2016). Benign rabbit caliciviruses exhibit evolutionary dynamics similar to those of their virulent relatives. *J. Virol.* 90, 9317–9329. doi:10.1128/JVI.01212-16.

Mansky, L. M., and Cunningham, K. S. (2000). Virus mutators and antimutators. *Trends Genet.* 16, 512–517. doi:10.1016/S0168-9525(00)02125-9.

Martín Alonso, J. M., Casais, R., Boga, J. a, and Parra, F. (1996). Processing of rabbit hemorrhagic disease virus polyprotein. *J. Virol.* 70, 1261–1265.

Mastrangelo, E., Pezzullo, M., Kramer, D., Germani, F., Petazzi, R., Tarantino, D., et al. (2012). Structure-based inhibition of norovirus RNA-dependent RNA polymerases. *J. Mol. Biol.* 419, 198–210. doi:10.1016/j.jmb.2012.03.008.

McCune, B. T., Tang, W., Lu, J., Eaglesham, J. B., Thorne, L., Mayer, A. E., et al. (2017). Noroviruses co-opt the function of host proteins VAPA and VAPB for replication via a phenylalanine–phenylalanine- acidic-tract-motif mimic in nonstructural viral protein NS1/2. *MBio* 8, 668–685. doi:10.1128/mBio.00668-17.

McFadden, N., Bailey, D., Carrara, G., Benson, A., Chaudhry, Y., Shortland, A., et al. (2011). Norovirus regulation of the innate immune response and apoptosis occurs via the product of the alternative open reading frame 4. *PLoS Pathog.* 7. doi:10.1371/journal.ppat.1002413.

Medvedev, A., Viswanathan, P., May, J., and Korba, B. (2017). Regulation of human norovirus VPg nucleotidylylation by ProPol and nucleoside triphosphate binding by its amino terminal sequence in vitro. *Virology* 503, 37–45. doi:10.1016/j.virol.2017.01.003.

Meyers, G., Wirblich, C., and Thiel, H. J. (1991a). Genomic and subgenomic RNAs of rabbit hemorrhagic disease virus are both protein-linked and packaged into particles. *Virology* 184, 677–686. doi:10.1016/0042-6822(91)90437-G.

Meyers, G., Wirblich, C., and Thiel, H. J. (1991b). Rabbit hemorrhagic disease virus-molecular cloning and nucleotide sequencing of a calicivirus genome. *Virology* 184, 664–676. doi:10.1016/0042-6822(91)90436-F.

Meyers, G., Wirblich, C., Thiel, H. J., and Thumfart, J. O. (2000). Rabbit hemorrhagic disease virus: Genome organization and polyprotein processing of a calicivirus studied after

transient expression of cDNA constructs. *Virology* 276, 349–363. doi:10.1006/viro.2000.0545.

Miller, W. A., and Koev, G. (2000). Synthesis of subgenomic RNAs by positive-strand RNA viruses. *Virology* 273, 1–8. doi:10.1006/viro.2000.0421.

Min, B. S., Han, K. R., Lee, J. I., and Yang, J. M. (2012). cDNA cloning of Korean human norovirus and nucleotidylylation of VPg by norovirus RNA-Dependent RNA polymerase. *J. Microbiol.* 50, 625–630. doi:10.1007/s12275-012-2087-4.

Mitra, T., Sosnovtsev, S. V, and Green, K. Y. (2004). Mutagenesis of tyrosine 24 in the VPg protein is lethal for feline calicivirus. *J. Virol.* 78, 4931–4935. doi:10.1128/JVI.78.9.4931-4935.2004.

Morales, M., Bárcena, J., Ramírez, M. A., Boga, J. A., Parra, F., and Torres, J. M. (2004). Synthesis in vitro of rabbit hemorrhagic disease virus subgenomic RNA by internal initiation on (-)sense genomic RNA: Mapping of a subgenomic promoter. *J. Biol. Chem.* 279, 17013–17018. doi:10.1074/jbc.M313674200.

Morrey, J. D., Taro, B. S., Siddharthan, V., Wang, H., Smee, D. F., Christensen, A. J., et al. (2008). Efficacy of orally administered T-705 pyrazine analog on lethal West Nile virus infection in rodents. *Antiviral Res.* 80, 377–379. doi:10.1016/j.antiviral.2008.07.009.

Neill, J. D. (1990). Nucleotide sequence of a region of the feline calicivirus genome which encodes picornavirus-like RNA-dependent RNA polymerase, cysteine protease and 2C polypeptides. *Virus Res.* 17, 145–160. doi:10.1016/0168-1702(90)90061-F.

Neill, J. D., Meyer, R. F., and Seal, B. S. (1995). Genetic relatedness of the caliciviruses: San Miguel sea lion and vesicular exanthema of swine viruses constitute a single genotype within the Caliciviridae. Available at: https://www.ncbi.nlm.nih.gov/pmc/articles/PMC189190/pdf/694484.pdf

Netzler, N. E., Enosi Tuipulotu, D., Eltahla, A. A., Lun, J. H., Ferla, S., Brancale, A., et al. (2017). Broad-spectrum non-nucleoside inhibitors for caliciviruses. *Antiviral Res.* 146, 65–75. doi:10.1016/j.antiviral.2017.07.014.

Neufeld, K. L., Galarza, J. M., Richards, O. C., Summers, D. F., and Ehrenfeld, E. (1994). Identification of terminal adenylyl transferase activity of the poliovirus polymerase 3Dpol. *J. Virol.* 68, 5811–8.

Ng, K. K. S., Arnold, J. J., and Cameron, C. E. (2008). Structure-function relationships among RNA-dependent RNA polymerases. *Curr. Top. Microbiol. Immunol.* 320, 137–156. doi:10.1007/978-3-540-75157-1_7.

Ng, K. K. S., Cherney, M. M., Vázquez, A. L., Machín, Á., Martín Alonso, J. M., Parra, F., et

al. (2002). Crystal structures of active and inactive conformations of a caliciviral RNA-dependent RNA polymerase. *J. Biol. Chem.* 277, 1381–1387. doi:10.1074/jbc.M109261200.

Ng, K. K. S., Pendás-Franco, N., Rojo, J., Boga, J. A., Machín, Á., Martín Alonso, J. M., et al. (2004). Crystal structure of Norwalk virus polymerase reveals the carboxyl terminus in the active site cleft. *J. Biol. Chem.* 279, 16638–16645. doi:10.1074/jbc.M400584200.

Oka, T., Katayama, K., Ogawa, S., Hansman, G. S., Kageyama, T., Ushijima, H., et al. (2005). Proteolytic Processing of Sapovirus ORF1 Polyprotein. *J. Virol.* 79, 7283–7290. doi:10.1128/JVI.79.12.7283-7290.2005.

Olspert, A., Truve, E., Chaudhry, Y., Hosmillo, M., Peil, L., and Goodfellow, I. (2016). Protein-RNA linkage and posttranslational modifications of feline calicivirus and murine norovirus VPg proteins. *PeerJ* 4, e2134. doi:10.7717/peerj.2134.

Parra, F., and Prieto, M. (1990). Purification and characterization of a Calicivirus as the causative agent of a lethal hemorrhagic disease in rabbits. *J. Virol.* 64, 4013–4015.

Patel, K., Bukh, J., Shi, S. T., Romano, P. R., Barber, G. N., Lai, M. M. C., et al. (2003). Triggering the interferon antiviral response through an IKK-related pathway. *Science (80- .).* 300, 1148–1151.

Pfeiffer, J. K., and Kirkegaard, K. (2003). A single mutation in poliovirus RNA-dependent RNA polymerase confers resistance to mutagenic nucleotide analogs via increased fidelity. doi:10.1073/pnas.1232294100.

Pfeiffer, J. K., and Kirkegaard, K. (2005). Increased fidelity reduces poliovirus fitness and virulence under selective pressure in mice. *PLoS Pathog.* 1, 0102–0110. doi:10.1371/journal.ppat.0010011.

Pierra, C., Amador, A., Benzaria, S., Cretton-Scott, E., D'Amours, M., Mao, J., et al. (2006). Synthesis and pharmacokinetics of valopicitabine (NM283), an efficient prodrug of the potent anti-HCV agent 2′-C-methylcytidine. *J. Med. Chem.* 49, 6614–6620. doi:10.1021/jm0603623.

Poch, O., Sauvaget, I., Delarue, M., and Tordo, N. (1989). Identification of four conserved motifs among the RNA-dependent polymerase encoding elements. *EMBO J.* 8, 3867–74. doi:10.1093/emboj/16.6.1248.

Prasad, B. V. V., Hardy, M. E., Dokland, T., Bella, J., Rossmann, M. G., and Estes, M. K. (1999). X-ray crystallographic structure of the Norwalk virus capsid. *Science (80-.).* 286, 287–290. doi:10.1126/science.286.5438.287.

Prasad, B. V. V., Matson, D. O., and Smith, A. W. (1994). Three-dimensional structure of

calicivirus. *J. Mol. Biol.* 240, 256–264. doi:10.1006/jmbi.1994.1439.

Ranjith-Kumar, C. T., Gajewski, J., Gutshall, L., Maley, D., Sarisky, R. T., and Cheng Kao, C. (2001). Terminal nucleotidyl transferase activity of recombinant flaviviridae RNA-dependent RNA polymerases: implication for viral RNA synthesis. *J. Virol.* 75, 8615–8623. doi:10.1128/JVI.75.18.8615-8623.2001.

Ranjith-Kumar, C. T., Kim, Y.-C., Gutshall, L., Silverman, C., Khandekar, S., Sarisky, R. T., et al. (2002). Mechanism of de novo initiation by the hepatitis C virus RNA-dependent RNA polymerase: role of divalent metals. *J. Virol.* 76, 12513–12525. doi:10.1128/JVI.76.24.12513-12525.2002.

Rocha-Pereira, J., Jochmans, D., Dallmeier, K., Leyssen, P., Cunha, R., Costa, I., et al. (2012a). Inhibition of norovirus replication by the nucleoside analogue 2'-C-methylcytidine. *Biochem. Biophys. Res. Commun.* 427, 796–800. doi:10.1016/j.bbrc.2012.10.003.

Rocha-Pereira, J., Jochmans, D., Dallmeier, K., Leyssen, P., Nascimento, M. S. J., and Neyts, J. (2012b). Favipiravir (T-705) inhibits in vitro norovirus replication. *Biochem. Biophys. Res. Commun.* 424, 777–780. doi:10.1016/j.bbrc.2012.07.034.

Rocha-Pereira, J., Verbeken, E., Jochmans, D., Nascimento, M. S. J., Debing, Y., and Neyts, J. (2013). The viral polymerase inhibitor 2'-C-methylcytidine inhibits norwalk virus replication and protects against norovirus-induced diarrhea and mortality in a mouse model. *J. Virol.* 87, 11798–11805. doi:10.1128/jvi.02064-13.

Rohayem, J., Jäger, K., Robel, I., Scheffler, U., Temme, A., and Rudolph, W. (2006a). Characterization of norovirus 3Dpol RNA-dependent RNA polymerase activity and initiation of RNA synthesis. *J. Gen. Virol.* 87, 2621–2630. doi:10.1099/vir.0.81802-0.

Rohayem, J., Robel, I., Jager, K., Scheffler, U., and Rudolph, W. (2006b). Protein-primed and de novo initiation of RNA synthesis by norovirus 3Dpol. *J. Virol.* 80, 7060–7069. doi:10.1128/JVI.02195-05.

Ruis, C., Brown, L.-A. K., Roy, S., Atkinson, C., Williams, R., Burns, S., et al. (2018). Mutagenesis in norovirus in response to favipiravir treatment. *N. Engl. J. Med.* 22. doi:10.1056/NEJMc1806941.

Ruis, C., Roy, S., Brown, J. R., Allen, D. J., Goldstein, R. A., and Breuer, J. (2017). The emerging GII.P16-GII.4 Sydney 2012 norovirus lineage is circulating worldwide, arose by late-2014 and contains polymerase changes that may increase virus transmission. *PLoS One* 12. doi:10.1371/journal.pone.0179572.

Sanjuán, R., and Domingo-Calap, P. (2016). Mechanisms of viral mutation. *Cell. Mol. Life Sci.* 73, 4433–4448. doi:10.1007/s00018-016-2299-6.

Schlegel, A., Giddings, T. H., Ladinsky, M. S., and Kirkegaard, K. (1996). Cellular origin and ultrastructure of membranes induced during poliovirus infection. *J. Virol.* 70, 6576–88.

Schwartz, S., Vergoulidou, M., Schreier, E., Loddenkemper, C., Reinwald, M., Schmidt-Hieber, M., et al. (2011). Norovirus gastroenteritis causes severe and lethal complications after chemotherapy and hematopoietic stem cell transplantation. *Blood* 117, 5850–5856. doi:10.1182/blood-2010-12-325886.

Selisko, B., Papageorgiou, N., Ferron, F., and Canard, B. (2018). Structural and functional basis of the fidelity of nucleotide selection by flavivirus RNA-dependent RNA polymerases. *Viruses* 10. doi:10.3390/v10020059.

Sharp, T. M., Guix, S., Katayama, K., Crawford, S. E., and Estes, M. K. (2010). Inhibition of cellular protein secretion by norwalk virus nonstructural protein p22 requires a mimic of an endoplasmic reticulum export signal. *PLoS One* 5, 13130. doi:10.1371/journal.pone.0013130.

Shivanna, V., Kim, Y., and Chang, K. O. (2014a). Endosomal acidification and cathepsin L activity is required for calicivirus replication. *Virology* 464–465, 287–295. doi:10.1016/j.virol.2014.07.025.

Shivanna, V., Kim, Y., and Chang, K. O. (2014b). The crucial role of bile acids in the entry of porcine enteric calicivirus. *Virology* 456–457, 268–278. doi:10.1016/j.virol.2014.04.002.

Simmonds, P., Karakasiliotis, I., Bailey, D., Chaudhry, Y., Evans, D. J., and Goodfellow, I. G. (2008). Bioinformatic and functional analysis of RNA secondary structure elements among different genera of human and animal caliciviruses. *Nucleic Acids Res.* 36, 2530–2546. doi:10.1093/nar/gkn096.

Sit, T. L., Vaewhongs, A. A., and Lommel, S. A. (1998). RNA-mediated trans-activation of transcription from a viral RNA. *Science (80-.).* 281, 829–832. doi:10.1126/science.281.5378.829.

Sosnovtseva, S. a, Sosnovtsev, S. V, and Green, K. Y. (1999). Mapping of the feline calicivirus proteinase responsible for autocatalytic processing of the nonstructural polyprotein and identification of a stable proteinase-polymerase precursor protein. *J. Virol.* 73, 6626–6633.

Sosnovtsev, S. V, Belliot, G., Chang, K.-O., Onwudiwe, O., and Green, K. Y. (2005). Feline calicivirus VP2 is essential for the production of infectious virions. *J. Virol.* 79, 4012–4024. doi:10.1128/JVI.79.7.4012-4024.2005.

Steitz, T. A. (1998). A mechanism for all polymerases. *Nature* 391, 231–232. doi:10.1038/34542.

Strive, T., Wright, J., Kovaliski, J., Botti, G., and Capucci, L. (2010). The non-pathogenic

Australian lagovirus RCV-A1 causes a prolonged infection and elicits partial cross-protection to rabbit haemorrhagic disease virus. *Virology* 398, 125–134. doi:10.1016/j.virol.2009.11.045.

Subba-Reddy, C. V., Yunus, M. A., Goodfellow, I. G., and Kao, C. C. (2012). Norovirus RNA synthesis is modulated by an interaction between the viral RNA-dependent RNA polymerase and the major capsid protein, VP1. *J. Virol.* 86, 10138–10149. doi:10.1128/JVI.01208-12.

Subba-Reddy, C. V., Yunus, M. A., Goodfellow, I. G., and Kao, C. C. (2017). Retraction for Subba-Reddy et al., "Norovirus RNA synthesis is modulated by an interaction between the viral RNA-dependent RNA polymerase and the major capsid protein, VP1". *J Virol* 91. doi:10.1128/JVI.01708-17.

Subba-Reddy, C. V, Goodfellow, I., and Cheng Kao, C. (2011). VPg-primed RNA synthesis of norovirus RNA-dependent RNA polymerases by using a novel cell-based assay. *J. Virol.* 85, 13027–13037. doi:10.1128/JVI.06191-11.

Swanstrom, J., Lindesmith, L. C., Donaldson, E. F., Yount, B., and Baric, R. S. (2013). Characterization of blockade antibody responses in GII.2.1976 Snow mountain virus-infected subjects. *J. Virol.* 88, 829–837. doi:10.1128/jvi.02793-13.

Tarantino, D., Pezzullo, M., Mastrangelo, E., Croci, R., Rohayem, J., Robel, I., et al. (2014). Naphthalene-sulfonate inhibitors of human norovirus RNA-dependent RNA-polymerase. *Antiviral Res.* 102, 23–28. doi:10.1016/j.antiviral.2013.11.016.

Thumfart, J. O., and Meyers, G. (2002). Rabbit hemorrhagic disease virus: Identification of a cleavage site in the viral polyprotein that is not processed by the known calicivirus protease. *Virology* 304, 352–363. doi:10.1006/viro.2002.1660.

Urakova, N., Frese, M., Hall, R. N., Liu, J., Matthaei, M., and Strive, T. (2015). Expression and partial characterisation of rabbit haemorrhagic disease virus non-structural proteins. *Virology* 484, 69–79. doi:10.1016/j.virol.2015.05.004.

Urakova, N., Netzler, N., Kelly, A. G., Frese, M., White, P. A., and Strive, T. (2016). Purification and biochemical characterisation of rabbit calicivirus RNA-dependent RNA polymerases and identification of non-nucleoside inhibitors. *Viruses* 8. doi:10.3390/v8040100.

Urakova, N., Strive, T., and Frese, M. (2017a). RNA-dependent RNA polymerases of both virulent and benign Rabbit caliciviruses induce striking rearrangement of Golgi membranes. *PLoS One* 12, 1–15. doi:10.1371/journal.pone.0169913.

Urakova, N., Warden, A. C., White, P. A., Strive, T., and Frese, M. (2017b). A motif in the F

homomorph of rabbit haemorrhagic disease virus polymerase is important for the subcellular localisation of the protein and its ability to induce redistribution of golgi membranes. *Viruses* 9, 202. doi:10.3390/v9080202.

Vashist, S., Bailey, D., Putics, A., and Goodfellow, I. (2009). Model systems for the study of human norovirus biology. *Future Virol.* 4, 353–367. doi:10.2217/fvl.09.18.

Vazquez, A. L., Alonso, J. M. M., Casais, R., Boga, J. A., and Parra, F. (1998). Expression of enzymatically active rabbit hemorrhagic disease virus RNA-dependent RNA polymerase in Escherichia coli. *J. Virol.* 72, 2999–3004. doi:10.7551/mitpress/9780262033589.003.0011.

Voogd, T. E., Vansterkenburg, E. L. M., Wilting, J., and Janssen, L. H. M. (1993). Recent research on the biological activity of Suramin. *Pharmacol. Rev.* 45.

Wang, F., Wang, M., Dong, Y., Zhang, B., and Zhang, D. (2017). Genetic characterization of a novel calicivirus from a goose. *Arch. Virol.* 162, 2115–2118. doi:10.1007/s00705-017-3302-8.

Ward, C. D., Stokes, M. A., and Flanegan, J. B. (1988). Direct measurement of the poliovirus RNA polymerase error frequency in vitro. *J. Virol.* 62, 558–62.

Wei, L., Huhn, J. S., Mory, A., Pathak, H. B., Sosnovtsev, S. V., Green, K. Y., et al. (2001). Proteinase-polymerase precursor as the active form of feline calicivirus RNA-dependent RNA polymerase. *J. Virol.* 75, 1211–1219. doi:10.1128/JVI.75.3.1211-1219.2001.

Weir, M. L., Klip, A., and Trimble, W. S. (1998). Identification of a human homologue of the vesicle-associated membrane protein (VAMP)-associated protein of 33 kDa (VAP-33): a broadly expressed protein that binds to VAMP. *Biochem. J.* 333, 247–51. doi:10.1042/bj3330247.

Wirblich, C., Thiel, H. J., and Meyers, G. (1996). Genetic map of the calicivirus rabbit hemorrhagic disease virus as deduced from in vitro translation studies. *J. Virol.* 70, 7974–83. doi:10.1006/viro.2000.0579.

Witkowski, J. T., Robins, R. K., Sidwell, R. W., and Simon, L. N. (1972). Design, synthesis, and broad spectrum antiviral activity of 1-β-D-ribofuranosyl-1,2,4-triazole-3-carboxamide and related nucleosides. *J. Med. Chem.* 15.

Wobus, C. E., Karst, S. M., Thackray, L. B., Chang, K. O., Sosnovtsev, S. V., Belliot, G., et al. (2004). Replication of Norovirus in cell culture reveals a tropism for dendritic cells and macrophages. *PLoS Biol.* 2. doi:10.1371/journal.pbio.0020432.

Wobus, C. E., Thackray, L. B., and Virgin, H. W. (2006). Murine norovirus: a model system to study norovirus biology and pathogenesis. *J. Virol.* 80, 5104–5112.

doi:10.1128/JVI.02346-05.

Wu, G., and Kaper, J. M. (1994). Requirement of 3'-terminal guanosine in (−)-stranded RNA for in vitro replication of cucumber mosaic virus satellite rna by viral RNA-dependent RNA polymerase. *J. Mol. Biol.* 238, 655–657. doi:10.1006/jmbi.1994.1326.

Wu, H., Zu, S., Sun, X., Liu, Y., Tian, J., and Qu, L. (2016). N-terminal domain of feline calicivirus (FCV) proteinase-polymerase contributes to the inhibition of host cell transcription. *Viruses* 8. doi:10.3390/v8070199.

Xie, X., Wang, H., Zeng, J., Li, C., Zhou, G., Yang, D., et al. (2014). Foot-and-mouth disease virus low-fidelity polymerase mutants are attenuated. *Arch. Virol.* 159, 2641–2650. doi:10.1007/s00705-014-2126-z.

Yang, X., Smidansky, E. D., Maksimchuk, K. R., Lum, D., Welch, J. L., Arnold, J. J., et al. (2012). Motif D of viral RNA-dependent RNA polymerases determines efficiency and fidelity of nucleotide addition. *Structure* 20, 1519–1527. doi:10.1016/j.str.2012.06.012.

Yunus, M. A., Lin, X., Bailey, D., Karakasiliotis, I., Chaudhry, Y., Vashist, S., et al. (2015). The Murine norovirus core subgenomic RNA promoter consists of a stable stem-loop that can direct accurate initiation of RNA synthesis. *J. Virol.* 89, 1218–1229. doi:10.1128/JVI.02432-14.

Zamyatkin, D. F., Parra, F., Martín Alonso, J. M., Harki, D. A., Peterson, B. R., Grochulski, P., et al. (2008). Structural insights into mechanisms of catalysis and inhibition in Norwalk virus polymerase. *J. Biol. Chem.* 283, 7705–7712. doi:10.1074/jbc.M709563200.

Zeng, J., Wang, H., Xie, X., Li, C., Zhou, G., Yang, D., et al. (2014). Ribavirin-resistant variants of foot-and-mouth disease virus: the effect of restricted quasispecies diversity on viral virulence. *J. Virol.* 88, 4008–4020. doi:10.1128/JVI.03594-13.

Zhu, J., Miao, Q., Tan, Y., Guo, H., Liu, T., Wang, B., et al. (2017). Inclusion of an Arg-Gly-Asp receptor-recognition motif into the capsid protein of rabbit hemorrhagic disease virus enables culture of the virus in vitro. *J. Biol. Chem.* 292, 8605–8615. doi:10.1074/jbc.M117.780924.

Chapter 3. Calicivirus non-structural proteins: potential functions in replication and host cell manipulation

Declaration of Co-Authored Publications

UNIVERSITY OF CANBERRA

For use in theses which include co-authored publications. This declaration must be completed for each co-authored publication and to be placed at the start of the thesis chapter in which the publication appears, or as a preface to the thesis.

Declaration for Thesis Chapter 3

DECLARATION BY CANDIDATE

Declaration for the following publication: Calicivirus Non-structural Proteins: Potential Functions in Replication and Host Cell Manipulation. Front. Microbiol., 14 July 2021 | https://doi.org/10.3389/fmicb.2021.712710

Nature of Contribution	Extent of Contribution (%)
Conceived the idea, performed literature search, wrote the first draft and addressed reviewers' comments	70%

The following co-authors contributed to the work:

Name	Nature of Contribution	Contributor is also a UC student (Yes/No)
Robyn N. Hall	Prepared some of the figures and helped with the review structure, contributed to writing and revision of the manuscript	No
Nadya Urakova	Helped with literature search, revised the manuscript	No
Tanja Strive	Supervisor, helped with the review structure and revised the manuscript	No
Michael Frese	Supervisor, helped with the review structure and figures, revised the manuscript	No

Candidate's Signature   Date 21/04/2022

DECLARATION BY CO-AUTHORS

The undersigned hereby certify that:

(1) the above declaration correctly reflects the nature and extent of the candidate's contribution to this work, and the nature of the contribution of each of the co-authors.

(2) they meet the criteria for authorship in that they have participated in the conception, execution, or interpretation, of at least that part of the publication in their field of expertise;

(3) they take public responsibility for their part of the publication, except for the responsible author who accepts overall responsibility for the publication;

(4) there are no other authors of the publication according to these criteria.

(5) potential conflicts of interest have been disclosed to (a) granting bodies, (b) the editor or publisher of journals or other publications, and (c) the head of the responsible academic unit; and

(6) the original data are stored at the following location(s) and will be held for at least five years from the date indicated below:

[Please note that the location(s) must be institutional in nature, and should be indicated here as a department, centre or institute, with specific campus identification where relevant.]

Location(s):   CSIRO Black Mountain; University of Canberra

Signatures	Date
	20/04/2022
Nadya Urakova	20/04/2022
(Michael Frese)	20-04-2022
	22/04/2022

1 of 1

73

Calicivirus Non-Structural Proteins: Potential Functions in Replication and Host Cell Manipulation

Elena Smertina[1,2], Robyn N. Hall[1], Nadya Urakova[3], Tanja Strive[1,4], Michael Frese[1,2*]

[1] Commonwealth Scientific and Industrial Research Organisation, Health and Biosecurity, Canberra, ACT, Australia

[2] Faculty of Science and Technology, University of Canberra, Canberra, ACT, Australia

[3] Leiden University Medical Center, Leiden, The Netherlands

[4] Centre for Invasive Species Solutions, Canberra, ACT, Australia

* Correspondence:
  Michael Frese
  michael.frese@canberra.edu.au

Abstract

The *Caliciviridae* are a family of viruses with a single-stranded, non-segmented RNA genome of positive polarity. The ongoing discovery of caliciviruses has increased the number of genera in this family to 11 (*Norovirus*, *Nebovirus*, *Sapovirus*, *Lagovirus*, *Vesivirus*, *Nacovirus*, *Bavovirus*, *Recovirus*, *Salovirus*, *Minovirus*, and *Valovirus*). Caliciviruses infect a wide range of hosts that include fish, amphibians, reptiles, birds, and marine and land mammals. All caliciviruses have a genome that encodes a major and a minor capsid protein, a genome-linked viral protein, and several non-structural proteins. Of these non-structural proteins, only the helicase, protease, and RNA-dependent RNA polymerase share clear sequence and structural similarities with proteins from other virus families. In addition, all caliciviruses express two or three non-structural proteins for which functions have not been clearly defined. The sequence diversity of these non-structural proteins and a multitude of processing strategies suggest that at least some have evolved independently, possibly to counteract innate and adaptive immune responses in a host-specific manner. Studying these proteins is often difficult as many caliciviruses cannot be grown in cell culture. Nevertheless, the study of recombinant proteins has revealed many of their properties, such as intracellular localization, capacity to oligomerize, and ability to interact with viral and/or cellular proteins. Whether transfected cells secrete non-structural proteins has also been investigated. Here we will summarize these findings and discuss recent *in silico* studies that identified previously overlooked putative functional domains and structural features, including transmembrane domains that suggest the presence of viroporins.

Introduction

The *Caliciviridae* family of highly diverse RNA viruses currently includes 11 genera, i.e., *Norovirus*, *Nebovirus*, *Sapovirus*, *Lagovirus*, *Vesivirus*, *Nacovirus*, *Bavovirus*, *Recovirus*, *Salovirus*, *Minovirus*, and *Valovirus* (Vinjé et al., 2019; Desselberger, 2019). Viruses of the genera *Norovirus*, *Nebovirus*, *Sapovirus*, *Lagovirus*, *Recovirus*, and *Valovirus* are enteric viruses of mammals. Some of these viruses are associated with severe gastroenteritis or systemic disease, while others cause only mild or asymptomatic infections. Noroviruses cause an estimated 684 million gastroenteritis episodes and 200,000 deaths annually imposing a significant economic burden (Bartsch et al., 2016; Kirk et al., 2015; Pires et al., 2015). Human norovirus and sapovirus infections can also lead to chronic disease and are often associated with severe complications, especially in the elderly, very young, and immunocompromised patients (Petrignani et al., 2018; Wright et al., 2020). Neboviruses are enteric pathogens of cattle in which mortality rates reach up to 30% (Alkan et al., 2015). *Tulane virus* (genus *Recovirus*; Farkas et al., 2008) was isolated from stool samples of rhesus macaques; another recovirus (Bangladesh/289/2007) was later discovered from human patients with diarrhea in Bangladesh (Smits et al., 2012). Remarkably, and in contrast to other human caliciviruses, *Tulane virus* easily propagates in cell culture (Farkas, 2015), which promises to turn this newly discovered virus into an important model for enteric caliciviruses. Valoviruses were first isolated from the faeces of asymptomatic farmed pigs; these viruses were named St. Valerien-like viruses and were found to be closely related to noroviruses and recoviruses (L'Homme et al., 2009). Bavoviruses and nacoviruses were recovered from faeces and intestinal contents of poultry—chicken, turkey, and geese (Liao et al., 2014; S. Wolf et al., 2012). The *Rabbit calicivirus* (RCV) is an enteric lagovirus (the name makes a reference to the narrow host range of these viruses; they infect only members of the order Lagomorpha, i.e., hares, rabbits, and pikas). RCV usually causes asymptomatic infections in rabbits in contrast to many other lagoviruses that have been discovered to date (Strive et al., 2010).

Pathogenic lagoviruses, including *Rabbit hemorrhagic disease virus* (RHDV) and *European brown hare syndrome virus* (EBHSV), are hepatotropic and cause a peracute hepatitis with mortality rates approaching 100% (Abrantes et al., 2012b; Hall et al., 2017). Vesiviruses are the caliciviruses with the widest host range; so far, viruses have been isolated from cats (*Feline calicivirus*, FCV), pigs (*Vesicular exanthema of swine virus*, VESV), and seals (*San Miguel sea lion virus*-8, SMSV-8) (Neill, 2014; Oglesby et al., 1971; Radford et al., 2007). Infection with vesiviruses can cause multiple organ failure, vesicular lesions, and respiratory and reproductive system diseases, depending on virus and host species (Radford et al., 2007). Saloviruses and

minoviruses are viruses that infect fish. *Atlantic salmon calicivirus* (ASCV, genus *Salovirus*) was isolated from heart tissue of farmed Atlantic salmons with symptoms of heart and skeletal muscle inflammation (Mikalsen et al., 2014). *Fathead minnow calicivirus* (FHMCV, genus *Minovirus*) was first identified in diseased fathead minnows with widespread hemorrhaging; however, all analyzed fish samples showed a co-infection with fathead minnow picornavirus. Thus, further studies are needed to elucidate whether FHMCV is associated with haemorrhagic disease or requires a co-infection to cause the disease (Mor et al., 2017).

Picornaviridae and *Caliciviridae* are closely related families of the order *Picornavirales*, which comprises non-enveloped viruses with a positive-sense RNA genome. Both families translate a polyprotein that is cleaved by viral proteases, a process that, in some caliciviruses, is assisted by cellular proteases (Sosnovtsev et al., 2006; Thumfart & Meyers, 2002). In the case of caliciviruses, mature non-structural proteins include the RNA-dependent RNA polymerase (RdRp), a 3C-like protease, VPg (virion protein, genome-linked), a helicase (NTPase), and several poorly characterized non-structural proteins that can be termed NS1, NS2, and NS4. The overall gene organization of caliciviruses resembles that of picornaviruses with one major difference (**Figure 1**). In caliciviruses, the coding sequence for the capsid proteins is located at the 3'-end, while in picornaviruses, the capsid genes precede the polyprotein and are the first to be translated. Thus, the positional homologues of the calicivirus non-structural proteins NS1, NS2, and NS4 in picornaviruses are 2A, 2B, and 3A, respectively.
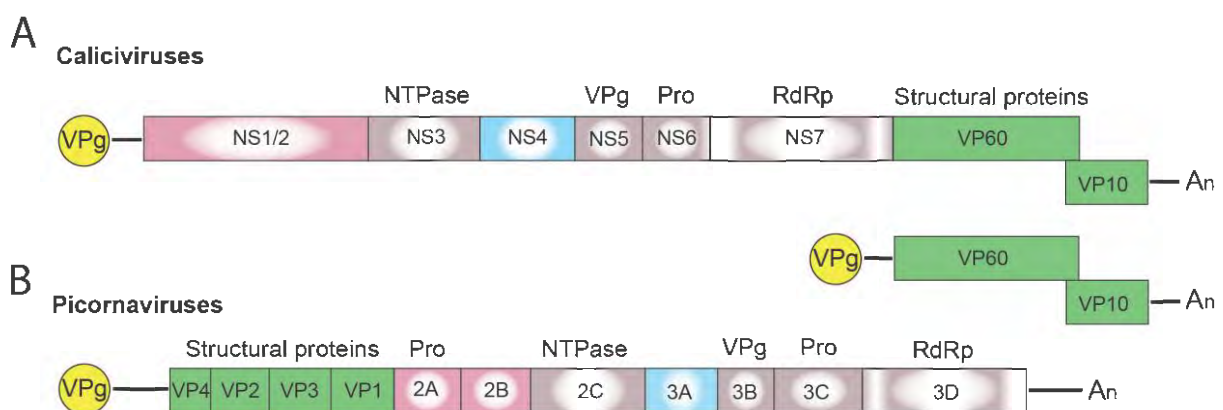
Figure 1. Schematic representation of the genome organization for a typical (A) calicivirus and (B) picornavirus. Untranslated and translated sequences are depicted as lines and boxes, respectively. Structural (capsid) proteins are shown in green, the signature proteins of the picornavirus-like superfamily are shown in grey, namely the helicase (NTPase), VPg, protease (Pro) and the RNA-dependent RNA polymerase (RdRp), the non-structural calicivirus proteins NS1/2 and their positional homologues in picornaviruses (2A, 2B) are shown in pink, and the

non-structural calicivirus protein NS4 and its homologue in picornaviruses (3A) are shown in blue. Covalently linked VPg proteins at the 5'end are shown in yellow, and An represents the poly(A) tail at the 3' end.

The genetic material of all caliciviruses consists of two types of positive-sense, single-stranded RNA molecules, full-length genomic and subgenomic RNAs (by contrast, picornaviruses produce only full-length genomic RNA). Calicivirus particles contain a single copy of genomic RNA (ca 7.5 kb) and one or more copies of a subgenomic RNA (ca 2 kb) (Ehresmann and Schaffer, 1977; Meyers et al., 1991a, b). Both RNAs have a 5′ end that is covalently linked to VPg, a polyadenylated 3′ end, and coding sequences in two or more partially overlapping open reading frames (ORFs) that are flanked by untranslated regions (UTRs). While the genomic full-length RNA encodes all structural and non-structural proteins, the subgenomic RNA encodes only the structural proteins VP1 and VP2. In caliciviruses, the subgenomic RNA ensures efficient particle formation through the translation of additional capsid proteins (Miller & Koev, 2000). It is tempting to speculate that picornaviruses do not require subgenomic RNAs, as the positioning of the coding sequences for the structural proteins at the 5′ end increases protein output. Why caliciviruses have evolved a different coding strategy is not clear, however having a small RNA molecule for the enhanced expression of structural proteins may allow for more sophisticated control of protein production (Meyers, 2003).

The functions of the calicivirus RdRp, protease, helicase, and VPg have been identified based on sequence similarities to homologous proteins from picornaviruses and other positive-sense single-stranded RNA viruses (Clarke & Lambden, 1997; Lambden & Clarke, 1995; Neill, 1990). The presence of conserved motifs and domains in these proteins often indicates the function of the protein (e.g., almost all RNA polymerases have a GDD motif in their active site). The RdRp replicates the viral genome, a process that, due to the lack of proof reading, constantly generates considerable genetic drift. The resulting gradual change to the genome determines the base speed of virus evolution, which can be accelerated by recombination events that occur either via template switching, most commonly at the junction of RdRp and structural protein genes, and less commonly elsewhere in the genome (Mahar et al., 2013). The calicivirus protease, also referred to as the 3C-like protease after its counterpart in picornaviruses, participates in the proteolytic cleavage of the viral polyprotein (Boniotti et al., 1994). The calicivirus helicase unwinds double-stranded RNA intermediates in an ATP-dependent reaction during viral replication (similar to homologous proteins in other viruses). However, the

calicivirus helicase has additional functions. It acts as an RNA chaperone that remodels structured RNA in an ATP-independent manner (Li et al., 2017), and it facilitates the formation of vesicular structures that house the replication complexes (Cotton et al., 2016). The VPg protein is usually listed among the non-structural proteins, but as it is covalently bound to the 5'-end of both genomic and subgenomic RNAs and is therefore present in mature virus particles, it could arguably be categorized as a structural protein. In infected cells, the VPg serves as a primer for the replication of the viral genome and plays a critical role in the initiation of translation (Goodfellow, 2011; Herbert et al., 1997). The functions of the remaining non-structural proteins (i.e., NS1/2, NS1, NS2, and NS4) are more challenging to determine, as they lack sequence homologies to other proteins. Even within the *Caliciviridae* family, the sequence diversity is so great that non-structural protein sequences cannot be used to produce meaningful phylogenetic trees, except for sequences from closely related viruses (**Figure 2B** and **2C**). Highly conserved RdRp sequences, in contrast, are much more suitable for phylogenetic analyses (Koonin, 1991; Y. I. Wolf et al., 2018) (**Figure 2A**). The location of the non-structural protein genes in the viral genome, however, is rather conserved. In all caliciviruses, the coding sequence of NS1/2 is located at the 5'end, while the NS4 sequence follows the helicase sequence. Some, but not all, NS1/2 proteins undergo proteolytic cleavage. In vesiviruses, lagoviruses, neboviruses, and sapoviruses, the NS1/2 precursor protein is cleaved by viral and/or host cell proteases, generating the proteins NS1 and NS2. In other viruses the cleavage efficiency is less clear and more stable precursor proteins may exist.

Although function(s) of the non-structural proteins NS1/2 and NS4 remain elusive, recent studies suggest that mutations in their coding sequences may influence tissue tropism, virulence, and epidemiological fitness. For example, Mahar and co-workers (2021) provided evidence for a role of NS proteins in epidemiological fitness while investigating the evolution of lagoviruses. The recent introduction of the highly pathogenic RHDV2 to Australia quickly led to the emergence of recombinant lagoviruses that contain the capsid genes of RHDV2, and the non-structural protein coding sequences of non-pathogenic RCV strains that had been circulating in Australian rabbits for some time. These recombinants are hepatotropic and pathogenic (as is the parental RHDV2), suggesting that phenotype and tropism is conferred by the structural genes. Furthermore, the new recombinant strains quickly replaced RHDV2, which suggests that the non-structural proteins are important drivers of epidemiological fitness (Mahar et al., 2021). It would be interesting to extend these studies and explore which non-structural proteins are responsible for the evolutionary success of the recombinant lagovirus strains. Non-structural proteins have also been shown to influence the tissue tropism in some caliciviruses.

For example, in *Murine norovirus* (MNV), a single amino acid substitution in NS1 is associated with better virus growth and persistent infection of the proximal colon. A non-persistent strain becomes persistent with a single change of aspartic acid to glutamic acid (D93E) in NS1 (Nice et al., 2013). Clearly, evidence is mounting for a role of the non-structural proteins as a key determinant of pathogenicity and epidemiological fitness. In this review we summarize the current knowledge of these calicivirus proteins.
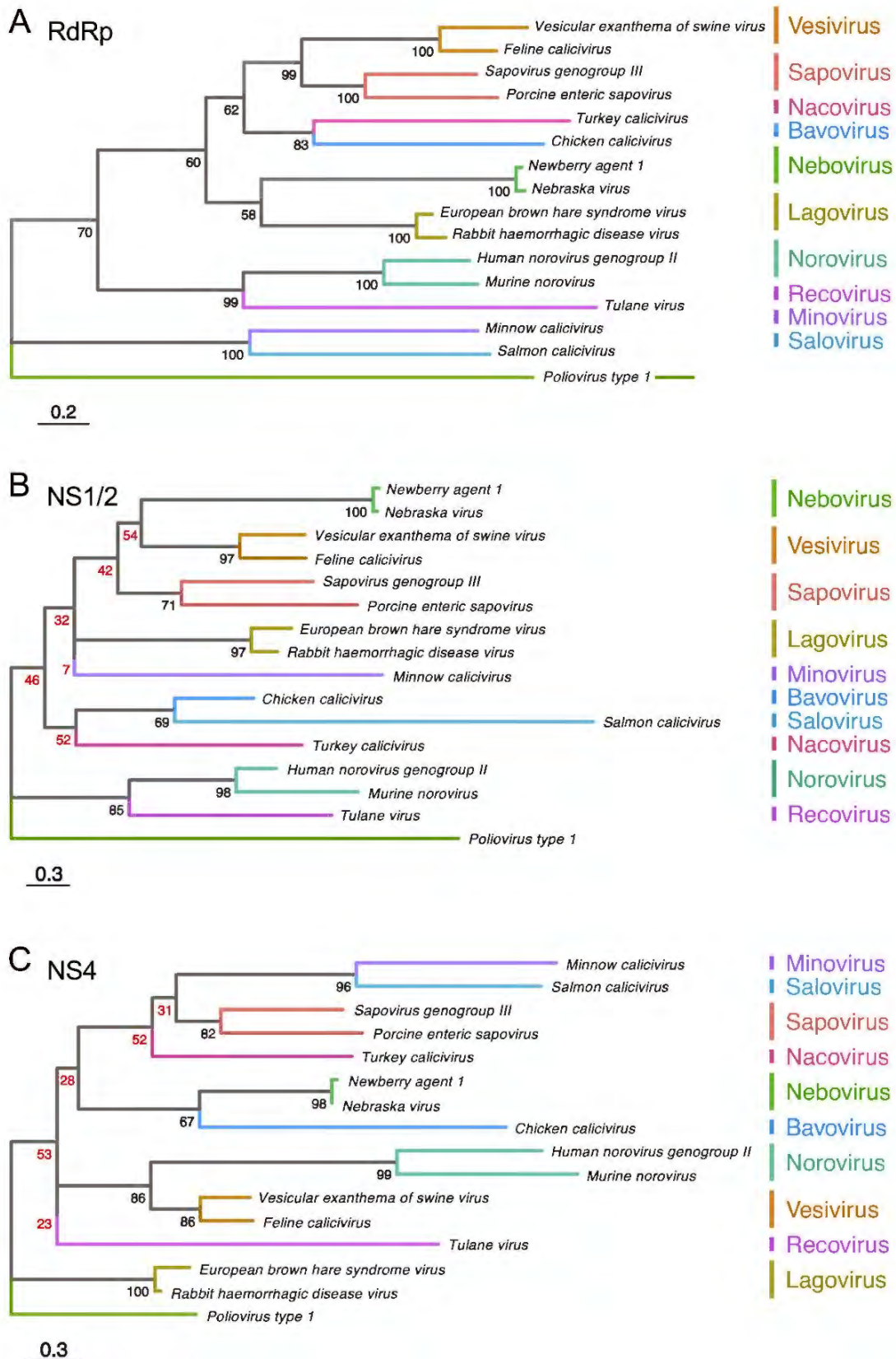
Figure 2. Phylogenetic analysis of calicivirus protein sequences. Maximum likelihood phylogenies were inferred for amino acid sequences of (**A**) RdRp, (**B**) NS1/2, and (**C**) NS4. First, the amino acid sequences of the complete ORF1 coding region of representative published

calicivirus sequences were aligned using MAFFT (Katoh et al., 2002). The alignment was then curated with trimal (Capella-Gutiérrez et al., 2009). The RdRp, NS1/2, and NS4 coding regions were extracted from this complete ORF1 alignment and phylogenies were inferred individually for each gene using IQ-TREE (Nguyen et al., 2015). Phylogenies were rooted using *Poliovirus type 1* (GenBank accession NC_002058). The following sequences were chosen for calicivirus genera: *Vesicular exanthema of swine virus* (NC_002551), *Feline calicivirus* (NC_001481), *Sapovirus genogroup III* (MG012434), *Porcine enteric sapovirus* (NC_000940), *Turkey calicivirus* (NC_043516), *Chicken calicivirus* (NC_033081), *Newbury agent 1* (NC_007916), *Nebraska virus* (NC_004064), *Rabbit haemorrhagic disease virus* (NC_001543), *European brown hare syndrome virus* (NC_002615), *Tulane virus* (NC_043512), *Human norovirus genogroup II* (NC_039477), *Murine norovirus* (NC_008311), *Minnow calicivirus* (NC_035675) and *Salmon calicivirus* (NC_024031). The tree is drawn to scale, with branch lengths measured in the number of substitutions per site. Ultrafast bootstrap values are shown for each node. Low confidence bootstrap values are highlighted in red.

Non-structural protein processing and secretion

The polyprotein of all caliciviruses is cleaved by the 3C-like virus protease into the non-structural proteins NS1/2, helicase, NS4, VPg, 3C-like protease, and the RdRp (**Figure 3**). In RHDV, FCV, and human sapovirus infected cells, the NS1/2 precursor is also cleaved by the 3C-like protease (Oka et al., 2005; Sosnovtsev et al., 2002; Wirblich et al., 1996). In contrast, the norovirus NS1/2 precursor is not processed further by the 3C-like protease (B. Liu et al., 1996). However, when the processing of a recombinant MNV NS1/2 precursor was analyzed *in vitro*, it was discovered that a cellular protease, caspase-3, cleaves the protein (Sosnovtsev et al., 2006). Subsequently, a cleavage site homologue was identified in human noroviruses and it was discovered that both the human norovirus and MNV secrete NS1 after the precursor has been cleaved (Lee et al., 2019). The cleavage occurs only at the late stages of viral life cycle (18–22 h post-infection) and is concurrent with activation of apoptosis (Robinson et al., 2019). Moreover, this process is required for intestinal tropism and persistence. A persistent MNV strain with a deleted caspase-3 cleavage site replicated less efficiently in the ileum (10-fold decrease) and was rarely detected in faeces compared with the corresponding wild-type strain (Robinson et al., 2019). Interestingly, the 'secretion' of NS1 is insensitive to brefeldin A, an inhibitor of trafficking from the endoplasmic reticulum (ER) to the Golgi (Lee et al., 2019).

This suggests that NS1 leaves infected cells through an unconventional pathway that still awaits characterization.

Non-structural protein oligomerization

The ability to oligomerize has been demonstrated for several non-structural proteins, including the NS1/2 of MNV and *Tulane virus*, NS2 of FCV, and NS2 of RHDV (**Table 1**). One of the best-studied examples is the NS2 (p23) of RHDV that was shown to oligomerise in both co-translocation and cross-linking assays (Urakova et al., 2015). Briefly, rabbit kidney (RK)-13 cells were transfected with expression plasmids that encoded either a NS2 protein with a nuclear localization sequence (NLS) and a FLAG-tag or with myc-tag but no NLS. When expressed separately, only the NS2 proteins with an NLS were transported to the nucleus. Upon co-expression, however, both proteins were detected in the nucleus, suggesting that NS2 proteins form dimers or higher order oligomers. This protein-protein interaction was confirmed in cross-linking experiments; subsequent Western blot analysis revealed a band of dimeric NS2 (Urakova et al., 2015). More evidence for the ability of NS2 proteins to oligomerize has been observed with FCV and *Tulane virus*. In the case of FCV, a NS2-NS2 dimer was detected by Western blot under non-reducing conditions in lysates from transfected cells (W. J. Kaiser, 2006). In the case of *Tulane virus*, a NS1/2 oligomerization was detected upon transient expression and subsequent Western blot analysis under non-reducing condition with unboiled samples (Strtak et al., 2019). Taken together, these findings suggest that the oligomerization domain in NS1/2 resides in the NS2 moiety of the protein. Interestingly, recent reports suggest that the NS2 part of the NS1/2 protein of noroviruses and *Tulane virus* possesses viroporin activity, for which oligomerization is essential.

Table 1. Cellular localization and functional properties of calicivirus non-structural proteins.

Protein name	Intracellular localization	Major functions/features	Reference
Human norovirus (genus *Norovirus*)			
NS1	Extracellular	NS1 is secreted and counteracts innate immune responses mediated by IFN-λ	Lee et al., 2019
NS1/2	Golgi	Golgi disassembly; inhibition of cellular protein secretion	Fernandez-Vega et al., 2004

			Ettayebi and Hardy, 2003
NS4	ER/Golgi	Golgi disassembly; inhibition of cellular protein secretion; formation of membranous web (replication factories)	Sharp et al., 2010 Doerflinger et al., 2017

Murine norovirus (genus *Norovirus*)			
NS1	Extracellular	NS1 is secreted and counteracts innate immune responses mediated by IFN-λ	Lee et al., 2019
NS1/2	ER	NS1/2 dimerization; NS1/2 cleavage is associated with persistence and apoptosis	Hyde and Mackenzie, 2010 Baker et al., 2012 Lee et al., 2019 Robinson et al., 2019
NS4	Golgi, endosomes	Golgi disassembly; moderate inhibition of cellular protein secretion	Sharp et al., 2012 Hyde and Mackenzie, 2010

Feline calicivirus (genus *Vesivirus*)			
NS2	ER	Dimerization; formation of membranous web (replication factories)	Bailey et al., 2010 Kaiser, 2006
NS4	ER	Formation of membranous web (replication factories); counteracts IFN response	Bailey et al., 2010 Tian et al., 2020

Rabbit haemorrhagic disease virus (genus *Lagovirus*)			
NS1	Nucleus and cytoplasm	Unknown	Urakova et al., 2015
NS2	Cytoplasm (ER?)	Dimerization	
NS4	Cytoplasm	Unknown	

Tulane virus (Recovirus)			
NS1/2	ER	Oligomerization; viroporin formation	Strtak et al., 2019

Membrane association of non-structural proteins

All positive-sense RNA viruses, including caliciviruses and picornaviruses, are known to manipulate host cell membranes to create a 'virus-friendly' environment (Romero-Brey &

Bartenschlager, 2014). A re-organization of the production and trafficking of cellular membranes has many consequences, e.g., interferons (IFNs) may no longer be secreted and major histocompatibility complex (MHC) molecules may no longer reach the plasma membrane. This allows viruses to become 'invisible' to the innate and adaptive immune system. In addition, re-directing cellular membranes enables the formation of new intracellular compartments for virus replication. In picornaviruses, the ability of 2A, 2B, and 3A to manipulate cellular membranes is well characterized (Doedens & Kirkegaard, 1995; Neznanov et al., 2001). It is tempting to speculate that these proteins are functional homologues of the calicivirus proteins NS1/2 and NS4. In the following, we will discuss findings that support this hypothesis.

Manipulation of cellular membrane trafficking

Poliovirus (genus *Enterovirus*) proteins 2B and 3A co-localize with ER and/or Golgi membranes in transfected cells, manipulating cellular membrane networks. For example, 3A is known to disrupt the Golgi architecture by inhibiting the vesicle transport from ER to Golgi (Teterina et al., 2011). Another consequence of 3A expression is the formation of vesicles that facilitate viral replication, most likely through the recruitment of ER-derived membranes (Cho et al., 1994; Suhy et al., 2000). Similarly, the calicivirus non-structural proteins NS1/2 and NS4 localize either to Golgi or ER membranes (**Table 1**); however, for some of the proteins, the intracellular localization was not determined in great detail, i.e., whether a protein is localized with a particular organelle or membrane structure not known.

The human norovirus protein NS4 localises to the ER and Golgi (**Table 1**). This protein contains a YXΦESDG motif (where X is any amino acid and Φ is a hydrophobic amino acid residue) that mimics cellular ER export signals, which typically contain a short YXXΦ motif (Nishimura & Balch, 1997). This norovirus motif was thus named MERES (mimic of an endoplasmic reticulum export signal) (Sharp et al., 2012). It should therefore not be surprising that NS4 antagonizes trafficking from the ER to Golgi (Sharp et al., 2012). By using a recombinant alkaline phosphatase as a reporter, it has been shown that norovirus NS4 hijacks COPII vesicles and inhibits protein secretion (Fernandez-Vega et al., 2004; Sharp et al., 2010). Similar but less prominent effects were demonstrated for the NS4 protein of MNV, which lacks a MERES motif, but nevertheless localises with Golgi membranes (Sharp et al., 2012). The interaction of the human norovirus NS4 with Golgi membranes occurs via a hydrophobic membrane association domain (MAD), that contains an amphipathic α-helix capable of membrane insertion (Sharp et al., 2010). When Doerflinger and co-authors used light and

electron microscopy to study the impact of recombinant NS4 proteins on vesicle formation, they found that NS4 is sufficient to induce the formation of single and double membrane vesicles (Doerflinger et al., 2017). Taken together, NS4 seems to play a key role in the manipulation of protein trafficking and the formation of the replication factories.

Inhibiting protein secretion in norovirus-infected cells is not restricted to NS4. The human norovirus protein NS1/2 also disrupts the Golgi and shows a vesicular localization pattern in transfected cells (Ettayebi & Hardy, 2003). To study the effect of recombinant NS1/2 expression, researchers traced the fate of the vesicular stomatitis virus (VSV) glycoprotein G. In the absence of NS1/2, the VSV G protein was transported to the cellular surface. In cells that expressed the human virus NS1/2, VSV G was no longer detectable on the cell surface, suggesting a disruption of the vesicular transport. Instead, VSV G was found to partially co-localize with NS1/2 (Ettayebi & Hardy, 2003). A yeast two-hybrid screen revealed an interaction of human NS1/2 with the vesicle-associated membrane protein VAP-A (Ettayebi & Hardy, 2003). Since VAP-A plays an important role in the ER to Golgi vesicle trafficking (M. Lynn Weir et al., 2001; M L Weir et al., 1998), Ettayebi and Hardy hypothesized that the interaction between NS1/2 and VAP-A contributes to the inhibition of secretory pathways. Subsequently, this interaction was found to be dependent on a motif in human NS1/2 that mimics the cellular phenylalanine-phenylalanine-acidic-tract (FFAT) motif (**Figure 3**) (McCune et al., 2017). FFAT motifs are present in many cellular proteins that bind VAP-A (S. E. Kaiser et al., 2005). A similar protein-protein interaction has been found for NS1/2 of MNV and VAP-A (McCune et al., 2017). Taken together these findings suggest that manipulating VAP-A might be an important strategy in the calicivirus life cycle. Future studies that investigate possible VAP-A interactions with other NS1/2 proteins (or their cleavage products) will reveal whether all caliciviruses rely on this strategy.

Formation of membrane-associated replication complexes

The NS2 and NS4 proteins of FCV are predicted to contain membrane-spanning hydrophobic protein domains, suggesting an association with membranes (Bailey et al., 2010). This might explain the ER localization of these proteins in immunofluorescence studies (**Table 1**). Further immunofluorescence and electron microscopy studies revealed that NS2 and NS4 of FCV cause a dramatic reorganization of the ER in transiently transfected Crandell Reese feline kidney (CRFK) cells (Bailey et al., 2010). Furthermore, the manipulation of the intracellular membrane traffic resulted in the formation of vesicles associated with virus replication (Bailey et al., 2010). Similar observations were made in FCV-infected 293T cells;

however, an impairment of cellular secretory functions was not detected (Bailey et al., 2010). An association of FCV NS2 and NS4 with viral replication complexes has long been postulated based on protein-protein interaction. Green et al. (Green et al., 2002) isolated active replication complexes from FCV-infected cells and identified the presence of NS2, NS4, helicase, capsid proteins, the polymerase precursor protein Pol-Pro, and the NS4-VPg precursor. These results were later confirmed using a yeast two-hybrid system and co-immunoprecipitations (W. J. Kaiser, 2006). Taken together, the finding that FCV infection induces ER rearrangements and vesicle formation, suggests that the non-structural proteins NS2, NS4, and the helicase assist in the formation of replication complexes.

In MNV infections, NS1/2 localizes to the ER but NS4 to the Golgi (**Table 1**). Nevertheless, both NS1/2 and NS4 are associated with replication complexes. To study the involvement of NS4 in replication, an infectious MNV variant with a FLAG-tagged NS4 protein was generated using transposon-mediated insertional mutagenesis (Thorne et al., 2012). Immunofluorescence staining revealed a co-localization of NS4 with the RdRp, and co-immunoprecipitation showed an interaction of NS4 with NS1/2. This demonstrates that both NS1/2 and NS4 were present at the site of MNV replication (Thorne et al., 2012). Furthermore, intracellular localization studies with specific marker proteins suggest that active MNV replication complexes contain membranous vesicles derived from the ER, medial- and trans-Golgi apparatus, and endosomes (Hyde et al., 2009). Thus, the role of the NS1/2 and NS4 proteins in this process is believed to be recruiting ER and Golgi membranes, respectively (Hyde & Mackenzie, 2010; Thorne et al., 2012). To further characterize the viral replication machinery, Hosmillo et al. (2019) used infectious MNV variants with FLAG tags at either NS1/2 or NS4 for immunoprecipitating active replication complexes. The researchers found that these complexes contained all viral proteins and interestingly, a number of cellular proteins associated with fatty acid metabolism and vesicular transport, such as protein VAP-A (Hosmillo et al., 2019).
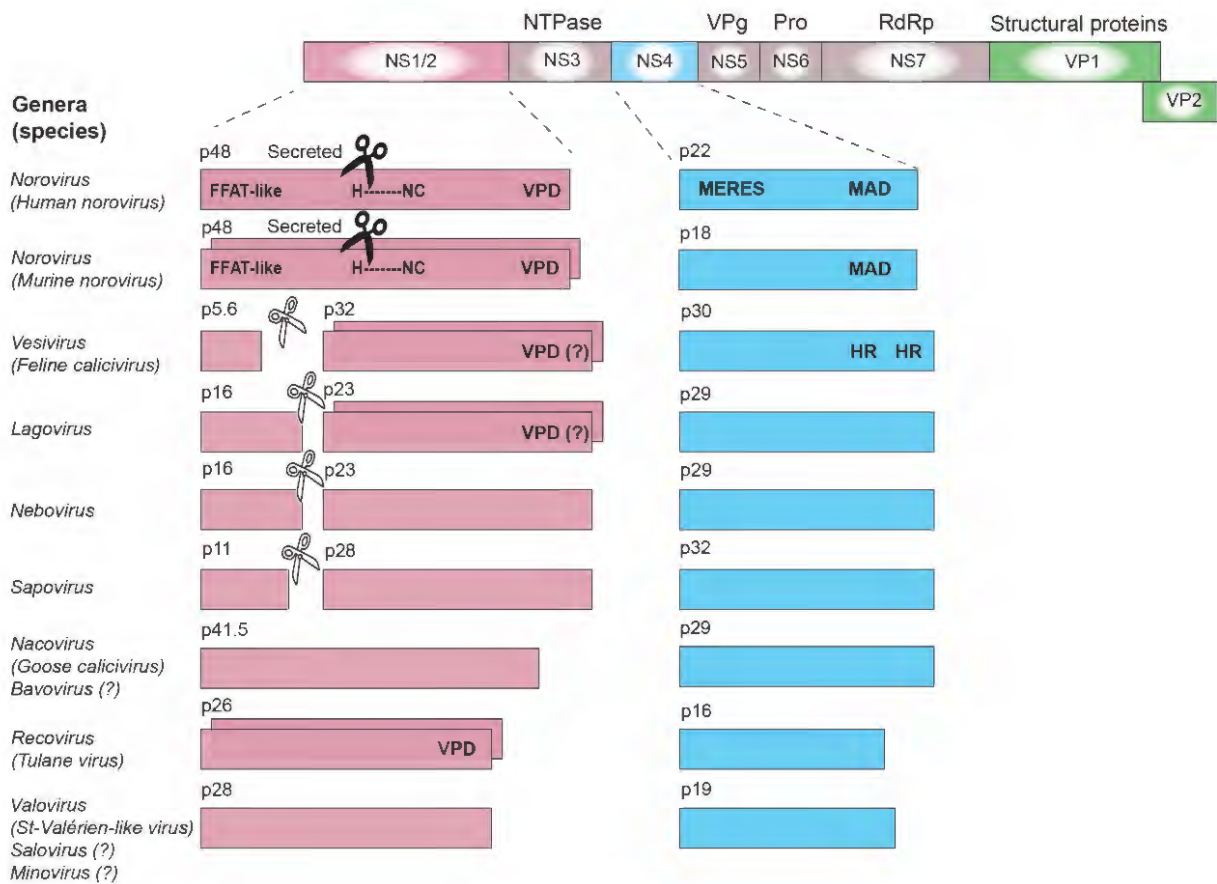
Figure 3. Calicivirus non-structural protein processing, oligomerization and domains. The coding sequences for non-structural proteins are shown in pink (NS1/2), blue (NS4), or grey (all other non-structural proteins), while coding sequences for structural proteins are shown in green (VP1 and VP2). The ability of some proteins to oligomerize is illustrated by staggered boxes. Black scissors indicate the presence of a caspase-3 cleavage site; white scissors indicate a viral 3C-like protease cleavage site; VPD, viroporin domain; HR, hydrophobic region; MAD, membrane-associated domain; H-NC, H-box and NC motif (asparagine-cysteine); MERES, mimic of an endoplasmic reticulum export signal; FFAT, phenylalanine-phenylalanine acidic tract. Genes and gene products are drawn to scale.

Viroporin activity

Viroporins are viral proteins that feature one, two, or three transmembrane α-helices (Hyser et al., 2010). The helices possess amphipathic properties that allow an efficient membrane incorporation: hydrophobic amino acid residues face the membrane, and polar residues line the pore. These proteins oligomerize to form a functional transmembrane ion channel, which can be selective or non-selective and voltage dependent or independent (reviewed in Nieva et al., 2012). For example, the influenza virus protein M2 has only one

transmembrane helix; however, through the formation of tetramers, enough transmembrane helices are brought together to form a small pore that is selectively permeable to protons (Pinto et al., 1997). A remarkable function mediated by many viroporins is the disruption of cellular Ca^{2+} homeostasis through leakage from intracellular depots (mitochondria, ER, Golgi) to the cytoplasm (Aldabe et al., 1997; Pham et al., 2017). Changes to the intracellular Ca^{2+} concentration can favour viral replication and induce apoptosis (Hajnóczky et al., 2003; Zhou et al., 2009).

The picornavirus protein 2B has multiple functions including that of a viroporin, i.e., it has the ability to form a membrane channel. In poliovirus-infected cells, 2B oligomerizes and forms ion channels in ER and Golgi membranes (Martinez-Gil et al., 2011). When expressed as recombinant proteins, 2B and interestingly, also 3A disrupted Ca^{2+} signaling suggesting that polioviruses encode two independent viroporins (Aldabe et al., 1997; Doedens & Kirkegaard, 1995; Martinez-Gil et al., 2011).

Similar activities were described for calicivirus non-structural proteins. For example, the Tulane virus NS1/2 was shown to form an ion channel in ER membranes and to elevate cytoplasmic Ca^{2+} levels (Strtak et al., 2019). Its ability to form an ion channel was initially predicted using bioinformatics which identified amphipathic transmembrane helices in the C-terminal (NS2) part of NS1/2. The functionality of the domain has since been confirmed *in vitro* using a classic bacterial viroporin assay. This assay takes advantage of a genetically modified *E. coli* strain that constitutively expresses low levels of the T7 lysozyme to control T7 RNA polymerase-dependent gene expression. The low-level expression of the lysozyme is normally well tolerated but co-expression of proteins that form membrane channels/pores can lead to the leakage of the lysozyme into the periplasmic space, cleavage of peptidoglycan, and subsequent lysis of the cell (Studier & Moffatt, 1986). The expression of full-length NS1/2 but not that of several deletion mutants caused cell lysis in T7 lysozyme producing *E. coli* (Strtak et al., 2019). Furthermore, eukaryotic cells stably expressing a fluorescent Ca^{2+} sensor were infected with *Tulane virus* and the intensity of fluorescence was measured over time. After 8 hours, the cytoplasmic Ca^{2+} concentration in infected cells was significantly higher than that in mock-infected cells. Moreover, when Ca^{2+} levels were depleted in the cell culture medium and in the cytoplasm using the Ca^{2+} chelator BAPTA-AM (1,2-bis(o-aminophenoxy)ethane-N,N,N′,N′-tetraacetic acid), virus replication decreased dramatically, suggesting that Ca^{2+}-mediated 'signalling' is crucial for the Tulane virus life cycle (Strtak et al., 2019). The ability of NS1/2 to alter intracellular Ca^{2+} concentrations in eukaryotic cells was demonstrated in a transfection

experiment, and by expressing a series of deletion mutants, the viroporin domain was mapped and characterized (Strtak et al., 2019).

It becomes increasingly clear that similar viroporins exist among all *Caliciviridae*. In 2003, Ettayebi and Hardy identified a hydrophobic transmembrane domain in the NS1/2 of human and murine noroviruses (**Figure 3**), even though it was not clear at the time that this domain is part of a viroporin (Ettayebi and Hardy, 2003). The C-terminal region of all NS2 proteins shows a remarkable degree of conservation among caliciviruses—relative to other parts of the protein (**Figure 4**). In noroviruses, the C-terminal part of the NS1/2 protein includes a number of relatively hydrophobic regions that form a distinct secondary structure, whereas most of the N-terminal is largely hydrophilic and disordered (i.e., a secondary structure is lacking) (Baker et al., 2012). The C terminal hydrophobic transmembrane domain (along with upstream sequences) is responsible for the observed co-localization of the human norovirus NS1/2 with Golgi membranes in transfected cells and is essential for the disassembly of the Golgi apparatus (Fernandez-Vega et al., 2004). When a fusion construct of the hydrophobic domain of NS1/2 (without upstream sequences) and GFP was expressed, it co-localized with Golgi but did not disrupt its membranes. Thus, sequences upstream of the hydrophobic region are required for Golgi disruption (Fernandez-Vega et al., 2004). In another experiment, transposon-based insertional mutagenesis was used to probe MNV genome tolerance for a 15-nt exogenous sequence (Thorne et al., 2012). In the C-terminal region of NS2, most of these 15-nt insertions were lost after three passages, suggesting that this part of the protein is required for virus replication (Thorne et al., 2012). Moreover, functional assays measuring intracellular Ca^{2+} levels revealed that the NS1/2 of human norovirus also disrupts calcium homeostasis, similar to the experiments with Tulane virus; Strtak et al., 2019).

Bioinformatic predictions suggest that the lagovirus proteins NS2 and NS4 contain amphipathic helices that may interact with membranes to form ion channels and possibly act as viroporins similar to the transmembrane domains in picornavirus homologues 2B and 3A, respectively (**Figure 5**). This hypothesis is further supported by the observation that RHDV NS2 oligomerizes in transfected cells (Urakova et al., 2015), which would allow to bring together a sufficient number of transmembrane helices to form a functional viroporin. However, functional studies are needed to confirm this hypothesis.
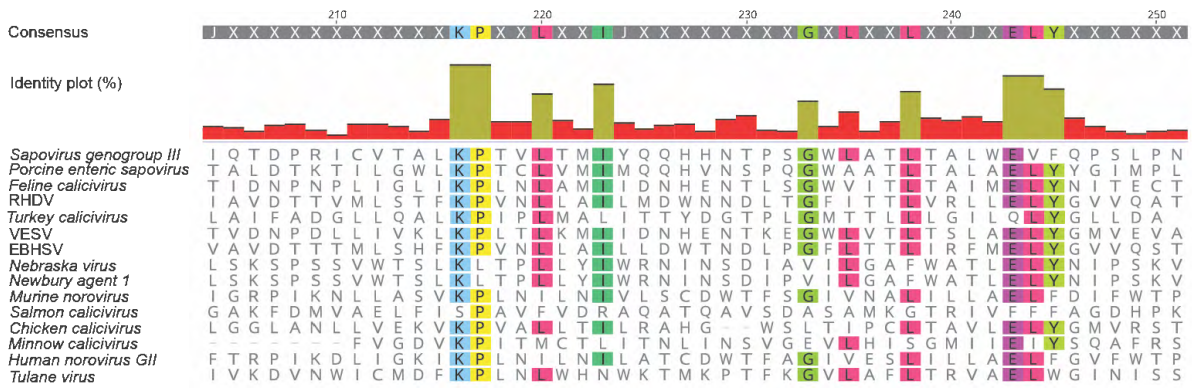
Figure 4. Amino acid sequence alignment of the putative viroporin domain region of protein NS2 of caliciviruses. Higher degree of conserved amino acid residues is observed in the C-terminal region corresponding to the described viroporin domain of *Tulane virus* compared to the rest of the protein sequence. For sequence IDs refer to Figure 2.

Counteracting innate immune responses

Poliovirus protein 2A (a chymotrypsin-like protease) counteracts the IFN-induced antiviral defense: wild-type poliovirus can efficiently replicate in cells pre-treated with IFN-α. In contrast, a poliovirus variant with a mutation in 2A that affects the cleavage of cellular but not viral substrates, no longer replicates in IFN-treated cells (Morrison & Racaniello, 2009). The exact mechanism for this phenomenon is not known. Not all picornaviruses have 2A proteins that counteract the IFN system, e.g., the 2A of *Encephalomyocarditis virus* (EMCV) seems to lack the ability to interfere with innate immune responses. The replication of EMCV is IFN-sensitive: the virus does not replicate in cells pre-treated with IFN-α, but IFN resistance can be engineered by substituting the EMCV 2A gene with the gene of its poliovirus homologue, demonstrating the importance of 2A in counteracting innate immune responses (Morrison & Racaniello, 2009). Other poliovirus non-structural proteins have additional immune evasion functions, e.g., the proteins 2B and 3A inhibit the secretion of IFN-β, proinflammatory interleukins (IL)-6 and 8, and the intracellular trafficking of the receptor for the tumor necrosis factor (TNF) (Dodd et al., 2001; Neznanov et al., 2001).

The calicivirus proteins NS1/2 and NS4 are likely the homologues of the picornavirus proteins 2A/2B and 3A, respectively (see Fig. 1). Evidence is accumulating that all of these proteins are involved in the downregulation of host defense responses. The norovirus protein NS1 is cleaved from its precursor protein NS1/2 by caspase-3 (a cellular protease) and is 'secreted' through an unconventional pathway. Extracellular NS1 seems to be essential for overcoming epithelial defences induced by IFN-λ. A recombinant MNV variant with a mutation

in the caspase-3 cleavage site of NS1/2 failed to replicate in wild-type mice after oral infection, although replication upon intraperitoneal injection was unaffected. Virus replication after oral infection can be rescued in type III IFN receptor deficient but not in type I IFN or type II IFN receptor deficient mice (Lee et al., 2019), suggesting that type III IFNs such as IFN-λ play a critical role in epithelial host defences against noroviruses.

Another mechanism through which the norovirus protein NS1/2 counteracts host immune responses is the regulation of gene transcription. A transcriptome analysis of transiently transfected monocytes revealed that norovirus NS1/2 reduces the expression of Toll-like receptors (TLR)-4, -7, -8 and -9, increases expression of several pro-inflammatory cytokines/chemokines, and induces a pro-apoptotic phenotype, suggesting that the norovirus NS1/2 protein regulates innate and adaptive immune responses (Lateef et al., 2017). In addition, norovirus NS1/2 protein may manipulate innate immune responses at the protein level. The aforementioned interaction between the norovirus NS1/2 protein and the vesicle-associated membrane protein VAP-A suggests that caliciviruses manipulate intracellular trafficking, which would inhibit or block the transport of critical innate immune proteins to the cellular surface (TLRs, IFNs, MHCs, etc.).

Interestingly, in FCV, it is the NS4 (p30) protein (picornavirus 3A homologue) that interferes with the host cell's innate immune responses. Tian and co-workers analyzed the IFN signalling in FCV-infected cells that were pre-treated with the transcription inhibitor actinomycin D (to stop any virus-induced transcription). When they analyzed the mRNA levels of the IFN-α/β receptor subunit 1 and 2 (IFNAR1 and IFNAR2, respectively), they found that the half-life of IFNAR1 but not IFNAR2 mRNAs is drastically reduced in virus-infected cells compared to control cells (6.3 vs 100 h, respectively). This showed that FCV downregulates expression of a functional IFN type I receptor through mRNA degradation of the IFN-α/β receptor subunit 1 (IFNAR1) (Tian et al., 2020). To identify the protein responsible for the IFNAR1 mRNA degradation, cells were transiently transfected with each of the FCV non-structural proteins and the IFNAR1 mRNA concentrations were measured. NS4 was the only protein that significantly affected IFNAR1 mRNA stability (Tian et al., 2020).

The picture emerges that caliciviruses have evolved various mechanisms to counteract innate immune defences. What is presently known is likely the equivalent of the tip of the iceberg, i.e., many more counter defence mechanisms exist but their discovery is hampered by a lack of robust cell culture models and replicon systems for many caliciviruses.

Miscellaneous features

Enteroviruses are well-known for their ability to shutoff host cell protein expression (Barco et al., 2000). This function is largely attributed to the viral proteases 2A and 3C proteins that participate in the viral polyprotein cleavage, but also cleave several host proteins (Agol & Gmyl, 2010; Ventoso et al., 1998). For example, 2A manipulates the nuclear pore by cleaving one of the nuclear pore components, thereby inhibiting mRNA export (Belov et al., 2004; Castelló et al., 2009). Furthermore, 2A and 3C attack the poly(A) binding protein (PABP) (Joachims et al., 1999) and 2A cleaves a component of the translation initiation factor eIF4F, which effectively stops translation of capped mRNAs (Kräusslich et al., 1987). Caliciviruses also interfere with the cellular protein expression, but the mechanistic details are less clear. The viral 3C-like proteases of human noroviruses, MNV and FCV were shown by several researchers to be associated with translational shutoff and the cleavage of PABP, similar to poliovirus proteases (Emmott et al., 2017; Kuyumcu-Martinez et al., 2004). Other researchers did not find an involvement of the MNV 3C-like protease, but observed that cellular protein synthesis was inhibited by NS3 (the helicase) through an unknown mechanism (Fritzlar et al., 2019). Clearly, future research is warranted to resolve this discrepancy.

Interestingly, the 2A proteins of enteroviruses and the NS1/2 protein of caliciviruses possess an H-NC motif (**Figure 3**). This motif contains an H-box with a characteristic histidine amino acid residue and an NC motif with an asparagine and cysteine dipeptide (Fernandez-Vega et al., 2004; Hughes & Stanway, 2000; Johansson et al., 2002). Why these non-structural proteins have a conserved H-NC motif is unknown, but the occurrence of the motif in a cellular protein may give some clues to its function. The class II tumour suppressor protein H-rev107 is a phospholipase that also possesses the H-NC motif (Hughes & Stanway, 2000; Uyama et al., 2009). Through its ability to bind K-Ras, H-rev107 inhibits cell growth and differentiation and regulates apoptosis (Han et al., 2017, 2020). It is tempting to speculate that viral proteins such as 2A and NS1/2 manipulate key signalling proteins like K-Ras, but there is presently no evidence to support this hypothesis.
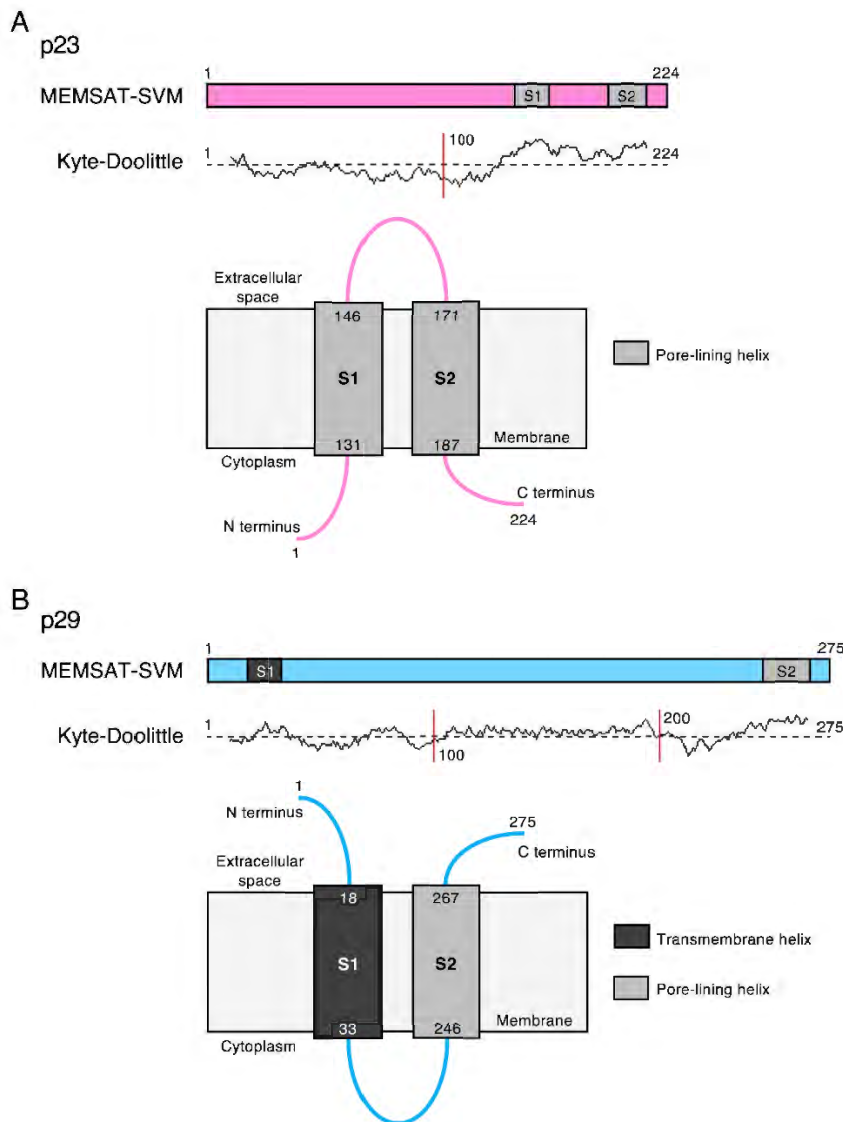
Figure 5. Potential viroporin domain domains in lagovirus (RHDV) non-structural proteins. Sequence analysis using PSIPRED (Buchan & Jones, 2019) secondary structure prediction tools revealed transmembrane (dark grey) and/or amphipathic pore-lining helices (light grey) in (**A**) p23 (pink) and (**B**) p29 (light blue); the MEMSAT-SVM algorithm (Nugent & Jones, 2012) was used for protein topology prediction; Kyte-Doolittle plots indicate the hydrophobicity of amino acids. Note that the exact intracellular localization of the potential viroporins and their orientation in cellular membrane(s) is currently unknown; in the case of an ER localization, the term 'cytoplasm' indicates the lumen of the organelle.

Outlook

Until now, research into the non-structural proteins of caliciviruses has mostly been focussed on human noroviruses, MNV, and FCV (mainly because these viruses can be cultivated easily in a laboratory). The development of new organoid culture systems, e.g. the

development of rabbit intestinal organoids (Kardia et al., 2021; Mussard et al., 2020), may soon allow growing lagoviruses and other caliciviruses in cell culture. This is a prerequisite for detailed studies on the role of non-structural proteins in building replication complexes, counteracting innate and adaptive immune responses, redirecting cellular resources, and other activities.

Conflict of interest

The authors declare that the work was conducted in the absence of any commercial or financial relationships that could be construed as a potential conflict of interest.

Author contributions

ES developed the conceptual outline and drafted the manuscript. ES, RH, NU, TS, and MF wrote the manuscript. All authors contributed to editing and revising the manuscript. All authors read and approved the final manuscript.

References

Abrantes, J., Van Der Loo, W., Le Pendu, J., and Esteves, P. J. (2012). Rabbit haemorrhagic disease (RHD) and rabbit haemorrhagic disease virus (RHDV): a review. *Vet. Res.* 43. doi:10.1186/1297-9716-43-12.

Agol, V. I., and Gmyl, A. P. (2010). Viral security proteins: counteracting host defences. *Nat. Rev. Microbiol.* 8, 867–878. doi:10.1038/nrmicro2452.

Aldabe, R., Irurzun, A., and Carrasco, L. (1997). Poliovirus protein 2BC increases cytosolic free calcium concentrations. *J. Virol.* 71, 6214–6217. doi:10.1128/jvi.71.8.6214-6217.1997.

Alkan, F., Karayel, I., Catella, C., Bodnar, L., Lanave, G., Bányai, K., et al. (2015). Identification of a bovine enteric calicivirus, kírklareli virus, distantly related to neboviruses, in calves with enteritis in Turkey. *J. Clin. Microbiol.* 53, 3614–3617. doi:10.1128/JCM.01736-15.

Bailey, D., Kaiser, W. J., Hollinshead, M., Moffat, K., Chaudhry, Y., Wileman, T., et al. (2010). Feline calicivirus p32, p39 and p30 proteins localize to the endoplasmic reticulum to initiate replication complex formation. *J. Gen. Virol.* 91, 739–749. doi:10.1099/vir.0.016279-0.

Baker, E. S., Luckner, S. R., Krause, K. L., Lambden, P. R., Clarke, I. N., and Ward, V. K. (2012). Inherent structural disorder and dimerisation of murine norovirus ns1-2 protein. *PLoS One* 7. doi:10.1371/journal.pone.0030534.

Barco, A., Feduchi, E., and Carrasco, L. (2000). A stable HeLa cell line that inducibly expresses poliovirus 2Apro: effects on cellular and viral gene expression. *J. Virol.* 74, 2383–2392. doi:10.1128/jvi.74.5.2383-2392.2000.

Bartsch, S. M., Lopman, B. A., Ozawa, S., Hall, A. J., and Lee, B. Y. (2016). Global economic burden of norovirus gastroenteritis. *PLoS One* 11, 1–16. doi:10.1371/journal.pone.0151219.

Belliot, G., Sosnovtsev, S. V., Chang, K. O., McPhie, P., and Green, K. Y. (2008). Nucleotidylylation of the VPg protein of a human norovirus by its proteinase-polymerase precursor protein. *Virology* 374, 33–49. doi.org/10.1016/j.virol.2007.12.028.

Belov, G. A., Lidsky, P. V., Mikitas, O. V., Egger, D., Lukyanov, K. A., Bienz, K., et al. (2004). Bidirectional increase in permeability of nuclear envelope upon poliovirus infection and accompanying alterations of nuclear pores. *J. Virol.* 78, 10166–10177. doi:10.1128/jvi.78.18.10166-10177.2004.

Boniotti, B., Wirblich, C., Sibilia, M., Meyers, G., Thiel, H. J., and Rossi, C. (1994). Identification and characterization of a 3C-like protease from rabbit hemorrhagic disease virus, a calicivirus. doi:10.1128/jvi.68.10.6487-6495.1994.

Buchan, D. W. A., & Jones, D. T. (2019). The PSIPRED Protein Analysis Workbench: 20 years on. *Nucleic Acids Research*, *47*, W402–W407. https://doi.org/10.1093/nar/gkz297.

Capella-Gutiérrez, S., Silla-Martínez, J. M., and Gabaldón, T. (2009). trimAl: A tool for automated alignment trimming in large-scale phylogenetic analyses. *Bioinformatics* 25, 1972–1973. doi:10.1093/bioinformatics/btp348.

Castelló, A., Izquierdo, J. M., Welnowska, E., and Carrasco, L. (2009). RNA nuclear export is blocked by poliovirus 2A protease and is concomitant with nucleoporin cleavage. *J. Cell Sci.* 122, 3799–3809. doi:10.1242/jcs.055988.

Cho, M. W., Teterina, N., Egger, D., Bienz, K., and Ehrenfeld, E. (1994). Membrane rearrangement and vesicle induction by recombinant poliovirus 2C and 2BC in human

cells. *Virology* 202, 129–45. doi:10.1006/viro.1994.1329.

Clarke, I. N., and Lambden, P. R. (1997). The molecular biology of caliciviruses. *J. Gen. Virol.* 78, 291–301. doi:10.1099/0022-1317-78-2-291.

Cotton, B. T., Hyde, J. L., Sarvestani, S. T., Sosnovtsev, S. V., Green, K. Y., White, P. A., et al. (2016). The norovirus NS3 protein is a dynamic lipid- and microtubule-associated protein involved in viral RNA replication. *J. Virol.* 91, 2138–2154. doi:10.1128/jvi.02138-16.

Deval, J., Jin, Z., Chuang, Y. C., and Kao, C. C. (2017). Structure(s), function(s), and inhibition of the RNA-dependent RNA polymerase of noroviruses. *Virus Res.* 234, 21–33. doi.org/10.1016/j.virusres.2016.12.018.

Desselberger, U. (2019). Caliciviridae other than noroviruses. *Viruses* 11. doi:10.3390/v11030286.

Dodd, D. A., Giddings, T. H., and Kirkegaard, K. (2001). Poliovirus 3A protein limits interleukin-6 (IL-6), IL-8, and beta interferon secretion during viral infection. *J. Virol.* 75, 8158–8165. doi:10.1128/jvi.75.17.8158-8165.2001.

Doedens, J. R., and Kirkegaard, K. (1995). Inhibition of cellular protein secretion by poliovirus proteins 2B and 3A. *EMBO J.* 14, 894–907. doi:10.1016/j.virol.2005.03.036.

Doerflinger, S. Y., Cortese, M., Romero-Brey, I., Menne, Z., Tubiana, T., Schenk, C., et al. (2017). Membrane alterations induced by nonstructural proteins of human norovirus. *PLoS Pathog.* 13. doi:10.1371/journal.ppat.1006705.

Ehresmann, D. W., and Schaffer, F. L. (1977). RNA synthesized in calicivirus infected cells is atypical of picornaviruses. *J. Virol.* 22, 572–576.

Emmott, E., Sorgeloos, F., Caddy, S. L., Vashist, S., Sosnovtsev, S., Lloyd, R., et al. (2017). Norovirus-mediated modification of the translational landscape via virus and host-induced cleavage of translation initiation factors. *Mol. Cell. Proteomics* 16, 215–229. doi:10.1074/mcp.M116.062448.

Ettayebi, K., Crawford, S. E., Murakami, K., Broughman, J. R., Karandikar, U., Tenge, V. R., et al. (2016). Replication of human noroviruses in stem cell-derived human enteroids. *Science* 353, 1387–1393. doi.org/10.1126/science.aaf5211.

Ettayebi, K., and Hardy, M. E. (2003). Norwalk virus nonstructural protein p48 forms a complex with the SNARE regulator VAP-A and prevents cell surface expression of vesicular stomatitis virus G protein. *J. Virol.* 77, 11790–7. doi:10.1128/JVI.77.21.11790.

Farkas, T. (2015). Rhesus enteric calicivirus surrogate model for human norovirus gastroenteritis. *J. Gen. Virol.* 96, 1504–1514. doi:10.1099/jgv.0.000020.

Fernandez-Vega, V., Sosnovtsev, S. V, Belliot, G., King, A. D., Mitra, T., Gorbalenya, A., et al. (2004). Norwalk virus N-terminal nonstructural protein is associated with disassembly of the Golgi complex in transfected cells. *J. Virol.* 78, 4827–4837. doi:10.1128/JVI.78.9.4827.

Fritzlar, S., Aktepe, T. E., Chao, Y. W., Kenney, N. D., McAllaster, M. R., Wilen, C. B., et al. (2019). Mouse norovirus infection arrests host cell translation uncoupled from the stress granule-PKR-eIF2α axis. *MBio* 10. doi:10.1128/mBio.00960-19.

Fullerton, S. W. B., Blaschke, M., Coutard, B., Gebhardt, J., Gorbalenya, A., Canard, B., et al. (2007). Structural and functional characterization of sapovirus RNA-dependent RNA polymerase. *J. Virol.* 81, 1858–1871. doi.org/10.1109/BIOCAS.2017.8325071.

Goodfellow, I. (2011). The genome-linked protein VPg of vertebrate viruses—a multifaceted protein. *Curr. Opin. Virol.* 1, 355–362. doi:10.1016/j.coviro.2011.09.003.

Green, K. Y., Mory, A., Fogg, M. H., Weisberg, A., Belliot, G., Wagner, M., et al. (2002). Isolation of enzymatically active replication complexes from feline calicivirus-infected cells. *J. Virol.* 76, 8582–8595. doi:10.1128/JVI.76.17.8582-8595.2002.

Hajnóczky, G., Davies, E., and Madesh, M. (2003). Calcium signaling and apoptosis. *Biochem. Biophys. Res. Commun.* 304, 445–454. doi:10.1016/S0006-291X(03)00616-8.

Hall, R. N., Peacock, D. E., Kovaliski, J., Mahar, J. E., Mourant, R., Piper, M., et al. (2017). Detection of RHDV2 in European brown hares (*Lepus europaeus*) in Australia. *Vet. Rec.* 180, 121. doi:10.1136/vr.104034.

Han, C. W., Jeong, M. S., Ha, S. C., and Jang, S. B. (2020). A H-REV107 peptide inhibits tumor growth and interacts directly with oncogenic KRAS mutants. *Cancers (Basel).* 12, 1–21. doi:10.3390/cancers12061412.

Han, C. W., Jeong, M. S., and Jang, S. B. (2017). Molecular interaction between K-Ras and H-REV107 in the Ras signaling pathway. *Biochem. Biophys. Res. Commun.* 491, 257–264. doi:10.1016/j.bbrc.2017.07.120.

Han, K. R., Choi, Y., Min, B. S., Jeong, H., Cheon, D., Kim, J., et al. (2010). Murine norovirus-1 3Dpol exhibits RNA-dependent RNA polymerase activity and nucleotidylylates on Tyr of the VPg. *J. Gen. Virol.* 91, 1713–1722. doi.org/10.1099/vir.0.020461-0.

Herbert, T. P., Brierley, I., and Brown, T. D. K. (1997). Identification of a protein linked to the genomic and subgenomic mRNAs of feline calicivirus and its role in translation. *J. Gen. Virol.* 78, 1033–1040. doi:10.1099/0022-1317-78-5-1033.

Hosmillo, M., Lu, J., McAllaster, M. R., Eaglesham, J. B., Wang, X., Emmott, E., et al. (2019). Noroviruses subvert the core stress granule component G3BP1 to promote viral VPg-

dependent translation. *eLife* 8, 1–35. doi:10.7554/eLife.46681.

Hughes, P. J., and Stanway, G. (2000). The 2A proteins of three diverse picornaviruses are related to each other and to the H-rev107 family of proteins involved in the control of cell proliferation. *J. Gen. Virol.* 81, 201–207. doi:10.1099/0022-1317-81-1-201.

Hyde, J. L., and Mackenzie, J. M. (2010). Subcellular localization of the MNV-1 ORF1 proteins and their potential roles in the formation of the MNV-1 replication complex. *Virology* 406, 138–148. doi:10.1016/j.virol.2010.06.047.

Hyde, J. L., Sosnovtsev, S. V, Green, K. Y., Wobus, C., Virgin, H. W., and Mackenzie, J. M. (2009). Mouse norovirus replication is associated with virus-induced vesicle clusters originating from membranes derived from the secretory pathway. *J. Virol.* 83, 9709–9719. doi:10.1128/JVI.00600-09.

Hyser, J. M., Collinson-Pautz, M. R., Utama, B., and Estes, M. K. (2010). Rotavirus disrupts calcium homeostasis by NSP4 viroporin activity. *MBio* 1, 1–11. doi:10.1128/mBio.00265-10.

Joachims, M., Breugel, P. C. V. A. N., and Lloyd, R. E. (1999). Cleavage of poly (A)-binding protein by enterovirus proteases concurrent with inhibition of translation *in vitro*. 73, 718–727.

Johansson, S., Niklasson, B., Maizel, J., Gorbalenya, A. E., and Lindberg, A. M. (2002). Molecular analysis of three Ljungan virus isolates reveals a new, close-to-root lineage of the *Picornaviridae* with a cluster of two unrelated 2A proteins. *J. Virol.* 76, 8920–8930. doi:10.1128/JVI.76.17.8920-8930.2002.

Kaiser, S. E., Brickner, J. H., Reilein, A. R., Fenn, T. D., Walter, P., and Brunger, A. T. (2005). Structural basis of FFAT motif-mediated ER targeting. *Structure* 13, 1035–1045. doi:10.1016/j.str.2005.04.010.

Kaiser, W. J. (2006). Analysis of protein-protein interactions in the feline calicivirus replication complex. *J. Gen. Virol.* 87, 363–368. doi:10.1099/vir.0.81456-0.

Kardia, E., Frese, M., Smertina, E., Strive, T., Zeng, X. L., and Estes, M. (2021). Culture and differentiation of rabbit intestinal organoids and organoid-derived cell monolayers. *Sci. Rep.*, 1–12. doi:10.1038/s41598-021-84774-w.

Katoh, K., Misawa, K., Kuma, K. I., and Miyata, T. (2002). MAFFT: A novel method for rapid multiple sequence alignment based on fast Fourier transform. *Nucleic Acids Res.* 30, 3059–3066. doi:10.1093/nar/gkf436.

Kirk, M. D., Pires, S. M., Black, R. E., Caipo, M., Crump, J. A., Devleesschauwer, B., et al. (2015). World Health Organization estimates of the global and regional disease burden of

22 foodborne bacterial, protozoal, and viral diseases, 2010: a data synthesis. *PLoS Med.* 12, 1–21. doi:10.1371/journal.pmed.1001921.

Koonin, E. V. (1991). The phylogeny of RNA-dependent RNA polymerases of positive-strand RNA viruses. *J. Gen. Virol.* 72, 2197–2206. doi:10.1099/0022-1317-72-9-2197.

Kräusslich, H. G., Nicklin, M. J. H., Toyoda, H., Etchison, D., and Wimmer, E. (1987). Poliovirus proteinase 2A induces cleavage of eucaryotic initiation factor 4F polypeptide p220. doi:10.1128/jvi.61.9.2711-2718.1987.

Kuyumcu-Martinez, M., Belliot, G., Sosnovtsev, S. V., Chang, K.-O., Green, K. Y., and Lloyd, R. E. (2004). Calicivirus 3C-like proteinase inhibits cellular translation by cleavage of poly(A)-binding protein. *J. Virol.* 78, 8172–8182. doi:10.1128/jvi.78.15.8172-8182.2004.

L'Homme, Y., Sansregret, R., Plante-Fortier, É., Lamontagne, A. M., Ouardani, M., Lacroix, G., et al. (2009). Genomic characterization of swine caliciviruses representing a new genus of Caliciviridae. *Virus Genes* 39, 66–75. doi:10.1007/s11262-009-0360-3.

Lambden, P. R., and Clarke, I. N. (1995). Genome organization in the caliciviridae. *Trends Microbiol.* 3, 261–265. doi:10.1016/S0966-842X(00)88940-4.

Lateef, Z., Gimenez, G., Baker, E. S., and Ward, V. K. (2017). Transcriptomic analysis of human norovirus NS1-2 protein highlights a multifunctional role in murine monocytes. *BMC Genomics* 18. doi:10.1186/s12864-016-3417-4.

Lee, J. H., Alam, I., Han, K. R., Cho, S., Shin, S., Kang, S., et al. (2011). Crystal structures of murine norovirus-1 RNA-dependent RNA polymerase. *J. Gen. Virol.* 92, 1607–1616. doi.org/10.1099/vir.0.031104-0.

Lee, S., Liu, H., Wilen, C. B., Sychev, Z. E., Desai, C., Hykes, B. L., et al. (2019). A secreted viral nonstructural protein determines intestinal norovirus pathogenesis. *Cell Host Microbe* 25, 845–857.e5. doi:10.1016/j.chom.2019.04.005.

Leen, E. N., Sorgeloos, F., Correia, S., Chaudhry, Y., Cannac, F., Pastore, C., et al. (2016). A conserved interaction between a C-terminal motif in norovirus VPg and the HEAT-1 domain of eIF4G is essential for translation initiation. *PLoS Pathogens* 12, 1–34. doi.org/10.1371/journal.ppat.1005379.

Li, T.-F., Hosmillo, M., Schwanke, H., Shu, T., Wang, Z., Yin, L., et al. (2017). Human norovirus NS3 has RNA helicase and chaperoning activities. *J. Virol.* 92, e01606-17. doi:10.1128/jvi.01606-17.

Liao, Q., Wang, X., Wang, D., and Zhang, D. (2014). Complete genome sequence of a novel calicivirus from a goose. *Arch. Virol.* 159, 2529–2531. doi:10.1007/s00705-014-2083-6.

Lin, S. C., Qu, L., Ettayebi, K., Crawford, S. E., Blutt, S. E., Robertson, M. J., et al. (2020). Human norovirus exhibits strain-specific sensitivity to host interferon pathways in human intestinal enteroids. *Proc. Natl. Acad. Sci. U. S. A.* 117, 23782–23793. doi.org/10.1073/pnas.2010834117.

Liu, B., Clarke, I. N., and Lambden, P. R. (1996). Polyprotein processing in Southampton virus: identification of 3C-like protease cleavage sites by *in vitro* mutagenesis. *J. Virol.* 70, 2605–2610. doi:10.1128/jvi.70.4.2605-2610.1996.

Mahar, J. E., Jenckel, M., Huang, N., Smertina, E., Holmes, E. C., Strive, T., et al. (2021). Frequent intergenotypic recombination between the non-structural and structural genes is a major driver of epidemiological fitness in caliciviruses. *bioRxiv* 2021.02.17.431744; doi.org/10.1101/2021.02.17.431744.

Martinez-Gil, L., Bano-Polo, M., Redondo, N., Sanchez-Martinez, S., Nieva, J. L., Carrasco, L., et al. (2011). Membrane integration of poliovirus 2B viroporin. *J. Virol.* 85, 11315–11324. doi:10.1128/JVI.05421-11.

McCune, B. T., Tang, W., Lu, J., Eaglesham, J. B., Thorne, L., Mayer, A. E., et al. (2017). Noroviruses co-opt the function of host proteins VAPA and VAPB for replication via a phenylalanine–phenylalanine-acidic-tract-motif mimic in nonstructural viral protein NS1/2. *MBio* 8, 668–685. doi:10.1128/mBio.00668-17.

Meyers, G. (2003). Translation of the minor capsid protein of a calicivirus is initiated by a novel termination-dependent reinitiation mechanism. *J. Biol. Chem.* 278, 34051–34060. doi:10.1074/jbc.M304874200.

Meyers, G., Wirblich, C., and Thiel, H. J. (1991). Rabbit hemorrhagic disease virus-molecular cloning and nucleotide sequencing of a calicivirus genome. *Virology* 184, 664–676. doi:10.1016/0042-6822(91)90436-F.

Meyers, G., Wirblich, C., and Thiel, H. J. (1991). Genomic and subgenomic RNAs of rabbit hemorrhagic disease virus are both protein-linked and packaged into particles. *Virology* 184, 677–686. doi:10.1016/0042-6822(91)90437-G.

Mikalsen, A. B., Nilsen, P., Frøystad-Saugen, M., Lindmo, K., Eliassen, T. M., Rode, M. R., et al. (2014). Characterization of a novel calicivirus causing systemic infection in Atlantic salmon (*Salmo salar* L.): proposal for a new genus of *Caliciviridae*. *PLoS One* 9. doi:10.1371/journal.pone.0107132.

Miller, W. A., and Koev, G. (2000). Synthesis of subgenomic RNAs by positive-strand RNA viruses. *Virology* 273, 1–8. doi:10.1006/viro.2000.0421.

Mor, S. K., Phelps, N. B. D., Ng, T. F. F., Subramaniam, K., Primus, A., Armien, A. G., et al.

(2017). Genomic characterization of a novel calicivirus, FHMCV-2012, from baitfish in the USA. *Arch. Virol.* 162, 3619–3627. doi:10.1007/s00705-017-3519-6.

Morrison, J. M., and Racaniello, V. R. (2009). Proteinase 2A pro is essential for enterovirus replication in type I interferon-treated cells. *J. Virol.* 83, 4412–4422. doi:10.1128/JVI.02177-08.

Mussard, E., Pouzet, C., Helies, V., Pascal, G., Fourre, S., Cherbuy, C., et al. (2020). Culture of rabbit caecum organoids by reconstituting the intestinal stem cell niche *in vitro* with pharmacological inhibitors or L-WRN conditioned medium. *Stem Cell Res.* 48, 101980. doi:10.1016/j.scr.2020.101980.

Neill, J. D. (1990). Nucleotide sequence of a region of the feline calicivirus genome which encodes picornavirus-like RNA-dependent RNA polymerase, cysteine protease and 2C polypeptides. *Virus Res.* 17, 145–160. doi:10.1016/0168-1702(90)90061-F.

Neill, J. D. (2014). The complete genome sequence of the San Miguel sea lion virus-8 reveals that it is not a member of the vesicular exanthema of swine virus/San Miguel sea lion virus species of the *Caliciviridae*. *Genome Announc.* 2, 693–694. doi:10.1128/genomeA.01286-14.

Neznanov, N., Kondratova, A., Chumakov, K. M., Angres, B., Zhumabayeva, B., Agol, V. I., et al. (2001). Poliovirus protein 3A inhibits tumor necrosis factor (TNF)-induced apoptosis by eliminating the TNF receptor from the cell surface. *J. Virol.* 75, 10409–10420. doi:10.1128/jvi.75.21.10409-10420.2001.

Ng, K. K. S., Cherney, M. M., Vázquez, A. L., Machín, Á., Martín Alonso, J. M., Parra, F., et al. (2002). Crystal structures of active and inactive conformations of a caliciviral RNA-dependent RNA polymerase. *J. Biol. Chem.* 277, 1381–1387. doi.org/10.1074/jbc.M109261200.

Ng, K. K. S., Pendás-Franco, N., Rojo, J., Boga, J. A., Machín, Á., Martín Alonso, J. M., et al. (2004). Crystal structure of Norwalk virus polymerase reveals the carboxyl terminus in the active site cleft. *J. Biol. Chem.* 279, 16638–16645. doi.org/10.1074/jbc.M400584200.

Nguyen, L. T., Schmidt, H. A., Von Haeseler, A., and Minh, B. Q. (2015). IQ-TREE: a fast and effective stochastic algorithm for estimating maximum-likelihood phylogenies. *Mol. Biol. Evol.* 32, 268–274. doi:10.1093/molbev/msu300.

Nice, T. J., Strong, D. W., McCune, B. T., Pohl, C. S., and Virgin, H. W. (2013). A single-amino-acid change in murine norovirus NS1/2 is sufficient for colonic tropism and persistence. *J. Virol.* 87, 327–334. doi:10.1128/jvi.01864-12.

Nieva, J. L., Madan, V., and Carrasco, L. (2012). Viroporins: structure and biological functions.

Nat. Rev. Microbiol. 10, 563–574. doi:10.1038/nrmicro2820.

Nishimura, N., and Balch, W. (1997). A di-acidic signal required for selective export from the endoplasmic reticulum. *Science* 277, 17–19.

Nugent, T., and Jones, D. T. (2012). Detecting pore-lining regions in transmembrane protein sequences. *BMC Bioinformatics* 13. doi:10.1186/1471-2105-13-169.

Oglesby, A. S., Schaffer, F. L., and Madin, S. H. (1971). Biochemical and biophysical properties of vesicular exanthema of swine virus. *Virology* 44, 329–341. doi:10.1016/0042-6822(71)90264-9.

Oka, T., Katayama, K., Ogawa, S., Hansman, G. S., Kageyama, T., Ushijima, H., et al. (2005). Proteolytic processing of sapovirus ORF1 polyprotein. *J. Virol.* 79, 7283–7290. doi:10.1128/JVI.79.12.7283-7290.2005.

Petrignani, M., Verhoef, L., de Graaf, M., Richardus, J. H., and Koopmans, M. (2018). Chronic sequelae and severe complications of norovirus infection: a systematic review of literature. *J. Clin. Virol.* 105, 1–10. doi:10.1016/j.jcv.2018.05.004.

Pham, T., Perry, J. L., Dosey, T. L., Delcour, A. H., and Hyser, J. M. (2017). The rotavirus NSP4 viroporin domain is a calcium-conducting ion channel. *Sci. Rep.* 7, 1–11. doi:10.1038/srep43487.

Pinto, L. H., Dieckmann, G. R., Gandhi, C. S., Papworth, C. G., Braman, J., Shaughnessy, M. A., et al. (1997). A functionally defined model for the M2 proton channel of influenza A virus suggests a mechanism for its ion selectivity. *Proc. Natl. Acad. Sci. U. S. A.* 94, 11301–11306.

Pires, S. M., Fischer-Walker, C. L., Lanata, C. F., Devleesschauwer, B., Hall, A. J., Kirk, M. D., et al. (2015). Aetiology-specific estimates of the global and regional incidence and mortality of diarrhoeal diseases commonly transmitted through food. *PLoS One* 10, 1–17. doi:10.1371/journal.pone.0142927.

Radford, A. D., Coyne, K. P., Dawson, S., Porter, C. J., and Gaskell, R. M. (2007). Feline calicivirus. *Vet. Res.* 38, 319–335.

Robinson, B. A., Van Winkle, J. A., McCune, B. T., Peters, A. M., and Nice, T. J. (2019). Caspase-mediated cleavage of murine norovirus NS1/2 potentiates apoptosis and is required for persistent infection of intestinal epithelial cells. *PLoS Pathog.* 15. doi:10.1371/journal.ppat.1007940.

Romero-Brey, I., and Bartenschlager, R. (2014). Membranous replication factories induced by plus-strand RNA viruses. *Viruses* 6, 2826–2857. doi:10.3390/v6072826.

Sharp, T. M., Crawford, S. E., Ajami, N. J., Neill, F. H., Atmar, R. L., Katayama, K., et al.

(2012). Secretory pathway antagonism by calicivirus homologues of Norwalk virus nonstructural protein p22 is restricted to noroviruses. *Virol. J.* 9, 181. doi:10.1186/1743-422X-9-181.

Sharp, T. M., Guix, S., Katayama, K., Crawford, S. E., and Estes, M. K. (2010). Inhibition of cellular protein secretion by norwalk virus nonstructural protein p22 requires a mimic of an endoplasmic reticulum export signal. *PLoS One* 5, e13130. doi:10.1371/journal.pone.0013130.

Smertina, E., Urakova, N., Strive, T., and Frese, M. (2019). Calicivirus RNA-dependent RNA polymerases: evolution, structure, protein dynamics, and function. *Front. Microbiol.* 10, 1280. doi.org/10.3389/fmicb.2019.01280.

Smits, S. L., Rahman, M., Schapendonk, C. M. E., van Leeuwen, M., Faruque, A. S. G., Haagmans, B. L., et al. (2012). Calicivirus from novel recovirus genogroup in human diarrhea, Bangladesh. *Emerg. Infect. Dis.* 18, 1192–1195. doi:10.3201/eid1807.120344.

Sosnovtsev, S. V., Belliot, G., Chang, K.-O., Prikhodko, V. G., Thackray, L. B., Wobus, C. E., et al. (2006). Cleavage map and proteolytic processing of the murine norovirus nonstructural polyprotein in infected cells. *J. Virol.* 80, 7816–7831. doi:10.1128/jvi.00532-06.

Sosnovtsev, S. V., Garfield, M., and Green, K. Y. (2002). Processing map and essential cleavage sites of the nonstructural polyprotein encoded by ORF1 of the feline calicivirus genome. *J. Virol.* 76, 7060–7072. doi:10.1128/jvi.76.14.7060-7072.2002.

Strive, T., Wright, J., Kovaliski, J., Botti, G., and Capucci, L. (2010). The non-pathogenic Australian lagovirus RCV-A1 causes a prolonged infection and elicits partial cross-protection to rabbit haemorrhagic disease virus. *Virology* 398, 125–134. doi:10.1016/j.virol.2009.11.045.

Strtak, A. C., Perry, J. L., Sharp, M. N., Chang-Graham, A. L., Farkas, T., and Hyser, J. M. (2019). Recovirus NS1-2 has viroporin activity that induces aberrant cellular calcium signaling to facilitate virus replication. *mSphere* 4, 1–21. doi:10.1128/msphere.00506-19.

Studier, F. W., and Moffatt, B. A. (1986). Use of bacteriophage T7 RNA polymerase to direct selective high-level expression of cloned genes. *J. Mol. Biol.* 189, 113–130. doi:10.1016/0022-2836(86)90385-2.

Suhy, D. A., Giddings, T. H., and Kirkegaard, K. (2000). Remodeling the endoplasmic reticulum by poliovirus infection and by individual viral proteins: an autophagy-like origin for virus-induced vesicles. *J. Virol.* 74, 8953–8965. doi:10.1128/jvi.74.19.8953-8965.2000.

Te Velthuis, A. J. W. (2014). Common and unique features of viral RNA-dependent polymerases. *Cell. Mol. Life Sci.* 71, 4403–4420. doi.org/10.1007/s00018-014-1695-z.

Teterina, N. L., Pinto, Y., Weaver, J. D., Jensen, K. S., and Ehrenfeld, E. (2011). Analysis of Poliovirus protein 3A interactions with viral and cellular proteins in infected cells. *J. Virol.* 85, 4284–4296. doi:10.1128/jvi.02398-10.

Thorne, L., Bailey, D., and Goodfellow, I. (2012). High-resolution functional profiling of the norovirus genome. *J. Virol.* 86, 11441–11456. doi:10.1128/jvi.00439-12.

Thumfart, J. O., and Meyers, G. (2002). Rabbit hemorrhagic disease virus: identification of a cleavage site in the viral polyprotein that is not processed by the known calicivirus protease. *Virology* 304, 352–363. doi:10.1006/viro.2002.1660.

Tian, J., Kang, H., Huang, J., Li, Z., Pan, Y., Li, Y., et al. (2020). Feline calicivirus strain 2280 p30 antagonizes type I interferon-mediated antiviral innate immunity through directly degrading IFNAR1 mRNA. *PLoS Pathog.* 16, 1–27. doi:10.1371/journal.ppat.1008944.

Urakova, N., Frese, M., Hall, R. N., Liu, J., Matthaei, M., and Strive, T. (2015). Expression and partial characterisation of rabbit haemorrhagic disease virus non-structural proteins. *Virology* 484, 69–79. doi:10.1016/j.virol.2015.05.004.

Uyama, T., Morishita, J., Jin, X. H., Okamoto, Y., Tsuboi, K., and Ueda, N. (2009). The tumor suppressor gene H-Rev107 functions as a novel Ca^{2+}-independent cytosolic phospholipase A1/2 of the thiol hydrolase type. *J. Lipid Res.* 50, 685–693. doi:10.1194/jlr.M800453-JLR200.

Ventoso, I., Barco, A., and Carrasco, L. (1998). Mutational analysis of poliovirus 2A(pro): distinct inhibitory functions of 2A(pro) on translation and transcription. *J. Biol. Chem.* 273, 27960–27967. doi:10.1074/jbc.273.43.27960.

Vinjé, J., Estes, M. K., Esteves, P., Green, K. Y., Katayama, K., Knowles, N. J., et al. (2019). ICTV virus taxonomy profile: *Caliciviridae*. *J. Gen. Virol.* 100, 1469–1470. doi:10.1099/jgv.0.001332.

Weir, M. L., Klip, A., and Trimble, W. S. (1998). Identification of a human homologue of the vesicle-associated membrane protein (VAMP)-associated protein of 33 kDa (VAP-33): a broadly expressed protein that binds to VAMP. *Biochem. J.* 333, 247–51. doi:10.1042/bj3330247.

Weir, M. L., Xie, H., Klip, A., and Trimble, W. S. (2001). VAP-A binds promiscuously to both v- and tSNAREs. *Biochem. Biophys. Res. Commun.* 286, 616–621. doi:10.1006/bbrc.2001.5437.

Wirblich, C., Thiel, H. J., and Meyers, G. (1996). Genetic map of the calicivirus rabbit

hemorrhagic disease virus as deduced from in vitro translation studies. *J. Virol.* 70, 7974–83. doi:10.1006/viro.2000.0579.

Wolf, S., Reetz, J., Hoffmann, K., Gründel, A., Schwarz, B. A., Hänel, I., et al. (2012). Discovery and genetic characterization of novel caliciviruses in German and Dutch poultry. *Arch. Virol.* 157, 1499–1507. doi:10.1007/s00705-012-1326-7.

Wolf, Y. I., Kazlauskas, D., Iranzo, J., Lucía-Sanz, A., Kuhn, J. H., Krupovic, M., et al. (2018). Origins and evolution of the global RNA virome. *MBio* 9, 1–31. doi:10.1128/mBio.02329-18.

Wright, S., Kleven, D., Kapoor, R., Kavuri, S., and Gani, I. (2020). Recurring norovirus & sapovirus infection in a renal transplant patient. *IDCases* 20, e00776. doi:10.1016/j.idcr.2020.e00776.

Zhou, Y., Frey, T. K., and Yang, J. J. (2009). Viral calciomics: interplays between Ca^{2+} and virus. *Cell Calcium* 46, 1–17. doi:10.1016/j.ceca.2009.05.005.

Chapter 4. Lagovirus non-structural protein p23: a putative viroporin that interacts with heat shock proteins, uses a disulfide bond for dimerization and plays a role in Ca^{2+} homeostasis

Declaration of Co-Authored Publications

UNIVERSITY OF CANBERRA

For use in theses which include co-authored publications. This declaration must be completed for each co-authored publication and to be placed at the start of the thesis chapter in which the publication appears, or as a preface to the thesis.

Declaration for Thesis Chapter 4

DECLARATION BY CANDIDATE

Declaration for the following publication: Lagovirus non-structural protein p23: a putative viroporin that interacts with heat shock proteins and uses a disulfide bond for dimerization

Nature of Contribution	Extent of Contributions (%)
Conceptualisation, methodology, writing of the first draft and addressing reviewers' comments	70%

The following co-authors contributed to the work:

Name	Nature of Contribution Help/guidance with:	Contributor is also a UC student (Yes/No)
Adam J. Carroll	Mass spectrometry proteomics, revision of the manuscript	No
Joseph Boileau	Mass spectrometry proteomics, revision of the manuscript	No
Edward Emmott	Mass spectrometry proteomics, revision of the manuscript	No
Maria Jenckel	Data analysis, revision of the manuscript	No
Harpreet Vohra	Flow cytometry, revision of the manuscript	No
Vivien Rolland	Confocal microscopy, revision of the manuscript	No
Philip Hands	Confocal microscopy, revision of the manuscript	No
Joanna Hayashi	Data analysis, revision of the manuscript	No
Matthew J. Neave	Data analysis, revision of the manuscript	No
Han-Wei Liu	Mass spectrometry proteomics, revision of the manuscript	No
Robyn N. Hall	Supervision, revision of the manuscript	No
Tanja Strive	Supervision, revision of the manuscript	No
Michael Frese	Supervision, revision of the manuscript	No

Candidate's Signature

Date 10/06/2022

DECLARATION BY CO-AUTHORS

The undersigned hereby certify that:

(1) the above declaration correctly reflects the nature and extent of the candidate's contribution to this work, and the nature of the contribution of each of the co-authors;

(2) they meet the criteria for authorship in that they have participated in the conception, execution, or interpretation, of at least that part of the publication in their field of expertise;

(3) they take public responsibility for their part of the publication, except for the responsible author who accepts overall responsibility for the publication;

(4) there are no other authors of the publication according to these criteria;

(5) potential conflicts of interest have been disclosed to (a) granting bodies, (b) the editor or publisher of journals or other publications, and (c) the head of the responsible academic unit; and

(6) the original data are stored at the following location(s) and will be held for at least five years from the date indicated below:

[Please note that the location(s) must be institutional in nature, and should be indicated here as a department, centre or institute, with specific campus identification where relevant.]

Location(s):	CSIRO Black Mountain, University of Canberra, Australian National University

Declaration of Co-Authored Publications

Signatures	Date
(Michael Frese)	10/06/2022
(Tanja Strive)	13/06/2022
(Maria Jenckel)	14/06/2022
(Robyn Hall)	14/6/2022
(Phil Hands)	16/06/2022
(Nina Kenting)	16/08/2022
(Matthew Neave)	17/06/2022
(Jian-Wei Liu)	20/06/2022
(Adam Carroll)	20/6/22
Joseph Boileau	20/6/2022	12:08 PM AEST
HARPREET VOHRA	21/06/2022
(Edward Emmott)	Edward Emmott 21/6/2022
(Junna Hayashi)	22/06/2022

Lagovirus non-structural protein p23: a putative viroporin that interacts with heat shock proteins and uses a disulfide bond for dimerization

Elena Smertina[1,2,4], Adam J. Carroll[5], Joseph Boileau[5], Edward Emmott[7], Maria Jenckel[1], Harpreet Vohra[6], Vivien Rolland[3], Philip Hands[3], Junna Hayashi[9], Matthew J. Neave[8], Jian-Wei Liu[10], Robyn N. Hall[1,4], Tanja Strive[1,4], and Michael Frese[1,2*]

[1] Commonwealth Scientific and Industrial Research Organisation, Health and Biosecurity, Canberra, ACT, Australia; [2] Faculty of Science and Technology, University of Canberra, Canberra, ACT, Australia; [3] Commonwealth Scientific and Industrial Research Organisation, Agriculture and Food, Canberra, ACT, Australia; [4] Centre for Invasive Species Solutions, Canberra, ACT, Australia; [5] RSB/RSC Joint Mass Spectrometry Facility, Research School of Chemistry, Australian National University, Canberra, ACT, Australia; [6] Imaging and Cytometry Facility, John Curtin School of Medical Research, Acton, Canberra, ACT, Australia; [7] Centre for Proteome Research, Department of Biochemistry & Systems Biology, Institute for Systems, Molecular and Integrative Biology, University of Liverpool, Liverpool, UK; [8] Commonwealth Scientific and Industrial Research Organisation, Australian Centre for Disease Preparedness, Geelong, VIC, Australia; [9] Research School of Chemistry, The Australian National University, Acton, ACT, 2601, Australia; [10] Commonwealth Scientific and Industrial Research Organisation, Land and Water, Canberra, ACT, Australia

* Correspondence:

Michael Frese

michael.frese@canberra.edu.au

Abstract

The exact function(s) of the lagovirus non-structural protein p23 is unknown as robust cell culture systems for Rabbit haemorrhagic disease virus (RHDV) and other lagoviruses have not been established. Instead, a range of *in vitro* and *in silico* models have been used to study p23, revealing that p23 oligomerizes, accumulates in the cytoplasm, and possesses a conserved C-terminal region with two amphipathic helices. Furthermore, the positional homologs of p23 in other caliciviruses have been shown to possess viroporin activity. Here, we report on the mechanistic details of p23 oligomerization. Site-directed mutagenesis revealed the importance of an N-terminal cysteine for dimerization. Furthermore, we identified cellular interactors of p23 using stable isotope labelling with amino acids in cell culture (SILAC)-based proteomics; heat shock proteins Hsp70 and 110 interact with p23 in transfected cells, suggesting that they 'chaperone' p23 proteins before their integration into cellular membranes. We investigated changes to the global transcriptome and proteome that occurred in infected rabbit liver tissue and observed changes to the misfolded protein response, calcium signaling, and the regulation of the endoplasmic reticulum (ER) network. Finally, flow cytometry studies indicate slightly elevated calcium concentrations in the cytoplasm of p23-transfected cells. Taken together, accumulating evidence suggests that p23 is a viroporin that might form calcium-conducting channels in the ER membranes.

Introduction

The *Rabbit haemorrhagic disease virus* (RHDV), genus *Lagovirus*, family *Caliciviridae*, infects only lagomorphs (i.e., rabbits, hares, and related leporids; the detailed classification and nomenclature of lagoviruses can be found in **Supplementary Text S1**). RHDV is of particular importance in Australia, as this virus is used as a biocontrol agent to manage the introduced European rabbit, one of the most devastating vertebrate pest species in the country (Kerr et al., 2021). Caliciviruses are small, non-enveloped viruses with a positive-sense, single-stranded RNA genome. Calicivirus particles contain two types of RNA molecules: a genomic RNA of about 7.5 kb (encodes all virus proteins) and a subgenomic RNA of about 2 kb that encodes only the capsid proteins (Ehresmann and Schaffer, 1977) (**Figure 1**). Genomic and subgenomic RNAs both contain two open reading frames (ORFs) (Meyers et al., 1991a, 1991b). The first ORF of the genomic RNA encodes a polyprotein that is cleaved by the viral protease into seven non-structural (NS) proteins, namely p16 (NS1), p23 (NS2), helicase (NS3), p29 (NS4), VPg (NS5), protease (NS6), RNA-dependent RNA polymerase (RdRp; NS7), and the major structural protein VP60 (Meyers et al., 2000; Thumfart and Meyers, 2002). The

second ORF encodes only the minor structural protein VP10. The subgenomic RNA is colinear with the 3'-end of the genomic RNA, i.e., it also encodes the two structural proteins (Boga et al., 1992; Morales et al., 2004). The main role of the structural proteins is to build the viral capsid while the non-structural proteins support viral replication and translation, counteract host immune responses and possibly execute other functions (reviewed in Smertina et al., 2021).
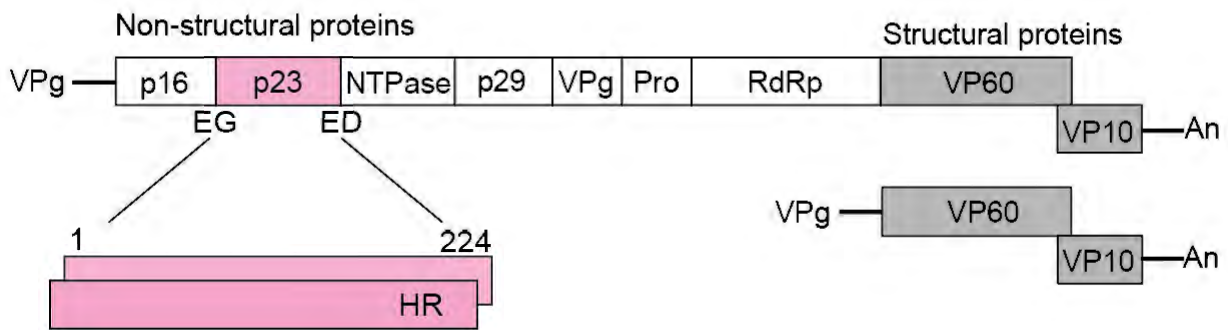
Figure 1. Schematic representation of a typical lagovirus genome. Both genomic (top) and subgenomic RNAs (bottom) contain two ORFs, are covalently linked to the viral protein VPg at the 5'-end and are polyadenylated at the 3'-end (An). The genomic RNA encodes non-structural (shown in white and pink) and structural proteins (shown in grey), whereas the subgenomic RNA encodes only structural proteins. The coding sequence for p23 (224 amino acid residues) is shown in pink; two copies are shown to indicate that p23 dimerizes; cleavage sites at the N-terminus (E, glutamine and G, glycine) and C-terminus (E, glutamine and D, aspartic acid) are indicated; HR, hydrophobic region.

Due to the lack of a robust cell culture system and reproducible reverse genetics system, rabbit caliciviruses remain poorly characterized. For example, the function(s) of the NS proteins p16, p23, and p29 have not yet been discovered. Nevertheless, recombinant proteins have been used to identify at least some features of these proteins. Here, we focus on p23 (originally named p23 after its apparent molecular weight, but later studies on the cleavage site between p23 and NS3 revealed that p23 is longer and has a molecular weight of approximately 25 kDa). The protein has an ER-like intracellular localization pattern and the ability to oligomerize (Urakova et al., 2015). The C-termini of p23 and homologous proteins from other caliciviruses are relatively conserved and hydrophobic, whereas the N-terminal part of these proteins is highly variable and largely disordered, i.e., it lacks secondary structure (Baker et al., 2012; Strtak et al., 2019). Using bioinformatic prediction tools, we previously identified two amphipathic membrane-spanning helices at the C-terminus of the p23 protein of RHDV

(Smertina et al., 2021). Similar helices have been described for the p23 homologs of other caliciviruses (Baker et al., 2012; Strtak et al., 2019). Furthermore, the NS1/2 precursor of the norovirus NS2, the NS2 of feline calicivirus (FCV, genus *Vesivirus*), and the NS1/2 of *Tulane virus* (genus *Recovirus*) localize to the ER (and/or Golgi membranes) and some of these proteins also oligomerize (reviewed in Smertina et al., 2021). These features led to the discovery of viroporin activity in cells expressing the NS1/2 of *Tulane virus* (Strtak et al., 2019). It is therefore tempting to speculate that the p23 protein of RHDV is also a viroporin that forms ion channels upon oligomerization.

Viroporins are small proteins that contain at least one membrane-spanning amphipathic helix (Nieva et al., 2012). As the formation of a functional membrane channel requires more than one transmembrane helix, small viroporins need to oligomerize. Viroporins often target intracellular membranes, especially those of the ER, thereby altering intracellular ion concentrations (Nieva et al., 2012). For example, the NS1/2 proteins of *Tulane virus* and some noroviruses cause a release of Ca^{2+} ions from the ER to the cytoplasm (Strtak et al., 2019). Many secreted proteins and cell surface membrane proteins (e.g., MHC proteins) acquire correct folding in the ER lumen, a process that depends on specific concentrations of Ca^{2+} and other ions. The elevated Ca^{2+} level in the ER (100 μM compared to 10–100 nM in the cytoplasm) is achieved by the sarco/endoplasmic reticulum Ca^{2+}-ATPase, which pumps Ca^{2+} from the cytoplasm into the ER lumen. Depleted Ca^{2+} levels in the ER can trigger an unfolded protein response, as chaperones and folding enzymes depend on high Ca^{2+} concentration (Kleizen and Braakman, 2004). On the other hand, increased levels of Ca^{2+} in the cytoplasm support many steps of the viral life cycle, from entry to replication, and the release of viral particles (Zhou et al., 2009).

In this study, we propose a mechanism of p23 oligomerization. We also identify heat shock proteins (Hsps) as cellular interaction partners of p23. Our results suggest that RHDV p23 is a viroporin that may form ion channels in ER membranes.

Materials and methods

Cell culture and SILAC labelling

Rabbit kidney (RK-13) cells (obtained from the European Collection of Cell Cultures, Porton Down, U.K.; 00021715) were cultured in Eagle's minimum essential medium (MEM) supplemented with 10% fetal bovine serum (FBS; Sigma-Aldrich, St. Louis, MI), 2 mM Glutamax (Gibco), 100 ug/ml of streptomycin (Gibco), and 100 units/ml of penicillin (Gibco). Cells were maintained in 5% CO_2 at 37°C in humidified incubators. For SILAC labelling, cells

were cultured in SILAC MEM (Thermo Fisher Scientific, MA, USA), a depleted medium that lacks the two amino acids lysine and arginine. Before use, SILAC MEM was supplemented with either unlabelled ('light') L-arginine and L-lysine (Sigma-Aldrich, St. Louis, MO) or isotope-labelled ('heavy') $^{13}C_6^{15}N_2$ L-lysine (Lys8) and $^{13}C_6^{15}N_4$ L -arginine (Arg10) (Sigma-Aldrich). To avoid unlabelled amino acid contamination, dialyzed FBS (10 kDa cut-off; Gibco, Thermo Fisher Scientific) was used (protocol adapted from Emmott and Goodfellow, 2014). For the same reason, a non-enzymatic cell dissociation solution (Sigma-Aldrich) was used to dislodge the cells for passaging (Sigma-Aldrich). Cells were cultured for at least seven passages in 'heavy' medium, and incorporation of heavy isotope-labelled amino acids was confirmed by mass spectrometry (MS) analysis. Cryopreserved aliquots of labelled cells were used in all subsequent experiments.

Rabbit liver samples

RHDV2-infected and uninfected control rabbit liver samples (described in a previous study (Neave et al., 2018)) were used for label-free quantification (LFQ). Briefly, rabbits were either infected with RHDV2 (genotype GI.1bP-GI.2) or mock-infected with PBS. The animals were humanely killed 24 h post-infection, and 25% liver homogenates were prepared in RNA-later buffer and stored at -20°C. Samples from three RHDV2-infected animals (K375, K376, K378) and three uninfected animals (K3, K14, K12) were used in this study. Liver samples were clarified at 0.2 g for 5 min at 4°C, and 100 mg of solid precipitate was collected into tubes with glass beads. Liver homogenates were lysed in 300 µl of PBS (pH 7.5) with 150 mM NaCl, 0.5 mM EDTA, 0.5% Igepal CA-630 with protease inhibitors (Roche), 1 mM $MgCl_2$, and 1 µl/ml benzonase nuclease (5 KU; Sigma-Aldrich). The suspension was homogenized using a Precellys homogenizer (Bertin Technologies) and incubated on ice for 30 min with gentle rocking to allow for full lysis. Finally, the lysates were cleared by centrifugation and supernatants were used for MS sample preparation.

Plasmids and transfections

Coding sequences for p23 (genotype GI.1cP) and green fluorescent protein (GFP) were cloned into the pCMV-Tag2C expression vector (Agilent Technologies, CA, USA) as described previously (Urakova et al., 2015) to generate N-terminally FLAG-tagged constructs (FLAG:p23 and FLAG:GFP). The Q5 site-directed mutagenesis kit (NEB) was used to generate constructs with cysteine to serine substitutions at the C-terminus of p23 (C451S, C456S, and a double substitution variant), at the N-terminus (C41S), a triple cysteine to serine variant, and p23 Δ146–224 truncated variant, as per manufacturer's instructions. All constructs were

verified by Sanger sequencing at the Biomolecular Resource Facility of The John Curtin School of Medical Research (Australian National University, Canberra, Australia). Lipofectamine P3000 (Invitrogen, Thermo Fisher Scientific) was used for transfections following the manufacturer's guidelines. For SILAC experiments, antibiotic- and FBS-free SILAC medium was used in place of Opti-MEM (Gibco, Thermo Fisher Scientific). All SILAC experiments were performed in triplicate with one label-swap sample. For affinity purifications, labelled RK-13 cells were plated on 10-cm dishes and, when 70–80% confluent, transfected with 14 µg of plasmid complexed with Lipofectamine 3000. After transfection, cells were incubated overnight in 5% CO_2 at 37°C prior to lysis and affinity purification.

Cell lysis and affinity purification

Transfected cells were washed with ice-cold PBS and scraped into a centrifuge tube with 1 ml PBS. Harvested cells were centrifuged at $200 \times g$, resuspended in 400 µl of lysis buffer (PBS, pH 7.5 with 150 mM NaCl, 0.5 mM EDTA, 0.5% Igepal CA-630, and protease inhibitors (Roche, Basel, Switzerland)) and incubated on ice for 20 min with gentle rocking. Remaining cell debris was removed by centrifugation, and the supernatants were subjected to affinity purification after a 50-µl sample was set aside for Western blotting. Total protein concentration in the lysates was estimated with the bicinchoninic acid (BCA) protein assay (Abcam, Cambridge, UK) to ensure that the same amount of protein lysate was used for all affinity purifications. To reduce the concentration of Igepal CA-630, the lysates were diluted with an equal volume of washing buffer without Igepal CA-630 prior to affinity purification. After equilibration with washing buffer, anti-FLAG M2 affinity gel beads (25 µl per sample) (Sigma-Aldrich) were incubated with the cell lysates overnight at 4°C with rotation. After binding, the beads were washed three times with 500 µl of washing buffer. To elute the proteins from the beads, 60 µl of elution buffer (100 mM triethylammonium bicarbonate (TEAB), pH 7.55 with 5% (w/v) sodium dodecyl sulphate (SDS)) was added and samples were incubated for 10 min at 95°C. To collect the eluates, samples were centrifuged at $8,600 \times g$ for 2 min at room temperature and another aliquot was set aside for Western blotting. Eluates from p23 affinity purifications were combined with eluates from GFP affinity purifications at a 1:1 ratio (by volume), resulting in a total of three samples per experiment.

Sample preparation for MS analysis

SILAC samples

Combined eluates (a 1:1 mixture of p23 and GFP or 1:1 RdRp and GFP) were subjected to MS sample preparation using suspension trapping (s-trap; Protifi, Huntington, NY)

(Zougman et al., 2014), as per the manufacturer's recommendations. Briefly, samples were reduced with 20 mM dithiothreitol and alkylated with 40 mM iodoacetomide (Sigma-Aldrich). S-trap micro columns were used for trypsin digestion; columns were incubated overnight at 37°C with 2.5 ng/µl of trypsin (Promega, Madison, WI) per sample. Resulting peptides were diluted as recommended by the manufacturer and dried using a SpeedVac concentrator. Dried peptides were stored at -20°C before resuspension in 0.1% formic acid. Samples were filtered (0.2 µm; Millex, Merck Millipore; Darmstadt, Germany) prior to MS processing.

Global proteome analysis (rabbit liver samples)

Liver lysates were subject to a BCA assay (Abcam), and a total of 100 µg of protein from each sample was loaded onto s-trap micro columns (Protifi), as described above. Trypsin digestion was performed overnight with 1.5 µl of trypsin (Promega) per sample. Eluted peptides were dried using a SpeedVac and fractionated with a High pH Reversed-Phase Peptide Fractionation kit (Pierce, Thermo Fisher Scientific), as recommended by the manufacturer. Briefly, the peptides were dissolved in 300 µl of 0.1% trifluoroacetic acid and loaded onto conditioned C18 columns (provided with the fractionation kit). After washing, the peptides were sequentially eluted with 5, 7.5, 10, 12.5, 15, 17.5, 20, and 50% acetonitrile in 0.1% triethylammonium bicarbonate. All fractions were dried and resuspended in 0.1% formic acid prior to MS processing.

Western blotting

Cell lysates were mixed with SDS-PAGE sample buffer (with or without β-mercaptoethanol to create reducing and non-reducing conditions, respectively), denatured by boiling for 5 min, and separated on 4–20% TruPAGE pre-cast gels (Sigma-Aldrich). Proteins were transferred onto a nitrocellulose transfer membrane (NitroBind, MSI, Cole-Parmer, US) using the Bio-Rad (Hercules, CA, USA) wet transfer blotting module. The membrane was subsequently blocked in 5% skim milk (Coles Supermarkets, Australia) in tris-buffered saline with 0.1% Tween-20 (TBST) for 2 h at room temperature. Incubation with primary antibodies was performed overnight at 4°C in TBST. Incubation with secondary antibodies conjugated to horseradish peroxidase was performed for 1 h at room temperature in TBST. SIGMAFAST 3,3'-diaminobenzidine tablets (Sigma-Aldrich) were used for visualization of bands according to the manufacturer's instructions. Staining of β-actin was used as a loading control where appropriate.

MS data acquisition and analysis

For LFQ, the digested protein samples were analyzed using data-dependent MS/MS on a Thermo Orbitrap Fusion ETD mass spectrometer coupled to a Dionex UltiMate 3000 RSLCnano liquid chromatography (LC) system via a Nanospray Flex nano-ESI ion source (Thermo Fisher Scientific). Following injection by the autosampler, peptides were initially trapped onto a C18 PepMap100 µ-precolumn (5-µm particle size, 100 Å pore size; Thermo Fisher Scientific; Part No. 160454) with a 15 µl/min flow of 5% (v/v) acetonitrile in water coming from the loading pump of the LC, for 10 min, at which point a valve was switched to place the trap between the nano pump and the nano LC column to begin chromatographic separation. The peptides were separated on a C18 column (ReproSil-Pur 120 C18-AQ, 1.9 µm particle size; Dr Maisch, Ammerbuch, Germany; Part No. r119.aq.0001) packed in-house at the Joint Mass Spectrometry Facility (Australian National University) (Richards et al., 2015). The nano LC mobile phase gradient was as follows: flow rate of 350 nL/min; solvent A = MilliQ Ultra-Pure water + 2% LC/MS-grade acetonitrile + 0.1% (v/v) Optima LC/MS-grade formic acid; solvent B = MilliQ Ultra-Pure Water + 80% Optima LC/MS-grade acetonitrile + 0.1 % (v/v) formic acid; 5% B from 0 to 15 min; 12.5% B at 20 min; 40% B at 95 min; 80% B at 97 min, hold at 80% B until 109 min; 5% B at 110 min; hold at 5% B until 120 min. Mass spectrometer settings were as follows: Application Mode = Peptide; Positive mode ESI with 2.3 kV static spray voltage; Ion Transfer Tube Temperature = 305 °C; Expected LC Peak Width = 30 s; Advanced Peak Determination = ON; Default Charge State = 2; Internal Mass Calibration = OFF; Survey Scans had Orbitrap Resolution = 120000, Scan Range 375-1500 m/z, RF Lens = 60%, Maximum Inject Time = 50 ms; Monoisotopic Peak Determination = Peptide; AGC Target = 400000; Intensity Threshold = 5.0E3; Include Charge States 2-7; Include undetermined charge states = OFF; Dynamic Exclusion was set to exclude for 60 s after 1 selection event with a mass tolerance of ± 10 ppm; Exclude Isotopes = ON; Perform dependent scan on single charge state per precursor only = OFF; Precursor Priority = Most Intense; MS2 scans where performed on the IonTrap detector with an isolation window of 1.6 m/z, Scan Range Mode = AUTO, Isolation Offset = OFF, Activation Type = CID, Collision Energy = 35%, Scan Rate = Rapid, Maximum Injection Time = 35 ms; Duty Cycle was limited to 3 seconds. The same acquisition parameters were used for the SILAC samples, except the spray voltage was set to 2.4 kV and the targeted Mass Difference filter was used with the following settings: number of precursors in the targeted group = 2, Mass List: Lys-8 and Arg-10, Partner Intensity Range Relative to the Most Intense Precursor (%) 5–100, Mass tolerance:

± 10 ppm, perform subsequent scan on: most intense ion in the pair, charge state requirement: ions must be the same.

MS raw data analysis

MaxQuant software (version 1.6.10.43) was used for peptide identification and protein quantification (Cox and Mann, 2008). The Andromeda search engine (Cox et al., 2011) was used to search against the *Oryctolagus cuniculus* (European rabbit) UniProt FASTA database (downloaded on 21st August 2019) and a custom library of RHDV2 FASTA protein sequences based on the BlMt-1 GI.1bP-GI.2 virus (GenBank accession KT280060.1). Default search parameters were used, including up to two 'missed trypsin cleavage sites', 'oxidation of methionine', and 'N-terminal acetylation' as variable modifications, and 'carbamidomethylation of cysteine' as a fixed modification. The data were searched against a reverse database and peptide-spectrum match and protein false discovery rate was set to 0.01. LFQ (Cox et al., 2014) was used for whole proteome analysis. The 'match between runs' option was not applied. For SILAC raw data analysis, the 'light' and 'heavy' labels were specified in MaxQuant. Re-quantify and match between runs options were applied in this case.

Statistical analysis and data visualization

Proteomics

The whole proteome data were analyzed in R version 4.0.2 (R Core Team, 2020) using the packages DEP (Zhang et al., 2018), Enhanced Volcano (Blighe et al., 2020), TopGO (Alexa and Rahnenfuhrer, 2020), and GOplot (Walter et al., 2015). Multiple testing adjusted p-values were used with a significance cut-off of <0.01.

SILAC data analysis was performed with the Perseus software (version 1.6.10.45; Tyanova et al., 2016). The following protein groups were filtered out: 'only identified by site', 'by reversed sequence', and 'potential contaminants'. Normalized heavy/light SILAC ratios were converted to a log scale ($\log_2$ SILAC ratio) and filtered for proteins identified in at least two out of three replicates. Significantly enriched proteins were identified using one sample *t*-test (compared to $\log_2$ ratio = 0, or no difference with internal 'light' GFP control) with an unadjusted p-value of <0.05.

Transcriptomics (RNA sequencing)

RNA sequencing for transcriptome analysis was conducted previously (Neave et al., 2018) using the same liver homogenates that were used for the whole proteome analysis described here. Briefly, TopHat 2.1.1 (Trapnell et al., 2009) was used to map the sequenced reads to the rabbit genome assembly OryCun2.0 (GenBank assembly accession

GCA_000003625.1). HTseq was used to count the reads for each gene (Anders et al., 2015). For statistical analysis and visualization, the R packages DESeq2 (Love et al., 2014), Enhanced Volcano (Blighe et al., 2020), and topGO (Alexa and Rahnenfuhrer, 2020) were used. The significance cut-off for differential gene expression was set to a multiple testing adjusted p-value <0.01.

Immunofluorescence and confocal microscopy

For the full list of antibodies used in this work, please refer to the **Supplementary Table S1**.

RK-13 cells grown on 8-chamber slides (Nunc Lab-Tek II, Thermo Fisher Scientific) were transfected as described above. After overnight incubation, cells were fixed with 4% paraformaldehyde in PBS for 15 min, permeabilized with 0.25% Triton X-100 in PBS for 10 min, and incubated for 90 min with blocking solution (5% bovine serum albumin; Sigma-Aldrich) in PBS. All incubations were performed at room temperature. Primary and secondary antibodies were diluted in 0.1% Tween-20 in PBS and were incubated overnight at 4°C and for 1 h at room temperature, respectively. Cell nuclei were stained with 4',6-diamidino-2-phenylindole (DAPI) (Sigma-Aldrich). Finally, cover slips were mounted onto glass slides with Fluoroshield mounting medium (Sigma-Aldrich). Samples were imaged using a Leica SP8 (Leica Microsystems, Germany) laser-scanning confocal microscope equipped with a 40x objective and controlled with the Leica Application Suite X 3.5.1.18803 software (Leica Microsystems, Germany). Cells were imaged in three separate tracks. In the first track, samples were excited with 405 nm and DAPI signals were collected between 420-440 nm, together with transmitted light; in a second track, samples were excited with 499 nm and AF488 signals were collected between 510 and 540 nm; and in the third track, samples were excited with 555 nm and AF555 signals were collected between 563 and 630 nm. Cells were imaged using z-stacks, but quantitative colocalization analysis was performed on single planes only, using Leica software. Data were statistically analyzed in RStudio (R version 4.2.0; R Core Team, 2020) using one-way analysis of variance (ANOVA) followed by a Tukey's honest significant difference test; graphs were produced with ggplot2 R package (Gómez-Rubio, 2017).

Flow cytometry: Ca^{2+} flux measurement

Fluo-4 acetyloxymethyl ester (Fluo-4 AM) (Thermo Fisher Scientific) 2 mM stock solution was prepared in anhydrous dimethyl sulfoxide (DMSO) (Sigma-Aldrich). RK-13 cells were grown on 60-mm dishes until 70–80% confluent and were transfected using lipofectamine 3000 as described above. After 14 hours incubation, cells were harvested with trypsin,

resuspended in FBS-free Dulbecco's Modified Eagle Medium (DMEM) and counted using a haemocytometer. Cells were diluted to 1×10^6 cells/ml with FBS-free DMEM and loaded with 1.5 µM final concentration of Fluo-4 AM (Thermo Fisher Scientific). Immediately after that, cell suspensions were vortexed and incubated for 30 mins at 37°C while being protected from light. Dulbecco's phosphate buffered saline (DPBS) supplemented with 2% FBS was used to wash excess Fluo-4 AM from cells. After centrifugation, cells were resuspended to 1×10^6 cells/ml in 2% FBS DPBS. LSRII flow cytometer (BD Biosciences) was used for data acquisition. Data analysis was performed using FlowJo software version 10.8.1 (Tree Star, Ashland, OR, USA) and R (R Core Team, 2020). To pool the results of four independent experiments, the mean fluorescence intensities for each condition in each experiment were summed and each mean values were divided by the sums, resulting in normalization coefficients. Individual fluorescence intensities values were then multiplied by the respective coefficient. These data were then analyzed using the one-way Kruskal-Wallis test and pairwise comparisons were performed using the Wilcoxon rank sum test with multiple testing correction.

In silico predictions

The Predictor of Natural Disordered Regions (PONDR, http://www.pondr.com/) was used to analyze p23 protein sequences of RHDV (NC_001543.1), EBHSV (NC_002615.1), and RCV (MF598302.1). The PONDR® output is a plot that indicates the strength of the prediction at each region with a cut-off value equal to 0.5 (Xue et al., 2010). The PSIPRED Protein Analysis Workbench server (http://bioinf.cs.ucl.ac.uk/psipred/) (Buchan and Jones, 2019) was used to analyze the secondary structure of p23 proteins, the potential presence of membrane helices was analyzed with the MEMSAT-SVM algorithm (Nugent and Jones, 2010, 2012). Membrane helix composition was studied using wheel diagrams generated with HeliQuest (https://heliquest.ipmc.cnrs.fr/; Gautier et al., 2008).

Lagovirus p23 protein sequence alignment

All publicly available lagovirus p23 sequences (n=2025; 6th August 2021) were downloaded from the GenBank nucleotide database based on the search term 'lagovirus'. Three sequences were excluded (EU552531, UGVC01000001, KY437668) because they were either not a lagovirus sequence or were provided as a circular sequence. A nucleotide alignment was generated from the remaining 2,022 sequences using MAFFTv7.450 in Geneious Prime 2021.1.1 (https://www.geneious.com) using default settings. The nucleotide alignment was truncated to the annotated p23/p26 coding sequence (672 nt) and partial p23 coding sequences were removed (leaving n=567 sequences). The alignment was translated, and an amino acid

sequence alignment (224 amino acids) was generated using MAFFTv7.450 with default amino acid settings.

Results

Oligomerization of p23 requires a disulfide bond

Previous experiments with recombinant proteins suggested that p23 forms dimers in transfected cells (Urakova et al., 2015). To better understand the molecular mechanism behind the oligomerization, we immunoprecipitated a N-terminally FLAG-tagged p23 (RHDV/GI.1) that was transiently expressed in rabbit kidney (RK-13) cells. Cell lysates were loaded on anti-FLAG antibody resin and proteins were eluted with either a reducing Laemmli buffer that contained β-mercaptoethanol or a non-reducing Laemmli buffer. Proteins in the eluate were separated and immunostained using SDS-PAGE and Western blotting. The experiment confirmed the previous observation that p23 forms dimers but also indicated that dimerization depends on the formation of one or more disulfide bonds, as the dimers were only observed in non-reducing conditions (**Figure 2A**). The protein sequence of p23 contains a total of three cysteine residues; one is located near the N-terminus (position 41) and two are located near the C-terminus (positions 207 and 212) (**Figure 2B**). All three cysteines are highly conserved, i.e., we found that all available lagovirus sequences contained cysteines at positions 41 and 212 and that nearly all contained a cysteine at position 207 (**Figure 2C**). These findings prompted us to investigate the role of cysteine residues in the oligomerization of p23 and check whether oligomerization depends on one or two intermolecular disulfide bonds. To find out whether one or more of these cysteines are indeed essential for oligomerization, site-directed mutagenesis was used to substitute cysteine with serine residues. Initially, we focused on the C-terminal cysteine residues and substituted: (*i*) the cysteine at position 207 (C207S), (*ii*) cysteine at position 212 (C212S), (*iii*) the cysteines at positions 207 and 212 (C207S/C212S, referred to as 'double'). These protein variants were expressed and immunoprecipitated as described above; eluates were collected using reducing or non-reducing loading buffers, and samples were analyzed by Western blotting (**Figure 2D**). The C207S and C212S variants migrated noticeably faster under non-reducing conditions, which may be indicative of an intramolecular disulfide bond between the neighboring cysteine residues at positions 207 and 212. However, both variants were still able to dimerize, indicating that neither of the C-terminal cysteine residues is involved in dimerization. The result further suggests that the N-terminal cysteine at position 41 is likely involved in the formation of an intermolecular disulfide bond that stabilizes dimers. To test this hypothesis, we generated two additional variants by substituting (*iv*) the cysteine at

position 41 (C41S) and (*v*) the cysteines at positions 41, 207, and 212 (C41S/C207S/C212S; referred to as 'triple'). Our results clearly show that the N-terminal cysteine at position 41 is essential for the dimerization of p23 or for stabilization of dimers, as no dimer was observed under non-reducing conditions for any of the variants that contain a serine at position 41 (**Figure 2E**). Moreover, additional bands indicate the presence of higher-order oligomers (trimers and tetramers) under non-reducing conditions (**Figure 2E**).

In order to test whether hydrophobic interactions aid in the stabilization of dimers (and perhaps higher-order oligomers), some samples were processed under non-reducing conditions and without boiling. Under these conditions, we did not detect any oligomerization (**Figure 2F**), suggesting that the formation of the disulfide bond between cysteines at position 41 is the main driver behind the dimerization of p23. Finally, a truncated p23 variant was generated that retains the cysteine at position 41 but lacks 78 C-terminal amino acids (FLAG:p23 Δ146–224). According to earlier *in silico* predictions (Smertina et al., 2021), such a truncation will remove two transmembrane helices, and it would be interesting to determine whether this protein variant can still oligomerize. However, we were not able to detect FLAG:p23 Δ146–224 in transiently transfected cells (**Figure 2G**), suggesting that the variant is unstable and rapidly degraded.
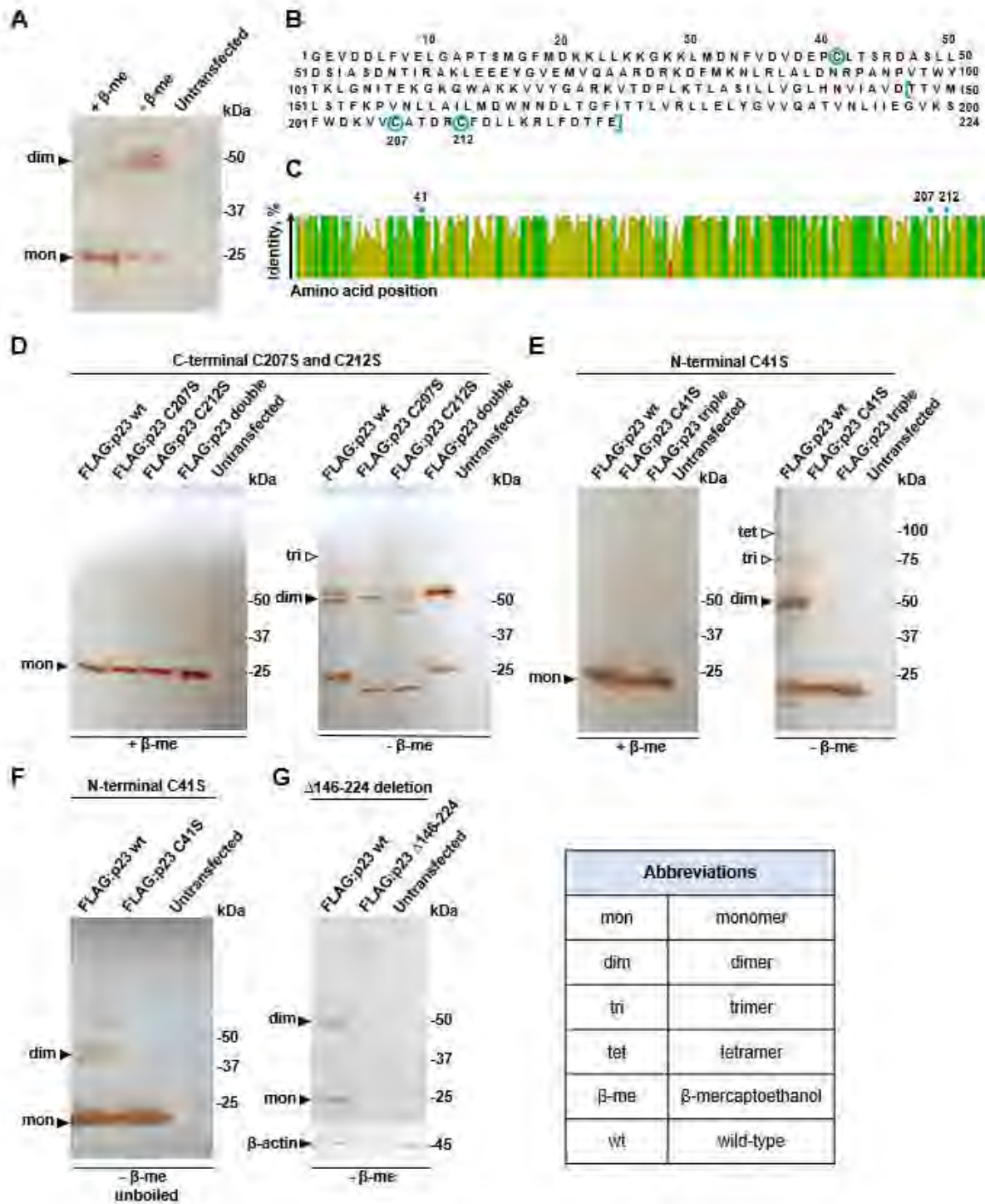
Figure 2. Dimerization of p23 depends on disulfide bond formation. (**A**) Recombinant FLAG-tagged p23 (wt, wild-type) expressed in transiently transfected RK-13 cells was eluted from an anti-FLAG resin with reducing or non-reducing Laemmli buffer containing β-mercaptoethanol (+ β-me) or without β-mercaptoethanol (- β-me), respectively. Affinity purified p23 was separated by SDS-PAGE and analyzed by Western blotting using anti-FLAG antibodies; bands corresponding to monomeric p23 and dimeric forms can be observed. Untransfected RK-13 cell lysate was subject to immunoprecipitation as a negative control. The

position of molecular mass standards is shown at the right. (**B**) RHDV/GI.1 p23 (NC_001543.1) protein sequence; the three cysteine residues at positions 41, 207, and 212 are highlighted in blue; and amino acids truncated in variant FLAG:p23 Δ146–224 are indicated using blue square brackets. (**C**) A consensus sequence and identity plot were generated using 567 lagovirus p23 sequences; the positions of the cysteine residues at position 41, 207 and 212 are indicated above the plot (also in blue). The percentage identity at each amino acid position is indicated by column height and color (green means completely conserved, olive means less than complete identity, and red refers to a low identity). (**D**) Variants with C-terminal cysteine substitutions. Dimer formation of p23 wild-type (wt) and variants with cysteine-to-serine substitutions at positions 207 (C207S) or 212 (C212S) or both, 'double' was not affected under non-reducing conditions; the possible formation of a trimer is suggested by a weak band. (**E**) Dimers did not form between p23 variants with a cysteine-to-serine substitution at position 41 or in variants that had all cysteines substituted to serine ('triple'); higher-order oligomers, trimers and tetramers are seen in non-reducing conditions. (**F**) Unboiled samples were analyzed in a gel that did not contain SDS. Under these conditions, the C41S variant did not form dimers and both the wt protein and the C41S variant failed to form higher-order oligomers. In panel D, 10-µl samples were loaded per lane, and in E and F, 20-µl samples were loaded per lane (to enhance the detection of higher- order oligomers). (**G**) The truncated p23 Δ146–224 variant without transmembrane helices was not detected in either monomeric or dimeric form.

Lagovirus protein p23 contains two amphipathic transmembrane helices

To better understand the mechanism and the role of p23 dimerization, we explored the secondary structure of p23 proteins from RHDV, *Rabbit calicivirus* (RCV), and *European brown hare syndrome* virus (EBHSV) using the predictor of natural disordered regions (PONDR) server (Xue et al., 2010) and the PSIPRED protein analysis workbench (Buchan and Jones, 2019). Most of the N-terminal 125 residues of all three proteins are hydrophilic and disordered, while the C-terminal region is hydrophobic and highly ordered (see Kyte-Doolittle and PONDR plots in **Figure 3**). Furthermore, the MEMSAT-SVM secondary structure prediction algorithm identified two pore-lining (amphipathic) helices near the C-terminus in all three lagovirus p23 proteins (**Figure 3A**, **C**, **E**, **G**, **I**, **K**), suggesting that all p23 proteins interact with membranes and possibly form a transmembrane channel. To further study the composition of these helices, HeliQuest (Gautier et al., 2008) was used to generate 'helix wheels'. The first helix ('Helix 1', aa 132–147) appears too short to build a wheel. Therefore, only wheels for the second helix ('Helix 2', aa 177–198) are shown (**Figure 3 B**, **F**, **J**). In all cases, the results show

a clear separation into mostly polar (hydrophilic) and non-polar (hydrophobic) regions, suggesting a conserved amphipathic nature of the predicted helices.
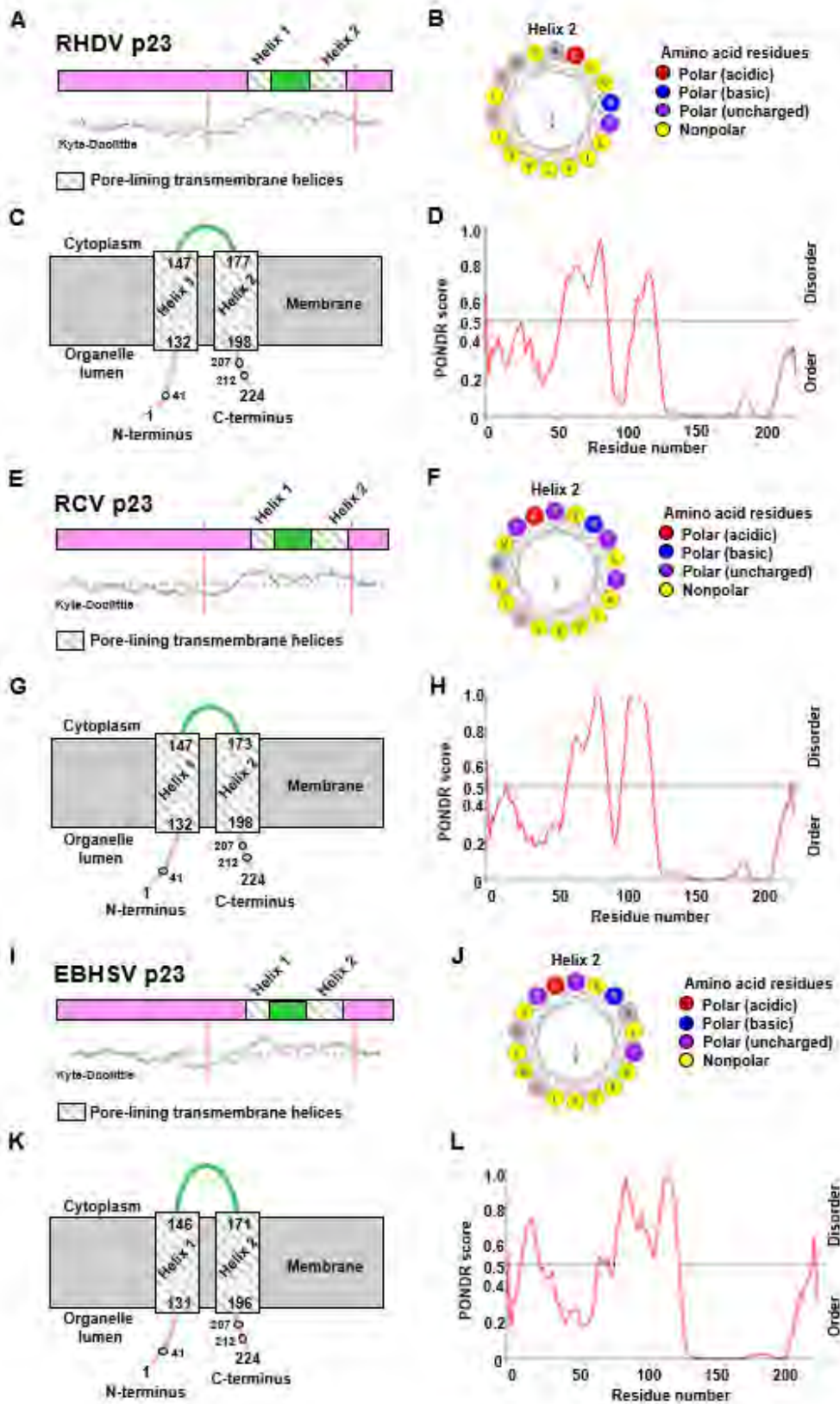
Figure 3. Prediction of transmembrane helices and disordered regions using *in silico* sequence analyses. (**A**–**D**) p23 protein sequences from *Rabbit haemorrhagic disease virus* (RHDV/GI.1; NC_001543.1), (**E**–**H**) *Rabbit calicivirus* (RCV/GI.4; MF598302.1), and (**I**–**L**) *European brown hare syndrome virus* (EBHSV/GII.1; NC_002615.1). (**A**, **C**, **E**, **G**, **I**, **K**) PSIPRED secondary structure prediction with MEMSAT-SVM algorithm and Kyte-Doolittle hydropathy plot revealed the presence of two putative transmembrane helices in the p23 proteins of all lagoviruses examined. The helices ('helix 1' and 'helix 2') are shown as striped boxes. (**D**, **H**, **L**) PONDR plot shows predicted disordered and ordered regions; the strength of the prediction is indicated by the score on the y-axis (>0.5 are considered disordered). (**B**, **F**, **J**) HeliQuest was used to generate a wheel diagram for the amino acid sequence of 'helix 2'. Arrows represent direction and magnitude of the hydrophobic moment. Note that the orientation of p23 within the membrane is not clear.

According to the secondary structure prediction, the cysteine at position 41 is further away from the membrane than cysteines 207 and 212, and is thus more accessible for a disulfide bond formation. The membrane orientation of the N- and C-termini are unknown; however, it is likely that both are located in the organelle lumen, e.g., the ER as this organelle provides a favorable oxidative environment for disulfide bond formation (Tu and Weissman, 2004). The observed oligomerization may lead to the formation of a transmembrane channel built from two or more p23 monomers.

Recombinant p23 localizes with the ER in transfected cells

The p23 proteins of RHDV and RCV show an ER-like localization in transfected RK-13 cells (Urakova et al., 2015). Homolog proteins of many other caliciviruses were also found to colocalize with ER membranes, with only the p23 homolog of human norovirus (NS1/2) colocalizing with the Golgi (Ettayebi and Hardy, 2003; reviewed in Smertina et al., 2021). Our hypothesis that the p23 protein of lagoviruses is a viroporin prompted us to look more closely at the intracellular localization of p23. RK-13 cells were seeded in chamber slides and transfected to transiently express a FLAG-tagged p23. The p23 protein was co-stained either with the ER marker calnexin or α-tubulin, a major structural component of the cytoskeleton (**Figure 4 A**–**C**, **E**–**G**). We found that p23 strongly colocalizes with calnexin in areas that contain ER membranes. In contrast, p23 does not always colocalize with α-tubulin, although p23 and α-tubulin staining often overlaps in the cytoplasm around the nucleus, the colocalization did not extend to the periphery where we detected strong α-tubulin signals but

only weak p23 staining (**Figure 4 I**–**K**). Furthermore, we quantified the colocalization of p23 and calnexin (**Figure 4 D**, **H**, **L**). We determined the mean Pearson correlation coefficient (0.62) and the mean colocalization rate (86.10%) for 7 cells (n=7). These data further support the earlier observation that these proteins colocalize. We also analyzed the potential colocalization of p23 and α-tubulin, for which we calculated a mean Pearson correlation coefficient and colocalization rate of 0.53 and 92.14%, respectively (n=7). However, when we restricted our analysis to the periphery of cells, we found a mean Pearson correlation coefficient and colocalization rate of 0.40 and 24.66%, respectively (n=7) suggesting that areas devoid of ER membranes do not contain much p23, likely because the majority of p23 is membrane associated. Nevertheless, it should be noted that p23 is translated by free ribosomes, which means that every p23 protein spends time in the cytoplasm, which would explain the weak staining in the periphery of cells and the observed Pearson correlation coefficient and colocalization rate with α-tubulin. Taken together, our results confirm a colocalization of p23 with the ER.
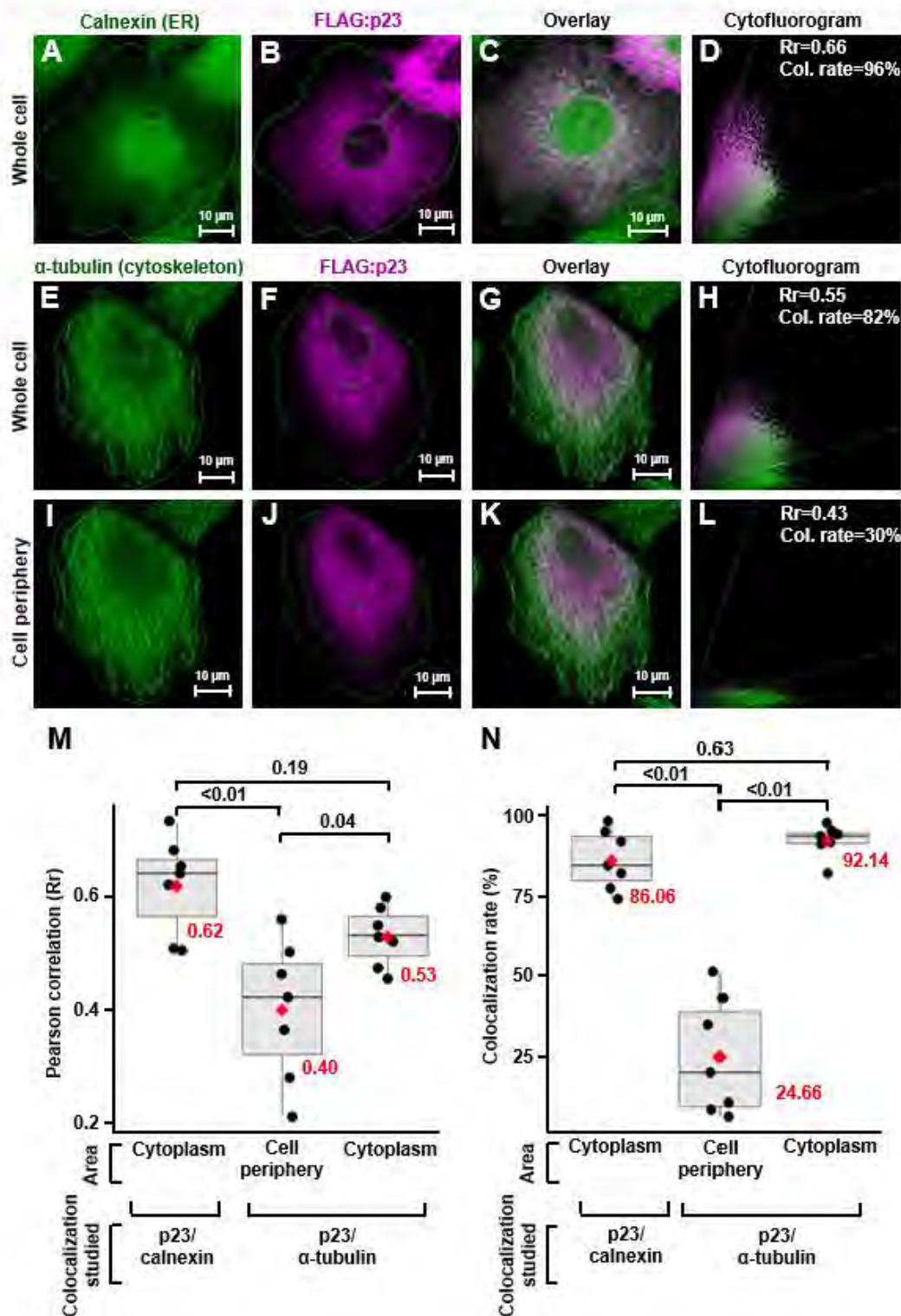
Figure 4. Transiently expressed recombinant p23 localises to the ER. RK-13 cells were transfected with FLAG-tagged p23 (RHDV), incubated overnight, fixed, immunostained, and analyzed by confocal microscopy. (**A**–**C**) The ER marker calnexin (green) and FLAG-tagged p23 (magenta) were detected by immunofluorescence using anti-calnexin and anti-FLAG antibodies, respectively; (**E**–**H**) The cytoskeleton protein α-tubulin (green) and FLAG-tagged p23 (magenta) were detected by immunofluorescence using anti-tubulin and anti-FLAG

antibodies, respectively. (**I–L**) The cell periphery lacks p23 expression and therefore this area was used to estimate the threshold for Rr (**D, H, L**) The cytofluorograms show the distribution of green and magenta pixels in the cytoplasm (areas under investigation are bounded by a green line); Rr, Pearson correlation coefficient and Col. rate (%), colocalization rate. (**M, N**) Boxplots represent the distribution of Rr and colocalization rates for seven individual cells (n=7), respectively. Each cell is depicted as a black dot, the median for each group is shown as a black line inside the boxes, the position of the mean is shown as a red diamond, and the value of mean is given in red numbers. Significance was analyzed using one-way ANOVA followed by Tukey's honest significant difference test;; adjusted *p*-values are shown above the plots; plots were produced using ggplot2 (Gómez-Rubio, 2017).

p23 interacts with heat shock proteins

To identify cellular interaction partners of p23, we used stable isotope labelling of amino acids in cell culture (SILAC) coupled with immunoprecipitation. In this approach, a population of cells was grown for several passages in culture medium that was supplemented with heavy isotope-labelled arginine and lysine while control cells were cultured in unlabelled medium that contained regular arginine and lysine. Heavy isotope-labelled ('heavy') and unlabelled ('light') RK-13 cells were transiently transfected to express recombinant FLAG-tagged p23 and GFP (for heavy to light (heavy/light) ratio quantification), respectively. As a labelling control, transfections were swapped in one out of three replicates (i.e., GFP and p23 was expressed in 'heavy' and 'light' cells, respectively). Using quantitative MS to analyze the composition of affinity-purified FLAG-tagged protein complexes, we found that p23 specifically interacts with heat shock proteins, namely Hsp70 member 2, Hsp70 member 4, and Hsp110. To investigate the specificity of the observed interaction between p23 and heat shock proteins, another SILAC experiment was conducted with the viral RNA-dependent RNA-polymerase (RdRp) as bait (**Figure 5B**). In this case, no interaction with heat shock proteins was detected. Instead, we identified a BRO1 domain-containing protein as a potential interactor of RdRp. Western blotting analysis of the individual eluate aliquots from anti-FLAG resin (before p23 and GFP samples were combined) further demonstrated that p23 specifically interacts with heat shock proteins, as a band corresponding to Hsp70 was only detected when p23 was used as bait (**Figure 5C**).
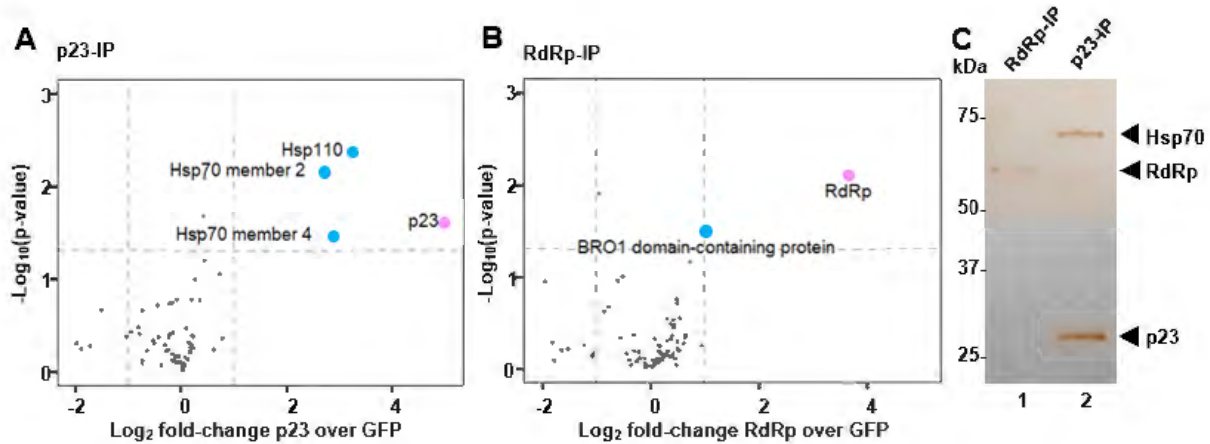
Figure 5. Heat shock proteins interact with p23 but not the viral polymerase. (**A**, **B**) A quantitative proteomics approach (SILAC) was used to identify cellular interaction partners of p23 and the RNA-dependent RNA polymerase (RdRp) of RHDV, respectively. Proteins identified in at least two out of three biological replicates were included in the analysis. Cellular proteins significantly enriched in comparison to an internal GFP control are shown as blue dots; the viral bait proteins p23 and RdRp are highlighted in pink. Significance was analyzed using a one-sample *t*-test with an unadjusted p-value of <0.05 and a $\log_2$ fold-change >1. Heat shock proteins Hsp70 and Hsp90 were identified as p23 interactors (A), and one or more BRO1 domain-containing proteins were identified as RdRp interactors (B). (**C**) Western blot analysis of immunoprecipitated complexes isolated from transfected cells expressing recombinant FLAG:p23 or FLAG:RdRp (p23-IP and RdRp-IP, respectively). Aliquots of affinity purified complexes were separated by SDS-PAGE and analyzed by Western blot using anti-FLAG and anti-Hsp70 antibodies. Hsp70 was detected in p23- but not in RdRp-expressing cells (we did not attempt to detect Hsp110 or BRO1 domain-containing proteins).

Global transcriptome and proteome characterization of RHDV2-infected liver samples confirm alterations in Ca²⁺ homeostasis

Due to the lack of a suitable cell culture system for RHDV, we investigated infected rabbit liver samples to identify cellular pathways that change during infection. We used RHDV2-infected rabbit liver tissue samples and data from a previous study (Neave et al., 2018) to characterize global changes to the transcriptome and proteome, respectively. The transcriptome analysis was performed using raw RNA sequencing data ('reads') as made available by Neave and co-workers (BioProject accession No. PRJNA434149). For the proteome analysis, three existing RHDV2-infected and three mock-infected liver samples that had been stored in RNA-later were processed for MS-based proteomic analysis. Differences in

gene expression (either at the mRNA or protein level) between infected and uninfected samples were identified and visualized using volcano plots (**Supplementary Figure S1**), full lists of differentially expressed genes and proteins can be found in **Supplementary Data File S1** and **Supplementary Data File S2**, respectively. Next, we performed a gene set enrichment analysis using topGO (Alexa and Rahnenfuhrer, 2020) to identify biological pathways and molecular functions of differentially expressed genes. This analysis yielded gene ontology (GO) terms that are associated with pathways such as fatty acid transport and metabolism, and cytoskeleton reorganization; pathways associated with unfolded protein and heat shock protein responses were also identified, although only at the transcript level (**Table 1**). We generated a 'graphical output' that shows the GO terms in the context of a greater network of pathways; a large amount of data was produced on numerous pathways of which only a small subset is displayed in **Figure 6** (for full-size figures, see **Supplementary Figure S2** and **Supplementary Figure S3).**

This analysis revealed changes to the Ca^{2+} homeostasis, which further supports our hypothesis that lagoviruses encode a viroporin that forms channels in intracellular membranes.

Table 1. Gene ontology analysis of differentially expressed genes and proteins in RHDV2-infected rabbit liver samples.

Transcriptome		
GO term*	**Description**	***p*-value**
Biological pathway		
0046719	regulation by virus of viral protein levels in host cell	0.003
0090150	establishment of protein localization to membrane	0.027
1903371	regulation of ER tubular network organization	0.028
1903076	regulation of protein localization to plasma membrane	0.033
Molecular function		
0003777	microtubule motor activity	0.0001
0051082	unfolded protein binding	0.0002
0004698	calcium-dependent protein kinase C activity	0.004
0042803	protein homodimerization activity	0.005

0030544	Hsp70 protein binding	0.020
Proteome		
GO term*	**Description**	*p*-**value**
Biological pathway		
1902001	fatty acid transmembrane transport	0.006
2000191	intracellular lipid transport	0.021
0031532	actin cytoskeleton reorganization	0.039
2001234	negative regulation of apoptotic signaling pathway	0.044
Molecular function		
0042803	protein homodimerization activity	0.003
0043495	protein-membrane adaptor activity	0.008
0005324	long-chain fatty acid transporter activity	0.008
0000146	microfilament motor activity	0.010
0051015	actin filament binding	0.011
*Gene ontology terms (only selected terms are shown)		
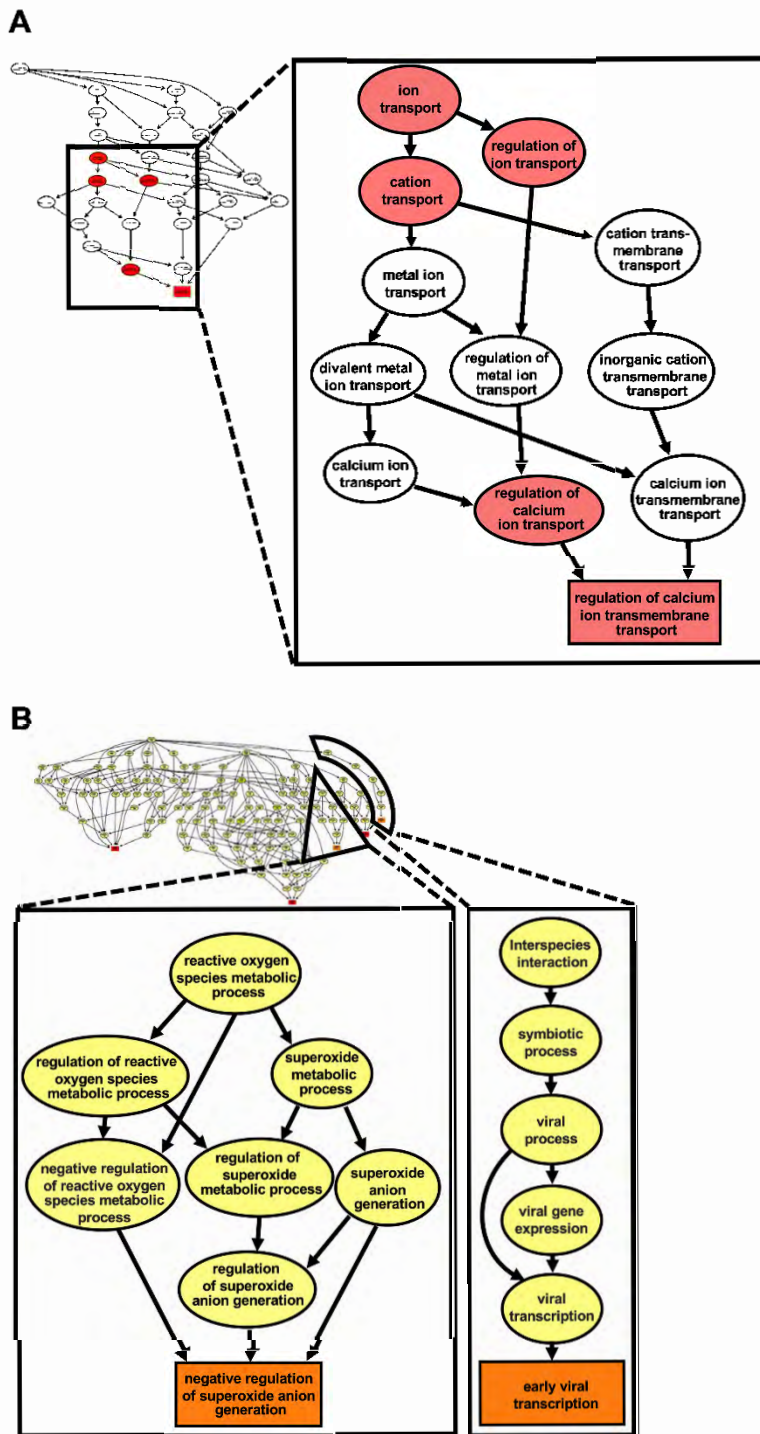
Figure 6. Ca²⁺ transmembrane transport pathways are altered in the liver of RHDV2-infected rabbits. A gene ontology (GO) enrichment analysis was conducted using the list of differentially expressed genes from RNA sequencing. (**A**) The graph induced by the top 5 GO terms identified by the weight01 algorithm (Alexa et al., 2006); the square shape indicates the most significant GO term. (**B**) The graph induced by the top 5 GO terms identified by weight01 algorithm with Fisher exact test also identified pathways associated with viral infection and

regulation of reactive oxygen species generation. Box colors represents the relative significance of GO terms, from white (least significant) to red (most significant).

Recombinant p23 expression in cultured cells slightly changes cytoplasmic Ca²⁺ level

RK-13 cells were transiently transfected with plasmids encoding either RHDV FLAG:p23 or a mutated FLAG:p23 with the C41S substitution, or the plasmid vector (pCMV-Tag2C). After transfection, the cells were loaded with the cell-permeable fluorescent dye Fluo-4 AM (that increases fluorescence intensity upon Ca^{2+} binding by more than 100-fold) and the mean fluorescence intensity was measured with a flow cytometer. We observed that the mean fluorescence intensity in the cytoplasm increased slightly in cells expressing wild-type p23 compared to cells expressing the C41S variant or cells that were transfected with the 'empty' vector (**Figure 7**). However, the pooled results of four independent experiments showed that these differences were not statistically significant.
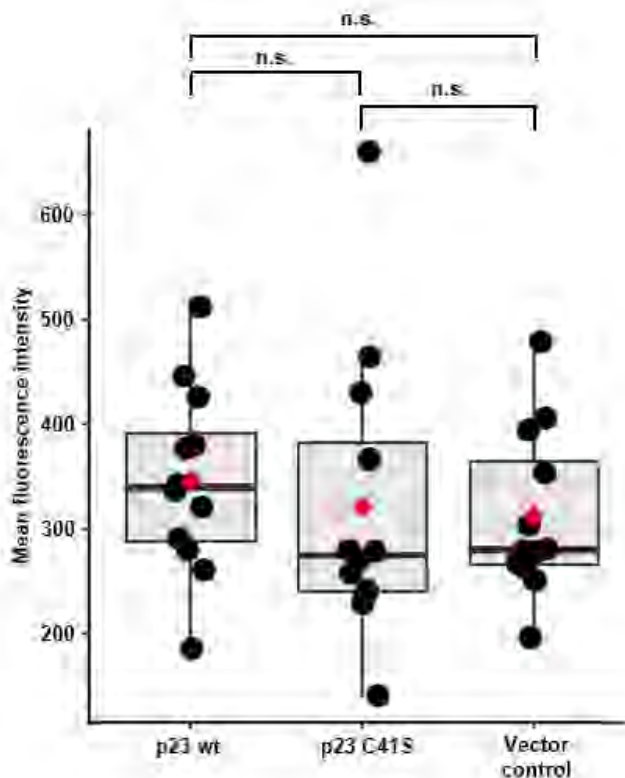
Figure 7. Flow cytometry Ca²⁺ flux measurements. Mean fluorescence intensity was measured for 25,000 cells in each condition, with three replicates per condition. Boxplots represent the distribution of mean fluorescence intensity value. Median values are shown as a horizontal line and mean values as a red diamond. The results from four independent experiments were normalized and combined. Significance was analyzed using one-way Kruskal-Wallis test and pairwise Wilcoxon rank test with multiple testing correction; adjusted

Discussion

Our knowledge about many key aspects of the lagovirus life cycle is limited. For example, the function(s) of three out of seven non-structural proteins are still unknown. Closing this research gap is difficult as many caliciviruses, including lagoviruses, do not grow in cell culture. Therefore, we and others mostly relied on the expression of recombinant proteins to study their intracellular localization, enzymatic activity, and oligomerization. Furthermore, various screening and multi-omics approaches have been used to identify cellular interaction partners and characterize the effects of NS proteins on cellular metabolism. For example, Hosmillo and co-authors used proteomics to describe the 'interaction network' for the norovirus protein NS1/2 (NS2 is a positional homolog of p23) (Hosmillo et al., 2019). In that study, NS1/2 was shown to interact with the stress granule component G3BP1 and regulate cellular protein translation (Hosmillo et al., 2019). Furthermore, global transcriptome characterizations revealed that the transient expression of norovirus NS1/2 in transfected cells and during genuine norovirus infection leads to changes in Ca^{2+} homeostasis; more specifically, Lateef and co-authors found evidence for the downregulation of the Ca^{2+} voltage-gated channel subunit alpha 1D (Lateef et al., 2017).

Here, we focused on the p23 proteins of lagoviruses; our data suggest that these proteins are viroporins that reside in ER membranes, form dimers (and possibly also higher-order oligomers), and may act as ion channels. Furthermore, we found that p23 dimers are stabilized by an intermolecular disulfide bond between the cysteine residues at position 41. This disulfide bond is likely formed in the lumen of the ER, but further structural studies are warranted to confirm this hypothesis. The presence of faint bands in some of our Western blots suggests that p23 also forms trimers and tetramers, but the mechanism behind the formation of these higher-order oligomers and their potential biological relevance remains unknown.

Secondary structure prediction tools suggested that p23 positions itself into a membrane using two amphipathic helices in the C-terminal region of the protein. Oligomerization is a common mechanism in the formation of membrane channels, especially for small proteins. Indeed, viroporins are usually small proteins that require oligomerization. For example, the hepatitis C viroporin protein p7 is only 63 amino acids long and requires six monomers to build a transmembrane channel (Luik et al., 2009). The p23 homolog in *Tulane virus* (family *Caliciviridae*, genus *Recovirus*) is 233 amino acids long and is also a viroporin that disrupts

calcium homeostasis by forming channels in the ER membranes after dimerization (Strtak et al., 2019). In noroviruses, the p23 homolog NS1/2 has a distinctly ordered hydrophobic C-terminal region, similar to that observed in lagoviruses and *Tulane virus* (Baker et al., 2012). A viroporin that also relies on disulfide bonds for oligomerization was recently described for *Feline calicivirus* (genus *Vesivirus*) (Peñaflor-Téllez et al., 2022). Moreover, the viroporins of *Feline calicivirus* (Barrera-Vázquez et al., 2019) and *Murine norovirus* (Robinson et al., 2019) trigger apoptosis, which may be a critical factor in efficient virus spreading. Accumulating evidence suggests that viroporin activity may be a feature that is conserved across the family *Caliciviridae* (reviewed in Smertina et al., 2021).

To confirm the hypothesis that p23 interacts with cellular membranes, we extended earlier confocal microscopy studies (Urakova et al., 2015) by conducting a quantitative colocalization analysis. We observed that RHDV p23 localizes with the ER marker calnexin in transfected cells, a finding that confirms previous results (Urakova et al., 2015). However, the detected colocalization was not complete, and multiple p23-specific puncta were located beyond the cytofluorogram colocalization threshold. This observation suggests that when p23 is overexpressed in cells, it may only be partially transported and incorporated into the membranes.

A quantitative proteomics approach (SILAC) coupled with immunoprecipitation identified several heat shock proteins as potential interactors of p23. Heat shock proteins are known as common contaminants in proteomics studies (Trinkle-Mulcahy et al., 2008). However, we believe that the observed interaction is specific and has biological relevance as the same experiment was performed for another viral protein, RNA-dependent RNA polymerase, and we did not observe the interaction with heat shock proteins. It is tempting to speculate that the interaction between p23 and heat shock proteins is important to stabilize the partially hydrophobic p23 proteins in the cytoplasm and 'guide' them towards cellular membranes. Many viroporins, including p23, do not have a signal sequence and thus do not trigger the cellular signal recognition system that co-translationally directs proteins to the ER, therefore requiring alternative mechanisms of transportation. In several cases, cellular chaperones have been observed to assist such proteins post-translationally (Martinez-Gil and Mingarro, 2015; Rabu et al., 2008). Furthermore, cytosolic Hsp70 and co-chaperones are responsible for keeping tail-anchored membrane proteins soluble, and assist their transportation to the ER membranes in yeast cells (Cho and Shan, 2018). This function is likely also used by mammalian cells, as an association between heat shock proteins and newly synthesized membrane proteins was also detected in rabbit reticulocyte lysates (Abell et al., 2007; Colombo

et al., 2009). In the case of viral infections, cellular chaperones switch their attention as protein quality assurers to viral proteins. Yellow fever virus polyprotein processing depends on Hsp40, a cochaperone that assists Hsp70-mediated protein folding (Bozzacco et al., 2016). Our observation that the p23 protein of RHDV interacts with heat shock proteins may therefore indicate that p23 requires additional stabilization prior to its oligomerization and interaction with cellular membranes.

Another point of discussion is whether the disulfide bonds between p23 monomers are formed in the ER or in the cytoplasm. It is known that the oxidative environment in the ER lumen promotes formation of disulfide bonds (Tu and Weissman, 2004); therefore, it is conceivable that monomeric p23 is transported to the ER where it interacts with the membranes in a manner that drives the N-terminus into the lumen of the organelle. Then, it becomes available for S-S bond formation with another p23. Moreover, we observed that p23 variants with C-terminal cysteine-to-serine substitutions show an altered SDS-PAGE mobility, which is indicative of an intramolecular disulfide bond. Therefore, p23 can be classified as a class IIA viroporin as both its N- and C-termini are located in the ER lumen, similar to the hepatitis C virus protein p7 (Martinez-Gil and Mingarro, 2015). The fact that the transmembrane helices are located at the C-terminus and the cysteine residue responsible for the oligomerization at the N-terminus, raises a question whether a 'classic' viroporin domain (as defined in Hyser and Estes, 2015) can be defined for p23.

Most of our work has been conducted using transiently transfected rabbit kidney cells. To corroborate our findings, we performed global proteome and transcriptome analysis of infected rabbit liver samples. The differentially expressed proteins and genes were used to identify pathways that changed during the infection. Pathways associated with calcium signaling and unfolded protein response were among those identified by our analyses, which suggests that p23 may affect the Ca^{2+} homeostasis.

Finally, we conducted flow cytometry-based Ca^{2+} flux measurements in transiently transfected cells. These experiments did not reveal statistically significant differences between the analyzed groups (i.e., wild-type p23, C41S p23, negative control). However, we observed a trend across four independent experiments pointing to slightly elevated Ca^{2+} levels in cells that expressed wild-type p23. Considering that the transfection efficiency was well below 100%, our experiments likely underestimated the effect of p23 expression on Ca^{2+} homeostasis. Furthermore, changes to intracellular Ca^{2+} levels are notoriously difficult to measure using fluorescent dyes (Perry et al., 2015), which means that additional studies are required to fully characterize the transport characteristics of ion channels in lagovirus replication.

Overall, our results extend the definition of a viroporin domain. These findings will benefit future work aimed at defining the 3D structure of p23 oligomers, an important step towards the development of new antiviral drugs.

Data Availability Statement

The authors confirm that all data underlying the findings are fully available without restriction. The RNAseq data set has been deposited in the NCBI Sequence Read Archive under the BioProject accession No. PRJNA434149. Proteomics data (label-free quantification) has been deposited to the ProteomeXchange Consortium via the PRIDE repository (Vizcaíno et al., 2016) with the dataset identifier PXD031027. The SILAC data set has been deposited to the ProteomeXchange Consortium via the PRIDE repository with PXD031619 identifier.

References

Abell, B. M., Rabu, C., Leznicki, P., Young, J. C., and High, S. (2007). Post-translational integration of tail-anchored proteins is facilitated by defined molecular chaperones. *J. Cell Sci.* 120, 1743–1751. doi:10.1242/jcs.002410.

Alexa, A., and Rahnenfuhrer, J. (2020). topGO: Enrichment analysis for gene ontology. https://github.com/ycl6/topGO-adrianalexa [Accessed on 30 March 2022].

Alexa, A., Rahnenführer, J., and Lengauer, T. (2006). Improved scoring of functional groups from gene expression data by decorrelating GO graph structure. *Bioinformatics* 22, 1600–1607. doi:10.1093/bioinformatics/btl140.

Anders, S., Pyl, P. T., and Huber, W. (2015). HTSeq-A Python framework to work with high-throughput sequencing data. *Bioinformatics* 31, 166–169. doi:10.1093/bioinformatics/btu638.

Baker, E. S., Luckner, S. R., Krause, K. L., Lambden, P. R., Clarke, I. N., and Ward, V. K. (2012). Inherent structural disorder and dimerisation of murine norovirus ns1-2 protein. *PLoS One* 7. doi:10.1371/journal.pone.0030534.

Barrera-Vázquez, O. S., Cancio-Lonches, C., Hernández-González, O., Chávez-Munguia, B., Villegas-Sepúlveda, N., and Gutiérrez-Escolano, A. L. (2019). The feline calicivirus leader of the capsid protein causes survivin and XIAP downregulation and apoptosis. Virology 527, 146–158. doi:10.1016/j.virol.2018.11.017.

Blighe, K., Rana, S., and Lewis, M. (2020). Publication-ready volcano plots with enhanced colouring and labeling. https://github.com/kevinblighe/EnhancedVolcano [Accessed on 30 March 2022].

Boga, J., Marín, M. S., Casais, R., Prieto, M., and Parra, F. (1992). In vitro translation of a subgenomic mRNA from purified virions of the Spanish field isolate AST/89 of Rabbit Hemorrhagic Disease Virus (RHDV). *Virus Res.* 26, 33–40. doi:10.1016/0168-1702(92)90144-X.

Bozzacco, L., Yi, Z., Andreo, U., Conklin, C. R., Li, M. M. H., Rice, C. M., et al. (2016). Chaperone-assisted protein folding is critical for Yellow fever virus NS3/4A cleavage and replication. *J. Virol.* 90, 3212–3228. doi:10.1128/jvi.03077-15.

Buchan, D. W. A., and Jones, D. T. (2019). The PSIPRED protein analysis workbench: 20 years on. *Nucleic Acids Res.* 47, W402–W407. doi:10.1093/nar/gkz297.

Cho, H., and Shan, S. (2018). Substrate relay in an Hsp70-cochaperone cascade safeguards tail-anchored membrane protein targeting. *EMBO J.* 37, 1–17. doi:10.15252/embj.201899264.

Colombo, S. F., Longhi, R., and Borgese, N. (2009). The role of cytosolic proteins in the

insertion of tail-anchored proteins into phospholipid bilayers. *J. Cell Sci.* 122, 2383–2392. doi:10.1242/jcs.049460.

Cox, J., Hein, M. Y., Luber, C. A., Paron, I., Nagaraj, N., and Mann, M. (2014). Accurate proteome-wide label-free quantification by delayed normalization and maximal peptide ratio extraction, termed MaxLFQ. MCP Papers in Press doi:10.1074/mcp.M113.031591.

Cox, J., and Mann, M. (2008). MaxQuant enables high peptide identification rates, individualized p.p.b.-range mass accuracies and proteome-wide protein quantification. *Nat. Biotechnol.* 26, 1367–1372. doi:10.1038/nbt.1511.

Cox, J., Neuhauser, N., Michalski, A., Scheltema, R. A., Olsen, J. V., and Mann, M. (2011). Andromeda: A peptide search engine integrated into the MaxQuant environment. *J. Proteome Res.* 10, 1794–1805. doi:10.1021/pr101065j.

Ehresmann, D. W., and Schaffer, F. L. (1977). RNA synthesized in calicivirus infected cells is atypical of picornaviruses. *J. Virol.* 22, 572–576.

Emmott, E., and Goodfellow, I. (2014). Identification of protein interaction partners in mammalian cells using SILAC-immunoprecipitation quantitative proteomics. *J. Vis. Exp.*, 1–8. doi:10.3791/51656.

Ettayebi, K., and Hardy, M. E. (2003). Norwalk virus nonstructural protein p48 forms a complex with the SNARE regulator VAP-A and prevents cell surface expression of vesicular stomatitis virus G protein. *J. Virol.* 77, 11790–7. doi:10.1128/JVI.77.21.11790.

Gautier, R., Douguet, D., Antonny, B., and Drin, G. (2008). HELIQUEST: A web server to screen sequences with specific α-helical properties. *Bioinformatics* 24, 2101–2102. doi:10.1093/bioinformatics/btn392.

Gómez-Rubio, V. (2017). ggplot2 - elegant graphics for data analysis (2nd Edition) . *J. Stat. Softw.* 77. doi:10.18637/jss.v077.b02.

Hosmillo, M., Lu, J., McAllaster, M. R., Eaglesham, J. B., Wang, X., Emmott, E., et al. (2019). Noroviruses subvert the core stress granule component G3BP1 to promote viral VPg-dependent translation. *eLife* 8, 1–35. doi:10.7554/eLife.46681.

Hyser, J. M., and Estes, M. K. (2015). Pathophysiological consequences of calcium-conducting viroporins. *Annu. Rev. Virol.* 2, 473–496. doi:10.1146/annurev-virology-100114-054846.

Kerr, P. J., Hall, R. N., and Strive, T. (2021). Viruses for Landscape-Scale Therapy: Biological Control of Rabbits in Australia. Humana, New York, NY: Lucas A.R. (eds) Viruses as Therapeutics. Methods in Molecular Biology doi:https://doi.org/10.1007/978-1-0716-1012-1_1.

Kleizen, B., and Braakman, I. (2004). Protein folding and quality control in the endoplasmic

reticulum. *Curr. Opin. Cell Biol.* 16, 343–349. doi:10.1016/j.ceb.2004.06.012.

Lateef, Z., Gimenez, G., Baker, E. S., and Ward, V. K. (2017). Transcriptomic analysis of human norovirus NS1-2 protein highlights a multifunctional role in murine monocytes. *BMC Genomics* 18. doi:10.1186/s12864-016-3417-4.

Love, M. I., Huber, W., and Anders, S. (2014). Moderated estimation of fold change and dispersion for RNA-seq data with DESeq2. *Genome Biol.* 15, 1–21. doi:10.1186/s13059-014-0550-8.

Luik, P., Chew, C., Aittoniemi, J., Chang, J., Wentworth, P., Dwek, R. A., et al. (2009). The 3-dimensional structure of a hepatitis C virus p7 ion channel by electron microscopy. *Proc. Natl. Acad. Sci. U. S. A.* 106, 12712–12716. doi:10.1073/pnas.0905966106.

Martinez-Gil, L., and Mingarro, I. (2015). Viroporins, examples of the two-stage membrane protein folding model. *Viruses* 7, 3462–3482. doi:10.3390/v7072781.

Meyers, G., Wirblich, C., and Thiel, H. J. (1991a). Genomic and subgenomic RNAs of rabbit hemorrhagic disease virus are both protein-linked and packaged into particles. *Virology* 184, 677–686. doi:10.1016/0042-6822(91)90437-G.

Meyers, G., Wirblich, C., and Thiel, H. J. (1991b). Rabbit hemorrhagic disease virus-molecular cloning and nucleotide sequencing of a calicivirus genome. *Virology* 184, 664–676. doi:10.1016/0042-6822(91)90436-F.

Meyers, G., Wirblich, C., Thiel, H. J., and Thumfart, J. O. (2000). Rabbit hemorrhagic disease virus: Genome organization and polyprotein processing of a calicivirus studied after transient expression of cDNA constructs. *Virology* 276, 349–363. doi:10.1006/viro.2000.0545.

Morales, M., Bárcena, J., Ramírez, M. A., Boga, J. A., Parra, F., and Torres, J. M. (2004). Synthesis in vitro of rabbit hemorrhagic disease virus subgenomic RNA by internal initiation on (-)sense genomic RNA: Mapping of a subgenomic promoter. *J. Biol. Chem.* 279, 17013–17018. doi:10.1074/jbc.M313674200.

Neave, M. J., Hall, R. N., Huang, N., McColl, K. A., Kerr, P., Hoehn, M., et al. (2018). Robust innate immunity of young rabbits mediates resistance to rabbit hemorrhagic disease caused by Lagovirus Europaeus GI.1 but not GI.2. *Viruses* 10, 1–22. doi:10.3390/v10090512.

Nieva, J. L., Madan, V., and Carrasco, L. (2012). Viroporins: Structure and biological functions. *Nat. Rev. Microbiol.* 10, 563–574. doi:10.1038/nrmicro2820.

Nugent, T., and Jones, D. T. (2010). Predicting transmembrane helix packing arrangements using residue contacts and a force-directed algorithm. *PLoS Comput. Biol.* 6. doi:10.1371/journal.pcbi.1000714.

Nugent, T., and Jones, D. T. (2012). Detecting pore-lining regions in transmembrane protein sequences. *BMC Bioinformatics* 13. doi:10.1186/1471-2105-13-169.

Peñaflor-Téllez, Y., Chavez-Munguia, B., Lagunes-Guillen, A., Salazar-Villatoro, L., and Gutierrez-Escolano, A.-L. (2022). The feline calicivirus leader of the capsid protein has the functional characteristics of a viroporin. *Viruses* 14. doi:https://doi.org/10.3390/v14030635.

Perry, J. L., Ramachandran, N. K., Utama, B., and Hyser, J. M. (2015). Use of genetically-encoded calcium indicators for live cell calcium imaging and localization in virus-infected cells. *Methods* 90, 28–38. doi: 10.1016/j.ymeth.2015.09.004.

Rabu, C., Wipf, P., Brodsky, J. L., and High, S. (2008). A precursor-specific role for Hsp40/Hsc70 during tail-anchored protein integration at the endoplasmic reticulum. *J. Biol. Chem.* 283, 27504–27513. doi:10.1074/jbc.M804591200.

Richards, A. L., Hebert, A. S., Ulbrich, A., Bailey, D. J., Coughlin, E. E., Westphall, M. S., et al. (2015). One-hour proteome analysis in yeast. *Nat. Protoc.* 10, 701–714. doi:10.1038/nprot.2015.040.

Robinson, B. A., Van Winkle, J. A., McCune, B. T., Peters, A. M., and Nice, T. J. (2019). Caspase-mediated cleavage of murine norovirus NS1/2 potentiates apoptosis and is required for persistent infection of intestinal epithelial cells. PLoS Pathog. 15. doi:10.1371/journal.ppat.1007940.

Smertina, E., Hall, R. N., Urakova, N., Strive, T., and Frese, M. (2021). Calicivirus non-structural proteins: potential functions in replication and host cell manipulation. *Front. Microbiol.* 12. doi:10.3389/fmicb.2021.712710.

Strtak, A. C., Perry, J. L., Sharp, M. N., Chang-Graham, A. L., Farkas, T., and Hyser, J. M. (2019). Recovirus NS1-2 has viroporin activity that induces aberrant cellular calcium signaling to facilitate virus replication. *mSphere* 4, 1–21. doi:10.1128/msphere.00506-19.

R Core Team (2020). R: A language and environment for statistical computing.

Thumfart, J. O., and Meyers, G. (2002). Rabbit hemorrhagic disease virus: identification of a cleavage site in the viral polyprotein that is not processed by the known calicivirus protease. *Virology* 304, 352–363. doi:10.1006/viro.2002.1660.

Trapnell, C., Pachter, L., and Salzberg, S. L. (2009). TopHat: Discovering splice junctions with RNA-Seq. *Bioinformatics* 25, 1105–1111. doi:10.1093/bioinformatics/btp120.

Trinkle-Mulcahy, L., Boulon, S., Lam, Y. W., Urcia, R., Boisvert, F. M., Vandermoere, F., et al. (2008). Identifying specific protein interaction partners using quantitative mass spectrometry and bead proteomes. *J. Cell Biol.* 183, 223–239. doi:10.1083/jcb.200805092.

Tu, B. P., and Weissman, J. S. (2004). Oxidative protein folding in eukaryotes: mechanisms and consequences. *J. Cell Biol.* 164, 341–346. doi:10.1083/jcb.200311055.

Tyanova, S., Temu, T., Sinitcyn, P., Carlson, A., Hein, M. Y., Geiger, T., et al. (2016). The Perseus computational platform for comprehensive analysis of (prote)omics data. *Nat. Methods* 13, 731–740. doi:10.1038/nmeth.3901.

Urakova, N., Frese, M., Hall, R. N., Liu, J., Matthaei, M., and Strive, T. (2015). Expression and partial characterisation of rabbit haemorrhagic disease virus non-structural proteins. *Virology* 484, 69–79. doi:10.1016/j.virol.2015.05.004.

Vizcaíno, J. A., Csordas, A., Del-Toro, N., Dianes, J. A., Griss, J., Lavidas, I., et al. (2016). 2016 update of the PRIDE database and its related tools. *Nucleic Acids Res.* 44, D447–D456. doi:10.1093/nar/gkv1145.

Walter, W., Sánchez-Cabo, F., and Ricote, M. (2015). GOplot: An R package for visually combining expression data with functional analysis. *Bioinformatics* 31, 2912–2914. doi:10.1093/bioinformatics/btv300.

Xue, B., Dunbrack, R. L., Williams, R. W., Dunker, A. K., and Uversky, V. N. (2010). PONDR-FIT: a meta-predictor of intrinsically disordered amino acids. 1804, 996–1010. doi:10.1016/j.bbapap.2010.01.011.PONDR-FIT.

Zhang, X., Smits, A. H., Van Tilburg, G. B. A., Ovaa, H., Huber, W., and Vermeulen, M. (2018). Proteome-wide identification of ubiquitin interactions using UbIA-MS. *Nat. Protoc.* 13, 530–550. doi:10.1038/nprot.2017.147.

Zhou, Y., Frey, T. K., and Yang, J. J. (2009). Viral calciomics: Interplays between Ca2+ and virus. *Cell Calcium* 46, 1–17. doi:10.1016/j.ceca.2009.05.005.

Zougman, A., Selby, P. J., and Banks, R. E. (2014). Suspension trapping (STrap) sample preparation method for bottom-up proteomics analysis. *Proteomics* 14, 1006–1000. doi:10.1002/pmic.201300553.

Supplementary materials

Supplementary Text 1

Lagoviruses are hierarchically classified based on the phylogeny of the major structural protein VP60 (Le Pendu et al., 2017). The classification system consists of genogroups (GI, GII), genotypes (e.g., GI.1, GI.2, GI.3, etc.), and variants (e.g., GI.1a, GI.1b, GI.1c, etc.). Genogroup II lagoviruses include benign enterotropic viruses and highly virulent hepatotropic viruses that typically infect hares (*Lepus* species) (Droillard et al., 2020). Genogroup I comprises several genotypes; those that are specific to rabbits such as the virulent and hepatotropic GI.1 viruses (Liu et al., 1984) and the benign enterotropic GI.3 (Le Gall-Reculé et al., 2011) and GI.4 (Strive et al., 2009) viruses; as well as GI.2 viruses (also known as RHDV2), which infect rabbits (*Oryctolagus*), hares (*Lepus*), jackrabbits (*Lepus*), and cottontails (*Sylvilagus*) (Lankton et al., 2021).

Caliciviruses frequently undergo recombination at the RdRp-VP60 junction, combining non-structural and structural genes from different genotypes and even different genogroups (Mahar et al., 2021; Szillat et al., 2020). Recombinant viruses are named Gx.xP-Gx.x, where P denotes the polymerase (or non-structural) variant. A characterisation of recombinant viruses by Mahar et al (2021) revealed that the determinants of tissue tropism and virulence are associated with the structural gene coding regions. Antigenicity and evasion of humoral immune responses are also conferred by the VP60 major capsid protein (Wang et al., 2013). However, the non-structural proteins are critical for viral replication and can also confer epidemiological fitness advantages independent of the capsid protein (Mahar et al., 2021).

References

Droillard, C., Lemaitre, E., Chatel, M., Quéméner, A., Briand, F. X., Guitton, J. S., et al. (2020). Genetic diversity and evolution of Hare Calicivirus (HaCV), a recently identified lagovirus from Lepus europaeus. *Infect. Genet. Evol.* 82, 104310. doi:10.1016/j.meegid.2020.104310.

Lankton, J. S., Knowles, S., Keller, S., Shearn-Bochsler, V. I., and Ip, H. S. (2021). Pathology of Lagovirus europaeus GI.2/RHDV2/b (Rabbit Hemorrhagic Disease Virus 2) in Native North American Lagomorphs. *J. wildl. dis* 57, 694–700. doi:10.7589/JWD-D-20-00207.

Le Gall-Recul, G., Zwingelstein, F., Boucher, S., Le Normand, B., Plassiart, G., Portejoie, Y., et al. (2011). Virology: Detection of a new variant of rabbit haemorrhagic disease virus in France. *Vet. Rec.* 168, 137–138. doi:10.1136/vr.d697.

Le Pendu, J., Abrantes, J., Bertagnoli, S., Guitton, J. S., Le Gall-Reculé, G., Lopes, A. M., et

al. (2017). Proposal for a unified classification system and nomenclature of lagoviruses. *J. Gen. Virol.* 98, 1658–1666. doi:10.1099/jgv.0.000840.

Liu, S. J., Xue, H. P., Pu, B. Q., and Qian, N. H. (1984). A new viral disease in rabbits. *Anim. Husb. Vet. Med. (Xumu yu Shouyi)* 16, 253–255.

Mahar, J. E., Jenckel, M., Huang, N., Smertina, E., Holmes, E. C., Strive, T., et al. (2021). Frequent intergenotypic recombination between the non-structural and structural genes is a major driver of epidemiological fitness in caliciviruses. *Virus Evol.* 7, 1–14. doi:10.1093/ve/veab080.

Strive, T., Wright, J. D., and Robinson, A. J. (2009). Identification and partial characterisation of a new lagovirus in Australian wild rabbits. *Virology* 384, 97–105. doi:10.1016/j.virol.2008.11.004.

Szillat, K. P., Hoper, D., Beer, M., and Konig, P. (2020). Full-genome sequencing of German rabbit haemorrhagic disease virus uncovers recombination between RHDV (GI.2) and EBHSV (GII.1). *Virus Evol.* 6, 1–11. doi:10.1093/ve/veaa080.

Wang, X., Xu, F., Liu, J., Gao, B., Liu, Y., Zhai, Y., et al. (2013). Atomic Model of Rabbit Hemorrhagic Disease Virus by Cryo-Electron Microscopy and Crystallography. *PLoS Pathog.* 9. doi:10.1371/journal.ppat.1003132.

Supplementary Table 1

Antibody	Product number	Supplier	Dilution	Conjugation
Primary antibodies				
Rat monoclonal anti-FLAG	NOVNBP106712SS	Novus Biologicals	1:1500 (WB*) 1:150 (IF**)	Unconjugated
Rabbit monoclonal anti-Hsp70	ab45133	Abcam	1:1500 (WB)	Unconjugated
Mouse monoclonal anti-β-actin	ab8226	Abcam	1:1500 (WB)	Unconjugated
Rabbit polyclonal anti-calnexin	ab75801	Abcam	1:100 (IF)	Unconjugated
Rabbit polyclonal anti-α-tubulin	PA5-19489	Thermo Scientific	1:100 (IF)	Unconjugated
Secondary antibodies				
Secondary goat anti-rabbit	ab150077	Abcam	1:300 (IF)	Alexa Fluor 488

Secondary goat anti-rat	ab150158	Abcam	1:300 (IF)	Alexa Fluor 555
Secondary goat anti-rat	3050-05	Cambridge Bioscience	1:3000 (WB)	HRP***
Secondary goat anti-mouse	170-6516	Bio-Rad	1:3000 (WB)	HRP
Secondary goat anti-rabbit	170-6515	Bio-Rad	1:3000 (WB)	HRP

* Western blotting; ** immunofluorescence; *** horseradish peroxidase

Supplementary Figure 1

A Transcriptome

B Proteome
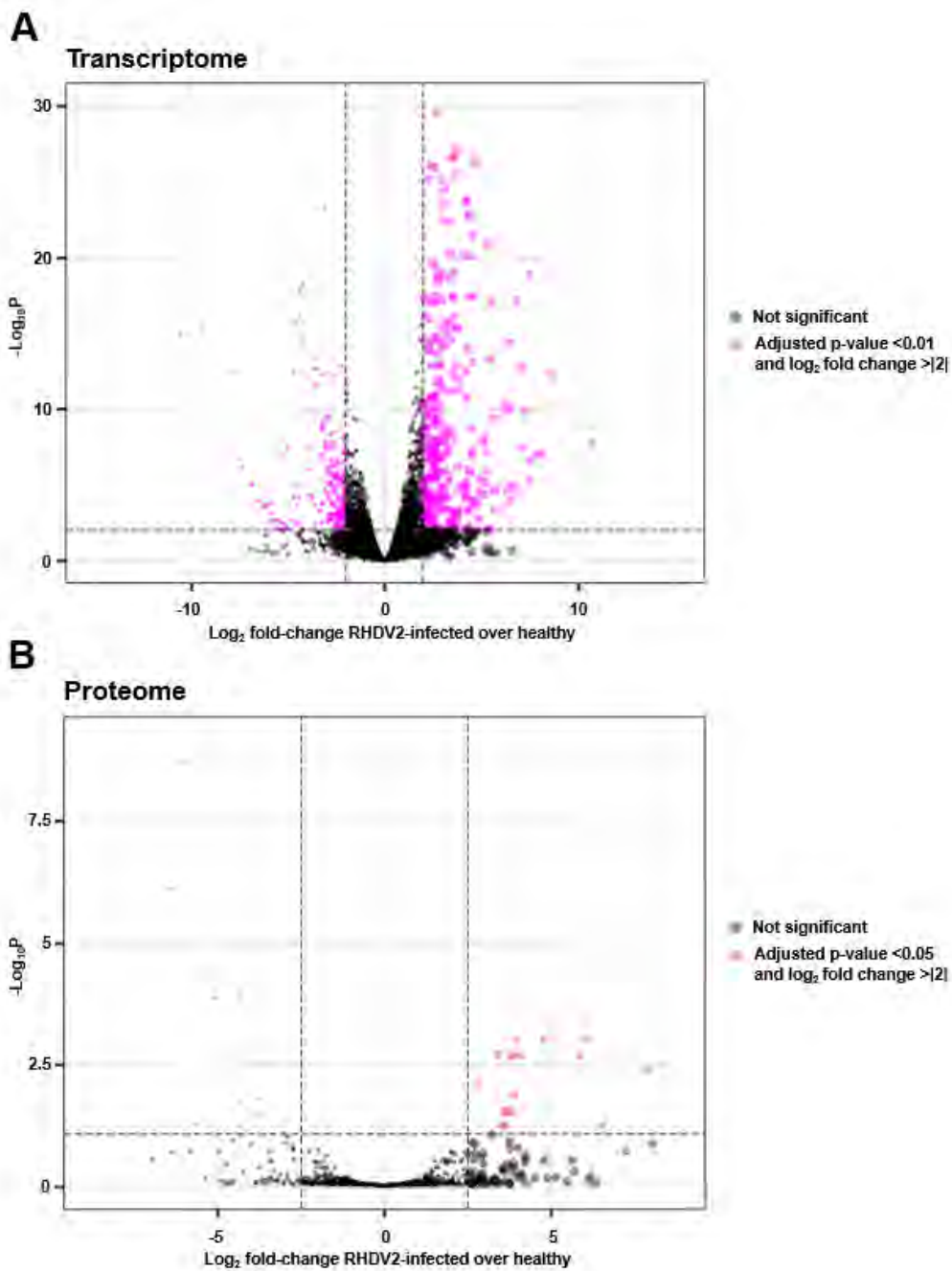
Differentially expressed genes in RHDV-infected livers. Volcano plots representing differentially expressed genes (**A**) and proteins (**B**) in liver samples from RHDV2-infected (24 hpi) and uninfected rabbits. Genes and proteins that were significantly upregulated or downregulated are depicted as large magenta dots, respectively. Non-significant gene and protein expression changes are shown in black. Dots are transparent to more easily distinguish overlapping points. The thresholds are derived at $\log_2$ fold change > 2 or < -2 and significance was determined using adjusted p-values of <0.01 (transcriptome) and <0.05 (proteome). Full lists of differentially expressed genes and proteins can be found in Supplementary data file **S1** and **S2** files, respectively.

Supplementary Figure 2
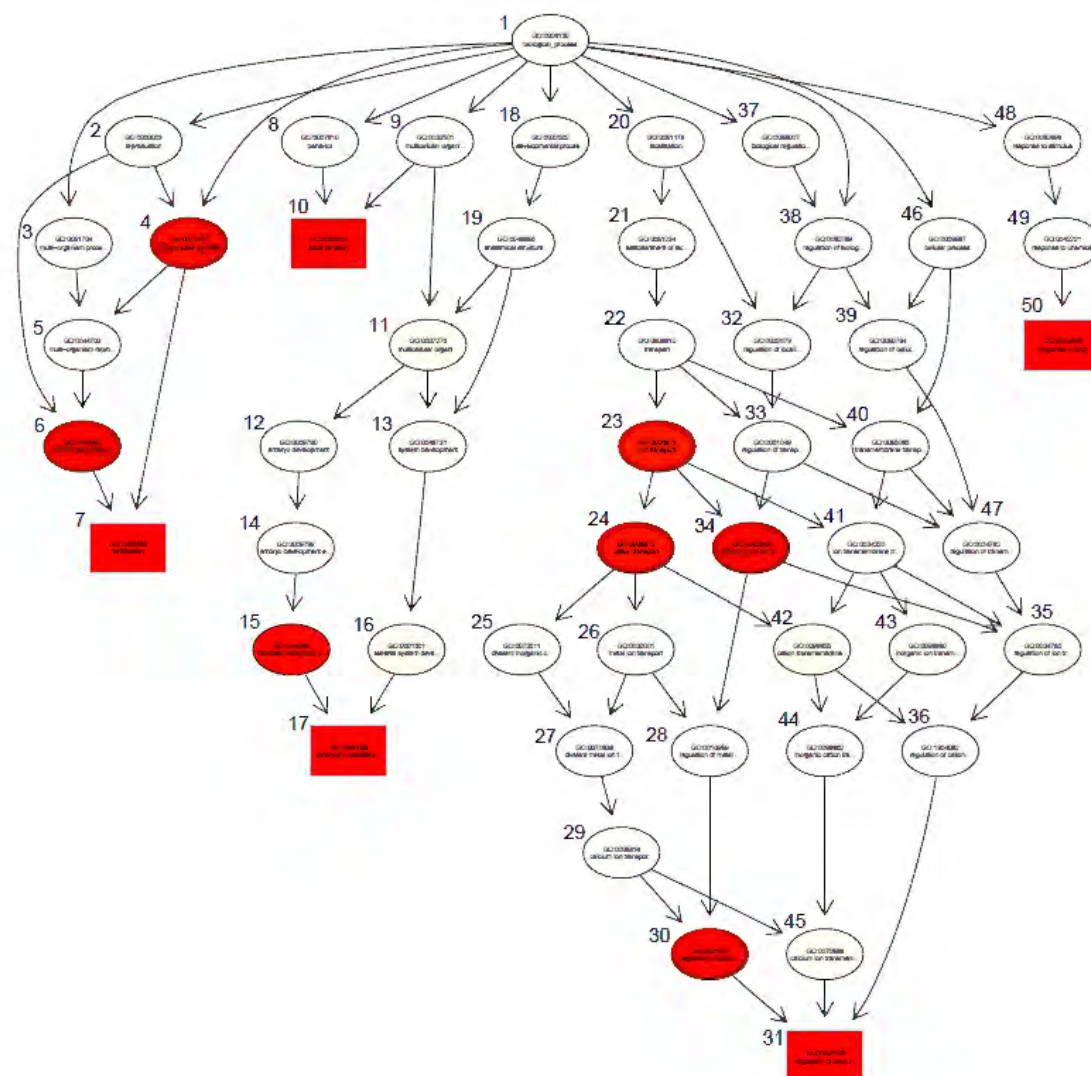
Molecular pathway analysis of RHDV2-infected liver transcriptome samples. The subgraph is induced by the top 5 gene ontology (GO) components (depicted in red squares) identified by the weight01 algorithm for scoring gene ontology components (Alexa et al., 2006).

White and red ovals depict gene ontology components that contribute to a pathway. Shapes colored red indicate the most significant components, whereas those colored white indicate less significant components. All the components are numbered and a description for each of the components can be found in table below. TopGO R package was used to build the network (Alexa and Rahnenfuhrer, 2020).

#	GO ID	GO component description
1	GO:0008150	Biological process
2	GO:0000003	Reproduction
3	GO:0051704	Multi-organism process
4	GO:0022414	Reproductive process
5	GO:0044703	Multi-organism reproductive process
6	GO:0019953	Sexual reproduction
7	GO:0009566	Fertilization
8	GO:0007610	Behaviour
9	GO:0032501	Multicellular organismal process
10	GO:0030534	Adult behaviour
11	GO:0007275	Multicellular organism development
12	GO:0009790	Embryo development
13	GO:0048731	System development
14	GO:0009792	Embryo development ending in birth or egg hatching
15	GO:0043009	Chordate embryonic development
16	GO:0001501	Skeletal system development
17	GO:0048706	Embryonic skeletal system development
18	GO:0032502	Developmental process
19	GO:0048856	Anatomical structure development
20	GO:0051179	Localization
21	GO:0051234	Establishment of localization
22	GO:0006810	Transport
23	GO:0006811	Ion transport
24	GO:0006812	Cation transport
25	GO:0072511	Divalent inorganic cation transmembrane transport
26	GO:0030001	Metal ion transport
27	GO:0070838	Divalent metal ion transport
28	GO:0010959	Regulation of metal ion transport
29	GO:0006816	Calcium ion transport
30	GO:0051924	Regulation of calcium ion transport
31	GO:1903169	Regulation of calcium ion transmembrane transport
32	GO:0032879	Regulation of localization
33	GO:0051049	Regulation of transport
34	GO:0043269	Regulation of ion transport
35	GO:0034765	Regulation of ion transmembrane transport
36	GO:1904062	Regulation of cation transmembrane transport
37	GO:0065007	Biological regulation
38	GO:0050789	Regulation of biological process
39	GO:0050794	Regulation of cellular process

| 40	GO:0055085	Transmembrane transport
41	GO:0034220	Ion transmembrane transport
42	GO:0098655	Cation transmembrane transport
43	GO:0098660	Inorganic ion transmembrane transport
44	GO:0098662	Inorganic cation transmembrane transport
45	GO:0070588	Calcium ion transmembrane transport
46	GO:0009987	Cellular process
47	GO:0034762	Regulation of transmembrane transport
48	GO:0050896	Response to stimulus
49	GO:0042221	Response to chemical
50	GO:0042493	Response to xenobiotic stimulus

Supplementary Figure 3
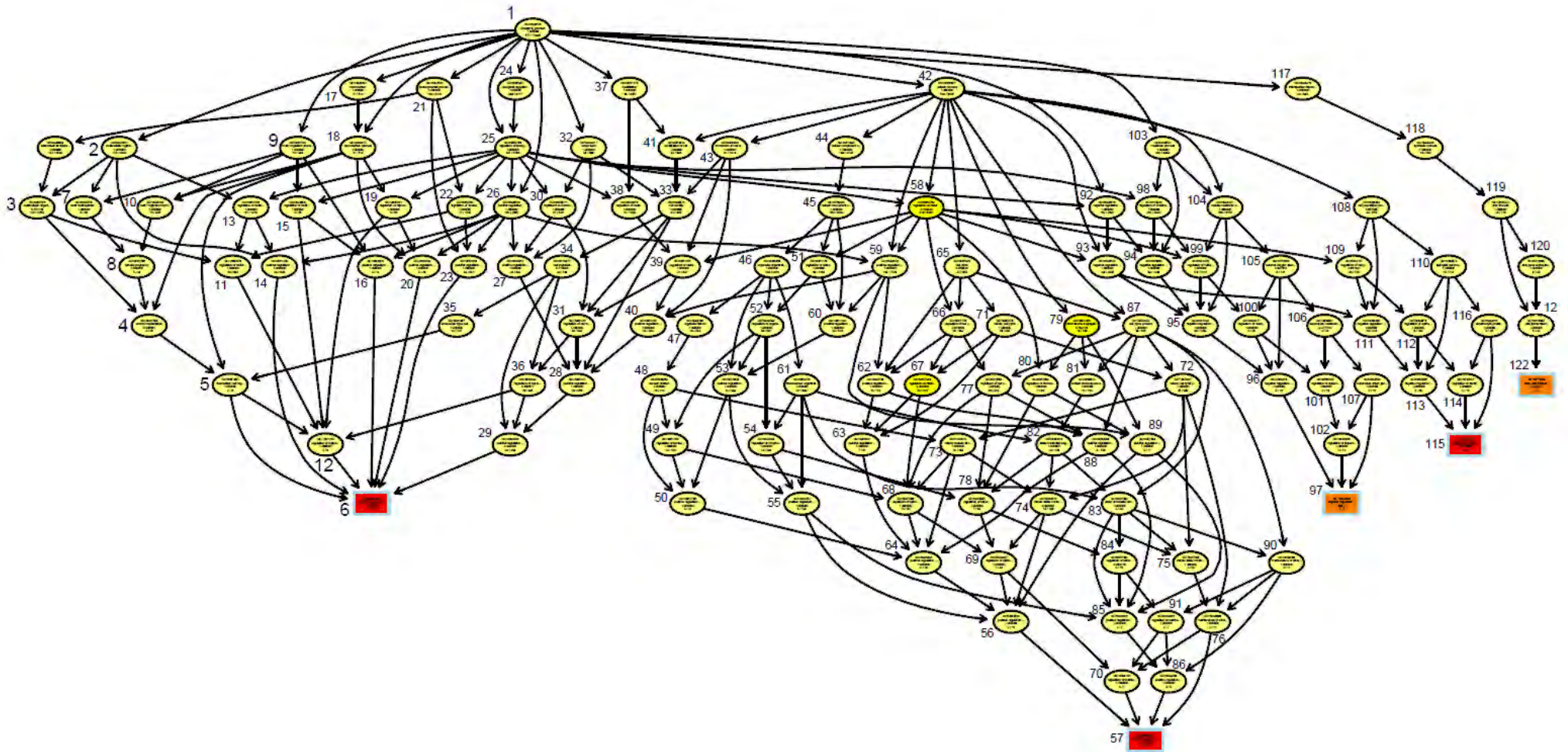
Molecular pathway analysis of RHDV2-infected liver samples (transcriptome). The network subgraph is induced by the top 5 gene ontology (GO) components (depicted in squares) identified by the weight01 algorithm with Fisher's exact test (Alexa et al., 2006). Box colors represent the relative significance of GO components, with yellow, orange, and red boxes and ovals indicating least and most significant GO terms, respectively. All the components are numbered and the description for each of the components can be found in table below. TopGO R package was used to build the network (Alexa and Rahnenfuhrer, 2020).

#	GO ID	GO component description
1	GO:0008150	Biological process
2	GO:0032501	Multicellular organismal process
3	GO:0007275	Multicellular organism development
4	GO:0007566	Embryo implantation
5	GO:0061450	Trophoblast cell migration
6	GO:1901165	Positive regulation of trophoblast cell migration
7	GO:0044706	Multi-multicellular organism process
8	GO:0007565	Female pregnancy
9	GO:0051704	Multi-organism process
10	GO:0044703	Multi-organism reproductive process
11	GO:2000026	Regulation of multicellular organismal development
12	GO:1901163	Regulation of trophoblast cell migration
13	GO:0051239	Regulation of multicellular organismal process
14	GO:0051240	Positive regulation of multicellular organismal process
15	GO:0043900	Obsolete regulation of multi-organism process
16	GO:0043902	Obsolete positive regulation of multi-organism process
17	GO:0000003	Reproduction
18	GO:0022414	Reproductive process
19	GO:2000241	Regulation of reproductive process
20	GO:2000243	Positive regulation of reproductive process
21	GO:0032502	Developmental process
22	GO:0050793	Regulation of developmental process
23	GO:0051094	Positive regulation of developmental process
24	GO:0065007	Biological regulation
25	GO:0050789	Regulation of biological process
26	GO:0048518	Positive regulation of biological process
27	GO:0040017	Positive regulation of locomotion
28	GO:2000147	Positive regulation of cell motility
29	GO:0030335	Positive regulation of cell migration
30	GO:0040012	Regulation of locomotion
31	GO:2000145	Regulation of cell motility
32	GO:0040011	Locomotion
33	GO:0048870	Cell motility
34	GO:0016477	Cell migration

35	GO:0001667	Ameboidal-type cell migration
36	GO:0030334	Regulation of cell migration
37	GO:0051179	Localization
38	GO:0032879	Regulation of localization
39	GO:0051270	Regulation of cellular component movement
40	GO:0051272	Positive regulation of cellular component movement
41	GO:0051674	Localization of cell
42	GO:0009987	Cellular process
43	GO:0006928	Movement of cell or subcellular component
44	GO:0071840	Cellular component organization or biogenesis
45	GO:0016043	Cellular component organization
46	GO:0006996	Organelle organization
47	GO:0048285	Organelle fission
48	GO:0000280	Nuclear division
49	GO:0051783	Regulation of nuclear division
50	GO:0051785	Positive regulation of nuclear division
51	GO:0051128	Regulation of cellular component organization
52	GO:0033043	Regulation of organelle organization
53	GO:0010638	Positive regulation of organelle organization
54	GO:0033044	Regulation of chromosome organization
55	GO:2001252	Positive regulation of chromosome organization
56	GO:0062033	Positive regulation of mitotic sister chromatid segregation
57	GO:0034184	Positive regulation of maintenance of mitotic sister chromatid cohesion
58	GO:0050794	Regulation of cellular process
59	GO:0048522	Positive regulation of cellular process
60	GO:0051130	Positive regulation of cellular component organization
61	GO:0051276	Chromosome organization
62	GO:0045787	Positive regulation of cell cycle
63	GO:0045931	Positive regulation of mitotic cell cycle
64	GO:0045840	Positive regulation of mitotic nuclear division
65	GO:0007049	Cell cycle
66	GO:0051726	Regulation of cell cycle
67	GO:0007346	Regulation of mitotic cell cycle
68	GO:0007088	Regulation of mitotic nuclear division
69	GO:0033047	Regulation of mitotic sister chromatid segregation
70	GO:0034182	Regulation of maintenance of mitotic sister chromatid cohesion
71	GO:0000278	Mitotic cell cycle
72	GO:1903047	Mitotic cell cycle process
73	GO:0140014	Mitotic nuclear division
74	GO:0000070	Mitotic sister chromatid segregation
75	GO:0007064	Mitotic sister chromatid cohesion
76	GO:0034088	Maintenance of mitotic sister chromatid cohesion
77	GO:0010564	Regulation of cell cycle process
78	GO:0033045	Regulation of sister chromatid segregation
79	GO:0007059	Chromosome segregation
80	GO:0051983	Regulation of chromosome segregation
81	GO:0098813	Nuclear chromosome segregation
82	GO:0000819	Sister chromatid segregation

83	GO:0007062	Sister chromatid cohesion
84	GO:0007063	Regulation of sister chromatid cohesion
85	GO:0045876	Positive regulation of sister chromatid cohesion
86	GO:0034093	Positive regulation of maintenance of sister chromatid cohesion
87	GO:0022402	Cell cycle process
88	GO:0090068	Positive regulation of cell cycle process
89	GO:0051984	Positive regulation of chromosome segregation
90	GO:0034086	Maintenance of sister chromatid cohesion
91	GO:0034091	Regulation of maintenance of sister chromatid cohesion
92	GO:0048519	Negative regulation of biological process
93	GO:0048523	Negative regulation of cellular process
94	GO:0009892	Negative regulation of metabolic process
95	GO:0031324	Negative regulation of cellular metabolic process
96	GO:2000378	Negative regulation of reactive oxygen species metabolic process
97	GO:0032929	Negative regulation of superoxide anion generation
98	GO:0019222	Regulation of metabolic process
99	GO:0031323	Regulation of cellular metabolic process
100	GO:2000377	Regulation of reactive oxygen species metabolic process
101	GO:0090322	Regulation of superoxide metabolic process
102	GO:0032928	Regulation of superoxide anion generation
103	GO:0008152	Metabolic process
104	GO:0044237	Cellular metabolic process
105	GO:0072593	Reactive oxygen species metabolic process
106	GO:0006801	Superoxide metabolic process
107	GO:0042554	Superoxide anion generation
108	GO:0008283	Cell population proliferation
109	GO:0042127	Regulation of cell population proliferation
110	GO:0050673	Epithelial cell proliferation
111	GO:0008285	Negative regulation of cell population proliferation
112	GO:0050678	Regulation of epithelial cell proliferation
113	GO:0050680	Negative regulation of epithelial cell proliferation
114	GO:0010837	Regulation of keratinocyte proliferation
115	GO:0010839	Negative regulation of keratinocyte proliferation
116	GO:0043616	Keratinocyte proliferation
117	GO:0044419	Biological process involved in interspecies interaction between organisms
118	GO:0044403	Biological process involved in symbiotic interaction
119	GO:0016032	Viral process
120	GO:0019080	Viral gene expression
121	GO:0019083	Viral transcription
122	GO:0019085	Early viral transcription

Future directions

To further improve the Ca^{2+} measurement flow cytometry-based experiment, I generated constructs that include mCherry fluorescent protein. In these constructs, N-terminal FLAG is followed by mCherry-tagged p23. The fluorescence emission spectrum of mCherry is distinct from the calcium-binding fluorescent dye Fluo-4 and therefore, transfected cells can be selected using mCherry. This way, Ca^{2+} will be measured in transfected cells only, reducing the background noise generated by the analysis of untransfected cells.

I checked whether mCherry-tagged p23 still dimerises using immunoprecipitation and Western blotting as described in chapter 4. The result indicates that mCherry-tagged wild-type p23 dimerises under non-reducing conditions and C41S variant does not:
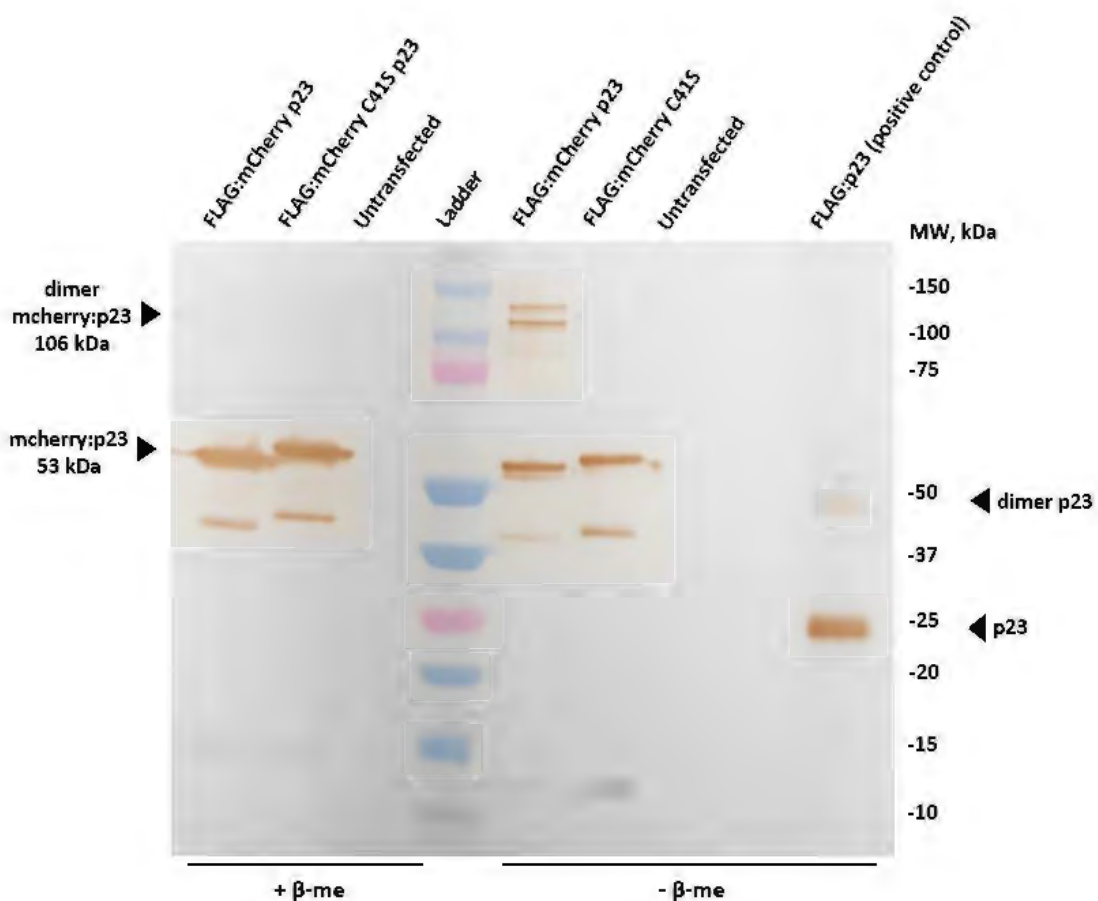
Therefore, these constructs can be used for Ca^{2+} measurements of p23-transfected cells.

Chapter 5. RHDV non-structural protein expression in *E. coli* and mammalian cell lines

Introduction

Protein expression in *E. coli* was attempted for RHDV non-structural proteins p16, p23 and p29. These proteins have not been expressed in bacteria before and therefore there were no protocols available to follow. Protein expression and purification with the subsequent possibility of crystallisation opens the opportunity to study the 3D structure of proteins. Moreover, in the case of viral membrane-associated channel-forming proteins, such as p23, protein expression in *E. coli* can be used to confirm viroporin activity. Monitoring bacterial growth upon the expression of potential viroporins is a 'classic' viroporin assay (Studier & Moffatt, 1986). For this assay, specific *E. coli* strains (e.g., BL21(DE3)pLysS) are used that carry a plasmid responsible for constitutive T7 lysozyme production and express T7 RNA polymerase under the control of a lac promoter. The T7 lysozyme is a selective inhibitor of T7 RNA polymerase and thus, the background expression of the gene of interest under a T7 promotor in the absence of isopropyl β-D-1-thiogalactopyranoside (IPTG) or lactose is minimal, making these *E. coli* strains suitable for the expression of toxic proteins. The classic viroporin assay is based on the leakage of lysozyme into the periplasmic space through the channels formed by viroporins in the inner membrane, causing dissociation of peptidoglycan and cell lysis, which can be detected by a declining optical density of the culture after IPTG induction.

This assay has previously been used to characterise viroporin activity of poliovirus (family *Picornaviridae*) proteins 2B and 3A (Lama & Carrasco, 1992), rotavirus (family *Rotaviridae*) protein NSP4 (Browne et al., 2000), *Tulane virus* (family *Caliciviridae*) protein NS1/2 (Strtak et al., 2019) and many other viroporins. Full-length viroporin expression in *E. coli* may be challenging as these proteins usually contain transmembrane helices and thus can be tightly associated with *E. coli* membranes resulting in poor solubility. Therefore, transmembrane helices are often truncated, and a shorter protein is expressed. Often the expression of a shortened protein that only contains the transmembrane helices is enough to induce the cell lysis in the classic viroporin assay (Browne et al., 2000).

Apart from expressing these proteins in *E. coli*, I also attempted to express p16, p23 and p29 in mammalian cells, such as the RK-13 (rabbit kidney) cell line. Transient expression of tagged viral proteins in mammalian cells with subsequent immunofluorescence staining, Western blotting or immunoprecipitations facilitates characterisation of many important aspects

of a protein, e.g., its subcellular localisation, ability to oligomerise and interactions with other proteins. These basic approaches are essential for successful characterisation of a given protein. Immunofluorescence staining was used previously to determine the cellular localisation of RHDV proteins p16, p23 and p29 in transfected cells (Urakova et al., 2015). In my work, I used immunoprecipitations with subsequent Western blotting to study the mechanisms of p23 oligomerisation in transfected mammalian cells (results are presented in the previous chapter). Here I discuss my attempts to express and detect proteins p16 and p29 that were transiently expressed in RK-13 cells.

Materials and methods

Plasmids and constructs

Constructs for protein expression in *E. coli*

RHDV sequences of p16, p23 and p29 were generated to contain *Nco*I (5') and *Xho*I (3') restriction enzyme sites and submitted to Twist Bioscience (CA, USA) for synthesis and codon optimisation. Codon optimised sequences arrived cloned into a pTwist kanamycin high copy plasmid. Sequences were PCR amplified, purified using the Wizard PCR purification kit (Promega, Madison, WI) and digested with *Nco*I and *Xho*I restriction enzymes (Promega) as per the manufacturer's instructions. The following primers were used:

Insertion	Primers for cloning (5'->3')	Restriction sites
p16 in pET28a (codon optimised)	F: ATATACCATGGGCTTAACAGG R: TATATCTCGAGTTCGAAGATCG	*Nco*I (5')- *Xho*I (3')
p23 in pET28a (codon optimised)	F: ATATACCATGGGCGGAGAAG R: TATATCTCGAGCTCGAAGGTGTC	*Nco*I (5')- *Xho*I (3')
p29 in pET28a (codon optimised)	F: ATATACCATGGGCGGAGC R: TATATCTCGAGCTGGAAGGC	*Nco*I (5')- *Xho*I (3')

pET28a(+) vector (a kind gift from Michelle Williams (CSIRO, Land & Water)) was digested with the same restriction enzymes and purified. The concentration of the fragments and vector was measured using Qubit double stranded DNA broad range assay (Life Technologies, Carlsbad, CA, USA). After that, the ligation reaction was set up with T4 DNA ligase (NEB, Ipswich, Massachusetts, United States) as per the manufacturer's instructions. The ligation reaction was incubated at 16°C overnight. After that, 10 μl of each reaction was transformed into chemically competent *E. coli* TOP10 cells (Invitrogen, Carlsbad, CA, USA). TOP10 cells were incubated on ice for 30 min, heat-shocked for 30 s at 42°C and 350 μl of Super Optimal broth with Catabolite repression (SOC) was added to the reaction. Then, the tubes were incubated at 37°C with constant shaking. The reaction was plated onto LB plates with 50 μg/ml kanamycin and the plates were incubated overnight at 37°C.

A pET14b (ampicillin resistance) construct with green fluorescence protein (GFP) was a kind gift from Raquel Rocha Aguiar (CSIRO Land & Water). This construct was used as a non-toxic protein expression control. All constructs were verified by Sanger sequencing at the

Biomolecular Resource Facility of the John Curtin School of Medical Research (Australian National University, Canberra, Australia).

Constructs for protein expression in mammalian cells

RHDV (GI.1) sequences of p16, p23, p29, RdRp and coding sequence of GFP were cloned into a pCMV-Tag2C expression vector using restriction enzyme-based cloning using the following primers:

Insertion	Primers for cloning (5'->3')	Restriction sites
p29 RHDV	F: ATATA<u>GAATTC</u>TTATGGGTGCCAACAAATTTAACTTTG R: ATATA<u>CTCGAG</u>CTACTGAAAAGCTTTCGTTGCAACTG	*Eco*RI (5')-*Xho*I (3')
GFP	F: ATATA<u>GGATCC</u>TTATGGTGAGCAAGG R: ATATA<u>AAGCTT</u>CTACTACTTGTACAGCTCGTC	*Bam*HI (5')-*Hind*III (3')
RdRp RHDV	F: ATATA<u>GAATTC</u>TTATGACGTCAAACTTCTTCTGTGG R: ATATA<u>GTCGAC</u>CTACTCCATAACATTCACAAATTC	*Eco*RI (5')-*Sal*I (3')

Plasmids encoding RHDV p16 and p23 were generated previously (Urakova et al., 2015).

Antibodies

Table 1. List of the antibodies used.

Antibody	Product number	Supplier	Dilution	Conjugation**
Primary antibodies				
Rat monoclonal anti-FLAG	NOVNBP106712SS	Novus Biologicals	1:1500 (WB*)	Unconjugated
Rabbit monoclonal anti-Hsp70	ab45133	Abcam	1:1500 (WB)	Unconjugated
Mouse monoclonal anti-β-actin	ab8226	Abcam	1:1500 (WB)	Unconjugated
Mouse monoclonal anti 6xHIS-tag	ab18184	Abcam	1:1500 (WB)	Unconjugated
Secondary antibodies				
Secondary goat anti-rat	3050-05	Cambridge Bioscience	1:3000 (WB)	HRP**
Secondary goat anti-mouse	170-6516	Bio-Rad	1:3000 (WB)	HRP
Secondary goat anti-rabbit	170-6515	Bio-Rad	1:3000 (WB)	HRP

* Western blotting; **Horseradish peroxidase.

Western blotting

E. coli cell lysates or mammalian cell lysates were mixed with sodium dodecyl sulphate polyacrylamide gel electrophoresis (SDS-PAGE) sample buffer (125 mM tris pH 6.8, 4% SDS, 20% (v/v) glycerol, 0.004% bromophenol blue, 5% β-mercaptoethanol), denatured by boiling at 95°C for 5 min and separated on 4–20% TruPAGE pre-cast gels (Sigma-Aldrich, St. Louis, MO). Proteins were transferred onto a nitrocellulose membrane (NitroBind, MSI, Cole-Parmer, US) using the Bio-Rad (Hercules, CA, USA) wet transfer blotting module. The membrane was subsequently blocked in 5% skim milk (Coles Supermarkets, Australia) in tris-buffered saline with 0.1% Tween-20 (TBST) for 1.5 h at room temperature. Incubation with primary antibodies was performed overnight at 4°C in TBST (for HIS-tagged proteins, mouse anti-HIS tag antibodies were used). Incubation with secondary antibodies conjugated to horseradish peroxidase was performed for 1 h at room temperature in TBST (goat anti-mouse HRP). SIGMAFAST 3,3'-diaminobenzidine tablets (Sigma-Aldrich) were used for visualization of bands according to the manufacturer's instructions.

Protein expression in *E. coli*

BL21(DE3) E. coli strain, IPTG induction

BL21DE3 chemically competent cells were provided by Michelle Williams (CSIRO Land & Water). The cells were transformed with p16, p23, p29 and empty pET28a vector as described above. The next day, a single colony was picked and resuspended in 5 ml Luria Bertani (LB) broth with 50 μg/ml kanamycin. The culture was incubated overnight at 37°C with constant shaking. After that, 2 ml of the overnight culture was inoculated into 100 ml of fresh LB with 20 mM glucose and 50 μg/ml kanamycin. This culture was incubated at 37°C with shaking until optical density (OD600) reached 0.6–0.8. At this point, protein expression was induced with 1 mM IPTG. The flask was swirled to ensure mixing, and 10 ml of culture was aliquoted into 50-ml Corning tubes. After that, aliquots were incubated at different temperatures (25°C, 31°C, 37°C) to determine optimal conditions for protein expression. The next day, a 1-ml aliquot was taken from each tube and centrifuged at 3000 × g for 5 min at 4°C to harvest the cells. The cell pellets were resuspended in 500 μl BugBuster lysis buffer (Roche, Basel, Switzerland). To prepare the lysis buffer, 10x stock solution was diluted in 50 mM Tris pH 7.5. Cell suspensions were incubated with rocking at room temperature for 20 min and a 2-μl sample was mixed with 8 μl of milliQ water and 5 μl of loading dye (whole lysate). The suspensions were then centrifuged at 16,000 × g for 20 min at 4°C to obtain a soluble lysate, and 10 μl of

the supernatant were mixed with 5 µl of loading dye. The samples were heated at 95°C for 3 min and loaded onto a precast 4–20% TruPAGE gel (Sigma-Aldrich).

BL21(DE3)pLysE and BL21(DE3)pLysS *E. coli* strains, IPTG induction

BL21(DE3)pLysE chemically competent cells were purchased from Thermo Fisher Scientific (MA, USA) and BL21(DE3)pLysS cells were purchased from Promega. These cells were used for the classic viroporin assay to detect lysozyme-mediated lysis of bacteria. The cells were transformed with a pET28a construct encoding the codon-optimised sequence of p23 (as described above); the transformation mixture was plated onto an LB plate with 20 mM glucose and 50 µg/ml kanamycin. A single colony was picked and resuspended in 5 ml LB containing 20 mM glucose and 50 µg/ml kanamycin. Bacteria were grown at 37°C with constant shaking until an optical density (OD600) of 0.4–0.6 was reached. After that, the suspension was split into two flasks; 1 mM IPTG was added to one of the flasks, while the other culture served as a negative (uninduced) control. Optical density measurements were taken every 10 min after induction for total of 90 min and aliquots tested for protein expression.

Autoinduction (lactose induction)

For this type of induction, terrific broth (TB) medium with 24 g/l yeast extract, 20 g/l tryptone, 4 ml/l glycerol and 10% potassium phosphate buffer mix (23.1 g/l KH_2PO_4, 125.4 g/l K_2HPO_4) was used, the potassium buffer mix serves as a buffer system and maintains pH of the culture medium. In a 250 ml flask, 50 ml of TB broth supplemented with 2.5 ml 20% glucose (1% w/v) was inoculated with a freshly transformed single *E. coli* colony. The suspension was incubated overnight at 37°C with shaking. The next day, 2 ml of the overnight culture (1:50) was inoculated in 100 ml of TB supplemented with 2 ml 10% lactose (0.2% w/v). The suspension was cultured overnight at 37°C with shaking.

Ni-NTA protein purification

Freshly transformed BL21(DE3)pLysS were grown overnight in 5 ml of LB with 50 mg/ml kanamycin, 30 mg/ml chloramphenicol and 20 mM glucose and 2 ml of overnight culture was inoculated in 100 ml of fresh LB medium. Cells were grown until an OD600 of 0.6–0.7 was reached and then centrifuged at 3000 × g for 20 min at 4°C. The cell pellet was resuspended in 100 ml of fresh LB with 50 mg/ml kanamycin and 30 mg/ml chloramphenicol, and protein expression was induced with 1 mM IPTG. The culture was incubated overnight at 25°C with shaking. The next day, cells were harvested by centrifugation at 3000 × g for 20 min at 4°C and resuspended in lysis buffer (20 mM tris pH 8.5, 500 mM NaCl, 5% glycerol, 2 mM

PMSF, 5 mM β-mercaptoethanol, 1% triton X-100). The cell suspension was sonicated for 5 min (15 s sonication and cooling on ice cycles) and the cell lysate was cleared by centrifugation at $6500 \times g$ for 30 min at 4°C. For affinity purification of HIS-tagged p23, 100 µl of Ni-NTA affinity resin (Thermo Fisher Scientific) was added to a 2-ml tube. Two volumes of equilibration buffer (20 mM tris pH 8.5, 500 mM NaCl, 10% glycerol and 5 mM β-mercaptoethanol) were added to the resin, and it was centrifuged for 2 min at $700 \times g$ at 4°C. This washing step was repeated twice, and then the cell lysate was applied onto the resin and incubated with rocking at room temperature for 30 min. After that, the resin was washed twice with the equilibration buffer and once with the equilibration buffer containing 15 mM imidazole, and proteins were eluted. The elution buffer consisted of equilibration buffer with 300 mM imidazole. The elution buffer was added to the resin (100 µl) and the resin was centrifuged for 2 min at $700 \times g$. The supernatant was removed and prepared for analysis with SDS-PAGE.

Protein toxicity check: colony formation

For this experiment, GFP-expressing plasmid served as a non-toxic protein expression control. BL21(DE3)pLysS cells were transformed with either a p23- or a GFP-encoding plasmid as described above, and a single colony was resuspended in 5 ml of LB medium with 20 mM glucose and 50 µg/ml kanamycin. This suspension was incubated overnight as described above. A serial dilution of the overnight cultures was prepared, ranging from 10^{-1} to 10^{-8}. A 5-µl drop of each dilution was plated onto two plates, either with 0.2 mM IPTG or without IPTG (uninduced control). After that, plates were incubated overnight at 37°C and colony formation was checked the next day.

Protein expression in mammalian cells
Transient transfection

RK-13 cells were transfected with plasmids encoding proteins p16, p23 and p29 with a FLAG tag. The coding sequences of these proteins were cloned into pCMV-Tag2C expression vector as described previously (Urakova et al., 2015). Lipofectamine 3000 reagent was used for transfection according to the manufacturer's instructions. Briefly, RK-13 were grown in culture plates (usually 60-mm plates) until 70–90% confluent. Transfections were conducted with 5.5 µg of plasmid DNA and 8.25 µl of lipofectamine reagent per plate; OptiMEM culture medium (Gibco, Thermo Fisher Scientific) was used to prepare the DNA-lipofectamine mixtures. The mixture was incubated at room temperature for 15 min and then added dropwise to the culture

plates with fresh antibiotic-free DMEM medium (3.5 ml in case of 60-mm plates). Transfected cells were incubated overnight at 37°C to allow for protein expression.

Cell lysis and Western blotting

Transfected cells were washed with ice-cold PBS and scraped into a centrifuge tube with 1 ml of PBS. Harvested cells were centrifuged at $200 \times g$, resuspended in 400 µl of lysis buffer (PBS, pH 7.5 with 150 mM NaCl, 0.5 mM EDTA, 0.5% Igepal CA-630 and protease inhibitors (Roche, Basel, Switzerland)) and incubated on ice for 20 min with gentle rocking. Remaining cell debris was removed by centrifugation, and the supernatants were used for SDS-PAGE and Western blot analysis.

Cell lysates were mixed with SDS-PAGE sample buffer (125 mM tris pH 6.8, 4% SDS, 20% (v/v) glycerol, 0.004% bromophenol blue, 5% β-mercaptoethanol), denatured by boiling for 5 min, and separated on 4–20% TruPAGE pre-cast gels (Sigma-Aldrich). Proteins were transferred onto a nitrocellulose transfer membrane (NitroBind, MSI) using the Bio-Rad (Hercules, CA, USA) wet transfer blotting module. The following buffers were used for transfer: Towbin buffer (25 mM tris, 192 mM glycine, 20% v/v methanol, pH 8.3), N-cyclohexyl-3-aminopropanesulfonic acid (CAPS) buffer (10 mM CAPS, 10% v/v methanol, pH 10.5), Dunn carbonate buffer (10 mM $NaHCO_3$, 3 mM Na_2CO_3, 20% v/v methanol, pH 9.9). The nitrocellulose membrane was blocked in 5% skim milk (Coles Supermarkets, Australia) in tris-buffered saline with 0.1% Tween-20 (TBST) for 2 h at room temperature. Incubation with primary antibodies, rat anti-FLAG (1:2000) and rabbit anti-heat shock protein 70 (1:3000) was performed overnight at 4°C in TBST. Incubation with secondary antibodies, goat anti-rat and goat anti-rabbit conjugated to horseradish peroxidase (both 1:3000), was performed for 1 h at room temperature in TBST. SIGMAFAST 3,3'-diaminobenzidine tablets (Sigma-Aldrich) were used for visualisation of bands according to the manufacturer's instructions.

TCA precipitation

The protocol for trichloroacetic acid (TCA; Sigma Aldrich) precipitation from Lee et al., 2019 was used with modifications. RK-13 and African green monkey kidney cells (Vero) cells were transfected as described above with pCMV-Tag2C constructs encoding for RHDV proteins p16, p23 and p29. The next day, the culture supernatants were collected and centrifuged at $0.3 \times g$ for 5 min at 4°C to purify the cultured medium from cells and cell debris. After that, the supernatants were further purified by filtering through a 0.2-µm syringe filter. To prepare 100% v/v TCA, 2.2 g were dissolved in 1 ml of milliQ water. Water was added slowly and dropwise. For protein precipitation, 125 µl of TCA was added to 500 µl of culture

supernatant (20% TCA v/v) and incubated overnight at 4°C. The next day, solutions were centrifuged at 18,000 × g for 10 min at 4°C and the protein pellet was resuspended with 1 ml ice-cold acetone and centrifuged again. After that, the pellet was resuspended with 2x Laemmli loading buffer, boiled at 95°C for 5 min and analysed by SDS-PAGE and Western blotting.

In silico predictions

The Predictor of Natural Disordered Regions (PONDR, http://www.pondr.com/) was used to analyse p16, p23 and p29 protein sequences of RHDV (NC_001543.1). The PONDR® output is a plot that indicates the strength of the prediction at each region with a cut-off value equal to 0.5 (Xue et al., 2010). The PSIPRED Protein Analysis Workbench server (http://bioinf.cs.ucl.ac.uk/psipred/) (Buchan et al., 2019) was used to analyse the secondary structure of the proteins, the potential presence of membrane helices was analysed with the MEMSAT-SVM algorithm (Nugent and Jones, 2010, 2012).

Results

In silico predictions

For an initial characterisation of the proteins, I used various *in silico* prediction tools. This information helps to identify potential complications in protein expression and purification, for example, the presence of hydrophobic regions that could lead to poor protein solubility (Francis et al., 2010). First, the predictor of intrinsic disordered regions (PONDR) server was used to identify ordered and disordered regions in p16, p23 and p29 RHDV protein sequences (**Figure 1**) (Xue et al., 2010).
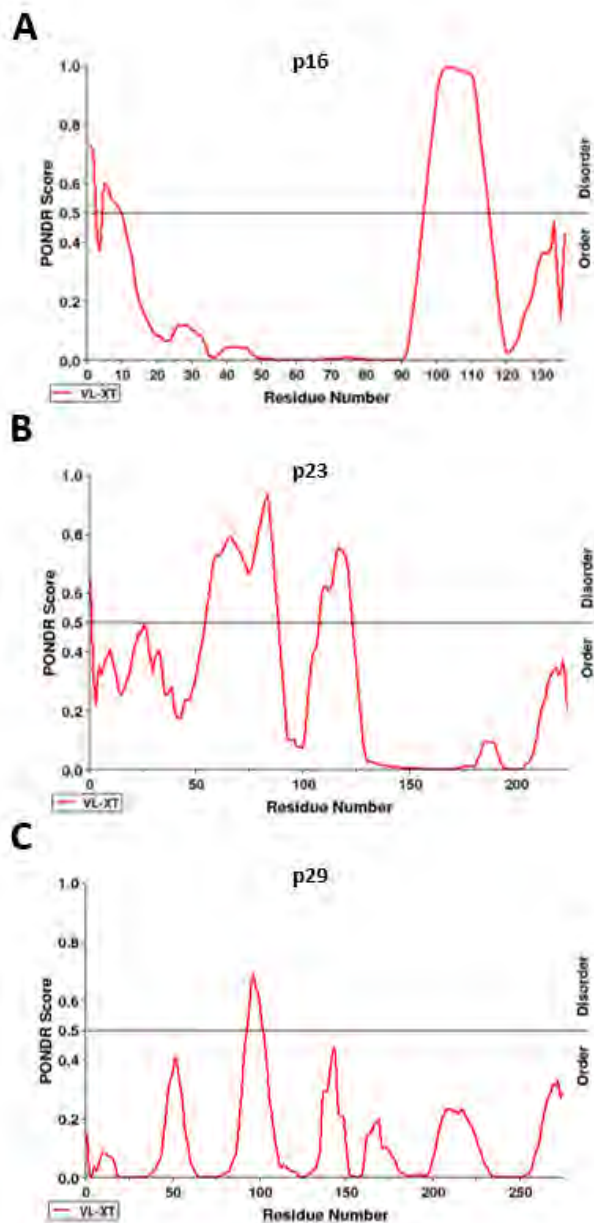
Figure 1. Disordered regions predictions for RHDV non-structural proteins. PONDR server (http://www.pondr.com/) (Xue et al., 2010) was used to generate the graphs for proteins (**A**) p16, (**B**) p23 and (**C**) p29. The PONDR score on the y-axis indicates the strength of the prediction; regions above 0.5 are considered disordered.

These results suggest that p16 has disordered regions at the N- and C-termini. Protein p23 is largely disordered except for the C-terminal region where potential transmembrane helices are located (Smertina et al., 2021), and protein p29 is the most ordered of the three proteins analysed. In general, disordered proteins lack stable secondary and tertiary structures, but still execute vital functions in cells, e.g., cyclin-dependent kinase inhibitor proteins that regulate cell cycle, are intrinsically disordered proteins (Xie et al., 2007). Intrinsic disorder was

also observed in other calicivirus proteins, such as NS1/2 of MNV, the positional homolog of proteins p16 and p23 in RHDV. NS1/2 contains an ordered region in the C-terminal part of the protein with a predicted transmembrane domain (Baker et al., 2012). Baker and co-authors successfully expressed and purified a truncated NS1/2 without the transmembrane domain (Baker et al., 2012). Hydrophobic helices are likely to decrease protein solubility upon overexpression in *E. coli*. In this work, NS1/2 was expressed as a fusion protein with a chitin binding fusion partner and purified using a chitin bead column (Baker et al., 2012).

Proteins with disordered regions often exhibit 'aberrant' migration on SDS-PAGE due to unusual amino acid compositions (Tompa et al., 2002). In some instances, this can be attributed to the binding of less SDS by hydrophilic regions, a high content of negatively charged amino acids and/or the presence of multiple proline residues. Proline residues often cause disorder because of their helix breaking nature (Vacic et al., 2007). Sequence analysis of the RHDV protein p16 shows a high proline content of 8% (similar to that of norovirus NS1/2; Baker et al., 2012). The mean percentage of proline in proteins of the human proteome is 6.2% (Morgan et al., 2013).

Another prediction tool, PSIPRED Protein Structure Prediction Server was used to predict the secondary structure of the proteins and transmembrane domains with MEMSAT-SVM algorithm (Nugent and Jones, 2012) (**Figure 2**).
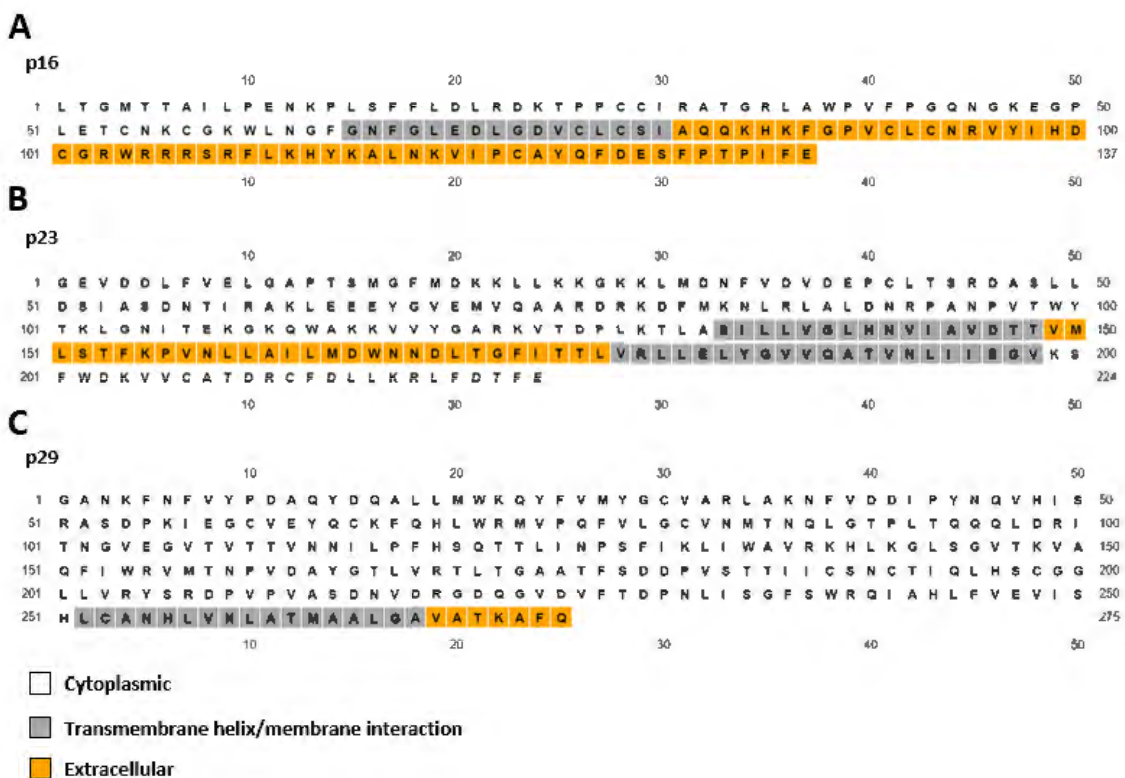

165

Figure 2. Secondary structure and transmembrane domains prediction for RHDV non-structural proteins. The MEMSAT-SVM algorithm of the PSIPRED workbench server was used to predict transmembrane helices in proteins (**A**) p16, (**B**) p23 and (**C**) p29. Non-highlighted areas are predicted to be cytoplasmic, areas highlighted grey constitute transmembrane helices and areas highlighted orange are predicted to be 'extracellular' or on the opposite side of a membranous organelle.

According to the MEMSAT-SVM prediction, p16 has a long 'extracellular' domain (**Figure 2**). This might mean that p16 is a membrane-spanning protein and this part of the protein is oriented to the cytoplasmic side of a membranous organelle or is located outside of a cell in case of a plasma membrane integration. Interestingly, the cleavage product of MNV NS1/2, protein NS1 was shown to be an extracellular protein, secreted via an unconventional mechanism triggered by caspase-3 cleavage of NS1/2 (Lee et al., 2019). These data may be indicative of RHDV p16 secretion. In this case, analysis of p16-transfected cells might not lead to successful detection of this protein.

Transmembrane helices predictions for proteins p23 and p29 were described in chapters 3 and 4. Briefly, according to the prediction tool, both proteins have at least one transmembrane helix. This may be a hindrance for protein expression because of their tight association with cellular membranes and poor solubility (Francis and Page, 2010).

Protein expression in *E. coli*

BL21(DE3) *E. coli* cells were used for p16, p23 and p29 protein expression optimisation as described above. Various temperatures were tested to determine the appropriate expression conditions. Insoluble (whole lysates) and soluble (centrifuged lysates) fractions were tested on SDS-PAGE gel to detect protein expression (**Figure 3A**, **B**). Only protein p16 was expressed and clearly detected in whole lysates upon expression at 37 and 31°C (**Figure 3A**). In centrifuged lysates it was only detected upon expression at 25°C (**Figure 3B**). It is known that lower expression temperatures usually improve the solubility of overexpressed proteins in *E. coli* (Sahdev et al., 2008). This protein was also detected using Western blotting with anti-HIS antibodies in the whole lysate fraction (**Figure 4**). Protein p16 was observed to be migrating aberrantly at ~20 kDa as this protein has high proline residue content and disordered regions. This was also observed previously (Urakova et al., 2015). In addition, the presence or absence of a reducing agent in the loading buffer, sample boiling temperature and duration may contribute to the variation in observed molecular weight of p16 as this 137 amino acid-long protein contains 10 cysteine residues.

Proteins p23 and p29 were not detected. Most likely, these proteins are membrane-associated as they contain transmembrane helices according to *in silico* predictions (Smertina et al., 2021).
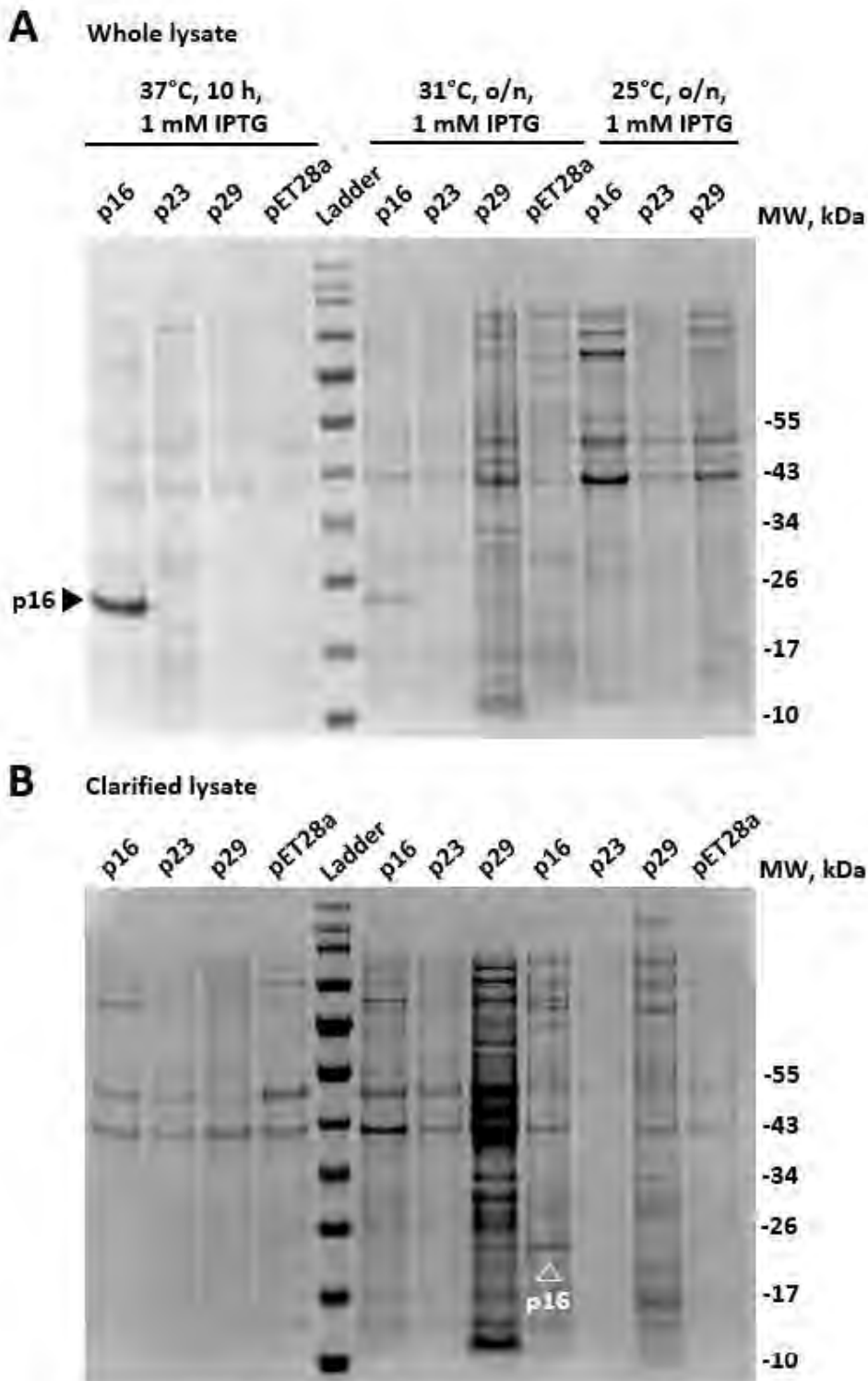

Figure 3. RHDV non-structural proteins expression (p16, p23, p29) in BL21(DE3) *E. coli* cells. (A) Whole lysates and **(B)** clarified lysates (soluble fraction) were analysed with SDS-PAGE and stained with Coomassie. Protein p16 is indicated by an arrow (black arrow in whole

lysate and white arrow in clarified lysate). MW, molecular weight in kilodaltons (kDa); o/n, overnight; h, hours.
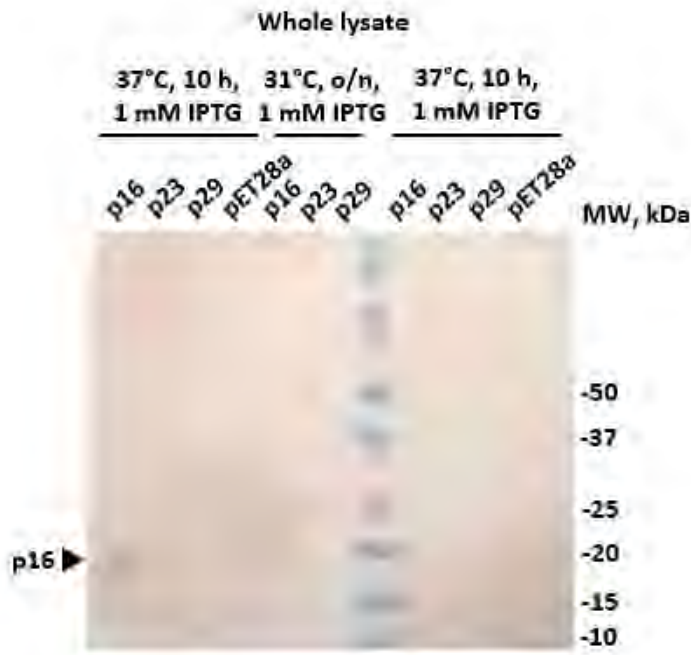

Figure 4. Western blot analysis of the whole cell BL21(DE3) lysates. A band between 15 and 20 kDa corresponding to protein p16 can be observed (indicated by a black arrow). MW, molecular weight in kilodaltons (kDa); o/n, overnight; h, hours.

Autoinduction

In the autoinduction method, lactose is used instead of IPTG for the induction of protein expression (Fox and Blommel, 2009), which, in some cases, results in higher protein yields. However, for proteins p16, p23 and p29, there was no difference in protein expression as compared to the IPTG induction (**Figure 5**). Protein p16 was detected in whole cell lysates and was best expressed at 37°C. Bands corresponding to proteins p23 and p29 were not detected, in accordance with my previous results; *E. coli* transformed with the empty pET28a vector was used as a negative control. Therefore, IPTG was used for subsequent inductions and protein p16 received more focus.
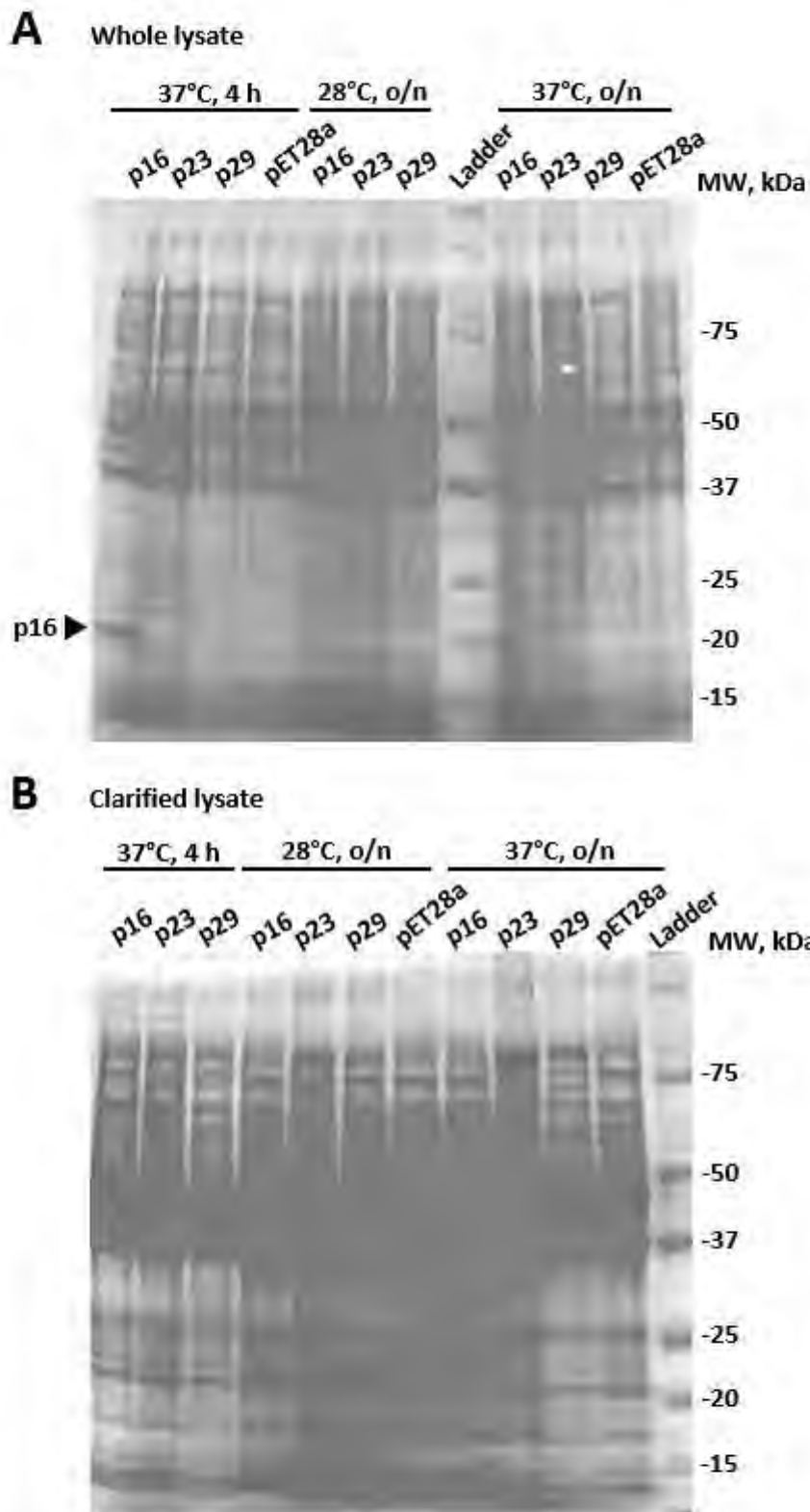
Figure 5. Autoinduction with lactose of p16, p23 and p29 expression. SDS-PAGE analysis of the whole cell lysates (BL21(DE3) *E. coli*). (**A**) Whole lysates and (**B**) clarified lysates (soluble fraction) were analysed with SDS-PAGE and stained with Coomassie. Protein p16 is indicated by a black arrow. MW, molecular weight; o/n, overnight; kDa, kilodaltons; h, hours.

Ni-NTA protein purification in a small volume

Ni-NTA affinity resin was used to purify the soluble p16 expressed using IPTG induction as described above. A small volume of culture (100 ml) was lysed as described in the materials and methods and applied onto Ni-NTA affinity resin. After the incubation, the resin was centrifuged, and the supernatant was analysed for p16 ('unbound' fraction). The resin was washed three times with the washing buffer and an aliquot from the last washing step was also analysed for p16 (last wash) (**Figure 6A**). Finally, the proteins bound to the resin were eluted with the elution buffer (eluate). All fractions were loaded onto SDS-PAGE to check for the presence of p16 (**Figure 6A, B**). Three different temperature conditions were used for protein expression (28, 32 and 37°C). A HIS-tagged purified protein (phosphoenolpyruvate carboxykinase (PEPCK)) was kindly provided by Dr Mihir Shah (CSIRO Land & Water) and used as a positive control for anti-HIS antibodies. Cells transformed with the vector pET28a were used as a negative control. Insoluble p16 was detected at all temperatures with the largest amount expressed at 37°C (**Figure 6A**). No p16 was detected in soluble (clarified) lysates and none was purified with the Ni-NTA affinity resin (**Figure 6B**). These results indicate at poor solubility of p16 in *E. coli* cells or inaccessibility of the HIS-tag. The abundance of cysteine residues in this protein may account for intramolecular disulfide bond(s) formation similar to what was observed with p23 (chapter 4). Such structures may 'mask' an epitope tag.

An unspecific band of ~25 kDa can be observed in Figure 6B. These are likely *E. coli* proteins that bind to Ni-NTA resin.
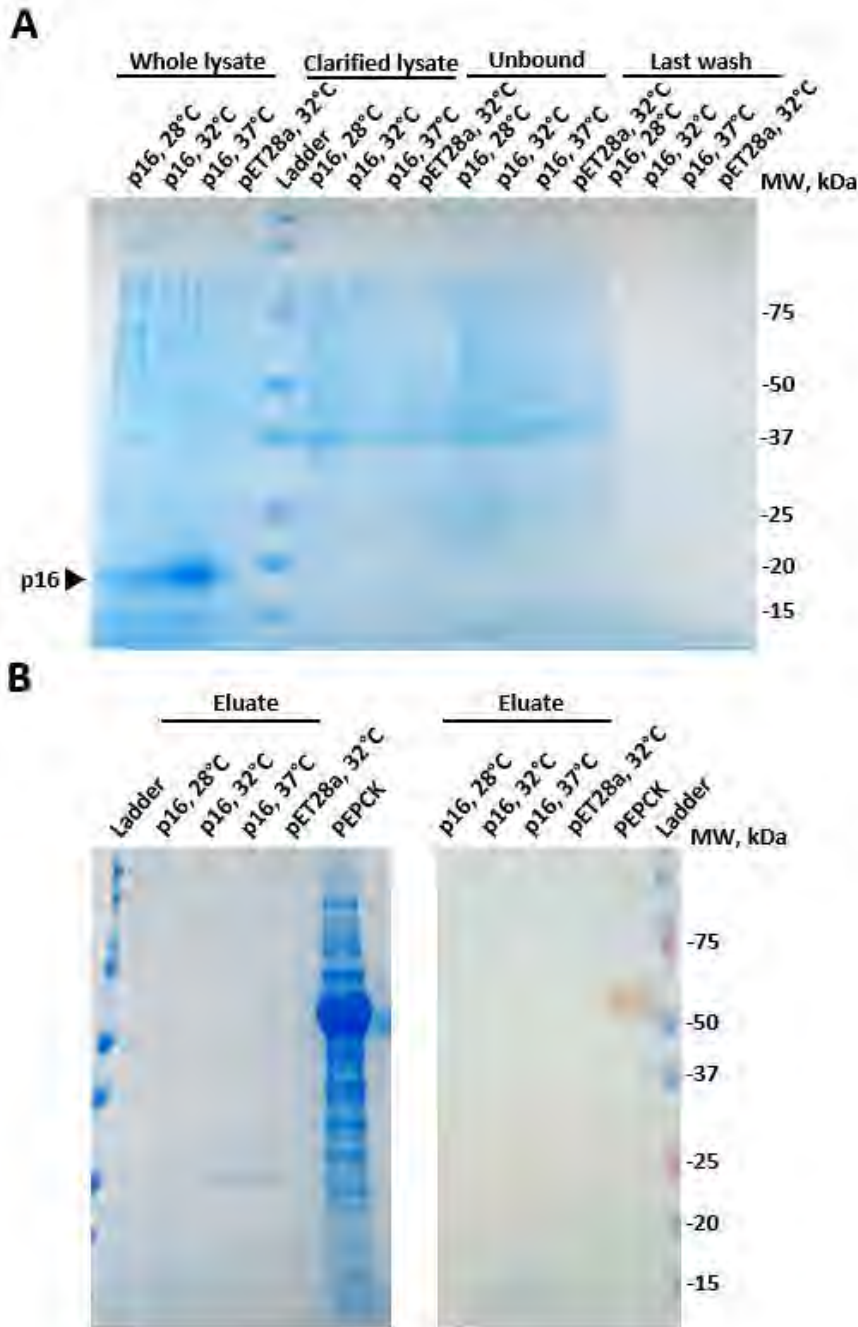
Figure 6. p16 protein expression and purification on Ni-NTA affinity resin. (**A**) p16 expression in BL21(DE3) *E. coli* cells was induced with IPTG at different temperatures; whole lysate and clarified lysate were analysed with SDS-PAGE. Empty vector pET28a was used as a negative control. Clarified lysates were applied onto Ni-NTA resin and fractions at different purification steps were analysed: unbound, last wash and (**B**) eluate. An unspecific band is present at ~25 kDa in Figure 6B (SDS-PAGE gel). A purified HIS-tagged protein (PEPCK) was used as a positive control. MW, molecular weight in kilodaltons (kDa).

Protein expression in mammalian cells (RK-13)

Transient expression of p16, p23 and p29

RK-13 cells were transfected with plasmids encoding RHDV non-structural proteins p16, p23 and p29 with an N-terminal FLAG-tag. The cells were lysed and the clarified lysates were subject to SDS-PAGE and Western blotting with rat anti-FLAG primary antibodies and goat anti-rat HRP-conjugated secondary antibodies (see materials and methods, **Table 1**). Only protein p23 was detected on Western blot (**Figure 7**). Two different conditions of protein transfer were tested for Western blotting. First, a conventional Towbin tris-glycine buffer (pH 8.3) was used to transfer the proteins from an SDS-PAGE gel to a nitrocellulose membrane. When proteins p16 and p29 were not detected (**Figure 7A**), I checked the isoelectric point (pI) for these proteins (**Figure 7C**). The pI value for p16 and p29 was above 8, whereas for the readily detected proteins p23, RdRp and GFP it was between 5.58 and 6.16. Proteins with high pI value require a higher pH to obtain the negative charge necessary for efficient transfer onto the positively charged nitrocellulose membrane. Therefore, I used N-cyclohexyl-3-aminopropanesulfonic acid (CAPS) buffer (pH 10.5). However, even in these conditions, proteins p16 and p29 were either not transferred or not expressed (**Figure 7B**).
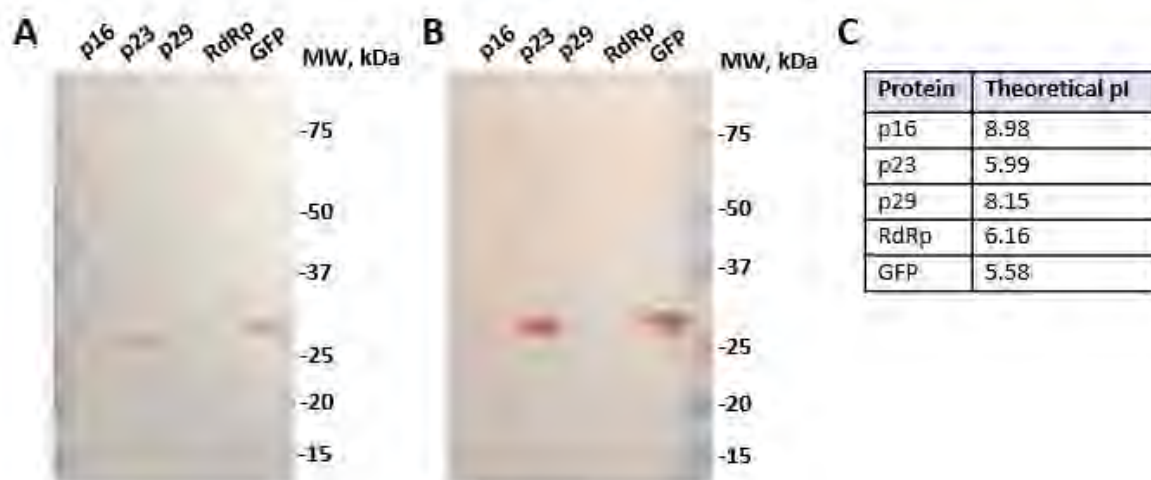
Figure 7. Western blot analysis of transfected RK-13 lysates. (**A**) Towbin (tris-glycine) buffer pH 8.3 was used for transfer of proteins from SDS-PAGE to nitrocellulose membrane; (**B**) CAPS pH 10.5 buffer was used for transfer; (**C**) isoelectric point for the analysed proteins. Proteins RdRp and GFP were used as positive controls. MW, molecular weight; kDa, kilodaltons; pI, isoelectric point.

Next, I used a different type of high-pH buffer, Dunn carbonate buffer (10 mM $NaHCO_3$ and 3 mM Na_2CO_3, pH 9.9) and analysed both the cell debris and supernatant after cell lysis.

With these conditions, p23 was clearly detected in both fractions but proteins p16 and p29 were not detected in either of the fractions (**Figure 8**). Moreover, RdRp that was used as a positive control was also not detected. High pH transfer buffer does not seem to be suitable for efficient transfer of this protein.
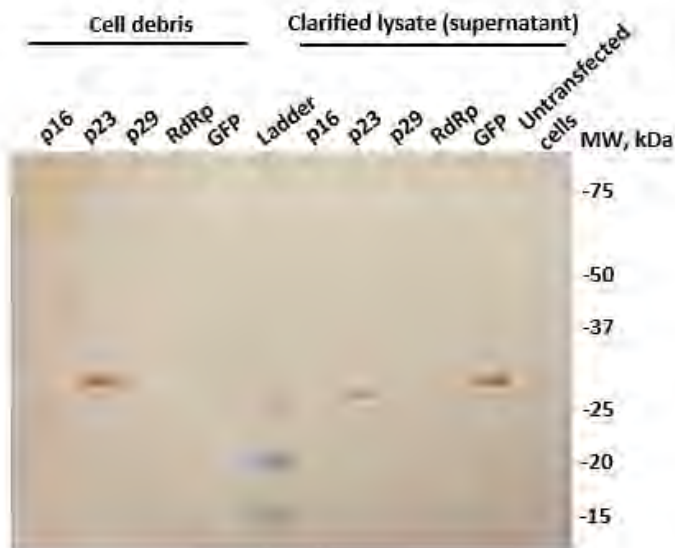

Figure 8. Western blot analysis of transfected RK-13 lysates (cell debris and supernatant). Dunn carbonate buffer pH 9.9 was used for protein transfer from SDS-PAGE gel to nitrocellulose membrane. Two fractions were analysed: cell debris after cell lysis and the supernatant. MW, molecular weight; kDa, kilodaltons.

TCA precipitation of cultured medium

I next checked the cell culture medium in case proteins p16 and/or p29 are secreted. Trichloroacetic acid (TCA) was used to precipitate proteins from culture medium that was collected from transfected cells (approximately 16 hours post transfection). Both RK-13 cells and Vero cells were analysed for protein secretion. Vero cells are interferon-deficient cells and therefore they were used in this experiment along with RK-13 cells, considering that interferon produced by RK-13 cells may inhibit the trafficking of viral proteins (Field et al., 1968). Heat shock protein 70 (Hsp70) was used as a loading control in this experiment, as Hsp70 was shown to be secreted (Mambula et al., 2007). However, none of the proteins p16, p23 or p29 was detected in cultured medium precipitates (**Figure 9**). Lysates of p23-transfected cells were used as a positive control for the detection of FLAG-tagged proteins and culture medium collected from untransfected cells was used as a negative control.

Overall, these results suggest that proteins p16 and p29 are either not expressed or expressed at very low levels, or quickly degraded making it extremely difficult to detect using Western blotting.
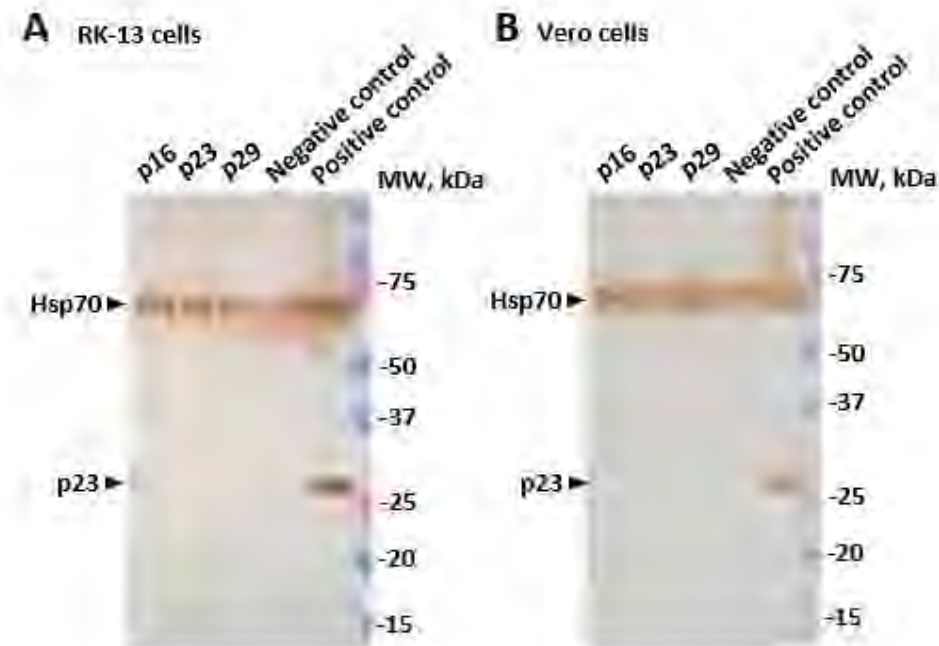

Figure 9. Western blot analysis of cell culture medium collected and precipitated from transfected cells. (**A**) Culture medium was collected from transfected RK-13 cells, precipitated with TCA and analysed with SDS-PAGE and Western blotting; (**B**) culture medium was collected from transfected Vero cells. Hsp70 was used as a loading control and cell lysate from RK-13 p23-transfected cells was used as a positive control for detection of FLAG-tagged proteins. MW, molecular weight; kDa, kilodaltons.

Expression of truncated protein p23 without transmembrane helices

Baker and co-authors successfully expressed in *E. coli* and purified a truncated variant of MNV NS1/2 that did not contain transmembrane helices; this protein variant was also expressed and detected in transfected mammalian cells (Baker et al., 2012). To test whether a similar truncation may enable the expression of p23, a p23 variant was generated that lacks 78 C-terminal amino acids (FLAG:p23 Δ146–224). RK-13 cells were transfected with this construct and Western blotting was used to detect the truncated p23 variant with anti-FLAG antibodies (**Figure 10**). The truncated p23 was not detected, suggesting that this protein variant without the transmembrane helices is not stable and may be rapidly degraded in cells. As showed previously (chapter 4; Smertina et al., 2022), p23 localises to the ER membranes and

interacts with heat shock proteins. Most likely, the transmembrane helices are necessary for this interaction and effective translocation of p23 to the ER.

Considering the instability of the truncated p23 in mammalian cells, I did not attempt to express this protein variant in *E. coli*.
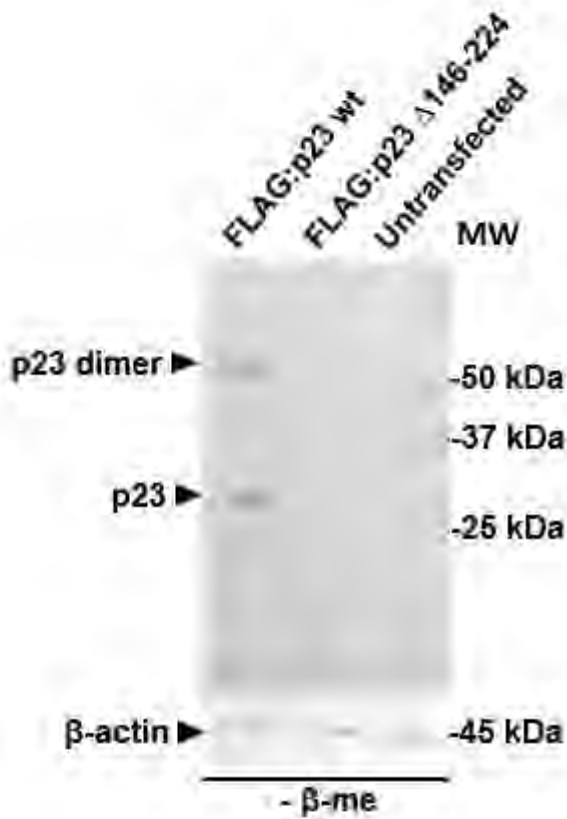
Figure 10. Western blot analysis of RK-13 cells transfected with a truncated p23 variant without transmembrane helices. Full length p23 (wild type, wt) was used as a positive control and untransfected cell lysate as a negative control. β-actin staining represents the loading control. MW, molecular weight; kDa, kilodaltons. Note that the samples were prepared in non-reducing conditions and therefore, p23 dimers are stable. For more details on p23 dimerisation, please see chapter 4.

Supplementary material

Verification of protein expression constructs with Sanger sequencing

Sanger sequencing was used to verify each construct before use. Here I present Sanger sequencing results for constructs used in this chapter that did not express any detectable proteins in mammalian cells and/or *E. coli*. The pCMV-Tag2C constructs were sequenced using T3 and T7 primers (**Supplementary Figure 1** and **Supplementary Figure 2**):

T3 forward primer: GCAATTAACCCTCACTAAAGG

T7 reverse primer: TAATACGACTCACTATAGGG

The pET28a constructs (**Supplementary Figure 3** and **Supplementary Figure 4**) were sequenced with the following primers:

Forward primer: AAAAAACCCCTCAAGACC

Reverse primer: TAATACGACTCACTATAGGGG

The resulting sequences were aligned to a reference (a respective *in silico* construct used for cloning design) with Geneious Prime 2021.1.1 (https://www.geneious.com) software using the default Geneious Alignment algorithm.

A RHDV p29 in pCMV-Tag2C (NCBI sequence ID: KF594476)

B 5'-end

C 3'-end
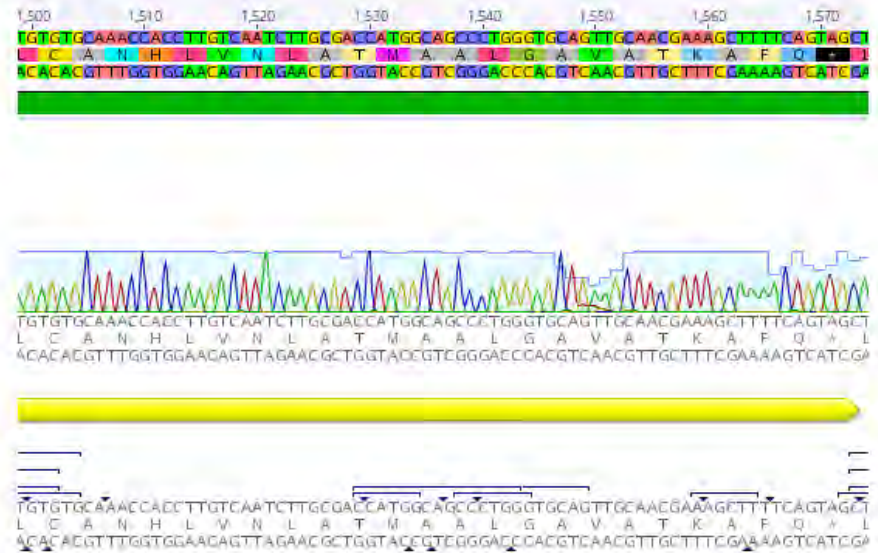
Supplementary Figure 1. Sequence alignment for RHDV p29 in pCMV-Tag2C. (**A**) Full sequence alignment of forward (T3) and reverse (T7) sequences to the reference sequence of RHDV p29 (NCBI ID KF594476); (**B**) enlarged 5'end area showing the FLAG-tag sequence and the beginning of the gene; (**C**) enlarged 3'-end area showing the stop codon at the end of the gene.

The sequence appears correct with only one synonymous nucleotide substitution in the third position of the codon:

A RHDV p16 in pCMVTag2C

Consensus
Identity

FWD 1. FLAG p16 plasmid
FWD 2. p161F-T3_C06_044.ab1
REV 3. p161R-T7_D06_042.ab1

p16

B 5'-end

Kozak seq...
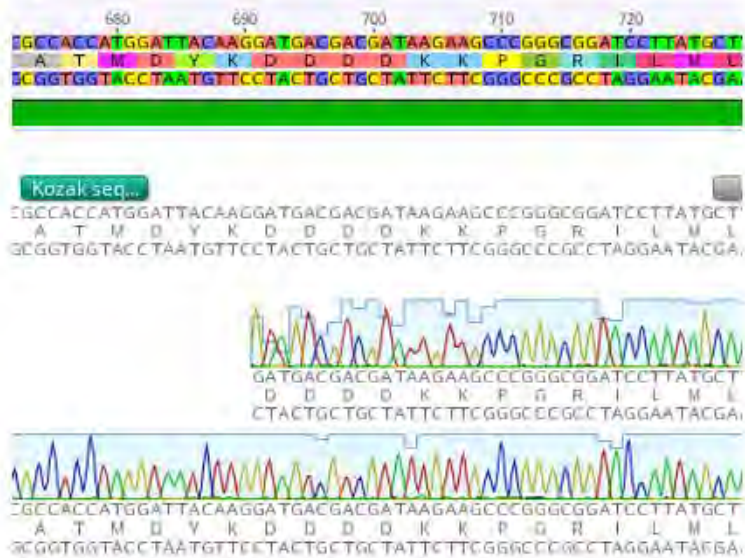
C 3'-end
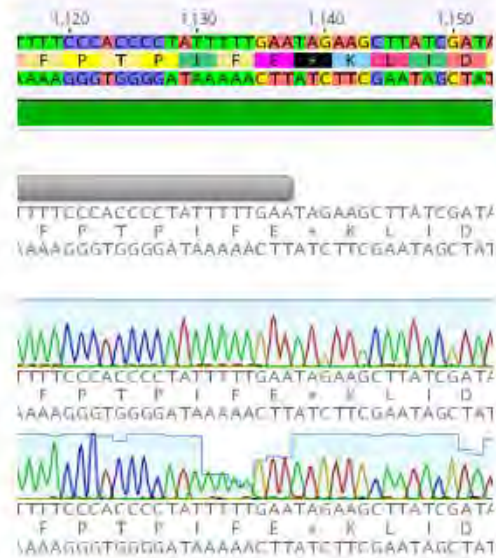
Supplementary Figure 2. Sequence alignment for RHDV p16 in pCMV-Tag2C. (**A**) Full sequence alignment of forward (T3) and reverse (T7) sequences to the reference sequence of RHDV p29 (NCBI ID KF594476); (**B**) enlarged 5'end area showing the FLAG-tag sequence and the beginning of the gene; (**C**) enlarged 3'-end area showing the stop codon at the end of the gene.

The sequence appears correct with only one non-synonymous nucleotide substitution that resulted in asparagine to lysine substitution:

A Codon-optimised RHDV p23 in pET28a
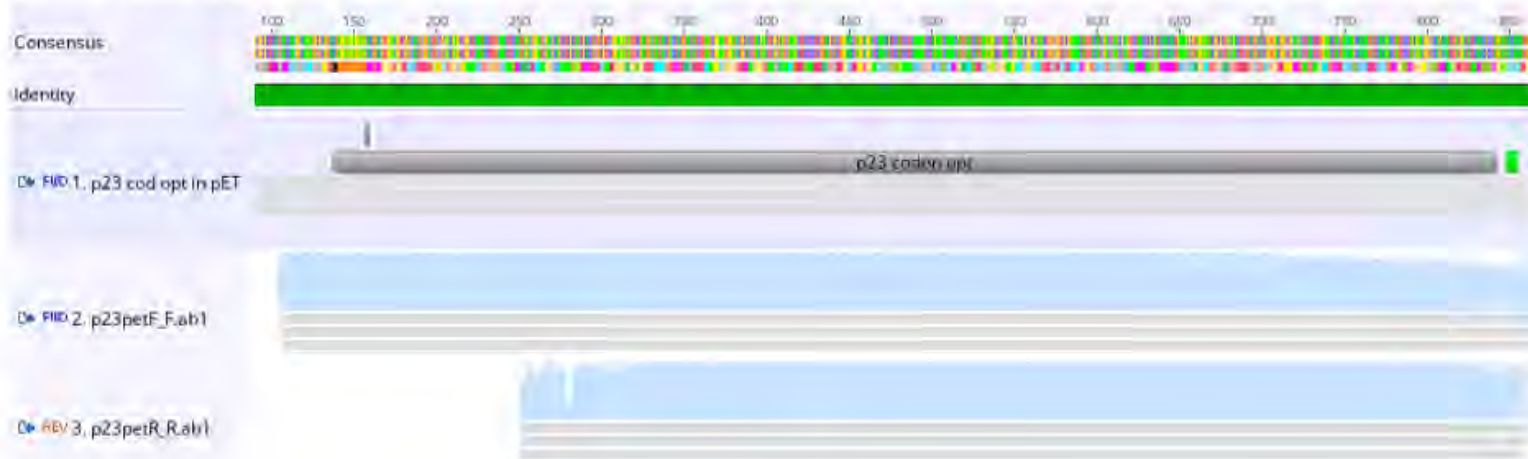
B 5'-end
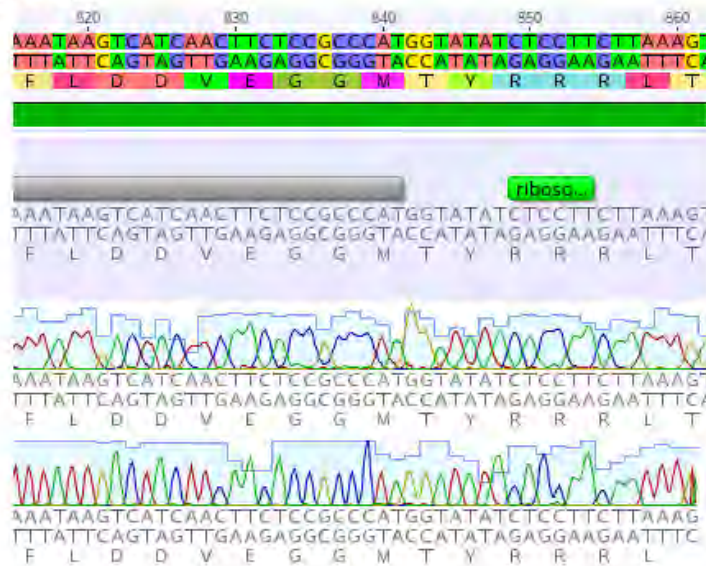
C 3'-end

Supplementary Figure 3. Sequence alignment for codon optimised RHDV p23 in pET28a.
(**A**) Full sequence alignment of forward and reverse sequences to the reference sequence of codon-optimised p23 cloned into pET28a; (**B**) enlarged 5'-end area showing the ribosome binding site and the beginning of the gene; (**C**) enlarged 3'-end area showing the 6xHIS-tag sequence and a stop codon.

The sequence appears correct with no mutations.

A Codon-optimised RHDV p29 in pET28a

B 5'-end

C 3'-end

183

Supplementary Figure 4. Sequence alignment for codon optimised RHDV p29 in pET28a.
(**A**) Full sequence alignment of forward and reverse sequences to the reference sequence of codon-optimised p29 cloned into pET28a; (**B**) enlarged 5'-end area showing the ribosome binding site and the beginning of the gene; (**C**) enlarged 3'-end area showing the 6HIS-tag sequence and a stop codon.

The sequence appears correct with no mutations.

Discussion

I generated constructs to express C-terminally HIS-tagged versions of the RHDV non-structural proteins p16, p23 and p29 in *E. coli*. I was able to find suitable expression conditions only for one protein, p16. However, a very small proportion of p16 was detected in a soluble form, but none was purified using Ni-NTA affinity resin. Further attempts to improve p16 solubility could be attempted in the future, e.g., by inserting a small ubiquitin-like modifier (SUMO) tag that is known to improve protein solubility (Butt et al., 2005). The observed migration pattern of p16 is typical for a protein with disordered regions and high content of proline residues (Baker et al., 2012). The HIS-tagged variant migrated at a molecular weight of around 20 kDa, a similarly aberrant migration was observed previously (Urakova et al., 2015) Moreover, p16 has an unusually high content of cysteine residues (10 cysteine residues in 137 amino acid-long protein). It is possible that formation of multiple intramolecular disulfide bonds upon cell lysis 'masks' an epitope tag hindering protein purification. This could be addressed using a highly reducing lysis buffer in future experiments.

Expression of p23 and p29 in *E. coli* was not detected upon induction of protein expression with either IPTG or lactose. This did not come as a complete surprise as both proteins are predicted to contain transmembrane helices (Smertina et al., 2021) and are therefore likely to be poorly soluble, interact with membranes and/or form inclusion bodies. Moreover, the disulfide bond formation that was shown to be essential for p23 dimerisation (Smertina et al., 2022) may not occur in the cytoplasm of bacteria, leading to incorrect protein folding and protein instability (reviewed in Francis et al., 2010). In addition, a C-terminal tag might not be suitable for p23 expression, as it can be buried in membranes along with the C-terminal transmembrane helices. Therefore, I suggest the following for future protein expression optimisation: (i) a truncation of one of the transmembrane helices, which could potentially improve the solubility of p23 while retaining protein stability; (ii) the use of Origami (DE3)pLysS *E. coli* as these cells facilitate proper disulfide bond formation that may be necessary for the correct folding of both p23 and p29; (iii) the use of a N-terminal instead of a C-terminal epitope tag.

A successful p23 expression in *E. coli* will allow to expand our knowledge on viroporin properties of this protein (introduced in chapter 4). The ability of a recombinant protein to form functional membrane channels can be assessed using *E. coli* strains that produce lysozyme. If a candidate channel protein is expressed and channels are formed in the bacterial plasma membrane, lysozyme leaks through the channels into the periplasmic space and lyses the cell wall, leading to cell death. This effect can be quantified by measuring the optical density of

cultured cells and is usually detected as a dramatic decrease in optical density. This assay was previously used to characterise viroporins from various virus families (e.g., Browne et al., 2000; Lama and Carrasco, 1992; Strtak et al., 2019). The 'classic' viroporin assay can be attempted once p23 protein expression is achieved.

In this work, I encountered problems trying to detect the RHDV non-structural proteins p16 and p29 after a transient expression in RK-13 cells although various Western blotting conditions were used to optimise the detection. These proteins are highly basic, with pI values higher than 8. Therefore, I tried high pH buffers for protein transfer from SDS-PAGE to a nitrocellulose membrane. This did not lead to a successful detection. As described in chapter 3, protein p29 has a transmembrane helix, and thus I sought to check whether it is associated with membranes in mammalian cells. Transfected RK-13 cells were lysed, and both the pellet and supernatant were analysed by Western blotting for the expression of p16, p23 and p29. Proteins p16 and p29 were not detected in this experiment in either of the fractions, whereas p23 was detected in both fractions, suggesting that some p23 proteins accumulate in the cytoplasm and others are associated with membranes. Interestingly, the positional homolog of p23 in *Tulane virus*, viroporin protein NS1/2, was not detected in the clarified supernatants, but only in the insoluble membrane fractions (Strtak et al., 2019).

Another possible explanation to the unsuccessful detection of proteins p16 and p29 may be that they are degraded upon overexpression in transfected cells. This hypothesis can be tested using a proteasome inhibitor. In addition, the proteins could be expressed using a cell-free rabbit reticulocyte lysate system. However, it is worth noting that both proteins were successfully detected in transiently transfected cells using immunofluorescence (Urakova et al., 2015), which can be explained by the significantly higher sensitivity of this technique compared to Western blotting.

The next step was motivated by the behaviour of the positional homolog of p16 in human and murine noroviruses (protein NS1) that was shown to be secreted and detectable in the cultured medium after transfection (Lee et al., 2019). Lee and co-authors precipitated proteins from the cultured medium with TCA and NS1 was detected using Western blotting (Lee et al., 2019), however, a possibility exists that some cells underwent lysis during the experiment, and this resulted in some NS1 protein being released into cell culture medium. In my experiment, neither p16, p23 nor p29 were detected in the cultured medium. These results indicate that p23 is not a secreted protein and that recombinant versions of p16 and p29 are likely not stable in mammalian cells or expressed at very low levels.

The results described in this chapter largely explain why most of my work was focused on p23, because p16 and p29 were not detected by me in transfected cells. In contrast, p23 was readily expressed in mammalian cells, which allowed me to study its interaction partners, cellular localisation and the mechanism of oligomerisation (Smertina et al., 2022).

References

Baker, E. S., Luckner, S. R., Krause, K. L., Lambden, P. R., Clarke, I. N., and Ward, V. K. (2012). Inherent structural disorder and dimerisation of murine norovirus ns1-2 protein. *PLoS One* 7. doi:10.1371/journal.pone.0030534.

Butt, T. R., Edavettal, S. C., Hall, J. P., & Mattern, M. R. (2005). SUMO fusion technology for difficult-to-express proteins. *Protein Expression and Purification*, 43(1), 1–9. https://doi.org/10.1016/j.pep.2005.03.016.

Browne, E. P., Bellamy, A. R., and Taylor, J. A. (2000). Membrane-destabilizing activity of rotavirus NSP4 is mediated by a membrane-proximal amphipathic domain. *J. Gen. Virol.* 81, 1955–1959. doi:10.1099/0022-1317-81-8-1955.

Field, A. K., Tytell, A. A., Lampson, G. P., and Hilleman, M. R. (1968). Inducers of interferon and host resistance, V. In vitro studies. *Proc. Natl. Acad. Sci. U. S. A.* 61, 340–346. doi:10.1073/pnas.61.1.340.

Fox, B. G., and Blommel, P. G. (2009). Autoinduction of protein expression. *Curr. Protoc. Protein Sci.*, 1–18. doi:10.1002/0471140864.ps0523s56.

Francis, D. M., and Page, R. (2010). Strategies to optimize protein expression in E. coli. *Curr. Protoc. Protein Sci.*, 1–29. doi:10.1002/0471140864.ps0524s61.

Lama, J., and Carrasco, L. (1992). Expression of poliovirus nonstructural proteins in Escherichia coli cells: Modification of membrane permeability induced by 2B and 3A. *J. Biol. Chem.* 267, 15932–15937. doi:10.1016/s0021-9258(19)49623-3.

Lee, S., Liu, H., Wilen, C. B., Sychev, Z. E., Desai, C., Hykes, B. L., et al. (2019). A Secreted viral nonstructural protein determines intestinal norovirus pathogenesis. *Cell Host Microbe* 25, 845–857.e5. doi:10.1016/j.chom.2019.04.005.

Lissemore, J. L., Bayes, J., Calvey, M., Reineke, L., Colagiavanni, A., Tscheiner, M., et al. (2009). Green fluorescent protein is superior to blue fluorescent protein as a quantitative reporter of promoter activity in E. coli. *Mol. Biol. Rep.* 36, 1107–1112. doi:10.1007/s11033-008-9285-5.

Mambula, S. S., Stevenson, M. A., Ogawa, K., and Calderwood, S. K. (2007). Mechanisms for Hsp70 secretion: crossing membranes without a leader. *Methods* 43, 168–175. doi:10.1016/j.ymeth.2007.06.009.

Nugent, T., and Jones, D. T. (2010). Predicting transmembrane helix packing arrangements using residue contacts and a force-directed algorithm. *PLoS Comput. Biol.* 6. doi:10.1371/journal.pcbi.1000714.

Nugent, T., and Jones, D. T. (2012). Detecting pore-lining regions in transmembrane protein

sequences. *BMC Bioinformatics* 13. doi:10.1186/1471-2105-13-169.

Oscar, T. P., Dulal, K., and Boucaud, D. (2006). Transformation of *Escherichia coli* K-12 with a high-copy plasmid encoding the green fluorescent protein reduces growth: Implications for predictive microbiology. *J. Food Prot.* 69, 276–281. doi:10.4315/0362-028X-69.2.276.

Peñaflor-Tellez, Y., Chavez-Munguia, B., Lagunes-Guillen, A., Salazar-Villatoro, L., and Gutierrez-Escolano, A.-L. (2022). The feline calicivirus leader of the capsid protein has the functional characteristics of a viroporin. *Viruses* 14. doi:https://doi.org/10.3390/v14030635.

Sahdev, S., Khattar, S. K., and Saini, K. S. (2008). Production of active eukaryotic proteins through bacterial expression systems: A review of the existing biotechnology strategies. *Mol. Cell. Biochem.* 307, 249–264. doi:10.1007/s11010-007-9603-6.

Smertina, E., Hall, R. N., Urakova, N., Strive, T., and Frese, M. (2021). Calicivirus non-structural proteins: potential functions in replication and host cell manipulation. *Front. Microbiol.* 12. doi:10.3389/fmicb.2021.712710.

Strtak, A. C., Perry, J. L., Sharp, M. N., Chang-Graham, A. L., Farkas, T., and Hyser, J. M. (2019). Recovirus NS1-2 has viroporin activity that induces aberrant cellular calcium signaling to facilitate virus replication. *mSphere* 4, 1–21. doi:10.1128/msphere.00506-19.

Studier, F. W., and Moffatt, B. A. (1986). Use of bacteriophage T7 RNA polymerase to direct selective high-level expression of cloned genes. *J. Mol. Biol.* 189, 113–130. doi:10.1016/0022-2836(86)90385-2.

Urakova, N., Frese, M., Hall, R. N., Liu, J., Matthaei, M., and Strive, T. (2015). Expression and partial characterisation of rabbit haemorrhagic disease virus non-structural proteins. *Virology* 484, 69–79. doi:10.1016/j.virol.2015.05.004.

Wickham, H. (2016). ggplot2: elegant graphics for data analysis. Available at: https://ggplot2.tidyverse.org.

Xie, H., Vucetic, S., Iakoucheva, L. M., Oldfield, C. J., Dunker, A. K., Uversky, V. N., et al. (2007). Functional anthology of intrinsic disorder. 1. Biological processes and functions of proteins with long disordered regions. *J. Proteome Res.* 6, 1882–1898. doi:10.1021/pr060392u.

Xue, B., Dunbrack, R. L., Williams, R. W., Dunker, A. K., and Uversky, V. N. (2010). PONDR-FIT: a meta-predictor of intrinsically disordered amino acids. 1804, 996–1010. doi:10.1016/j.bbapap.2010.01.011.PONDR-FIT.

General discussion

This work was aimed at the characterisation and identification of virulence factors in lagoviruses. Lagoviruses, such as RHDV, are understudied because they do not grow in a conventional cell culture. By contrast, MNV (genus *Norovirus*) readily infects cultured cells, in this case murine macrophage-derived cell lines. This has made MNV a popular model to study human noroviruses that also do not easily propagate in a conventional cell culture. Furthermore, FCV (genus *Vesivirus*) infects Crandell-Rees feline kidney (CRFK) cells and *Tulane virus* (genus *Recovirus*) can be grown in rhesus monkey kidney epithelial cells (LLC-MK2). Therefore, all these viruses received more attention and were studied in more detail compared to lagoviruses. Recent advances towards human intestinal organoid cultures allowed researchers to cultivate human noroviruses *ex vivo* (Estes et al., 2019). Steps are now being taken towards the development of similar organoid culture systems for lagoviruses. We published our results on the rabbit intestinal organoids (Kardia et al., 2021). These organoids were developed to study enterotropic rabbit caliciviruses but were not susceptible to RCV infection (Kardia et al., 2021). Recently, hepatobiliary organoids were established in our laboratory to study hepatotropic caliciviruses (Kardia et al., 2022, *preprint*). Although a first set of experiments showed encouraging results, more work is required to optimise and characterise this new cell culture system for RHDV and potentially other lagoviruses. However, the inability to reliably infect cultured cells with RHDV at the commencement of this project defined the choice of methodological approaches used in this work. Therefore, in this work, I mostly used transient expression of recombinant proteins, where cultured cells were transfected with a viral protein of interest and the effects of its expression were studied. For example, cellular localisation, interactions with other proteins, mechanisms of oligomerisation were identified.

Earlier characterisation of candidate virulence factors in RHDV started with the transient expression of non-structural proteins in RK-13 cells. The RdRp was observed to disaggregate the Golgi apparatus (Urakova et al., 2015), therefore this protein may have multiple functions and is a virulence factor candidate. The rearrangement of Golgi membranes may be indicative of a lagovirus interference with cellular trafficking, which is a common strategy to impair host immune responses in other viruses. For example, poliovirus infections also result in Golgi fragmentation, which inhibits cellular protein secretion, e.g., the secretion of type I interferons (IFNs) and the presentation of antigens by MHC class I molecules on cellular surface (Beske et al., 2007; Deitz et al., 2000). In this work, using quantitative

proteomics, I identified BRO1 domain-containing protein as a cellular interactor of RHDV RdRp (chapter 4; Smertina et al., 2022). BRO1 domain-containing proteins, e.g., the cellular protein Alix, are known to be involved in membrane trafficking and cytoskeletal remodeling (Odorizzi et al., 2011). Moreover, protein C of *Sendai virus* (family *Paramyxoviridae*) interacts with Alix, and this interaction is necessary for efficient virus budding (Sakaguchi et al., 2005). Protein C is a virulence factor that counteracts host cell IFN type I signaling (Didcock et al., 1999). Perhaps, this is also true for RHDV RdRp and its interaction with Alix inhibits IFN signaling, contributing to the high speed with which RHDV infection progresses. However, more research is needed to confirm this suggestion. For example, once a suitable cell culture system is established, Alix can be knocked down its effects on virus infection and replication can be assessed.

RdRps are highly conserved proteins that share a similar structure and show a high level of sequence similarity across RNA viruses. These proteins contain short, highly conserved functional motifs which participate in the viral replication process (reviewed in Deval et al., 2017). In chapter 2, I describe a novel motif termed 'motif I' that was identified using a sequence alignment for RdRp sequences from representative members of the families *Caliciviridae*, *Picornaviridae* and the order *Picornavirales* (Smertina et al., 2019). The order *Picornavirales* includes RNA viruses with a very diverse host range, from plants to insects and vertebrates; the fact that motif I is conserved among so many viruses suggests that it has an important role. Amino acid substitutions in the newly identified motif of the *Foot-and-mouth disease virus* (FMDV, family *Picornaviridae*) RdRp were either lethal for the virus or affected the RdRp fidelity (Xie et al., 2014; Zeng et al., 2014). My work on the RHDV RdRp will facilitate further research into the mechanism of the Golgi rearrangement and the function of the newly described motif I.

Apart from the RdRp, other virulence factor candidates for RHDV are proteins p16 (NS1), p23 (NS2) and p29 (NS3). Similar to lagoviruses, human noroviruses did not grow in cultured cells until recently and many aspects of their life cycle were inferred from studying the closely related *Murine norovirus* and using recombinant protein techniques (Hosmillo et al., 2019; McCune et al., 2017). For example, the cleavage product of protein NS1/2, protein NS1, counteracts innate immune responses (Lee et al., 2019). Furthermore, both NS1/2 and NS4 disrupt the Golgi and inhibit cellular protein secretion (Ettayebi and Hardy, 2003; Sharp et al., 2010). Recently, the NS1/2 protein of another calicivirus, *Tulane virus* (genus *Recovirus*), a virus that grows in cell culture, was described to have a viroporin activity. In the same work, Strtak and co-authors also showed that NS1/2 of human and murine noroviruses have viroporin

activity. Viroporins are proteins that form ion channels in cellular membranes upon oligomerisation (reviewed in Nieva et al., 2012). This finding prompted me to focus more closely on p23, a positional homolog of NS2, that was previously shown to dimerise and localise with ER membranes in transfected cells (Urakova et al., 2015). To study this protein in more detail and check whether it also possesses viroporin activity, I identified its cellular interactors using a quantitative proteomics approach. Heat shock proteins were found to interact with p23 (chapter 4; Smertina et al., 2022). It is likely that p23 requires assistance in reaching the ER membranes as it does not contain a signal sequence. Many other viroporins also do not encode a signal sequence and are stabilised and guided by cellular chaperones post-translationally (reviewed in Martinez-Gil and Mingarro, 2015). It would be worthwhile to investigate the role of Hsp70 and/or Hsp110 in the RHDV life cycle once a robust culture system becomes available. For example, one could create a knockout cell line (RHDV-permissible) that no longer expresses these chaperones and then the replication efficiency can be assessed. It is worth noting that heat shock proteins are common contaminants in such proteomics experiments due to their high abundance and overexpression in transfected cells (Trinkle-Mulcahy et al., 2008). For this reason, a quantitative proteomics approach was utilised: in this experiment, the interactors of the protein of the interest (p23) were quantitatively compared to the interactors of GFP, a protein of a similar size that served as an internal control. Moreover, to confirm that heat shock proteins do not non-specifically interact with any viral proteins in transfected cells, the same experiment was performed for another viral protein, the RdRp. An interaction with heat shock proteins was not observed in this case.

To form functional channels, all viroporins identified to date oligomerise. Interestingly, RHDV p23 has previously been shown to form dimers (Urakova et al., 2015). In this work, I confirmed the dimerisation and also detected putative higher order oligomers (trimers and tetramers), demonstrating that oligomers can only be formed in non-reducing conditions (chapter 4; Smertina et al., 2022). This discovery prompted me to a hypothesis that p23 oligomers are likely stabilised by a disulfide bond. To address this hypothesis, I individually substituted each of the three cysteines in p23 with a serine. When expressed in transfected cells and analysed by Western blotting, only one variant did not form detectable oligomers, namely, C41S. Therefore, a disulfide bond formed between two cysteine residues at the position 41 is essential for p23 oligomerisation. However, the mechanism underlying the formation of higher order oligomers remains unclear, as this bond can be formed between two molecules only. To check whether there are other interactions that are weaker than a covalent disulfide bond, I prepared the samples without boiling and in non-reducing conditions. Even in these conditions,

the C41S p23 variant was not able to oligomerise. It is likely that higher order oligomers can only be formed between dimers, e.g., between two dimers resulting in a tetramer. However, a weak band indicative of putative trimeric and tetrameric forms was also observed. This type of oligomers could be stabilised by lipid mimetic SDS in the running buffer as described previously for other viroporins (Hyser et al., 2010), which would make it an artefact. Cross-linking can be attempted in the future to detect stronger oligomer bands if they are formed. Moreover, structural studies such as x-ray crystallography or NMR spectroscopy are warranted to reveal the 3D structure of the channel formed by p23. chapter 5 describes the proceedings towards expression of recombinant HIS-tagged variants p23 in *E. coli*; although my attempts were unsuccessful, these results will assist future attempts to express and purify this protein. In my experiments, a C-terminal tag was used, perhaps it would be beneficial to attempt expression with a N-terminal tag, to prevent potential 'burying' of the tag into the membranes with p23 transmembrane helices and hence inaccessibility of the tag for detection. Moreover, the bacterial cytoplasm is highly reducing, which may prevent the correct folding of p23 and reduce protein stability.

To check whether p23-formed channels conduct Ca^{2+}, I used a flow cytometry-based Ca^{2+} concentration measurement in transfected RK-13 cells with a fluorescent cell-permeable Ca^{2+} sensor. This method presents a few limitations: (i) the cells were transiently transfected with p23 and Ca^{2+} measurement was undertaken after overnight incubation of cells, which does not result in accurate monitoring of Ca^{2+} over time upon p23 expression; (ii) the efficiency of transient transfection is never 100% and therefore the detected signal is likely to be 'diluted' by the presence of untransfected cells. However, a slight increase in Ca^{2+} concentration was observed, and further studies are necessary to confirm that p23 forms Ca^{2+}-conducting ion channels and/or also conducts other ions.

The presence of a viroporin in lagoviruses may explain the high speed with which the rabbit haemorrhagic disease progresses. Viroporins are known for penetration of host plasma membrane which may contribute to fast spread of the virus (reviewed in Xia et al., 2022). Moreover, in hepatitis C virus infection, the viroporin p7 has been observed to play a key role in liver pathogenesis and the development of hepatitis (Farag et al., 2016).

The other two RHDV proteins that might be virulence factors, namely p16 and p29, were previously shown to localise to the cytoplasm using immunofluorescence (Urakova et al., 2015). In chapter 5, I describe my efforts to detect these two proteins in transfected RK-13 cells using Western blotting. These proteins have a high pI value, meaning that in order to transfer these proteins from an SDS-PAGE gel onto a nitrocellulose membrane, higher pH buffer might

be required. Various buffers with pH ranging from 8.5 to 10.5 were used. I also tried to detect these proteins in culture medium in case they are secreted, and in the cellular debris fraction. However, these attempts were not successful and ultimately, I could not detect these proteins by Western blotting. Therefore, I could not use these proteins in SILAC immunoprecipitation assays as I cannot confirm the presence of the transfected (bait) proteins. This was one of the reasons why protein p23 received much more attention in my work. It is possible that these proteins are rapidly degraded in transfected cells and Western blotting does not allow detection, as these proteins were previously detected in transiently transfected cells using immunofluorescence (Urakova et al., 2015).

Despite the inability to detect these proteins in mammalian cells, I also tried to express these proteins in *E. coli* along with p23. Surprisingly, p16 was the only protein detectable in *E. coli* lysates after the induction of protein expression. A large fraction of this protein appeared in insoluble (whole lysate) fraction; however, some of it was also observed in clarified (soluble) lysate. Therefore, in my work, I established a protocol for the expression of p16 in *E. coli*. This protocol can be further optimised to increase the amount of soluble p16, e.g., by introducing a SUMO tag.

To summarise, this thesis provides the information on a novel motif in calicivirus RdRps that is likely to be responsible for the enzyme fidelity; describes a viroporin function for the lagovirus protein p23 and the mechanism of its dimerisation; and provides a protocol for RHDV p16 expression in *E. coli*.

Future directions summary

To improve our understanding of the RdRp I motif in lagovirus replication, a suitable cell culture system is warranted. With such a tool, changes can be introduced to the motif and the effects on virus replication can be measured. In addition, *in vitro* assays could be utilised to assess the speed and fidelity of the enzyme. This could be tested for different members of the *Caliciviridae* family to investigate whether these features are conserved across the family.

A number of further viroporin characterisations require a successful expression of protein p23 in *E. coli*. Once this protein is expressed and detected, the classic viroporin assay can be used to check whether this protein permeabilises *E. coli* membranes similar to other viroporins (Browne et al., 2000). Moreover, it must be confirmed which ions the formed channels conduct. Ca^{2+} concentration measurements are best assessed using genetically encoded Ca^{2+} sensors that exhibit fluorescence in response to changes in Ca^{2+} concentrations,

e.g., GCaMP6s (reviewed in Hyser et al., 2015; Perry et al., 2015). In this experiment, changes to fluorescence can be observed in live cells over time using fluorescent microscopy.

Regarding recombinant protein expression in *E. coli*, an approach similar to that used by Baker and co-authors could be attempted. Baker et al. successfully expressed and purified the non-structural protein NS1/2 of murine norovirus by using a chitin binding fusion partner (Baker et al., 2012).

For p16 and p29 expression in mammalian cells, a proteasome inhibitor treatment can be attempted to check whether this helps to stabilise these rapidly degraded proteins. In addition, expression of this proteins in rabbit reticulocyte lysates can be trialed.

References (introduction and general discussion)

Abrantes, J., Droillard, C., Lopes, A. M., Lemaitre, E., Lucas, P., Blanchard, Y., et al. (2020). Recombination at the emergence of the pathogenic rabbit haemorrhagic disease virus Lagovirus europaeus/GI.2. *Sci. Rep.* 10, 1–11. doi:10.1038/s41598-020-71303-4.

Abrantes, J., Van Der Loo, W., Le Pendu, J., and Esteves, P. J. (2012). Rabbit haemorrhagic disease (RHD) and rabbit haemorrhagic disease virus (RHDV): a review. *Vet. Res.* 43. doi:10.1186/1297-9716-43-12.

Alexa, A., and Rahnenfuhrer, J. (2020). topGO: enrichment analysis for gene ontology.

Angulo, E., and Cooke, B. (2002). First synthesize new viruses then regulate their release? The case of the wild rabbit. *Mol. Ecol.* 11, 2703–2709. doi:10.1046/j.1365-294X.2002.01635.x.

Bailey, D., Kaiser, W. J., Hollinshead, M., Moffat, K., Chaudhry, Y., Wileman, T., et al. (2010). Feline calicivirus p32, p39 and p30 proteins localize to the endoplasmic reticulum to initiate replication complex formation. *J. Gen. Virol.* 91, 739–749. doi:10.1099/vir.0.016279-0.

Beske, O., Reichelt, M., Taylor, M. P., Kirkegaard, K., and Andino, R. (2007). Poliovirus infection blocks ERGIC-to-Golgi trafficking and induces microtubule-dependent disruption of the Golgi complex. *J. Cell Sci.* 120, 3207–3218. doi:10.1242/jcs.03483.

Boga, J., Marín, M. S., Casais, R., Prieto, M., and Parra, F. (1992). In vitro translation of a subgenomic mRNA from purified virions of the Spanish field isolate AST/89 of Rabbit Hemorrhagic Disease Virus (RHDV). *Virus Res.* 26, 33–40. doi:10.1016/0168-1702(92)90144-X.

Buchan, D. W. A., and Jones, D. T. (2019). The PSIPRED protein analysis workbench: 20 years on. *Nucleic Acids Res.* 47, W402–W407. doi:10.1093/nar/gkz297.

Conley, M. J., McElwee, M., Azmi, L., Gabrielsen, M., Byron, O., Goodfellow, I. G., et al. (2019). Calicivirus VP2 forms a portal-like assembly following receptor engagement. *Nature*, 1. doi:10.1038/s41586-018-0852-1.

Cooke, B. D., and Fenner, F. (2002). Rabbit haemorrhagic disease and the biological control of wild rabbits, *Oryctolagus cuniculus*, in Australia and New Zealand. *Wildl. Res.* 29, 689–706. doi:10.1071/WR02010.

Crooks, G. E., Hon, G., Chandonia, J. M., and Brenner, S. E. (2004). WebLogo: A sequence logo generator. *Genome Res.* 14, 1188–1190. doi:10.1101/gr.849004.

Dalton, K. P., Nicieza, I., Balseiro, A., Muguerza, M. A., Rosell, J. M., Casais, R., et al. (2012). Variant rabbit hemorrhagic disease virus in young rabbits, Spain. *Emerg. Infect. Dis.* 18,

2009–2012. doi:10.3201/eid1812.120341.

Deitz, S. B., Dodd, D. A., Cooper, S., Parham, P., and Kirkegaard, K. (2000). MHC I-dependent antigen presentation is inhibited by poliovirus protein 3A. *Proc. Natl. Acad. Sci. U. S. A.* 97, 13790–13795. doi:10.1073/pnas.250483097.

Delibes-Mateos, M., Delibes, M., Ferreras, P., and Villafuerte, R. (2008). Key role of European rabbits in the conservation of the western Mediterranean Basin hotspot. *Conserv. Biol.* 22, 1106–1117. doi:10.1111/j.1523-1739.2008.00993.x.

Deval, J., Jin, Z., Chuang, Y. C., and Kao, C. C. (2017). Structure(s), function(s), and inhibition of the RNA-dependent RNA polymerase of noroviruses. *Virus Res.* 234, 21–33. doi:10.1016/j.virusres.2016.12.018.

Didcock, L., Young, D. F., Goodbourn, S., and Randall, R. E. (1999). Sendai virus and Simian virus 5 block activation of interferon-responsive genes: importance for virus pathogenesis. *J. Virol.* 73, 3125–3133. doi:10.1128/jvi.73.4.3125-3133.1999.

Ehresmann, D. W., and Schaffer, F. L. (1977). RNA synthesized in calicivirus infected cells is atypical of picornaviruses. *J. Virol.* 22, 572–576.

Eruera, A. R., McSweeney, A. M., McKenzie-Goldsmith, G. M., and Ward, V. K. (2021). Protein nucleotidylylation in +ssrna viruses. *Viruses* 13. doi:10.3390/v13081549.

Ettayebi, K., Crawford, S. E., Murakami, K., Broughman, J. R., Karandikar, U., Tenge, V. R., et al. (2016). Replication of human noroviruses in stem cell-derived human enteroids. *Science (80-.).* 353, 1387–1393. doi:10.1126/science.aaf5211.

Ettayebi, K., and Hardy, M. E. (2003). Norwalk virus nonstructural protein p48 forms a complex with the SNARE regulator VAP-A and prevents cell surface expression of vesicular stomatitis virus G protein. *J. Virol.* 77, 11790–7. doi:10.1128/JVI.77.21.11790.

Farag, N. S., Breitinger, U., El-Azizi, M., & Breitinger, H. G. (2017). The p7 viroporin of the hepatitis C virus contributes to liver inflammation by stimulating production of Interleukin-1β. *Biochimica et Biophysica Acta*, 1863(3), 712–720. https://doi.org/10.1016/j.bbadis.2016.12.006.

Fernandez-Vega, V., Sosnovtsev, S. V, Belliot, G., King, A. D., Mitra, T., Gorbalenya, A., et al. (2004). Norwalk virus N-terminal nonstructural protein is associated with disassembly of the Golgi complex in transfected cells. *J.Virol.* 78, 4827–4837. doi:10.1128/JVI.78.9.4827.

Goodfellow, I. (2011). The genome-linked protein VPg of vertebrate viruses - a multifaceted protein. *Curr. Opin. Virol.* 1, 355–362. doi:10.1016/j.coviro.2011.09.003.

Goodfellow, I., Chaudhry, Y., Gioldasi, I., Gerondopoulos, A., Natoni, A., Labrie, L., et al.

(2005). Calicivirus translation initiation requires an interaction between VPg and eIF4E. *EMBO Rep.* 6. doi:10.1038/sj.embor.7400510.

Hall, R. N., Mahar, J. E., Haboury, S., Stevens, V., Holmes, E. C., and Strive, T. (2015). Emerging Rabbit Hemorrhagic Disease Virus 2 (RHDVb), Australia. *Emerg. Infect. Dis.* 21, 2536–2543. doi:10.1056/NEJMoa0805715.

Hall, R. N., Peacock, D. E., Kovaliski, J., Mahar, J. E., Mourant, R., Piper, M., et al. (2017). Detection of RHDV2 in European brown hares (Lepus europaeus) in Australia. *Vet. Rec.* 180, 121. doi:10.1136/vr.104034.

He, J., Melnik, L. I., Komin, A., Wiedman, G., Fuselier, T., Morris, C. F., et al. (2017). Ebola virus delta peptide is a viroporin. *J. Virol.* 91, 1–14. doi:10.1128/jvi.00438-17.

Hosmillo, M., Lu, J., McAllaster, M. R., Eaglesham, J. B., Wang, X., Emmott, E., et al. (2019). Noroviruses subvert the core stress granule component G3BP1 to promote viral VPg-dependent translation. *Elife* 8, 1–35. doi:10.7554/eLife.46681.

Hyde, J. L., and Mackenzie, J. M. (2010). Subcellular localization of the MNV-1 ORF1 proteins and their potential roles in the formation of the MNV-1 replication complex. *Virology* 406, 138–148. doi:10.1016/j.virol.2010.06.047.

Jiang, X., Wang, M., Wang, K., and Estes, M. K. (1993). Sequence and genomic organization of Norwalk virus. *Virology* 195, 51–61. doi:10.1006/viro.1993.1345.

Jones, D. T., Taylor, W. R., and Thornton, J. M. (1992). The rapid generation of mutation data matrices. doi:doi.org/10.1093/bioinformatics/8.3.275.

Jones, M. K., Watanabe, M., Zhu, S., Graves, C. L., Keyes, L. R., Grau, K. R., et al. (2014). Enteric bacteria promote human and mouse norovirus infection of B cells. *Science (80-.).* 346, 755–759. doi:10.1126/science.1257147.

Kardia, E., Frese, M., Smertina, E., Strive, T., Zeng, X. L., and Estes, M. (2021). Culture and differentiation of rabbit intestinal organoids and organoid - derived cell monolayers. *Sci. Rep.*, 1–12. doi:10.1038/s41598-021-84774-w.

Kardia, E., Fakhri, O., Pavy, M., Mason, H., Huang, N., Smertina, E., et al. (2022). Hepatobiliary organoids derived from leporids support the replication of hepatotropic lagoviruses. *Preprint*. doi: https://doi.org/10.1101/2022.04.07.487566.

Kerr, P. J., Hall, R. N., and Strive, T. (2021). Viruses for landscape-scale therapy: biological control of rabbits in Australia. Humana, New York, NY: Lucas A.R. (eds) Viruses as therapeutics. *Methods in Molecular Biology* doi:https://doi.org/10.1007/978-1-0716-1012-1_1.

Kumar, S., Stecher, G., and Tamura, K. (2016). MEGA7: molecular evolutionary genetics

analysis version 7.0 for bigger datasets. *Mol. Biol. Evol.* 33, 1870–1874. doi:10.1093/molbev/msw054.

Le Gall-Reculé, G., Zwingelstein, F., Boucher, S., Le Normand, B., Plassiart, G., Portejoie, Y., et al. (2011). Virology: detection of a new variant of rabbit haemorrhagic disease virus in France. *Vet. Rec.* 168, 137–138. doi:10.1136/vr.d697.

Le Pendu, J., Abrantes, J., Bertagnoli, S., Guitton, J. S., Le Gall-Reculé, G., Lopes, A. M., et al. (2017). Proposal for a unified classification system and nomenclature of lagoviruses. *J. Gen. Virol.* 98, 1658–1666. doi:10.1099/jgv.0.000840.

Lee, S., Liu, H., Wilen, C. B., Sychev, Z. E., Desai, C., Hykes, B. L., et al. (2019). A secreted viral nonstructural protein determines intestinal norovirus pathogenesis. *Cell Host Microbe* 25, 845–857.e5. doi:10.1016/j.chom.2019.04.005.

Leen, E. N., Sorgeloos, F., Correia, S., Chaudhry, Y., Cannac, F., Pastore, C., et al. (2016). A conserved interaction between a C-terminal motif in norovirus VPg and the HEAT-1 domain of eIF4G is essential for translation initiation. *PLoS Pathog.* 12, 1–34. doi:10.1371/journal.ppat.1005379.

Liu, G., Zhang, Y., Ni, Z., Yun, T., Sheng, Z., Liang, H., et al. (2006). Recovery of infectious rabbit hemorrhagic disease virus from rabbits after direct inoculation with in vitro-transcribed RNA. *J. Virol.* 80, 6597–6602. doi:10.1128/JVI.02078-05.

Lopes, A. M., Dalton, K. P., Magalhães, M. J., Parra, F., Esteves, P. J., Holmes, E. C., et al. (2015). Full genomic analysis of new variant rabbit hemorrhagic disease virus revealed multiple recombination events. *J. Gen. Virol.* 96, 1309–1319. doi:10.1099/vir.0.000070.

Lopez Vazquez, A., Alonso, Jose M. Martin CASAIS, R., BOGA, J. A., and Parra, F. (1998). Expression of enzymatically active rabbit hemorrhagic disease virus RNA-dependent RNA polymerase in *Escherichia coli*. *J. Virol.* 72, 2999–3004. doi:10.7551/mitpress/9780262033589.003.0011.

Ludwig-Begall, L., Mauroy, A., and Thiry, E. (2018). Norovirus recombinants: Recurrent in the field, recalcitrant in the lab - a scoping review of recombination and recombinant types of noroviruses. *J. Gen. Virol.* 99, 970–988. doi:10.1099/jgv.0.001103.

Mahar, J. E., Jenckel, M., Huang, N., Smertina, E., Holmes, E. C., Strive, T., et al. (2021). Frequent intergenotypic recombination between the non-structural and structural genes is a major driver of epidemiological fitness in caliciviruses. *Virus Evol.* 7, 1–14. doi:10.1093/ve/veab080.

Marcotte, L. L., Wass, A. B., Gohara, D. W., Pathak, H. B., Arnold, J. J., Filman, D. J., et al. (2007). Crystal structure of poliovirus 3CD protein: virally encoded protease and precursor

to the RNA-dependent RNA polymerase. *J. Virol.* 81,3583–3596. doi:10.1128/JVI.02306-06.

Martín Alonso, J. M., Casais, R., Boga, J. a, and Parra, F. (1996). Processing of rabbit hemorrhagic disease virus polyprotein. *J. Virol.* 70, 1261–1265.

Martinez-Gil, L., and Mingarro, I. (2015). Viroporins, examples of the two-stage membrane protein folding model. *Viruses* 7, 3462–3482. doi:10.3390/v7072781.

Mccune, B. T., Tang, W., Lu, J., Eaglesham, J. B., Thorne, L., Krezel, A. M., et al. (2017). Noroviruses co-opt the function of host proteins VAPA and VAPB for replication. *MBio* 8, 1–17.

McFadden, N., Bailey, D., Carrara, G., Benson, A., Chaudhry, Y., Shortland, A., et al. (2011). Norovirus regulation of the innate immune response and apoptosis occurs via the product of the alternative open reading frame 4. *PLoS Pathog.* 7. doi:10.1371/journal.ppat.1002413.

Meyers, G., Wirblich, C., and Thiel, H.-J. (1991a). Rabbit hemorrhagic disease virus—molecular cloning and nucleotide sequencing of a calicivirus genome. *Virology* 184, 664–676. doi:10.1016/0042-6822(91)90436-F.

Meyers, G., Wirblich, C., and Thiel, H. J. (1991b). Genomic and subgenomic RNAs of rabbit hemorrhagic disease virus are both protein-linked and packaged into particles. *Virology* 184, 677–686. doi:10.1016/0042-6822(91)90437-G.

Meyers, G., Wirblich, C., Thiel, H. J., and Thumfart, J. O. (2000). Rabbit hemorrhagic disease virus: genome organization and polyprotein processing of a calicivirus studied after transient expression of cDNA constructs. *Virology* 276, 349–363. doi:10.1006/viro.2000.0545.

Morgan, A. A., & Rubenstein, E. (2013). Proline: The Distribution, Frequency, Positioning, and Common Functional Roles of Proline and Polyproline Sequences in the Human Proteome. *PLoS One*, 8(1). https://doi.org/10.1371/journal.pone.0053785.

Napthine, S., Lever, R. A., Powell, M. L., Jackson, R. J., Brown, T. D. K., and Brierley, I. (2009). Expression of the VP2 protein of murine norovirus by a translation termination-reinitiation strategy. *PLoS One* 4. doi:10.1371/journal.pone.0008390.

Neave, M. J., Hall, R. N., Huang, N., McColl, K. A., Kerr, P., Hoehn, M., et al. (2018). Robust innate immunity of young rabbits mediates resistance to rabbit hemorrhagic disease caused by Lagovirus Europaeus GI.1 but not GI.2. *Viruses* 10, 1–22. doi:10.3390/v10090512.

Neill, J. D. (1990). Nucleotide sequence of a region of the feline calicivirus genome which encodes picornavirus-like RNA-dependent RNA polymerase, cysteine protease and 2C

polypeptides. *Virus Res.* 17, 145–160. doi:10.1016/0168-1702(90)90061-F.

Nieva, J. L., Madan, V., and Carrasco, L. (2012). Viroporins: structure and biological functions. *Nat. Rev. Microbiol.* 10, 563–574. doi:10.1038/nrmicro2820.

Odorizzi, G. (2006). The multiple personalities of Alix. *J. Cell Sci.* 119, 3025–3032. doi:10.1242/jcs.03072.

Parra, F., and Prieto, M. (1990). Purification and characterization of a calicivirus as the causative agent of a lethal hemorrhagic disease in rabbits. *J. Virol.* 64, 4013–4015.

Parra, G. I. (2019). Emergence of norovirus strains: a tale of two genes. *Virus Evol.* 5, 1–9. doi:10.1093/ve/vez048.

Rademacher, C., Krishna, N. R., Palcic, M., Parra, F., and Peters, T. (2008). NMR experiments reveal the molecular basis of receptor recognition by a calicivirus. *J. Am. Chem. Soc*. 130, 3669–3675. doi:10.1021/ja710854r.

Peñaflor-Tellez, Y., Chavez-Munguia, B., Lagunes-Guillen, A., Salazar-Villatoro, L., and Gutierrez-Escolano, A.-L. (2022). The feline calicivirus leader of the capsid protein has the functional characteristics of a viroporin. *Viruses* 14. doi:https://doi.org/10.3390/v14030635.

Prasad, B. V. V., Hardy, M. E., Dokland, T., Bella, J., Rossmann, M. G., and Estes, M. K. (1999). X-ray crystallographic structure of the Norwalk virus capsid. *Science (80-.).* 286, 287–290. doi:10.1126/science.286.5438.287.

Prasad, B. V. V., Matson, D. O., and Smith, A. W. (1994). Three-dimensional structure of calicivirus. *J. Mol. Biol.* 240, 256–264. doi:10.1006/jmbi.1994.1439.

Rademacher, C., Krishna, N. R., Palcic, M., Parra, F., and Peters, T. (2008). NMR experiments reveal the molecular basis of receptor recognition by a calicivirus. *J. Am. Chem. Soc.* 130, 3669–3675. doi:10.1021/ja710854r.

Ruvoën-Clouet, N., Ganière, J. P., André-Fontaine, G., Blanchard, D., and Le Pendu, J. (2000). Binding of *Rabbit hemorrhagic disease virus* to antigens of the ABH histo-blood group family. *J. Virol.* 74, 11950–11954. doi:10.1128/jvi.74.24.11950-11954.2000.

Sakaguchi, T., Kato, A., Sugahara, F., Shimazu, Y., Inoue, M., Kiyotani, K., et al. (2005). AIP1/Alix is a binding partner of Sendai virus C protein and facilitates virus budding. *J. Virol.* 79, 8933–8941. doi:10.1128/jvi.79.14.8933-8941.2005.

Sharp, T. M., Guix, S., Katayama, K., Crawford, S. E., and Estes, M. K. (2010). Inhibition of cellular protein secretion by norwalk virus nonstructural protein p22 requires a mimic of an endoplasmic reticulum export signal. *PLoS One* 5, 13130. doi:10.1371/journal.pone.0013130.

Smertina, E., Hall, R. N., Urakova, N., Strive, T., and Frese, M. (2021). Calicivirus non-structural proteins: potential functions in replication and host cell manipulation. *Front. Microbiol.* 12. doi:10.3389/fmicb.2021.712710.

Smertina, E., Urakova, N., Strive, T., and Frese, M. (2019). Calicivirus RNA-dependent RNA polymerases: evolution, structure, protein dynamics, and function. *Front. Microbiol.* 10, 1280. doi:10.3389/fmicb.2019.01280.

Sosnovtsev, S. V, Belliot, G., Chang, K.-O., Onwudiwe, O., and Green, K. Y. (2005). Feline calicivirus VP2 is essential for the production of infectious virions. *J. Virol.* 79, 4012–4024. doi:10.1128/JVI.79.7.4012-4024.2005.

Sosnovtseva, S. a, Sosnovtsev, S. V, and Green, K. Y. (1999). Mapping of the feline calicivirus proteinase responsible for autocatalytic processing of the nonstructural polyprotein and identification of a stable proteinase-polymerase precursor protein. *J. Virol.* 73, 6626–6633.

Strtak, A. C., Perry, J. L., Sharp, M. N., Chang-Graham, A. L., Farkas, T., and Hyser, J. M. (2019). Recovirus NS1-2 has viroporin activity that induces aberrant cellular calcium signaling to facilitate virus replication. *mSphere* 4, 1–21. doi:10.1128/msphere.00506-19.

Thumfart, J. O., and Meyers, G. (2002). Rabbit hemorrhagic disease virus: identification of a cleavage site in the viral polyprotein that is not processed by the known calicivirus protease. *Virology* 304, 352–363. doi:10.1006/viro.2002.1660.

Tompa, P. (2003). Intrinsically unstructured proteins evolve by repeat expansion. *BioEssays*, 25(9), 847–855. https://doi.org/10.1002/bies.10324.

Urakova, N., Frese, M., Hall, R. N., Liu, J., Matthaei, M., and Strive, T. (2015). Expression and partial characterisation of rabbit haemorrhagic disease virus non-structural proteins. *Virology* 484, 69–79. doi:10.1016/j.virol.2015.05.004.

Vacic, V., Oldfield, C. J., Mohan, A., Radivojac, P., Cortese, M. S., Uversky, V. N., & Dunker, A. K. (2007). Characterization of molecular recognition features, MoRFs, and their binding partners. *Journal of Proteome Research*, 6(6), 2351–2366. https://doi.org/10.1021/pr0701411.

van Dycke, J., Ny, A., Conceição-Neto, N., Maes, J., Hosmillo, M., Cuvry, A., et al. (2019). A robust human norovirus replication model in zebrafish larvae. *bioRxiv*, 1–21. doi:10.1101/528364.

Vongpunsawad, S., Venkataram Prasad, B. V., and Estes, M. K. (2013). Norwalk virus minor capsid protein VP2 associates within the VP1 shell domain. *J. Virol*. 87, 4818–4825. doi:10.1128/jvi.03508-12.

Wang, X., Xu, F., Liu, J., Gao, B., Liu, Y., Zhai, Y., et al. (2013). Atomic model of rabbit

hemorrhagic disease virus by cryo-electron microscopy and crystallography. *PLoS Pathog.* 9. doi:10.1371/journal.ppat.1003132.

Wennesz, R., Luttermann, C., Kreher, F., and Meyers, G. (2019). Structure-function relationship in the "termination upstream ribosomal binding site" of the calicivirus rabbit hemorrhagic disease virus. *Nucleic Acids Res.* 47, 1920–1934. doi:10.1093/nar/gkz021.

Wirblich, C., Thiel, H. J., and Meyers, G. (1996). Genetic map of the calicivirus rabbit hemorrhagic disease virus as deduced from in vitro translation studies. *J. Virol.* 70, 7974–83. doi:10.1006/viro.2000.0579.

Xia, X., Cheng, A., Wang, M., Ou, X., Sun, D., Mao, S., Huang, J., Yang, Q., Wu, Y., Chen, S., Zhang, S., Zhu, D., Jia, R., Liu, M., Zhao, X. X., Gao, Q., & Tian, B. (2022). Functions of Viroporins in the Viral Life Cycle and Their Regulation of Host Cell Responses. *Front. Immunol.* (Vol. 13). https://doi.org/10.3389/fimmu.2022.890549.

Xie, X., Wang, H., Zeng, J., Li, C., Zhou, G., Yang, D., et al. (2014a). Foot-and-mouth disease virus low-fidelity polymerase mutants are attenuated. *Arch. Virol.* 159, 2641–2650. doi:10.1007/s00705-014-2126-z.

Zeng, J., Wang, H., Xie, X., Li, C., Zhou, G., Yang, D., et al. (2014). Ribavirin-resistant variants of foot-and-mouth disease virus: the effect of restricted quasispecies diversity on viral virulence. *J. Virol.* 88, 4008–4020. doi:10.1128/JVI.03594-13.

Zhu, J., Miao, Q., Tang, J., Wang, X., Dong, D., Liu, T., et al. (2018). Nucleolin mediates the internalization of rabbit hemorrhagic disease virus through clathrin-dependent endocytosis. *PLoS Pathog.* 14. doi:10.1371/journal.ppat.1007383.

Zinoviev, A., Hellen, C. U. T., and Pestova, T. V. (2015). Multiple mechanisms of reinitiation on bicistronic calicivirus mRNAs. *Mol. Cell* 57, 1059–1073. doi:10.1016/j.molcel.2015.01.039.

Appendix

1. Kardia E, Frese M, Smertina E, Strive T, Zeng XL, Estes MK & Hall RN. Culture and differentiation of rabbit intestinal organoids and organoid-derived cell monolayers. *Scientific Reports*, 2021; 1–12. https://doi.org/10.1038/s41598-021-84774-w.

2. Mahar JE, Jenckel M, Huang N, Smertina E, Holmes EC, Strive T & Hall RN. Frequent intergenotypic recombination between the non-structural and structural genes is a major driver of epidemiological fitness in caliciviruses. *Virus Evolution*, 2021; 7(2), 1–14. https://doi.org/10.1093/ve/veab080.

3. Kardia E, Fakhri O, Pavy M, Mason H, Huang N, Smertina E, Estes MK, Strive T, Frese M, Hall RN. Hepatobiliary organoids derived from leporids support the replication of hepatotropic lagoviruses. *Preprint*, 2022; https://doi.org/10.1101/2022.04.07.487566.

4. Smertina E, Urakova N, Strive T, Frese M. Calicivirus RNA-dependent RNA polymerases: evolution, structure, protein dynamics, and function. Frontiers in Microbiology, 2019; 10:1280. doi: 10.3389/fmicb.2019.01280.

5. Smertina E, Hall RN, Urakova N, Strive T, Frese M. Calicivirus Non-structural proteins: potential functions in replication and host cell manipulation. Frontiers in Microbiology, 2021; 12:712710. doi: 10.3389/fmicb.2021.712710.

6. Smertina E, Carroll AJ, Boileau J, Emmott E, Jenckel M, Vohra H, Rolland V, Hands P, Hayashi J, Neave MJ, Liu J-W, Hall RN, Strive T, Frese M. Lagovirus non-structural protein p23: a putative viroporin that interacts with heat shock proteins and uses a disulfide bond for dimerization. Frontiers in Microbiology, 2022; https://doi.org/10.3389/fmicb.2022.923256.